THE DEVELOPMENT AND STUDY OF CHELATING SUBSTRATES FOR THE SEPARATION OF METAL IONS IN COMPLEX SAMPLE MATRICES.

by

James Cowan

A thesis submitted to the University of Plymouth

in partial fulfilment for the degree of

DOCTOR OF PHILOSOPHY

Department of Environmental Sciences

Faculty of Science

In collaboration with DIONEX UK

January 2002

ABSTRACT

The Development and Study of Chelating Substrates for the Separation of Metal Ions in Complex Sample Matrices.

By James Cowan.

The fabrication and study of high performance chelating substrates for the separation of trace metals using a single column under both isocratic and gradient elutions were investigated.

Neutral polystyrene based resins from a variety of manufacturers including a hypercrosslinked resin (MN 200) were functionalised via impregnation with chelating dyestuffs or dynamically modified with small, low molecular weight organic molecules by physical adsorption and chemisorption processes respectively.

Improvements in the impregnation of substrates were developed, based upon ultrasonic agitation, along with improvements in the detection of metal ions by the use of a noise reduction system, eluent clean-up procedures and large volume injections.

The chelating substrates were characterised by studying their ability to retain metal cations (i.e. their capacity factors), column efficiency and separating power as well as their suitability for analytical applications. Other factors including ionic strength, pH, degree of crosslinking, column length and capacity were investigated to determine the separation capabilities of the substrates.

Those substrates deemed to have the most suitable capabilities were employed for the determination of trace metals in a variety of complex sample matrices. These applications included Cd(II), Pb(II) and Cu(II) in a highly mineralised commercially available water, U(VI) in a certified drinking water (High Purity Standards certified drinking water), a fortified soft water (TMDA-54.2), a seawater (NASS-4) and a sample of seawater from the Tamar Estuary. U(VI) and Bi(III) were determined in a certified stream sediment material (GBW07311) with U(VI) also being determined in certified soil materials (GBW0401 and GBW0403).

LIST OF CONTENTS

CHAPTER 2. Development of Dye Impregnated HPCIC Substrates.

CHAPTER 5. Determination of Trace Metals in Environmental Samples using HPCIC.

Part 1 - Determination of U(VI) in Environmental Waters using Dynamically Modified Chelating Substrates.

Part 2 - Determination of Bi(III) and U(VI) in Soils and Sediments using Dynamically Modified Chelating Substrates.

CHAPTER 6. Conclusions and Further Work.

LIST OF TABLES

CHAPTER 1.

CHAPTER 2.

CHAPTER 3.

CHAPTER 4.

CHAPTER 5.

LIST OF FIGURES

CHAPTER 1.

CHAPTER 2.

ACKNOWLEDGEMENTS

First and foremost, I would like to thank my supervisor, Dr. Phil Jones, for his continuous support, encouragement and friendship throughout the last four years. I would also like to thank Dr. Pavel Nesterenko, for helpful advice during his visits to Plymouth and for being another friendly face at the conferences I attended. Many thanks also to Derek and Paul for their invaluable assistance with the specialised analytical techniques required during this study.

For financial support of this work I would like to acknowledge the University of Plymouth and to DIONEX UK. I would like to thank also, the technical staff at the University (Andy, Andy, Ian, Derek, Sally and Roger) for their invaluable help during the past three years.

Major thanks to all my friends at the University for making my time here so enjoyable including Paul, Anita, Andy, Paul 'Mac', Emily, Emma, Neil (thanks for the job!) and everyone else. Thanks also to my ex lab partner Matt for all his help and friendship and to Helen for making things more interesting than I thought possible. Lastly I would like to thank Sarah for making these last few months much more enjoyable than they should have been.

Finally I would like to thank my family for all their support and encouragement throughout these last nine years without which I could never have made it this far.

A' the Best

AUTHORS DECLARATION

At no time during the registration for the degree of Doctor of Philosophy has the author been registered for any other University award.

This study was financed with the aid of a studentship from the University of Plymouth.
A programme of advanced study was undertaken, which included instruction in high performance liquid chromatography theory and instrument operation and metal chelation theory.

Relevant scientific seminars and conferences were regularly attended at which work was often presented, and a paper prepared for publication.

Publications

The ion chromatographic separation of high valence metal cations using a neutral polystyrene resin dynamically modified with dipicolinic acid. J. Cowan, M. J. Shaw, E. P. Achterberg, P. Jones and P. N. Nesterenko, *Analyst*, **125(12)** (2000) 2157.

Presentations and Conferences Attend

A Comparison of two high performance chelation ion chromatography substrates for the separation and determination of trace metals, J. Cowan, E. Achterberg and P. Jones, Poster Presentation, International Ion Chromatography Symposium, San Jose, USA, Sep 1999.

Recent Developments in the use of Dynamically formed high efficiency chelating substrates for the ion chromatography separation and determination of trace metals, J. Cowan, E. Achterberg, P. Jones and P. N. Nesterenko, Poster presentation, International Ion Chromatography Symposium, Nice, France, Sep 2000.

The use of chelating dyestuffs for the ion chromatography separation of trace metals, J. Cowan, Oral presentation, Departmental Research Lectures, University of Plymouth, UK, April 1998.

The development of novel methods for the determination of trace metals using high preformance chelation ion chromatography, Oral presentation, Departmental Research Lectures, University of Plymouth, UK, Feb 1999.

Chapter 1 - Introduction

1.1 Introduction.

The determination of trace metals in our environment is of great importance due to the potential danger that a number of them pose. All metals exist naturally in our environment, generally at levels which the surrounding ecosystem has evolved to handle [1]. However, industrialisation has resulted in the pollution of our environment with these natural metal concentrations at times becoming elevated to potentially lethal levels [1]. For example, industrial effluents from process streams can lead to an accumulation of metals in the local environment and if they contaminate the food chain they can build up to levels which are dangerous not only to plant and animal life but to human life as well [1]. Therefore, determination of trace metals in environmental and biological systems is of vital importance. It also affords a better understanding of the environmental and biological pathways by which these metals migrate through our environment. Many metals can be either toxic or non-toxic to their surrounding environment depending upon which species of the metal is present, for example, Cr(III) is essential to human nutrition while Cr(VI) is highly toxic towards aquatic plants and animal life [2]. Various environmental factors can also affect the toxicity of metals including temperature, pH and water hardness [3].

For many years now, increasing pollution incidents, along with our greater understanding of the ramifications of polluting our environment, have resulted in an increasing amount of legislation for pollution control and management. It is however beyond the scope of this thesis to discuss in detail the environmental legislation that is to be found in this country.

In the United Kingdom, many of our environmental laws are based upon proposals put forward by European legislation. This European Union (EU) legislation can take the form of one of three legally binding measures, namely **directives, regulations and decisions**. EU directives are the most common form of EU legislation to be found. These EU directives state the end result that a member state has to achieve, although it leaves it up to the individual country to decide how that result is to be achieved. Unfortunately, there is no single piece of EC legislation that covers for example, all aspects of water pollution or air pollution. There is in fact an extensive list of Directives which govern discharges, quality, sampling, handling, analysis, inspection etc. of various waters or air or soil etc..

One of the most important pieces of EC legislation of the past 25 years has been Directive 76/464, "Pollution caused by certain Dangerous Substances Discharged into the Aquatic Environment of the Community" and is commonly known as the dangerous substances directive. It should not however be confused with the "Dangerous Substances Directive 67/548" which governs the hazard labeling of chemicals. Directive 76/464 is a framework from which certain types of pollution have to be eliminated with other types only being reduced and is set out with two lists (I and II). List I (commonly known as the black list) contains substances which belong to specific families or groups of substances whose toxicity, persistence and bioaccumulation make it desirable that they be eliminated [1]. This list contains organohalogens, organophosphorus and organotin compounds, proven carcinogens, mercury and cadmium and their compounds, persistent mineral oils and hydrocarbons and persistent synthetic substances. The elimination of these substances is to be brought about by the setting of limit values by daughter Directives. List II (commonly known as the grey list) contains "families and groups of substances which have a deleterious effect on the aquatic environment but which can be confined to a given area

and which depend on the characterisation and location of the receiving water" [1]. These substances include metals, metalloids and their compounds including Zn, Cr, Pb, Be, U, Co, biocides not appearing in List I, substances that have a deleterious effect on the taste/smell of products derived for human consumption from the aquatic environment, toxic/persistent organic compounds of silicon, inorganic phosphorus compounds, non-persistent mineral oils, cyanides, fluorides and substances having an adverse affect on oxygen balance. Also List II contains all List I substances for which limit values have not yet been set.

This is by no means the only piece of water legislation implemented by the European community. Others include the Groundwater Directive (80/68) which is designed to prevent, reduce or eliminate pollution of groundwater arising from families and groups of substances. Directive 75/440 is concerned with the quality of surface waters whilst Directive 76/160 is concerned with the public health and environmental quality of bathing waters. The final principle Directive is 80/778, the drinking water directive which sets out the requirements for water for human consumption or to be used in cooking with the exception of natural mineral waters, provisions for which is made in Directive 80/777.

Books by Hughes [4], Helmer and Hespanhol [5] and Gillies [6] discuss environmental law and the various EC directives pertaining to water, land and air pollution.

Over the years many pollution incidents have resulted in increasing legislation to regulate discharge levels of metals from industrial sources and in order to enforce these regulations reliable, accurate and sensitive methods of analysis are required. Many modern analytical techniques such as atomic spectrometry, voltammetry and inductively coupled plasma

mass spectrometry (ICP-MS) are capable of quantifying total metal concentration at both natural and elevated levels. A disadvantage of these techniques is that they are not entirely suitable for certain sample matrices and can require complicated and/or time consuming methods for sample preparation before the analysis is carried out. The instrumentation used in these techniques can also be highly complex and expensive to run and maintain.

As previously noted, the speciation state of the metal plays an important part in the toxicity of the metal towards its local environment. These techniques cannot by themselves differentiate between the various species present and so are generally coupled with Liquid Chromatography (LC) in order to separate the individual species. LC offers a technique for the analysis of metal ions that is simple, reliable, robust and generally less costly to maintain and run. Also, complicated sample preparation is not necessarily required. The main disadvantage of LC techniques is the lack of highly sensitive detection systems, though modern conductivity detectors and the UV/VIS detectors discussed in this thesis are beginning to offer the sensitivity that is required by today's analyst. This thesis will describe studies carried out using an LC method for the separation of metal ions in complex matrices with detection by UV/VIS spectrometry.

1.2 Liquid Chromatography.

A Russian botanist called Mikhail Tswett [7] invented and named the technique called chromatography (from the Greek *chroma* meaning *colour* and *graphein* meaning *to write*) in 1903 when he separated various plant pigments by passing them through a glass column packed with finely divided calcium carbonate. For over 20 years this technique lay almost forgotten until in 1930 Lederer and Kuhn used chromatography in their research on

carotenoids. This work was well received and chromatography soon spread and became a standard laboratory technique. Izmailov and Schraiber in 1938 laid the foundations for thin layer chromatography, which was further refined by Stahl in 1958. Ion-exchange chromatography was also developed in the late 1930's when Taylor and Urey separated lithium and potassium isotopes on zeolites. The major advance came though with the application of synthetic ion-exchange resins to the separation of rare earth and transuranium elements in connection with the Manhattan project during World War II.

In 1941, Martin and Synge developed partition chromatography where the stationary phase was a liquid immobilised onto a solid support. This work was further strengthened by the development of paper chromatography in 1944 by Consden, Gorden and Martin. Martin was also instrumental in developing reversed-phase chromatography in 1950 and, with the introduction of gradient elutions in 1952, paved the way for modern column chromatography. The theoretical aspects of chromatography first realised by Martin and Synge were not put into practice until the late 1960s when, with the advances in technology, modern High Performance Liquid Chromatography (HPLC) was developed. With ionic suppression systems developed by the Dow chemical company, Small *et al* [8] in 1975, gave birth to modern ion chromatography.

During a chromatographic separation the analyte is constantly moving back and forth between a stationary and mobile phase. This process is called sorption. In LC there are 4 main types of sorption mechanisms to be found namely, **adsorption, partition, exchange** and **exclusion**.

1. **Adsorption Chromatography** - Adsorption or liquid-solid chromatography is the classic form of LC that was first introduced by Tswett. The stationary phases used are usually silica based though alumina based phases are also used. These stationary phases have polar surfaces and the analyte of interest (principally organic molecules) are adsorbed according to their own polarity i.e. the more polar the analyte is the greater its retention will be. The mobile phase used is generally non-polar though by increasing its polarity the analyte will be eluted quicker.

2. **Partition Chromatography** - Partition chromatography involves a stationary phase which has a liquid coated, or bonded, onto a solid support. Early partition chromatography involved the physical adsorption of the liquid stationary phase onto the solid support and was known as liquid-liquid chromatography. Today however, bonded-phase stationary phases are used. These substrates have the liquid stationary phase chemically bonded to a solid support and result in a much more robust and permanent phase. There are in fact two different types of partition stationary phases and these are *normal* and *reversed-phase*. Normal-phase involves the use of a polar stationary phase supported on silica or alumina particles along with a non-polar mobile phase as found in adsorption chromatography. Reversed-phase is the reverse of this i.e. a non-polar stationary phase and a polar mobile phase. The actual sorption mechanism exploits the fact that the analyte will distribute itself between the two immiscible liquids of the phases according to its distribution coefficient K_D.

3. **Ion-Exchange Chromatography** - Ion-exchange chromatography utilises a stationary phase which is usually a permeable polymeric solid containing fixed charge groups

with mobile counter ions which are exchanged with the analyte ions in the mobile phase. This sorption method will be discussed in the following section.

4. **Size-Exclusion Chromatography** - This sorption method, also called gel permeation or gel filtration chromatography, is based upon a physical sieving process and relies on the size selective diffusion of the analyte through a porous silica or polymer stationary phase.

The investigations discussed in this thesis entail the use of ion chromatography. Although the term ion chromatography traditionally refers to ion-exchange chromatography, today it also encompasses ion-exclusion and ion-pair chromatography. Of these techniques, the ion-exchange method is the most widely used and can be sub-divided into two further categories, namely **traditional ion-exchange** and **chelation ion-exchange**, the differences between these two methods have been discussed in a review paper by Jones and Nesterenko [9]. The actual studies undertaken in this thesis utilise the chelation ion-exchange method of chromatography.

1.2.1 Principles of Liquid Chromatography.

Chromatography is one of the most useful tools available to the analytical chemist. It provides a method for the separation and quantification of closely related compounds in complex mixtures, which may not be attainable by any other means. The IUPAC definition of chromatography states it as "*a method used primarily for the separation of the components of a sample, in which the components are distributed between two phases, one of which is stationary while the other moves*". Therefore, column liquid chromatography

consists of a liquid mobile phase which is forced through an immiscible stationary phase, which is a column containing a finely divided spherical solid or gel.

When a sample is introduced into this system, the individual components of the sample will be distributed between the two phases. The sample components that show a greater affinity for the stationary phase will be more strongly retained than those with a weaker affinity (or stronger affinity for the mobile phase). These differences in affinities allow for the individual sample components to migrate at different rates through the system and thereby result in their separation. The equilibrium, which a component forms between the mobile and stationary phases, is described by the **partition** (or distribution) **coefficient**, $\mathbf{K_D}$, which is defined as:

$$K_D = \frac{C_S}{C_M}$$

where C_S is the concentration of the component in the stationary phase and C_M is the concentration of the component in the mobile phase. K_D is related to the retention time of the component. Ideally this partition coefficient should be constant over as large a concentration range as possible. If so then this will produce a linear sorption isotherm as is shown in Figure 1.1 and will result in a gaussian shaped peak. As sorption charateristics can change at high concentrations this will lead to a change in the partition coefficient and result in a curved isotherm which will relate to distortions in peak shape known as *fronting* or *tailing*. Figure 1.1b and c show the effects of high concentration. Fronting occurs in systems where partition is the main separation process and where there is a small distribution ratio. Tailing occurs where adsorption is involved in the separation. As these

effects are more pronounced at high concentrations they are symptomatic of the overloading of the column.

The migration rate of a component can also be described by another very important parameter, namely the **capacity factor, k'**, which is defined as:

$$k' = \frac{t_R - t_0}{t_0}$$

where t_R is the retention time of the analyte of interest and t_0 is the retention time, also known as the dead time, of an unretained species. k' is directly proportional to K_D and is shown by the equation below, so therefore the greater the value for k' or K_D, the greater the retention of the analyte of interest will be.

$$k' = K_D \frac{V_S}{V_M}$$

where K_D is the partition coefficient, V_M is the volume of analyte in the mobile phase and V_S is the volume of analyte in the stationary phase. While k' and K_D are values for individual components, the actual separation between two components of a mixture can also be calculated. This relative separation is given by the **selectivity factor**, α, and is defined as:

$$\alpha = \frac{k'_2}{k'_1} \quad \text{or} \quad \frac{K_{D_2}}{K_{D_1}}$$

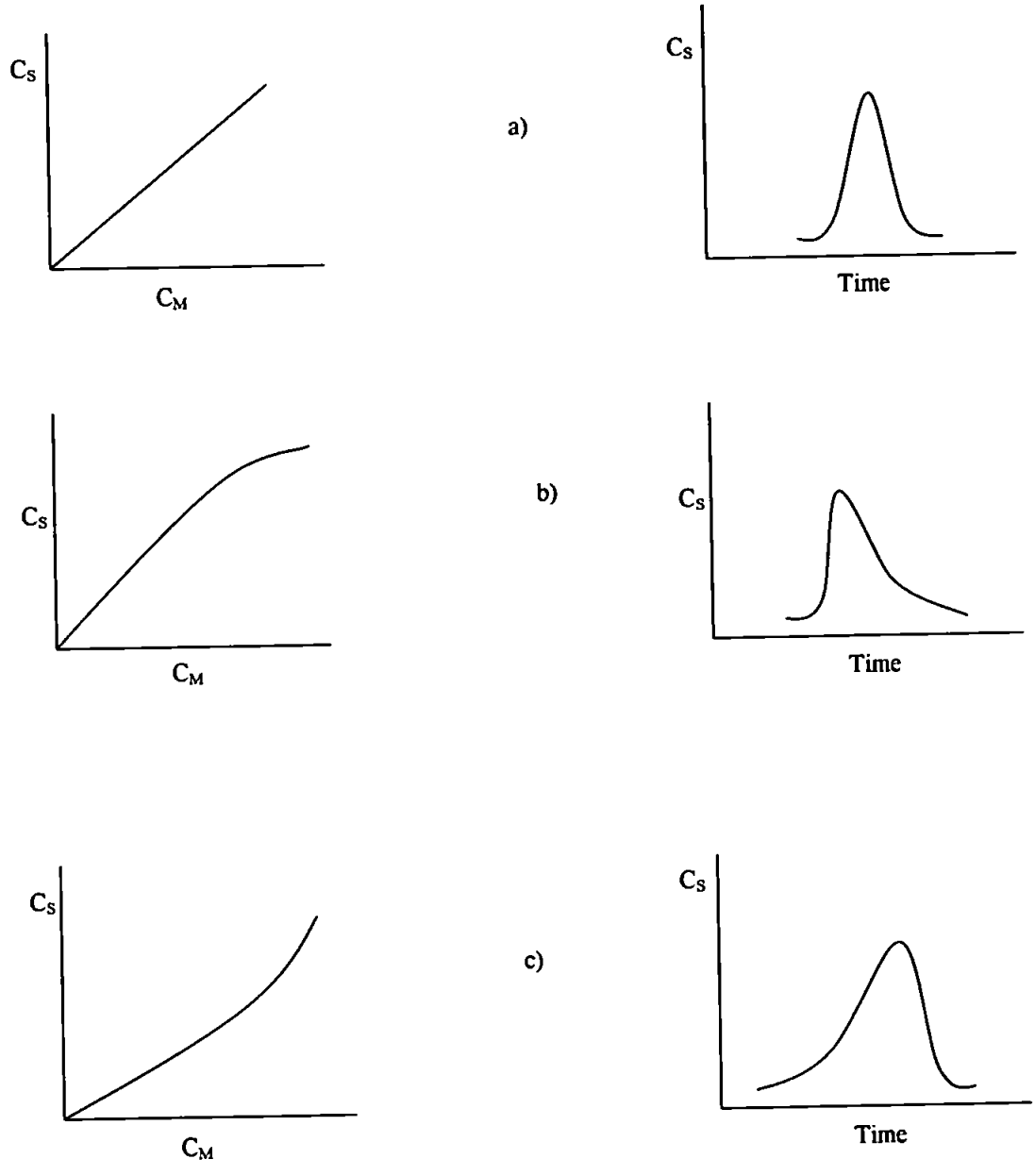

Figure 1.1. Sorption isotherms and concentration profiles: a) Linear Isothem; Gaussian Profile, b) Curved Isotherm; Tailing and c) Curved Isotherm; Fronting.

where k'_2 is the capacity factor for the more strongly retained component and k'_1 is the capacity factor for the less strongly held component. If the value of α is small the selectivity of the column and therefore, the separation of the components will usually be poor. If this is so, then modification of either the mobile or stationary phase (or both) may be required to increase the retention of one component over another. A major problem found though when retention is increased, is that of **band broadening**. This is a problem as when peaks broaden out the resolution between two peaks will decrease thereby resulting in the possible partial coelution of two separate analytes and unreliable quantitative data.

One way to minimise the band broadening effect is to increase the efficiency of the column. Column efficiency can be defined by the "Plate Theory", originally hypothesised by Martin and Singe and given by the following equation:

$$N = 16\left(\frac{t_R}{W}\right)^2 \quad \text{or} \quad N = 5.54\left(\frac{t_R}{W_{1/2}}\right)^2$$

where N is the number of theoretical plates, t_R is the retention time of the peak, W is the peak width and $W_{1/2}$ is the peak width at half the peak height. Generally $W_{1/2}$ is used as this is a more accurate and easily determined value than W. The greater the number of theoretical plates, the greater the efficiency of the column and therefore the greater the separating power of the column. Perhaps a better way of quoting column efficiency is in terms of plate height (or height equivalent to a theoretical plate) rather than the number of plates. The number of plates and the plate height are inversely proportional to one another and is given by the equation:

$$H = \frac{L}{N}$$

where L is the column length (usually in cm) and H is the plate height. This equation can be used to directly compare the efficiencies of two separate separation systems.

While the "plate theory" provides a method for the determination of column efficiencies it does not fully explain the causes of band broadening. This is because the "plate theory" is imperfect in that it does not treat a chromatographic system as a continuous dynamic system, however, the "rate theory" formulated by van Deemter, Zuiderberg and Klinkingberg does. Peak width is ultimately determined by the total amount of diffusion that occurs in the system and the rate at which it occurs. The **van Deemter** equation can be used to explain the different factors affecting the amount and rate of diffusion:

$$H = A + \frac{B}{u} + Cu$$

where A is the amount of *eddy diffusion* that occurs, B is the amount of *longitudinal (or molecular) diffusion* that occurs, C is the *resistance to mass transfer* and u is the velocity of the mobile phase. Eddy diffusion occurs due to the mobile phase taking an irregular path through the column rather than an ideal regular path whereas the longitudinal (or molecular) diffusion relates to the amount of diffusion of the solute in the mobile phase and to a lesser extent the stationary phase. As this is continuous, the longer the sample remains on the column the greater its diffusion will be and therefore, the greater the band broadening will be. The resistance to mass transfer term refers to the finite amount of time

taken for the sample to move between the two phases. This equation is shown graphically in Figures 1.2 and 1.3.

An ideal chromatographic column would not only be highly efficient but also offer good resolution between peaks. Peak resolution is the most commonly used parameter for describing the ability of a column to separate two peaks and is defined by the equation:

$$R_s = \frac{2(t_{R_2} - t_{R_1})}{(W_1 + W_2)}$$

This is a measure of the distance between the peak maxima of two adjacent peaks and is show in Figure 1.4. An R_s value of 1.5 means that the two peaks in question are quantitatively separated. The resolution can also be defined by the equation below which connects the parameters R_s, N, α and k' together.

$$R_s = \frac{\sqrt{N}}{4}\left(\frac{\alpha - 1}{\alpha}\right)\left(\frac{k'}{1 + k'}\right)$$

where N = number of theoretical peaks, α = selectivity factor and k' = capacity factor.

The parameters outlined here allow us to carry out an evaluation of the capabilities and performance of a chromatographic system.

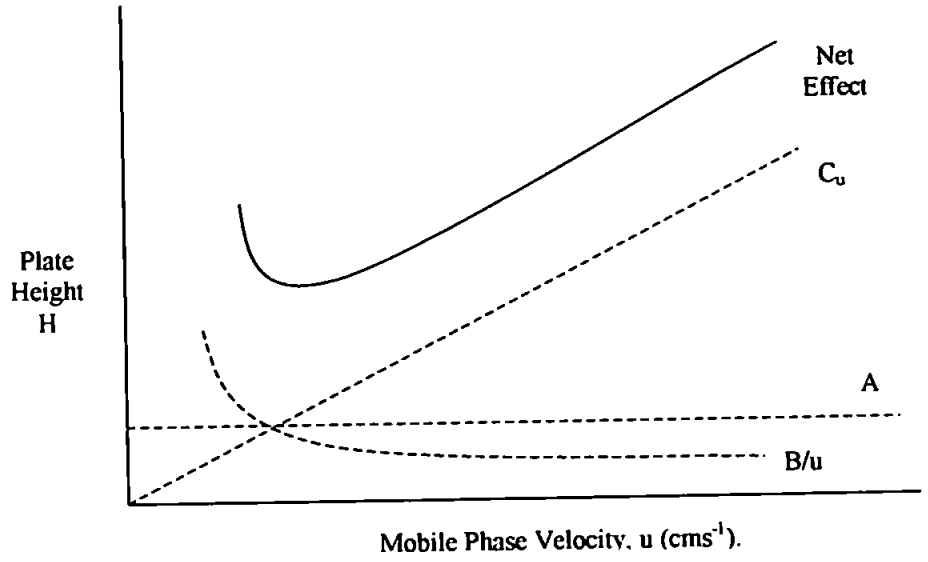

Figure 1.2. van Deemter Plot

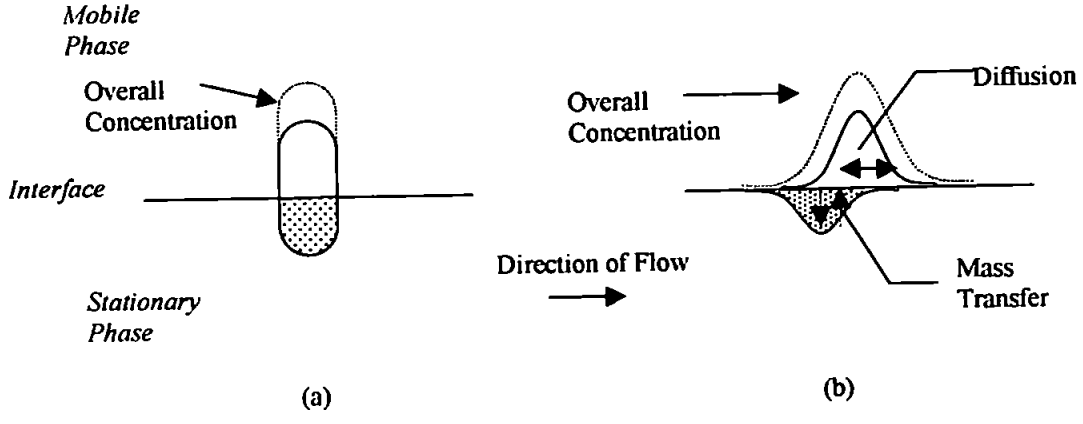

Figure 1.3. Effects of diffusion and mass transfer on peak width. (a) Concentration profiles of a solute at the beginning of a separation. (b) Concentration of a solute after passing some difference through a system.

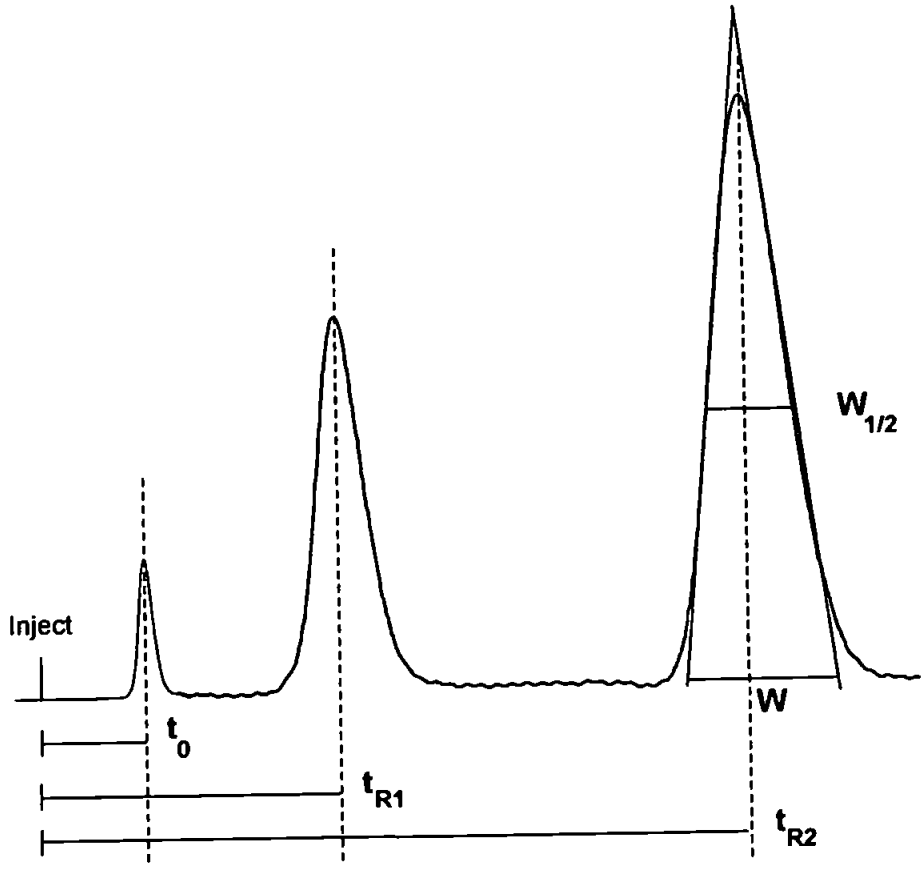

Figure 1.4. A chromatographic separation illustrating the parameters used in calculations.

1.2.2 Ion-exchange Methods

Ion-exchange methods are based upon a reversible exchange of ions between an external liquid phase and an ionic solid phase. Skoog and Leary [7] define an ion-exchange process as "*exchange equilibria between ions in solution and ions of like sign on the surface of an essentially insoluble, high molecular-weight solid*". The stationary (or solid) phase generally consists of a polymeric matrix, which is insoluble but permeable, containing covalently bonded ionic groups of fixed charge with exchangable counter ions of opposite

charge. Both anion and cation exchange resins can be found and both of these can be further subdivided into two separate classes of ion-exchanger, those being either strong or weak exchangers. A strong cation or anion exchanger would contain, for example, a sulphonic acid (a strong acid) or a quaternary amine (a strong base) functional group respectively whereas a weak cation or anion exchanger would contain, for example, a carboxylic acid (weak acid) or a primary amine (weak base) functional group respectively. Therefore, the more readily ionised the functional group is the stronger the ion-exchanger will be. The ion-exchange processes which occur are demonstrated by the following equations:

Strong Cation $nRSO_3^-H^+ + M^{n+} \rightleftharpoons (RSO_3^-)_nM^{n+} + nH^+$

Weak Cation $nRCOO^-H^+ + M^{n+} \rightleftharpoons (RCOO^-)_nM^{n+} + nH^+$

Strong Anion $nRN(CH_3)_3^+OH^- + A^{n-} \rightleftharpoons [RN(CH_3)_3^+]_nA^{n-} + nOH^-$

Weak Anion $nRNH_3^+OH^- + A^{n-} \rightleftharpoons (RNH_3^+)_nA^{n-} + nOH^-$

R = Resin backbone

Strong ion-exchangers are ionised over a wide pH range from 1-14 whereas weak ion-exchangers are ionised over a limited pH range, typically 5-14. Cation exchangers can start to lose their charge below pH6 and anion exchangers above pH9, with weak exchangers having a much higher capacity than the strong exchangers when fully ionised but only over a limited pH range.

The selectivity orders of cations on a strong cation exchange resin are dependent upon several controlling factors. One such factor is charge and as a general rule, trivalent ions

show greater retention than divalent ions which in turn show greater retention than monovalent ions [10] as is shown below:

$$Pu^{4+} \gg La^{3+} > Ce^{3+} > Pr^{3+} > Eu^{3+} > Y^{3+} > Sc^{3+} > Al^{3+} \gg$$

$$Ba^{2+} > Pb^{2+} > Sr^{2+} > Ca^{2+} > Ni^{2+} > Cd^{2+} > Cu^{2+} > Co^{2+} > Zn^{2+} > Mg^{2+} > UO_2^{2+} \gg$$

$$Tl^{+} > Ag^{+} > Cs^{+} > Rb^{+} > K^{+} > NH_4^{+} > Na^{+} > H^{+} > Li^{+}$$

Within each of these charge groups another controlling factor is the size of the hydrated ion. Those ions which are strongly hydrated have larger ionic radii than those which are weakly hydrated. For example, Mg^{2+} has a much larger charge density when compared to Ba^{2+} which has a greater atomic weight. Ba^{2+} is less hydrated in aqueous solution which results in a smaller hydrated radius and thereby greater retention. This is related to the pore size of the resin as the smaller the ion the more readily they will be trapped within the pores. Other factors which control the selectivity include, the type of functional group on the stationary phase, the composition of the mobile phase being used, the capacity of the stationary phase, dimensions of the column being used and whether or not a complexing agent is present in the mobile phase.

The presence of a complexing agent in the mobile phase can help to improve the efficiency of the separation especially when trying to separate metals. Addition of a complexing agent in effect reduces the effective charge on the metal ion. However, stability constants should not be too large otherwise retention times will be too short for good separations. Complexing agents which are used include carboxylic acids such as citric, tartaric and oxalic acid though weaker acids such as acetic and lactic acid can also be used. The

following example [11] shows how a complexing agent added to the eluent helps to improve the selectivity and efficiency of a column. Ethylenediamine (EDA) is added to the eluent of a system for the separation of transition metals to act as a competing ion. At the pH required for separation (usually between 3 and 5), the EDA is fully protonated and loses its ability to act as a ligand. Upon addition of a complexing ligand, the following equilibria is found to exist:

$$R\text{-}M + EDAH_2^{2+} + L^{2-} \rightleftharpoons R\text{-}EDAH_2 + M^{2+} + L^{2-} \rightleftharpoons R\text{-}EDAH_2 + ML$$

Without the complexing ligand (L^{2-}) being present the metal ions are strongly retained by a strong cation exchanger with elution being governed solely by the concentration of EDA present. When the complexing ligand is added, its anionic carboxylate groups compete with the sulphonic acid groups for the metal ion. This combined with the competition from the EDA counter ion results in the metal ion being released by the stationary phase, thereby resulting in a decrease in the retention time of the metal. As the protonation of the EDA and the deprotonation of the ligand are controlled by the pH of the eluent, which therefore controls the extent of complex formation, the pH of the eluent has to be carefully chosen as too much complexation will result in the metals being eluted too quickly with little or no separation occurring.

Further details on the theory and applications of ion chromatography can be found in books by Weiss [12], Fritz and Gjerde [13] and Robards *et al* [14].

1.2.3 Chelation-exchange Methods

So far only the ion-exchange mechanism has been discussed. As mention in section 1.2, the studies undertaken in this thesis employ a method that uses a chelation sorption mechanism rather than the traditional ion-exchange mechanism. This method of separation utilises a substrate that contains chelating functional groups that selectively form complexes with the metal ions in solution. The extent to which a metal ion will form a complex is given by its stability constant. As this constant is different for each metal, a metal mixture can be separated due to the differences between the stability constants using the chelation sorption mechanism. The differences between the traditional ion-exchange mechanism and the chelation-exchange mechanism are shown in Figure 1.5.

In the ion-exchange mechanism, alkali metal ions, if present, produce a major competitive effect on the exchange mechanism with this effect increasing as their concentration increases. In the chelation-exchange mechanism, the alkali metals form extremely weak coordinate bonds in comparison with other metals and can be considered negligible. This is partly why ionic strength does not affect the chelation separation mechanism. However, the concentration of H^+ ions (pH) does have a major significant effect on the chelation mechanism. This is due to the fact that most chelating ligands are the *conjugate base of a weak acid* and therefore have a very strong affinity for H^+ ions. The relative insensitivity of this chelating mechanism towards ionic strength is one of the major advantages of this method over the traditional ion-exchange method.

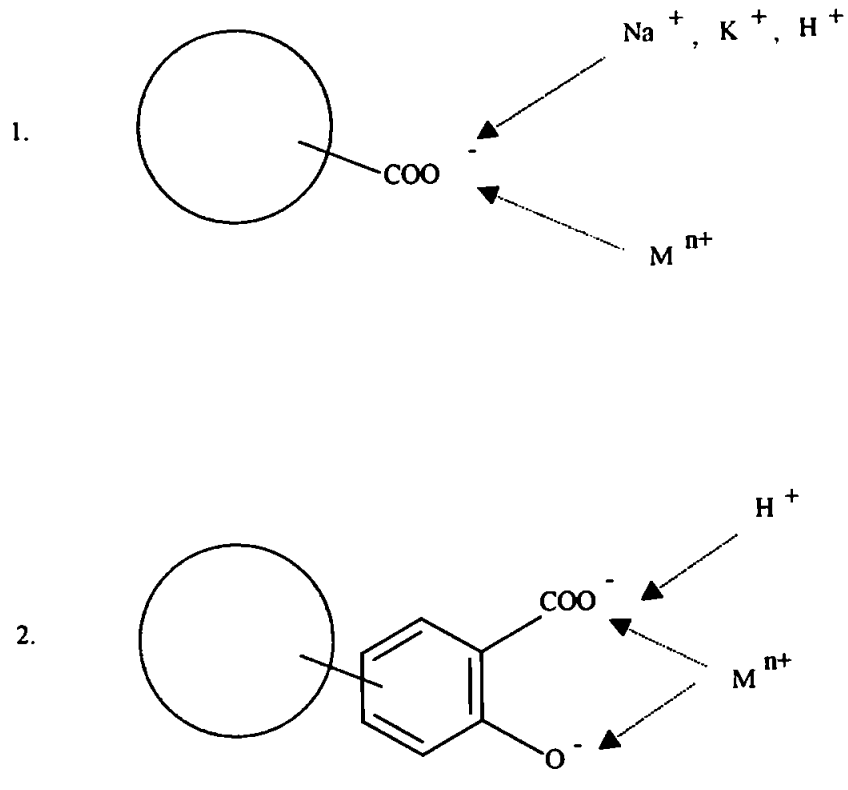

Figure 1.5. Traditional ion-exchange (1) and chelating ion-exchange (2) mechanisms.

1.2.4 Ion Chromatography Substrates

The stationary phase in ion chromatography consists of an insoluble but permeable resin which has had functional groups chemically bonded to it. Resins based on polystyrene-divinylbenzene (PS-DVB) copolymers are the most widely used, though polyacrylate and silica based resins are also to be found. The structure of a PS-DVB resin is shown in Figure 1.6.

Resins can be classified as either *microporous (or microreticular)* or *macroporous (or macroreticular)* resins. Microporous resins are gel-like, usually PS-DVB copolymers with 4-12% DVB crosslinking. A major problem with these types of resin is that they swell and shrink with changes in its ionic form. Increasing the degree of crosslinking can reduce the amount of swelling that occurs but too high a degree of crosslinking can affect the performance of the resin. Macroporous resins have a very different structure in comparison to the microporous resins. Again they are usually PS-DVB copolymers but contain greater than 15% crosslinking and are formed via a different polymerisation process. This time the resin bead comprises of thousands of smaller beads separated by wide pores and channels up to several hundred angstroms in size. This results in a very rigid structure with a much greater surface area (20-300 m^2g^{-1}). Also they do not shrink or swell due to the wide pores and channels present.

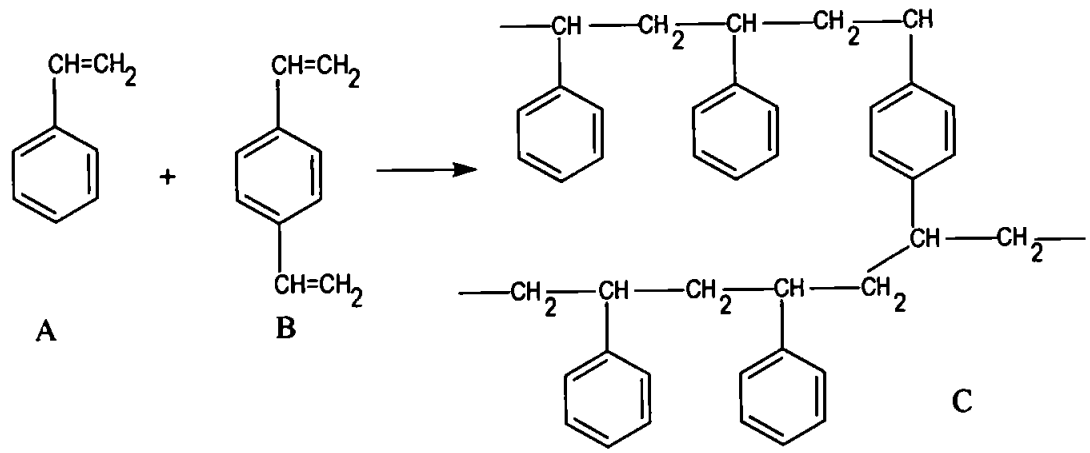

Figure 1.6. The synthesis and structure of: (1) polystyrene divinylbenzene (PS-DVB) (C) from styrene (A) and divinyl benzene (B).

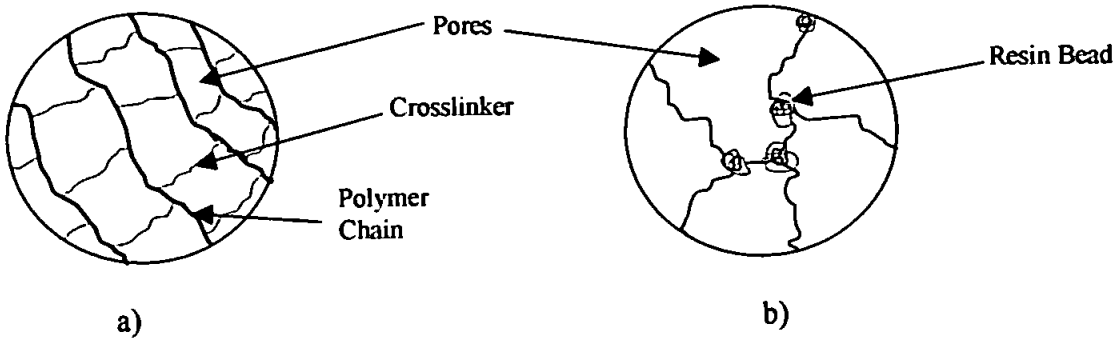

Figure 1.7. Structure of a) a microporous resin bead and b) a macroporous resin bead.

1.3 Coordination Chemistry.

The formation of a metal-ligand complex or coordination compound can be discussed using several concepts including acid/base theory, the chelate effect and the stabilility of these complexes.

One way to look at coordinate theory is to use the general acid/base definition as formulated by G. N. Lewis. He defined an acid as "*a substance which can accept a pair of electrons*" and a base as "*a substance which can donate a pair of electrons*" [15]. This theory allows us to understand the principles of coordination chemistry with the metal acting as a Lewis acid and the ligand acting as a Lewis base. This results in the formation of a coordinate bond where both electrons for the bond come from the ligand rather than one electron being donated by both the metal and ligand. For example BF_3 acts as a Lewis acid in the presence of NH_3 which acts as a Lewis base. The NH_3 donates its lone pair of electrons to form a coordinate covalent bond between the boron and nitrogen.

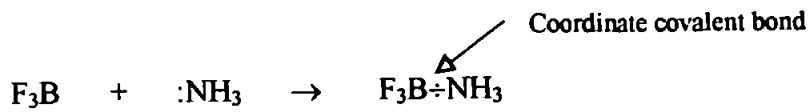

One model that is used to describe the interactions between Lewis acids and bases when dealing with metals and ligands is the concept of *hardness* and *softness* [16]. Metal ions which are small in size, with relatively high charge strongly retain their valence electrons, and therefore not readily polarisable are classified as *hard acids*. *Soft acids* are metal ions which are large, capable of losing their valence electrons readily and easily polarised. Ligands that contain highly electronegative donor atoms and therefore difficult to polarise are classified as *hard bases* whereas *soft bases* are those ligands which are easily polarised. Tables 1.1 and 1.2 shows some metal ions and ligands as hard and soft species [17].

Table 1.1. Metal ions as hard or soft acids

Hard	H^+ Li^+ Na^+ K^+ Rb^+ Cs^+ Be^{2+} Mg^{2+} Ca^{2+} Sr^{2+} Ba^{2+} Ra^{2+} Mn^{2+} UO_2^{2+} VO^{2+}
	Al^{3+} Sc^{3+} Ti^{3+} Cr^{3+} Fe^{3+} Co^{3+} Ga^{3+} In^{3+} MoO^{3+} Y^{3+} La^{3+} Lu^{3+} Zr^{4+} Hf^{4+} Th^{4+} U^{4+}
Intermediate	Cr^{2+} Fe^{2+} Ru^{2+} Os^{2+} Co^{2+} Ni^{2+} Cu^{2+} Zn^{2+} Sn^{2+} Pb^{2+} Rh^{3+} Ir^{3+} Sb^{3+} Bi^{3+}
Soft	Cu^+ Ag^+ Au^+ Hg^+ Tl^+ Pt^{2+} Pd^{2+} Cd^{2+} Tl^{3+} Pt^{4+} Te^{4+}

Table 1.2. Ligands as hard or soft bases

Hard	H_2O ROH R_2O HO^- RO^- RCO_2^- NO_3^- ClO_4^- F^- Cl^- CO_3^{2-} SO_4^{2-} PO_4^{2-}
Intermediate	NH_3 RNH_2 Aniline Pyridine N_2H_4 N_3^- NO_2^- ClO_3^- Br^- SO_3^{2-}
Soft	R_2S RSH R_3P $(RO)_3P$ RS^- SCN^- I^- CN^- $S_2O_3^{2-}$

As a general rule, the most stable complexes are generally formed between hard acids and hard bases with the stability increasing with charge and between soft acids and soft bases where the stability increases with a decrease in charge. The forces that bind hard acids and bases are usually electrostatic in nature whereas soft acids and bases tend to form mainly covalent bonds.

The ligands that are most commonly found are those that bond to the metal through lone pairs of electrons from donor atoms such as oxygen, nitrogen, sulphur or halogen. Coordination by oxygen is strongest for the carboxylate ion. For nitrogen it is the amino groups followed by diazo and ring nitrogens and for sulphur ligands it is strongest with thiolate (RS^- or R-SS-) groups. Oxygen containing ligands are harder than nitrogen containing ligands which in turn are harder than sulphur containing ligands. The categorisation of mixed ligands however is much more complex. If a compound contains for example, both hard and soft donor atoms then the presence of the hard donor atoms will increase the hardness of the soft donor atoms and the soft donor atoms will increase the softness of the hard donor atoms. This can result in either a decrease or increase in the stability of the resulting complex depending upon the nature of the metal ion.

1.3.1. Coordination Compounds.

When a complex (or coordination compound) is formed, a metal is surrounded by ligands which can either bond to the metal through a carbon bond, as is found in organometalic compounds or through interactions which can be thought of as Lewis acid-base reactions as discussed earlier. The number of donor atoms surrounding the central metal atom in a complex is termed the *coordination number* [15]. Coordination numbers range from 2-16,

though coordination numbers of 10 and above are generally only found in organometallic compounds rather than coordination compounds. The coordination number 6 is the most common number found as almost all metal cations form 6-coordinate complexes. The next most common is 4 with 2 being the most rare and limited to the +1 cations of Cu, Ag, and Au as well as Hg^{2+}.

As ligands can be thought of as electron-pair donors they can be further classified by the number of donor atoms present in the ligand. Those ligands which contain a single donor atom such as Cl^-, CN^-, CH_3OH and OH^- are called **monodentate** ligands. Ligands which contain two donor atoms which bond to a single metal ion are called **bidentate** ligands and include diamines, diethers, carboxylates and nitrates. **Tridentate, tetradentate** and even **hexadentate** ligands are also found.

1.3.1.1 The Chelate Effect.

All these polydentate ligands are also known as *chelate ligands* (from the Greek for claw). These chelate ligands form ring structures called chelates with the metal ions, with the ring formation called **chelation**. Complexes which contain one or several 5 or 6 membered chelate rings are more stable than those complexes which have fewer or none of these rings. The smaller the ring size the more strained the ring becomes while larger sized rings show a lesser tendency for coordination to the second site. This can be shown by the following example of the complexation between Cd^{2+} and methylamine and ethylenediamine (en) [18].

$$Cd^{2+} + 4CH_3NH_2 \rightleftharpoons [Cd(CH_3NH_2)_4]^{2+} \text{ -------Eq 1}$$

$$Cd^{2+} + 2en \rightleftharpoons [Cd(en)_2]^{2+} \text{ ------Eq 2}$$

The $[Cd(en)_2]^{2+}$ complex is nearly 10^4 times more stable than the $[Cd(CH_3NH_2)_4]^{2+}$ complex. This can be explained thermodynamically using the equation for Gibbs free energy, $\Delta G = \Delta H - T\Delta S$, the data for which is given in Table 1.3 [18].

Table 1.3. Stability Constants and Thermodynamic functions for Cd(II) complexes at 25°C and 0.1M ionic strength.

Complex	**Log β_n ($moldm^{-3}$)**	**ΔH ($kJmol^{-1}$)**	**ΔG ($kJmol^{-1}$)**	**$T\Delta S$ ($kJmol^{-1}$)**
$[Cd(CH_3NH_2)_4]^{2+}$	6.55	-57.32	-37.41	-19.91
$[Cd(en)_2]^{2+}$	10.62	-56.48	-60.67	4.19
Diff Eq2-Eq1	4.07	0.84	-23.26	24.10

Where β_n is the formation constant of the complex

Although both reactions have very similar enthalpy values, ΔH, the complexation of Cd^{2+} and ethylenediamine has a positive change in entropy, ΔS, which is a much more favorable change than the negative change shown by the complexation of Cd^{2+} and methylamine. Therefore, the more favorable the entropy change, the more stable the system.

This can be explained by the loss of water from the original aqua ion, $[Cd(H_2O)_6]^{2+}$. In an aqueous system the Cd (II) ion is coordinated with 6 water molecules. In both reactions, 4 of these water molecules are replaced. For the reaction with the methylamine (reaction1), 4 water molecules are replaced with 4 methylamine molecules which results in a zero net

change in the number of molecules whereas the reaction with en (reaction 2) results in the 4 water molecules being replaced with 2 en molecules which results in a net increase of 2 moles of molecules. Therefore, there is an increase in disorder and therefore ΔS is more positive (more favourable) for reaction 2. It can therefore be said that the chelate effect is essentially an entropy effect [19] though this definition is still a bit controversial.

1.3.1.2 Stability of Coordination Compounds.

The degree of complex formation can be quantified by the use of stability constants. The stability constant (or formation constant) of a coordination compound is "*the equilibrium constant for complex ion formation*" [15] or alternatively is "*a measure of the tendency of a metal ion to form a particular complex ion*" [119] and characterises the equilibria for the successive addition of ligands. Therefore, for a metal, M, and a monodentate ligand, L, the equilibria can be expressed as:

$$M + L = ML \qquad K_1 = \frac{[ML]}{[M][L]}$$

$$ML + L = ML_2 \qquad K_2 = \frac{[ML_2]}{[ML][L]}$$

$$ML_2 + L = ML_3 \qquad K_3 = \frac{[ML_3]}{[ML_2][L]}$$

$$\downarrow$$

$$ML_{n-1} + L = ML_n \qquad K_n = \frac{[ML_n]}{[ML_{n-1}][L]}$$

Where n is the maximum coordination number of the metal for the monodentate ligands. The equilibrium constants, K, are called the *stepwise formation constants*. An alternative way of representing these equilibria is:

$$M + L \rightleftharpoons ML_n \qquad \beta_n = \frac{[ML_n]}{[M][L]}$$

Where $\beta_n = K_1K_2K_3.....K_n$ and is called the *overall formation constant* and can also be referred to as the stability constant K_{STAB}. Therefore, K_{STAB} can be written as:

$$K_{STAB} = \frac{[ML]}{[M][L]} \qquad \text{for} \qquad M + L \rightleftharpoons ML$$

K_n normally steadily decreases with an increase in "n". This is simply because there are more ligands available and fewer places available in the coordination shell. This is shown in Table 1.4.

Table 1.4. Stepwise formation constants for ammonia complexes, $M(NH_3)n^{2+}$

Log K_n	Co^{2+}	Ni^{2+}	Cu^{2+}	Zn^{2+}	Cd^{2+}
K_1	2.1	2.8	4.2	2.4	2.65
K_2	1.6	2.2	3.5	2.4	2.10
K_3	1.1	1.7	2.9	2.5	1.44
K_4	0.8	1.2	2.1	2.2	0.93
K_5	0.2	0.8	-0.5		
K_6	-0.6	0.03			

The equation for K_{STAB} only holds true if each of the species present is only in the form stated i.e. M, L and ML. It assumes that all the factors which may affect complex formation, for example, ionic strength, temperature and pH remain constant. Essentially it represents the final equilibrium reached by the reaction of all the metal (in the form M) with all the ligand (in the form L) to form the metal/ligand complex (in the form ML). However, the reactants M and L may exist in several different forms to begin with or change form during the reaction process for example, $M(OH)_x$, MHL, MH_2L etc.. For example, the pH can dramatically alter the concentration of one or several species present. Therefore, K_{STAB} is generally used to refer to a single step in the formation process. Due to this a *conditional stability constant* can be used to measure the extent of complex formation to take into account this situation.

$$K_{COND} = K = \frac{[ML]}{[\Sigma M][\Sigma L]}$$

where [ΣM] is the concentration of the sum of all forms of uncomplexed M present and [ΣL] is the concentration of the sum of all forms of uncomplexed ligand present. Therefore, it can be seen that K_{COND} is not only governed by thermodynamics but also by experimental conditions, eluent pH being the most important as it controls the degree of dissociation of ligands and hence the magnitude of the conditional stability constants and this is why pH is a key factor in controlling separation in chelation ion-exchange chromatography.

These concepts can be explained by the following example which shows the reactions that occur between a metal ion and EDTA and the complexes that are produced. EDTA can exist as one of five different species, these being H_4Y, H_3Y^-, H_2Y^{2-}, HY^{3-} and Y^{4-}

depending upon the pH being used. Figure 1.8 shows the speciation curves of the various species of EDTA [16] and Figure 1.9 the conditional stability constants of various metal/EDTA complexes [16]. From Figure 1.8 we can seen that the pH used will determine which species is the more dominant and therefore dictate the degree of metal-EDTA complex formation i.e. at low pH (<3) the H_4Y species is the most dominant. It is also a non-complexing species and if this is so then the number of metal ions being complexed will decrease as will the K_{MY}'. At a high pH (>10) many metals form stable hydroxy species very readily. This prevents complexation with the EDTA. Therefore, the overall formation constant would have assumed that the EDTA was in its Y^{4-} form and complexing with the free metal ions which is not the case over a wide pH range.

Figure 1.8. Speciation curves for EDTA complexes.

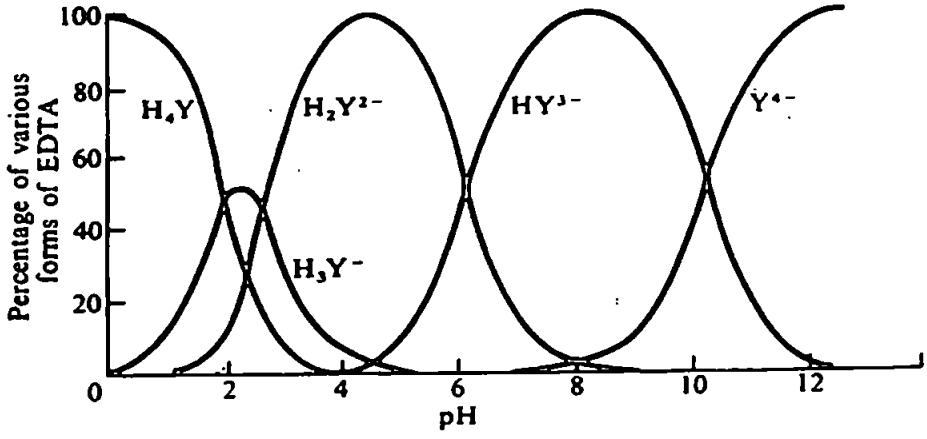

Figure 1.9. Conditional Stability Constants for M-EDTA complexes.

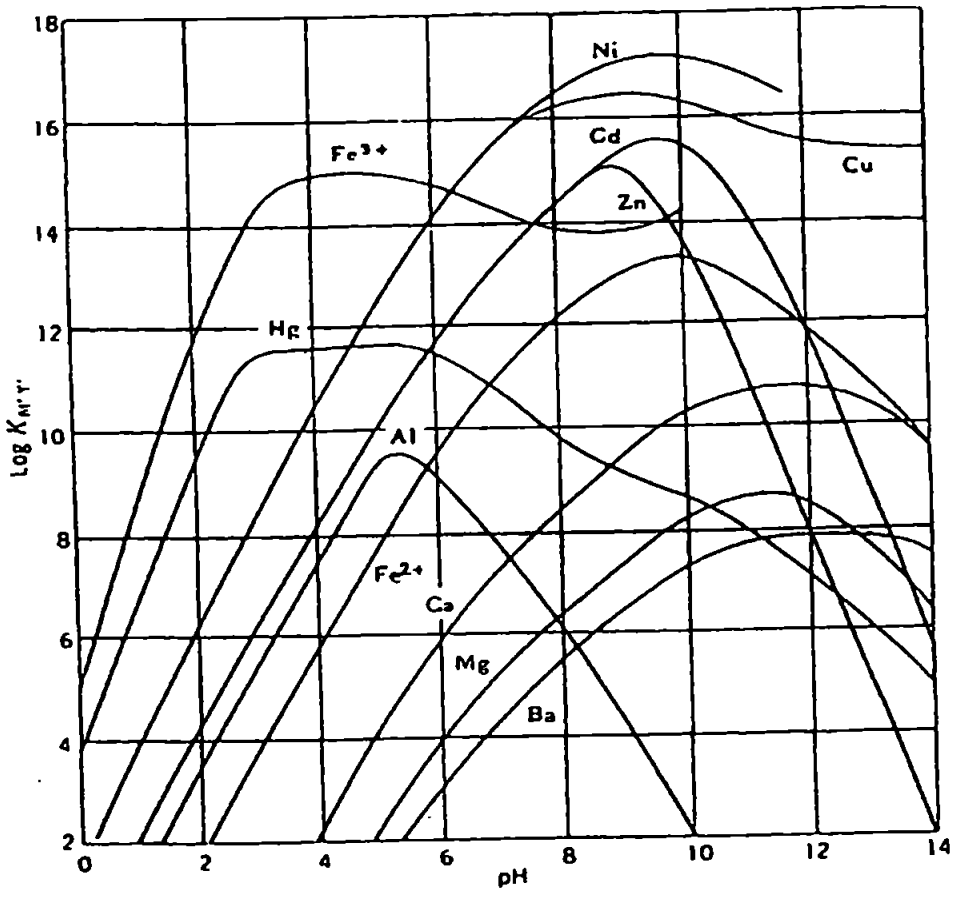

1.4. Ion Chromatography of Trace Metals - A Review.

Over the past 25 years, IC has evolved from the novel technique first described by Small *et al* [8] into a powerful analytical tool for the trace analysis of many organic and inorganic ionic species. A review by Small [20] details many of the advances that have made IC such an important technique for the modern analytical chemist. Over the past 10-12 years a lot of research has been aimed at developing suitable methods for this technique for the determination of various inorganic metal cations, particularly the transition metals, lanthanides and actinides in complex matrices as well as the development of increasingly more sensitive and selective detection systems. This review will discuss 3 principal IC

methods used for trace metal determinations with these methods being simple ion-exchange chromatography, chelation ion chromatography and high performance chelation ion chromatography.

Reviews by Robards *et al* [21] and Sarazanni [22, 23] detail the developments made in the area of inorganic metal speciation analysis, with reviews by Frankenberger *et al* [24] and Buldini *et al* [25] detailing the developments made in the application of this technique to the analysis of metals in complex sample matrices. Haddad *et al* [26] has reported on developments in sample preparation, while Pohl *et al* [27] has reviewed the various parameters that can affect ion selectivity and separation.

1.4.1 Traditional Ion-Exchange Methods.

The Dionex corporation produce a large number of various anion and cation exchange columns. The specifications of the IonPac columns that Dionex market vary considerably, for example, particle size varies from 5-50μm and the percentage of crosslinking varies from 2-55% [28]. An IonPac CS5 column has both sulphonic acid and quaternary ammonium functional groups, which allows for both anion and cation separations to be achieved via a mixed mode mechanism. This column is particularly suited to the separation of transition and lanthanide metals. The CS3 column on the other hand has only sulphonic acid functional groups and is suitable for alkali and alkaline earth metal separations. The CS14 column has carboxylic acid functional groups and is suitable for alkylamines and aromatic amines while the CS12 column has both carboxylic acid and phosphonic acid functional groups and is suitable for inorganic cations, alkylamines and

alkanol amines. These columns and others both from Dionex and other manufacturers have been used for the trace analysis of numerous sample types.

For example, Rahmalan *et al* [29] isocratically separated Cu^{2+}, Ni^{2+}, Zn^{2+}, Co^{2+}, Pb^{2+} and Fe^{2+} in airborne particular matter using an CS2 column with a complexing eluent of oxalic and citric acid. Detection was made with a UV/VIS detector using 4-(2-pyridylazo)resorcinol (PAR) as a post column reagent. The oxalic and citric acids are added as complexing agents so as to enhance the selectivity of the column by eluting the metals as anionic complexes. Ding *et al* [30] used a CS5A column to simultaneously separate and determine Hg(II) with other heavy and transition metals. 2,6-pyridinedicarboxylic acid (PDCA) was used as an eluent complexing agent. This method was based upon work developed by Ruth and Shaw [31]. Similar systems have also been used by Buldini *et al* [32, 33] for the determination of transition metals in edible fats and oils and the analysis of lead-acid battery electrolytes, Lu *et al* [34] for the determination of heavy and transition metals in biochemical samples, Vasconcelos and Gomes [35] for the determination of heavy metals in waters containing strong chelating agents, Janvion *et al* [36] and Cardellicchio *et al* [37, 38, 39] for the determination of transition metals in coastal marine sediments, natural waste and mineral waters. Ding *et al* [40] used a weakly acidic cation exchange column (Tosoh TSKgel Oapak-A) and a PDCA containing eluent for the similtaneous separation of common inorganic anions and cations in rainwater, tap water and snow waters with suppressed conductivity detection.

Several of these studies, for example Buldini *et al* [32] and Cardellicchio *et al* [37] also carried out separations using an oxalic acid containing eluent. This is because PDCA can affect the sensitivity of a post column reaction system. As the metal-oxalate complexes are

less stable than the metal-PDCA complexes they allow the metals to complex more readily with the post column reagent. An oxalic acid containing eluent together with a CS5 column has been used by Bruzzoniti *et al* [41, 42] for the determination of lanthanides, Lane *et al* [43] for the determination of Cu and Zn in blood plasma and by Al-Shawi and Dahl [44] for heavy metal determinations in nitrate/phosphate fertilisers. Bruzzoniti *et al* [45] has also used EDTA to separate various inorganic anions and metal ions on an IonPac AS9 strong anion exchange column.

All the studies reviewed so far have dealt with separations on polymer based resins however, silica based resins have also found extensive use. The main problem with silica based resins is their limited pH range (2-9); however, they do offer a highly effective alternative to polymer based resins within this pH range.

Alimarin *et al* [46] has utilised a silica based sulphonic acid cation exchanger for the concentration, separation and determination of Sc, Zr, Hf and Th. Alkali, alkaline-earth and transition metals were separated by Ohta *et al* [47] on an unmodified silica gel column which is a weakly acidic cation exchanger due to the silanol group on the surface of the silica, with various complexing agents in the eluent being investigated including PDCA, oxalic acid, $CuSO_4$ and ethylenediamine-oxalic acid at pH 5.5. Varying selectivities were found depending upon the complexing agent used. When $CuSO_4$ was used only the alkali metals were separated and the ethylenediamine-oxalic acid eluent produced a highly efficient separation of both the alkaline-earth and transition metals. The alkali and alkaline-earth metals have also been separated by Nair *et al* [48] on polybutadiene-maleic acid coated silica using mineral acid eluents and by Fernandez-Boy *et al* [49] on an identical system for the analysis of drainage waters and soil solutions.

Nesterenko *et al* [50] has determined transition metals using columns packed with silica gel grafted with hexadecyl and octodecyl residues with an eluent containing quinaldic acid as a complexing agent. Schnell *et al* [51] used a polymer coated silica based cation exchanger for the separation of Fe(III), Fe(II) and Mn(II) in environmental samples. Dipicolinic acid was also used by Chen and Adams [52] as an eluent for the separation of Mg(II) and Ca(II) from various inorganic anions in waters on an anion exchange column

The various studies reported in this section highlight some of the limitations of simple ion-exchange methods. These limitations include a lack of sensitivity as well as an intolerence to high ionic strength media. An alternative method that can be used for this type of analysis involves the use of chelating substrates. Over the past 15-20 years however, chelating ion-exchange systems have found increasing use as not only a preconcentration method but also as the separation system for trace metal analysis. There are however few commercially available chelating systems, the most widely used being Chelex-100 (BioRad), though silica based IDA and glass bead IDA can also be found, which has found widespread use for the preconcentration and separation of rare earth and transition metals particularly in sea waters. One of the main problems with this type of column is that it swells quite dramatically, therefore, it is an ongoing process to fabricate new and increasingly more efficient chelating substrates.

Chelating ion-exchangers utilise the chelating properties of numerous organic molecules and can be prepared in one of three ways. Firstly the chelating agent can be covalently bonded to the resin; however, this is a time consuming and complicated method of preparation. The second method is to permanently absorb or impregnate the chelating agent onto the resin. This second method offers a quicker and less complicated preparation

time and the ability to quickly evaluate the capabilities of the new chelating substrate. The third way to fabricate a chelating substrate is to dynamically modify a neutral substrate with a small organic chelating molecule. Reviews by Myasoedova and Savvin [53], Sahni and Reedijk [54] and Torre and Marina [55] report the wide variety of chelating groups that have been studied and their separation capabilities.

1.4.2 Chelation Ion Chromatography (CIC).

Traditionally chelation ion chromatography, where the substrate contains the chelating groups, has been used as a preconcentration method and/or for the separation of groups of metals i.e. to separate the +2 metals from the +3 metals, for trace metal analysis by ion chromatography. In 1990 Siriraks *et al* [56] developed a new system for the analysis of metal cations in complex samples. This method involved a complicated three column system connected via numerous valves. A low efficiency chelating column utilising the IDA functional group (MetPac CC-1) was used to preconcentrate transition and rare earth metals and separate them from alkali and alkaline-earth metals and other interfering matrix components before collection and concentration by a high capacity cation exchange column (TMC-1). Separation was carried out on an analytical ion-exchange column, (an IonPac CS5 column). Siriraks coined the term Chelation Ion Chromatography to describe this system.

Biernat *et al* [57] has investigated the use of silica based chelating systems for trace metal analysis while Kantipuly *et al* [58], Garg *et al* [59] and Liu [60] have carried out detailed studies on polymeric based chelating systems. The system developed by Siriraks has been used extensively over the past 10 years for various applications including the determination

of Cu, Ni, Zn, Co and Mn in seawater as reported by Caprioli and Torcini [61] and the determination of Cd, Co, Cu, Fe, Mn, Ni and Zn in coral skeletons as reported by Shotyk and Immenhauser-Potthast [62]. Lu *et al* [63, 64, 65] have used this system extensively for the determination of heavy metals in drinking water and for lanthanide determinations in various complex environmental and agricultural matrices. All of these studies used post column detection with PAR at a wavelength of 520nm.

Laikhtman *et al* [66] used a similar system for the study of Mg and Ca in brines though differed in that a CS12A analytical column was used instead of a CS5 column along with suppressed conductivity detection instead of post column derivitisation with PAR. Motellier *et al* [67] again used a similar system (a CS5A guard column was used instead of a TMC-1 column) for ultra-trace level transition metal determination in waters while Cardellicchio *et al* [68] used a dual column system for Cd and Pb in seawaters using differential-pulse anadic stripping voltammetry as the detection method. γ-aminobutyrohydroxamate resins were used as a preconcentration column along with a CS5 analytical column by Liu *et al* [69, 70] for the determination of lanthanides in seawater and transition metals in oyster tissue. PAR-ZnEDTA and PAR were used as post column reagents respectively. Kolpachnikova *et al* [71] have carried out studies on the effect of temperature on the retention of alkali and alkaline-earth metals using aminocarboxylic acids bonded to silica. Perchloric acid was used as an eluent with lysine, glutamic acid and iminodiacetic acids (IDA) used as the functional groups.

Abollino *et al* [72] investigated the retention of Cd(II), Pb(II) and Cu(II) on a three column system which utilised an anion exchange column, a reversed phase column and a chelating exchange column (Chelex-100) for their determination in seawaters. A Kelex-100 liquid

ion-exchanger was immobilised onto XAD-7 and Bondapack C-18 columns by Ferrarello *et al* [73] for the preconcentration of selected transition metals in seawaters. Warnken *et al* [74] used a Toyopearl AF-Chelate 650M IDA chelating resin for the preconcentration of Mn(II), Ni(II), Cu(II), Cd(II) and Pb(II) whilst Inagaki *et al* [75] used a Chelex-100 column to preconcentrate protein binding Zn and Cu in human blood as well as preconcentrating the rare earth elements in human blood serum [76]. A Metpac CC-1 column was utilised by Bloxham *et al* [77] for the preconcentration of Mn(II), Co(II), Cu(II), Zn(II) and Pb(II) in seawaters. Detection in the studies discussed in references Abollino – Bloxham was carried out using ICP-MS.

Kumar *et al* [78] used XAD-2 resin functionalised with *o*-aminophenol for the preconcentration of Co(II), Cd(II), Ni(II), Zn(II) and Pb(II) in well waters prior to detection by FAAS as well as XAD-2 functionalised with Tiron [79] for the preconcentration of selected transition metals and UO_2^{2+} before detection by FAAS. This method was used for UO_2^{2+} determinations in well waters and Co(II) determinations in pharmaceutical vitamin tablets. Bag *et al* [80] employed the imobilisation of Escherichia coli on sepiolite for the preconcentration of Cu(II), Zn(II), Fe(III), Ni(II) and Cd(II) in reference materials with Bagheri *et al* [81] using activated charcoal loaded with α-diphenylglyoxine for the preconcentration of Ni(II) from water samples before detection by AAS. Prado *et al* [82] used silica gel functionalised with the herbicide 2,4-dichlorophenoxyacetic acid for the preconcentration of Cu(II), Ni(II), Zn(II) and Cd(II) from both aqueous and ethanolic solutions before determination by ICP-AES.

Lee *et al* [83] used XAD-16 resin loaded with 4-(2-thiazoylazo)resorcinol (TAR) to study the sorption behaviour of thirteen metal ions including Cu(II), U(VI), Pb(II) and La(III).

Shah *et al* [84] used a dithizone containing poly(vinylpyridine) resin for the preconcentration and separation of Cu(II), Ni(II) and Zn(II) while a methacrylate-DVB copolymer with mercapto chelating groups was used by Maeda *et al* [85] for the sorption of Ag^{+}, Hg^{2+}, Cu^{2+}, Pb^{2+} and Cd^{2+} with a particularly high affinity for Ag^{+} and Hg^{2+}. Ahuja *et al* [86] has studied the use of hydroxamic acids as the chelating functional group on PS-DVB resins. Various hydroxamates including glycine and malonic hydroxamate were investigated with a greater selectivity found for the transition and high charged metals than for the alkaline-earth metals. Das *et al* [87] have reported the use of a PS-DVB resin with benzimidazolylazo functional groups. This chelating column was found to have no affinity at all for the alkali and alkaline-earth metals though was highly selective for Hg(II), Ag(I) and Pd(II). Inoue *et al* [88] chemically modified chitosan by immobilising EDTA and DTPA onto the polymer matrix while Chwastowska *et al* [89] used Bio-Rads SM-7 resin loaded with a 2-mercaptobenzothiazole for the preconcentration and separation of inorganic and alkyl mercury from natural waters. De Vito *et al* [90] investigated the use of a XAD-7 resin loaded with thorin as the chelating functionality for the preconcentration and separation of rare-earth elements including Sm(III), Eu(III) and Gd(III) whereas Dev *et al* [91] reported the use of a XAD-4 resin functionalised with bicine ligands for the analysis of La(III), Nd(III), Tb(III), Th(IV) and U(VI).

Glennon and Srijaranai [92] used hydroxamic acids immobilised on silica as a preconcentrating substrate while Ryan *et al* [93] used silica coated with carboxymethyl and hydroxamate dextrans for the online preconcentration of selected transition and heavy metals in aqueous environmental samples including tap and riverine waters. Separations were carried out on a Dionex CS5 analytical column. Hutchinson *et al* [94] used

calixarenes immobilised on silica and polymeric resins for the preconcentration and extraction of transition and heavy metals.

This review of CIC spotlights the main problem with the capabilities of this method i.e. it is suitable only for the preconcentration of metals before separation with traditional cation-exchange chromatography therefore increasing the complexity of the analytical system. The way to overcome this is to use a high efficiency substrate for the fabrication of the chelating system.

1.4.3 High Performance Chelation Ion Chromatography (HPCIC).

The difference between CIC and HPCIC is that with HPCIC both selective preconcentration and efficient analytical separations of various metals can be obtained on a single chelating column rather than preconcentration on a chelating column followed by separation on one or two cation-exchange columns as for CIC. One of the most useful functional groups used in chelation ion chromatography is the iminodiacetic acid (IDA) group, $[-N(CH_2COOH)_2]$ due to its reasonably fast kinetics, as well as selectivity coefficients that are not too large. Table 1.5 illustrates the similarity in the stability constants for selected metal ions with this ligand.

Bonn *et al* [96] used an IDA bonded silica based substrate to selectively separate transition metals in alkali and alkaline-earth rich sample matrices such as sea water. Nesterenko and Jones [97] has shown the effect of the substrate on the IDA functional group's chelating capabilities. A study by Yebra-Biurrum *et al* [98] shows the selectivity of a poly(aminophosphonic) acid chelating resin for transition metals over the alkali metals

Table 1.5. Log equilibrium constants of selected metal complexes with iminodiacetate 0.1M ionic strength [95].

M^{n+}	K_1	M^{n+}	K_1
Pb^{2+}	7.45	UO_2^{2+}	8.93
Ni^{2+}	8.19	Fe^{3+}	10.72
Zn^{2+}	7.27	In^{3+}	9.54
Co^{2+}	6.97	Al^{3+}	8.10
Cd^{2+}	5.73	La^{3+}	5.88
Cu^{2+}	10.63	Th^{4+}	10.66

over a pH range of 1-14. Nesterenko *et al* [99] has separated seven alkaline-earth and transition metals using silica chemically modified with aminophosphonic acid. Eluents used for this study were mineral acids over the pH range 2.5-7. Nesterenko has also used aminophosphonate functionalised silica to isocratically separate 8 transition and heavy metals [100] while Shaw *et al* [101] used this substrate for trace Be determinations in certified stream sediments. Merly *et al* [102] have used a different approach in the use of a porous graphitic carbon column for the separation of various transition metals. Again oxalic acid is used as a complexing agent in the eluent to enhance the selectivity. Elefterov *et al* [103] used an eluent containing dipicolinic acid for the separation of transition metals on an IDA bonded silica column as well as for the determination of alkali and alkaline-earth metals in drinking water and mineral water samples [104]. Voloschik *et al* [105] has used IDA bonded silica for Be determinations in rock and waste waters with Nesterenko and Jones [106, 107] performed the first ever isocratic separation of 14 Lanthanides and Yttrium using IDA bonded silica as well as investigating the effect of a variety of mineral acids on the retention of selected alkaline-earth and transition metals [108]. Bashir *et al*

has also used IDA bonded silica for trace alkaline-earth metal determinations in brines [109] and Be in waste waters [110].

This review shows the potential of HPCIC for trace metal analysis in complex environmental matrices without the need for complicated sample preparation procedures. Also the lack of sensitivity towards high ionic strength media shows how useful this technique is for seawaters, highly mineralised waters etc.. Many HPCIC columns are fabricated by the impregnation of a neutral substrate with chelating dyes, therefore a detailed review of dye impregnated systems is given in Chapter 2.

1.5 Detection of Metal Ions.

The ability to selectively separate trace metals in complex samples is without use if these metal ions cannot be detected. There are various techniques which can be employed to detect metals in ion chromatography and these techniques can be separated into two distinct groups, those being **electrochemical** and **spectroscopic** methods of detection.

Electrochemical methods of detection include *suppressed conductivity* as used by Jenson *et al* [111] when separating alkali and alkaline-earth metals on a CS12 cation exchanger and *non-suppressed conductivity* detection. *amperometric* and *potentiometric* detection while spectroscopic methods include *direct/indirect UV/VIS. Fluorescence* detection was used by Jones and Paull [112] when studying Al speciation in potable waters while a *chemiluminescence* method of detection was used by Beere and Jones [2] to detect Cr(III) and Cr(VI) species in aqueous samples.

Atomic spectrometry and mass spectrometry have also been used as detection techniques in hybrid systems, for example, by Truscott *et al* [113]. These methods while offering exceptional sensitivity are much more complicated and expensive when compared to other techniques.

The method of detection used for the studies reported in this thesis is a direct UV/VIS method. This method involves a post column complexation reaction between the eluted metal ions and a chelating agent that contains a chromophore which strongly absorbs in the visible region of the spectrum. Chelating agents suitable for this reaction include heterocyclic azo and triphenylmethane based dyes such as 4,2-(pyridylazo)resorcinol (PAR), Xylenol Orange (XO), Pyrocatechol Violet (PCV), Arsenazo III (AIII) and Metylthymol Blue (MTB), the structures of which are shown in Figure 1.10. This method of detection is probably the most common method used when dealing with trace metal analysis by ion chromatography and will be discussed in more detail in Chapter 3.

Reviews by Haddad [114], Rocklin [115] and Buchberger and Haddad [116] as well as book chapters by Fritz and Gjerde [13] and Weiss [12] discuss all of the above methods.

1.6 Aims and Objectives.

To date, research into the development of HPCIC as a viable and widespread technique for trace metal analysis has concentrated on the impregnation of both low and high efficiency substrates with chelating dyestuffs. Initial studies will investigate new substrates for impregnation with various dyestuffs and the subsequent effect of the ligating atoms on the retention of selected alkali-alkaline earth, transition and heavy metal ions as a function of

1.

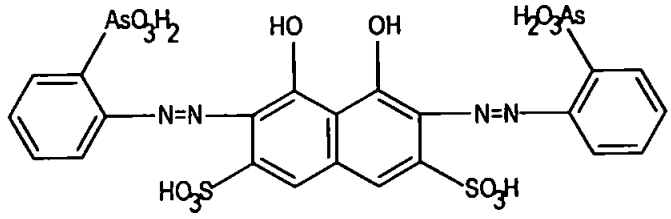

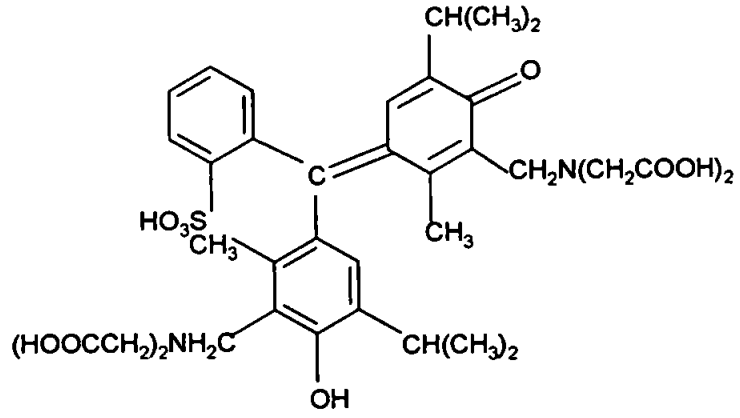

2.

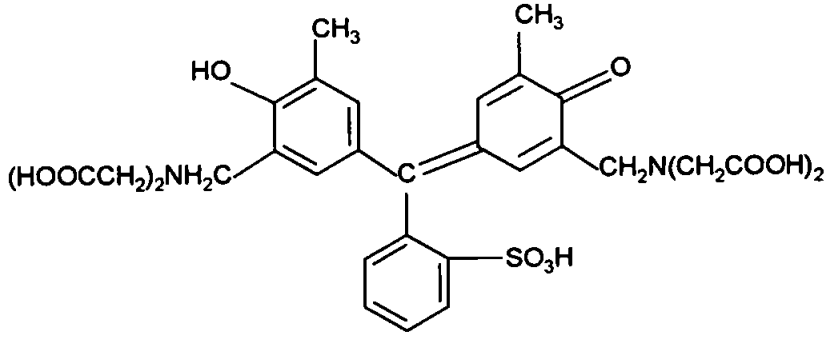

3.

4.

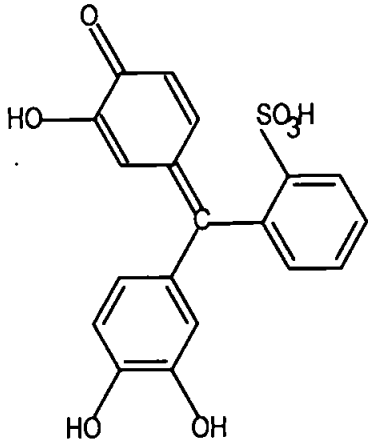

5.

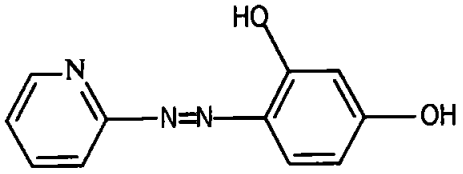

Figure 1.10. A selection of chromogenic reagents used to detect metal ions. 1: Arsenazo III, 2: Methylthymol Blue, 3: Xylenol Orange, 4: Pyrocatechol Violet and 5: 4-(2-pyridylazo)resorcinol.

pH with the construction of k' plots. A new impregnation method based upon ultrasonic agitation will also be developed with the aim of producing columns with more even dye coatings and greater dye loadings as well as reducing the time taken to fabricate these columns.

Investigations of dynamically modified substrates will also be carried out. This will entail dynamically modifying various neutral polystyrene based substrates of standard crosslinking and small particle size as well as the hypercrosslinked polystyrene based resin MN200. Small organic chelating molecules including dipicolinic acid, 2- and 4-chloromandelic acid and 4-chlorophenylalanine will be used to dynamically modify the substrates. This study will investigate the effect of these dynamically loaded molecules on the retention of selected alkali-alkaline earth, transition, heavy and high valency metals as a function of pH using k' plots. Other factors to be studied include the ligand concentration in the mobile phase, sample pH and the characteristics of the substrates and their effect on metal ion selectivity and retention.

The post column detection systems will also be studied with the aim of improving the sensitivity of the post column reagents used towards the metal ions (for example, the response of Cd with the PAR post column reagent). This will involve the study of new buffer systems including a disodium tetraborate based buffer for the PAR post column reagent, the possible use of biological buffers such as cyclohexylaminopropan sulphonic acid (CAPS) and the optimisation of the UV/VIS spectrometer's settings. Other factors such as eluent cleanup procedures, PCR parameters including pH, concentration and gradient elution programs will also be investigated. A newly developed noise reduction system will also be studied and applied to an optimised system with the aim of improving

signal-to-noise ratios and thereby lowering the limits of detection and producing a chromatographic system suitable for "real" sample analysis.

Finally, the most effective dye impregnated and/or dynamically modified HPCIC systems obtained will be applied to the analysis of trace metals in various complex samples. These samples will include high ionic strength media such as mineral and seawater samples and CRMs as well as complex environmental samples such as soil and sediment certified reference materials.

Chapter 2:- Development of Dye Impregnated HPCIC Substrates.

2.1 Introduction.

A chelating substrate can be prepared, as previously discussed in Chapter 1.4.1, in one of three ways. The simplest way to do this is to impregnate a neutral substrate with a chelating dyestuff. These dyestuffs, generally aromatic in nature, can be readily adsorbed onto polymeric substrates by exploiting π-π interactions between the aromatic groups of both the dyestuff and PS-DVB backbone as well as becoming entrapped within the pore structure of the substrate. These chelating dyestuffs have found widespread use in not only the preconcentration but also analytical separations of metal ions in various media. This use is generally dependent upon the type of substrate that is impregnated. The impregnation of substrates of large particle size are commonly used for preconcentration or batch extraction procedures due to the lower efficiency that they offer, whilst for HPCIC, high efficiency sorbents of small particle size are required for the single column separation of individual metal ions. Studies by Challenger [117], Sutton [118], Paull [119] and Shaw [120] have investigated many aspects of dye impregnated substrates.

2.1.1 Dye Impregnated Low Efficiency Substrates.

One of the most widely used dyestuffs for the impregnation method is Xylenol Orange (XO), the structure of which is shown in Figure 1.10. XO is a sulphonephthalein based dye with two IDA groups which is able to chelate with metals through a nitrogen and two oxygen atoms (N, O, O chelation). When impregnated onto a support of large particle size, a chelating substrate that is suitable for the selective preconcentration of groups of metal

ions is the result. To give some idea of the range of chelating dyestuffs employed, the following section reviews selected studies carried out using dye impregnated low efficiency columns for the preconcentration of metals only. This will be followed by a review of high efficiency dye impregnated substrates which is closely related to the work carried out here.

Brajter and Olbrych-Sleszynska [121] used a strong base anion exchange resin (Amberlite A-26) loaded with XO to selectively separate divalent and trivalent metal groups before detection by atomic absorption spectrometry (AAS). This method was used for the analysis of gallium-indium alloys. Handley *et al* [122, 123] used a Dowex1-X8 anion exchange column loaded with XO as a preconcentration column for Al(III), Ba(II), Ca(II), Mg(II), Sr(II) and Zn(II) in concentrated brine solutions before separation on a strong cation exchange resin (Benson BC-X10) for the on-line monitoring of Chlor-alkali process streams. Singh *et al* [124] used Dowex-2 anion exchange resin loaded with XO as a preconcentration column for Cu(II) and Cd(II) before analysis by flame AAS. Singh also investigated another sulphonephthalein dye, pyrocatechol violet (PCV) along with XO in this study. PCV (Figure 1.10) is an oxygen only chelator (O, O) and binds with metals via it's two hydroxyl groups. As this molecule only contains oxygen donor atoms it is a weaker acid than XO and therefore has a stronger conjugate base it forms stronger complexes. However, as a high pH is required for dissociation of the hydroxyl groups many oxygen chelators including PCV form weaker complexes than nitrogen containing chelators in lower pH media. Saxena *et al* [125] and Brajter *et al* [126] have also used PCV loaded onto Amberlite XAD-2 resin for the preconcentration and separation of metals including Zn(II), Ni(II) and Pb(II) in waters with detection by flame AAS and GF-AAS

along with Tewari *et al* [127] who preconcentrated Cd(II), Co(II), Cu(II), Fe(III), Ni(II) and Zn(II) in tap and river waters before determination by FAAS.

Chrome-Azurol S (CAS) (Figure 2.2) is another sulphonephthalein dye which chelates through oxygen atoms from both carboxyl and hydroxyl functional groups. CAS is even more weakly chelating than PCV due to the carboxylic acid being more acidic and therefore a weaker conjugate base than the phenol groups. CAS has been used used by Molodovan *et al* [128], loaded onto the strongly basic anion exchanger 2X4 as a preconcentration and separation system for various di, tri and tetravalent metals. Detection was made by ICP-AES while Almeida *et al* [129] used a Nova-Pak C_{18} guard column loaded with CAS as a preconcentration column with the separation of various transition metals carried out on a Nova-Pak C_{18} column with detection by post column derivatisation with 4-(2-pyridylazo)resorcinol (PAR) at 520nm.

PAR can also be used to impregnate resins. In fact, various azo dyes (Figures 1.10 and 2.1) such as PAR, 1-(2-pyridylazo)-2-napthol (PAN), 4-(2-thaizolylazo)resorcinol (TAR), 1-(2-thiasolylazo)-2-napthol (TAN) and Calmagite have all been used for substrate impregnation. Brajter and Olbrych-Sleszynska [130] used XAD-2 loaded with PAR to separate various transition metals as well as the selective extraction of Ag(I) from copper ores using flame AAS. Morosanova *et al* [131] investigated various triphenyl methane and azo based dyestuffs including XO, PAR and PAN for transition metal analysis in waters and foodstuffs using a silica based substrate with flame AAS used for detection. XAD-2 resin loaded with PAN and Calmagite was used by Ferreira *et al* [132, 133] for alkali, alkaline-earth and transition metal

1.

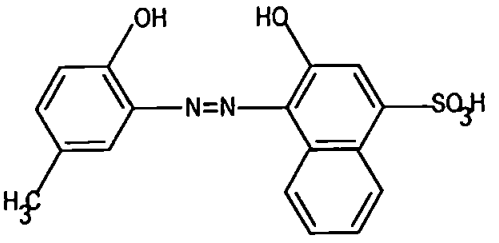

2.

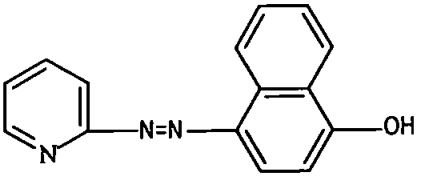

3.

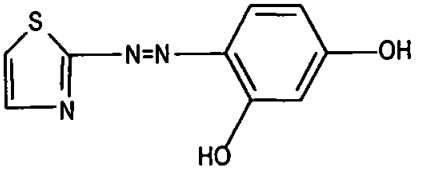

Figure 2.1. Structures of dye molecules used for the preconcentration and separation of metal ions: 1. Calmagite; 2. 1-(2-pyridylazo)-2-napthol; 3. 4-(2-thiazolylazo)resorcinol.

1.

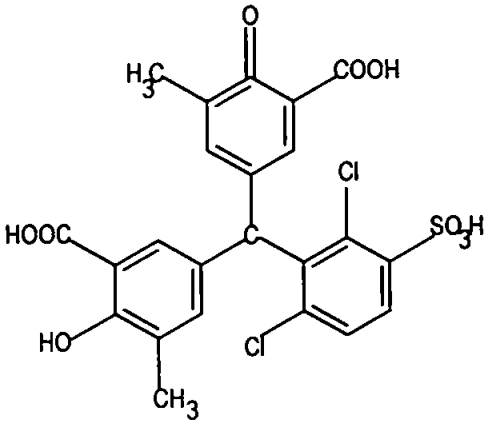

2.

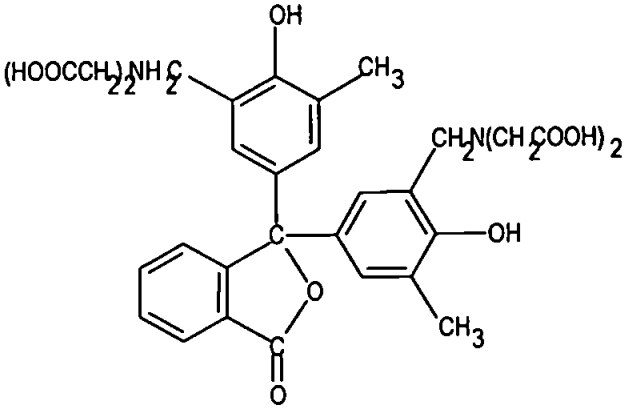

3.

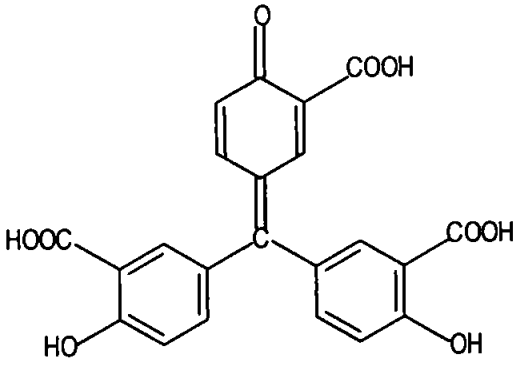

Figure 2.2. Structures of dye molecules used for the preconcentration and separation of metal ions: 1. Chrome Azurol S ,2. *O*-Cresolphthalein Complexone or Pthalein Purple and 3. Aurine Tricarboxylic Acid (ATA).

determinations with emphasis on Cu(II) in natural waters (with flame AAS detection) and Ni(II) alkaline and table salts (with ICP-AES detection).

Sutton *et al* [134] investigated different substrates for impregnation including highly cross-linked PS-DVB substrates such as Amberlite IRA 904 (a strong basic anion exchanger), XAD-2 (a neutral resin) and Purolite MN100 (a weakly basic anion exchanger) and MN200 (a neutral macronet resin) both of which showed higher capacities and better performance than the other PS-DVB resins. A cellulose based column impregnated with Procion Violet P-3R was also investigated.

Cornejo-Ponce *et al* [135] used silica gel loaded with PAN with detection by energy dispersive X-ray fluorescence for the preconcentration of rare earth metals while a resin loaded with TAR was used by Lee *et al* [136] to separate various transition and rare earth metals. Silica gel was loaded with TAN was used by Zaporozhets *et al* [137] for Cu(II) and Zn(II) determinations in natural and tap waters whilst Saxena *et al* [138] used XAD-2 loaded with Alizarin Red-S for the preconcentration of Pb(II), Cd(II), Zn(II) and Ni(II) in well waters before detection by flame AAS.

2.1.2 High Performance Dye Impregnated Substrates

So far only low efficiency chelating systems have been reviewed. However, dye impregnation of high efficiency substrates has also been widely investigated. The use of high efficiency dye impregnated substrates allows for not only the preconcentration but also analytical separations of metal ions on a single chelating column and is the main focus of attention in this work.

One of the first to exploit this technique was Jones *et al* [139] who used a 10μm HPLC grade neutral polystyrene resin coated with CAS to separate both divalent and trivalent metals. Jones reported that while pH produced a major affect on metal retention, the ionic strength did not. Challenger *et al* [140, 141, 142] continued these studies with a comparison of CAS, Calmagite and XO immobilised on resins of both large and small particle size that were either neutral or anion exchangers. A commercially available column, TOSOH TSK-GEL Chelate-5PW was also used in the comparison. Various alkaline-earth and transition metals in high ionic strength matrices such as brines and seawaters, were separated on these high efficiency chelating resins. Jones *et al* [143] also used an 8.8μm PS-DVB resin (DIONEX) coated with methylthymol blue (MTB) for barium and strontium determinations in mineral waters and coated with o-cresolphthaleine complexone also known as phtalein purple (PP) for strontium determinations in milk powder. With an eluent of 1M KNO_3 to suppress any ion-exchange processes that may occur, the selectivity of the chelating columns resulted in a reversed elution order for the alkaline-earth metals thereby allowing trace levels of strontium to be determined in the presence of large concentrations of Ca.

A comparitive study of ten different chelating dyes was carried out by Paull *et al* [144]. The results of this study showed that triphenylmethane based dyes that contained the IDA functionality offered the most stable and effective chelating system. Paull also reported the use of a XO impregnated column for the transition metal analysis of seawater [145], a MTB impregnated column for alkaline-earth metal determinations in oil well brines [146] and trace uranyl ion in saline samples [147]. Su and Huang [148] used a C_{18} bonded silica gel loaded with either PAR or 2-(2pyridylazo)-5-dimethylaminophenol for Cd determinations in seawaters. Zolotov *et al* [149] immobilised XO, PAN and (*p*-

sulfonphenylazo)-2'-sulpfo-4'-nitrodiazozminobenzene disodium salt (Cadion) on reverse phase silica substrates and hydrophobic capillary tubes for the similtaneous detection of 2 metals (Cu(II) and Co(II), Co(II) and Fe(III), Fe(III) and Zn(II), Mn(II) and Pb(II)) with flow spectrophotometric detection.

2.1.3 Dyes in the Mobile Phase.

Another way of utilising the chelating characteristics of these metallochromic ligands is to have them present in the mobile phase. This results in a dynamic dye coating on the substrate with an equilibrium being established between the dye adsorbed onto the substrate and that which remains in the mobile phase. This dynamic loading offers certain advantages over pre-coated substrates including greater capacities, improved separations, different selectivities and the ability to exploit the dye for the visible detection of the metal ions thereby simplifying the instrumentation required. One possible disadvantage of dynamically modified substrates is that complex samples may disturb the equilibrium that exists between the substrate and the mobile phase and thereby cause leaching of the dynamically sorbed layer which would in turn affect the baseline of any chromatogram obtained. However, few studies have been carried out which utilise these dynamically loaded dye systems.

DiNunzio *et al* [150] used a C_{18} silica column with an eluent that contained 0.1mM PAR for transition metal analysis while Walker [151] investigated both polymer and silica based substrates with an eluent containing Thymol Blue for the analysis of both organic and inorganic cations. Toei has extensively studied the use of metallochromic ligands in the mobile phase. Using an eluent containing 1mM PP, the alkaline-earth metals were

separated under a gradient on a carboxylic cation exchange column [152] while Ca(II) and Mg(II) were determined in seawater [153] using an IDA cation exchange column (TOSOH) with an eluent containing 0.1mM PP. This system was also used for Mg(II) and Ca(II) determinations in clinical samples [154]. Using an anion exchange column Toei also separated Ni(II) and Zn(II) using an eluent containing XO [155].

Paull *et al* has also carried out extensive studies in this area. Using a porous graphitic carbon column with an eluent containing PP, Ca(II) and Mg(II) determinations were carried out in seawater [156] and other environmental waters including saturated saline Antarctic lake samples [157]. Transition metals [158] were determined using a 5μm PS-DVB PRP-1 column (Hamilton) dynamically modified with MTB and the alkaline-earth metals using a PRP-1 column dynamically modified with PP [159] was applied to saturated brine samples. Various divalent and trivalent metals were determined on an ODS reversed phase column dynamically modified with MTB [160] and a review paper which compares pre-coated and dynamically coated chelating columns for metal ion separations is given by Paull and Haddad [161]. The dynamic loading of substrates with low molecular weight chelating molecules is a special case and is discussed in Chapter 4.

2.1.4 Aims of this Study.

The aim of this study is to fabricate a range of dye impregnated HPCIC columns which utilise the chelating properties of two triphenylmethane based dyestuffs, namely Xylenol Orange (XO) a N, O, O chelator and Aurin Tricarboxylic Acid (ATA) a O, O chelator. The development of these two columns and their subsequent application to the analysis of selected transition and heavy metals in highly mineralised waters is discussed in the

following pages. An improved dye impregnation procedure employing ultrasonic agitation to effect impregnation rather than continuous flow will also be developed with the aim of not only improving dye loadings but also reducing the time required to fabricate these columns.

2.2 Experimental

2.2.1 Instrumentation

The basic instrumentation used throughout the investigations presented in this work is shown schematically in Figure 2.3 and consists of a Dionex gradient pump module (Dionex, Sunnyvale, CA, USA), a six port PEEK injection valve (model number 9010, Rheodyne, Cutati, CA, USA) and a 100µl or 500µl PEEK sample loop. The post column detection system consisted of a Dionex IP20 isocratic pump (Dionex, Sunnyvale, CA, USA) to deliver the post column reagent (PCR) which was mixed with the eluent in a zero dead volume PEEK low pressure Tee followed by a 2m teflon reaction coil (0.5mm ID). Detection was made with a Shimadzu SPD-10AVvp UV/VIS detector (Shimadzu Corporation, Kyoto, Japan) connected via a Dionex Advanced Computer Interface to a computer which utilises the Dionex AI450 chromatographic software.

2.2.2 Reagents.

All reagents used for these investigations were obtained from BDH and of AnalaR grade unless otherwise stated. The eluent used for these studies consisted of either a 1M or 0.1M KNO_3 solution which contained 50mM acetic acid and was prepared in distilled deionised

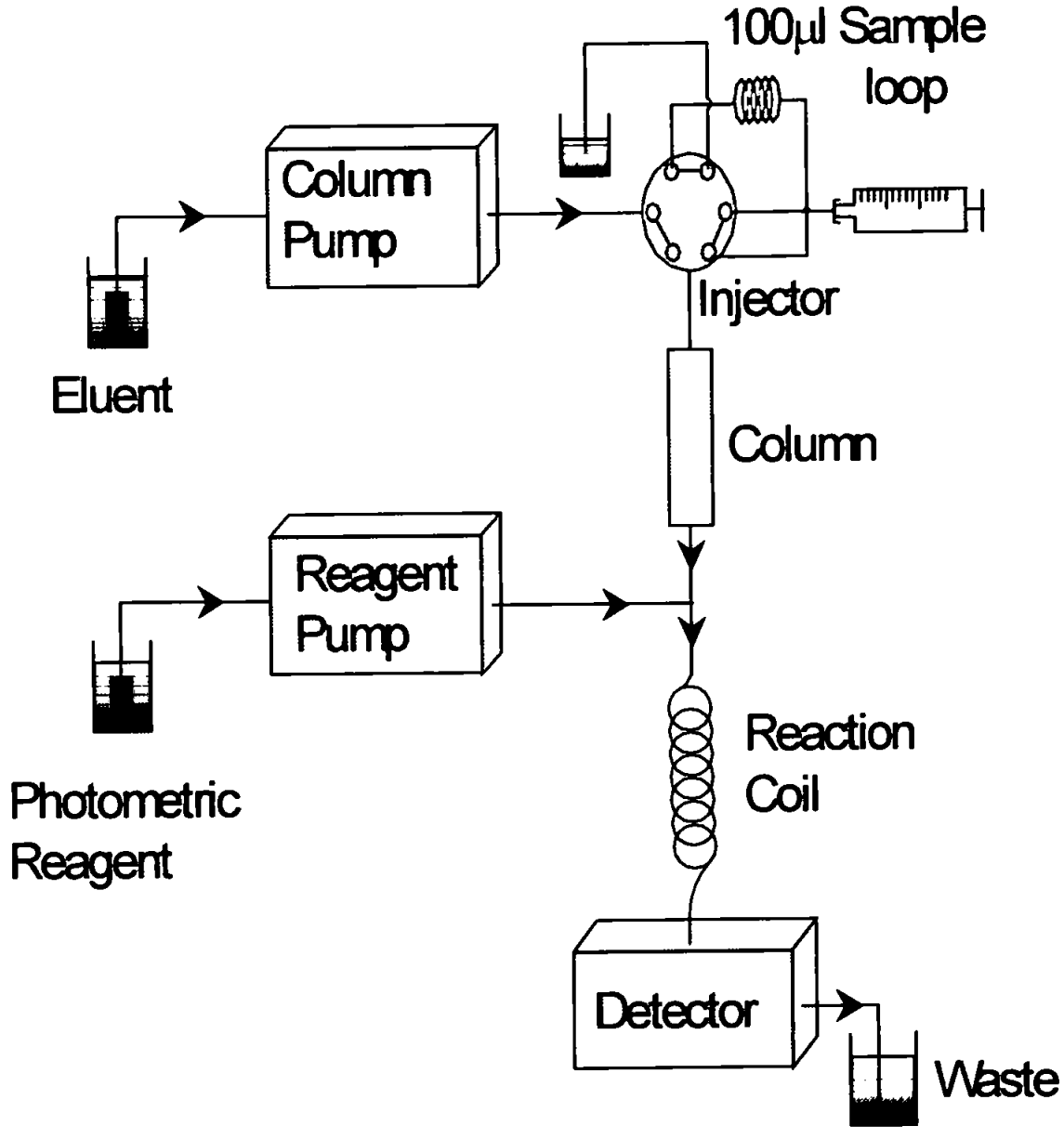

Figure 2.3. Schematic representation of HPCIC instrumentation used.

water (MilliQ, Millipore, Milford, MA, USA). The eluent was then filtered through 0.45μm, 47mm cellulose acetate filters and degassed before pH adjustment with either conc HNO_3, conc NH_3 or 5M NaOH. The PCR used was 4-(2-pyridylazo) resorcinol (PAR) from Fluka (Glossop, UK) and prepared in one of two ways.

PAR/NH_3 System:- 0.12mM PAR buffered to pH 10.2 with 2.6M NH_4OH and 0.85M NH_4NO_3 (30mls of 4mM PAR stock, 192mls of 35% NH_3, 54mls of 69% HNO_3 made up to 1 litre with MilliQ water).

PAR/Borate System:- 0.1mM PAR with 0.125M di-sodium tetraborate made up to 1litre with MilliQ water and adjusted to pH 10.5 with 5M NaOH.

More details of these systems are given in Chapter 3.

Detection of the metal ions was carried out at a wavelength of 490 or 520nm. A compensating wavelength of 445nm was employed when the noise reduction system was used. This system will be discussed in detail in Chapter 3. Both the eluent and PCR were delivered at a rate of $1 ml min^{-1}$. Metal standard solutions were prepared from $1000 mg l^{-1}$ Spectrosol stock solutions (BDH) and prepared in either dilute nitric acid or the eluent and were stored in poly (propylene) bottles.

2.2.3 Dyestuffs Studied.

For this study two different chelating dyestuffs were used for column impregnation, these being, Xylenol Orange (XO) and Aurin Tricarboxylic Acid (ATA). Both of these dyestuffs are triphenylmethane based dyes and are shown in their free acid forms in Figures 1.10 and

2.2. XO is one of the most widely used dyes for column impregnation due to its ability to chelate with a wide variety of metals over a pH range of 0-6. It contains two IDA functional groups and offers N, O, O chelation whereas ATA contains salicylic acid functional groups and offers O, O chelation. The triammonium salt of ATA is called "Aluminon" and has been used as a spectrophotometric reagent for the determination of Al(III) [162]. Table 2.1 shows the log stability constants of selected metal ions with ATA.

Table 2.1. Log equilibrium constants of metal complexes with ATA [95] (0.1M Ionic strength)

M^{n+}	K_1
Be^{2+}	5.38
Cu^{2+}	4.1
Fe^{3+}	4.68
Th^{4+}	5.04
UO_2^{2+}	4.77

The post column reagent (PCR) used is 4-(2-pyridylazo) resorcinol (PAR) which is shown in Figure 1.10. PAR is a heterocyclic azo dye which has found extensive use as a PCR particularly when looking at transition and heavy metals. It can complex with a large number of metals over a wide pH range with the complexation occuring through both the pyridyl and azo nitogen atoms and the hydroxyl oxygen thereby offering N, N, O chelation.

2.3 Procedures.

2.3.1 Column Preparation.

Two methods were used to impregnate the substrate with the dyestuff. Initial studies used a continuous flow impregnation procedure, whilst later studies utilised impregnation by ultrasonic agitation.

2.3.1.1 Continuous Flow Impregnation Method.

This method involved the continuous recycling of a dye solution through a column pre-packed with bare resin over a twenty four hour period at a rate of 1ml min^{-1}. 100ml of a 0.2% dye solution in 10% methanol at pH 5 was used. Previous studies [119] have shown that pH 5 was the optimum impregnation pH for triphenylmethane based dyestuffs using this method. Once loaded, the column was then conditioned by alternatively pumping 0.1M HNO_3, MilliQ water and 0.1M NH_3 through the column until all the loosely retained dye had been washed off the column. The dye washings were then collected for analysis by UV/VIS spectrometry to calculate the dye loading as detailed in Chapter 2.3.4.1.

2.3.1.2 Sonication Impregnation Method.

The method involving ultrasonic agitation entailed impregnation of the bare substrate before packing the substrate into the column rather than impregnating the substrate after packing. For a 10cm column approximately 1g of substrate is sonicated in 100ml of a 0.2% dye solution in 10% aqueous methanol. The pH was adjusted to pH 3 when using XO and pH 4 when using ATA. The substrate is then sonicated at room temperature (20-

30°C) in this dye solution for approximately ten hours then left to stand over night. The dye solution is decanted then the remaining resin centrifuged down till a volume of 15-20ml is obtained. This slurry is then packed into the column as detailed in section 2.3.2. The packed column is then conditioned using the same procedure as for the continuous flow impregnation procedure.

2.3.2 Column Packing.

The columns used for this study were 100mm or 250mm x 4.6mm internal diameter (ID) PEEK columns supplied by Alltech. Before packing, the column, frits and endcaps are all sonicated in a 40:60 Methanol:MilliQ solution for approximately one hour. The column is then connected to the column packer (Shandon Southern Products Ltd, Cheshire, UK). The reservoir is filled with the substrate in a slurry of 15-20ml of 30% methanol and topped up with the eluent to be used. The substrate is then pumped into the column at a pressure of 2000psi using an eluent of 5-10% methanol for approximately one hour. If the substrate has been pre-impregnated then the reservoir is topped up with the original dye solution, the remainder of which is used as the eluent followed by MilliQ water for one hour or until no more bleeding is observed.

2.3.3 Clean-up Columns.

Due to the very nature of chelating columns, it is not only the metals of interest in the sample that are retained but also any metals present in the eluent that is being used. This is not a problem under isocratic conditions, but when using gradient elution programs, large contaminant peaks are often found to be eluted off and often mask the sample peaks of

interest. The eluent used during these investigations contained KNO_3 which had relatively high levels of metal contaminants particularly Zn(II) and Cu(II). To combat this problem it was decided to clean up the eluent before use. This entailed pumping the eluent through a column, which had been impregnated with the same chelating dye as would be used for the analytical separation. The eluent was adjusted to approximately pH 9 so as to ensure that the transition metals were strongly adsorbed, then pumped through the clean-up column overnight at a rate of $1 ml min^{-1}$. This resulted in a marked decrease in contaminant levels. Figure 2.4 shows the gradient elution of a blank run on an ATA impregnated column both before and after clean-up. The clean-up column used for this was a 10cm column impregnated with ATA and was prepared by M. Shaw [120]. For clean-ups when using a XO impregnated column, column 10 in Table 2.2 was used.

2.3.4 Calculations.

2.3.4.1 Column Loadings.

The extent of impregnation that occurs is referred to as the "loading" of the column. This loading is determined using a UV/VIS spectrophotometer (model number 8453, Hewlett Packard, OR, USA) to measure the absorbance of the dye solution before and after impregnation along with the combined bleed solutions. The difference between the dye solution before and after impregnation is directly proportional to the amount of dye that is absorbed onto the substrate. The absorbances were measured at 434nm for XO and 520nm for ATA dye solutions. The loading is generally quoted as *millimoles of dye per gram of resin*.

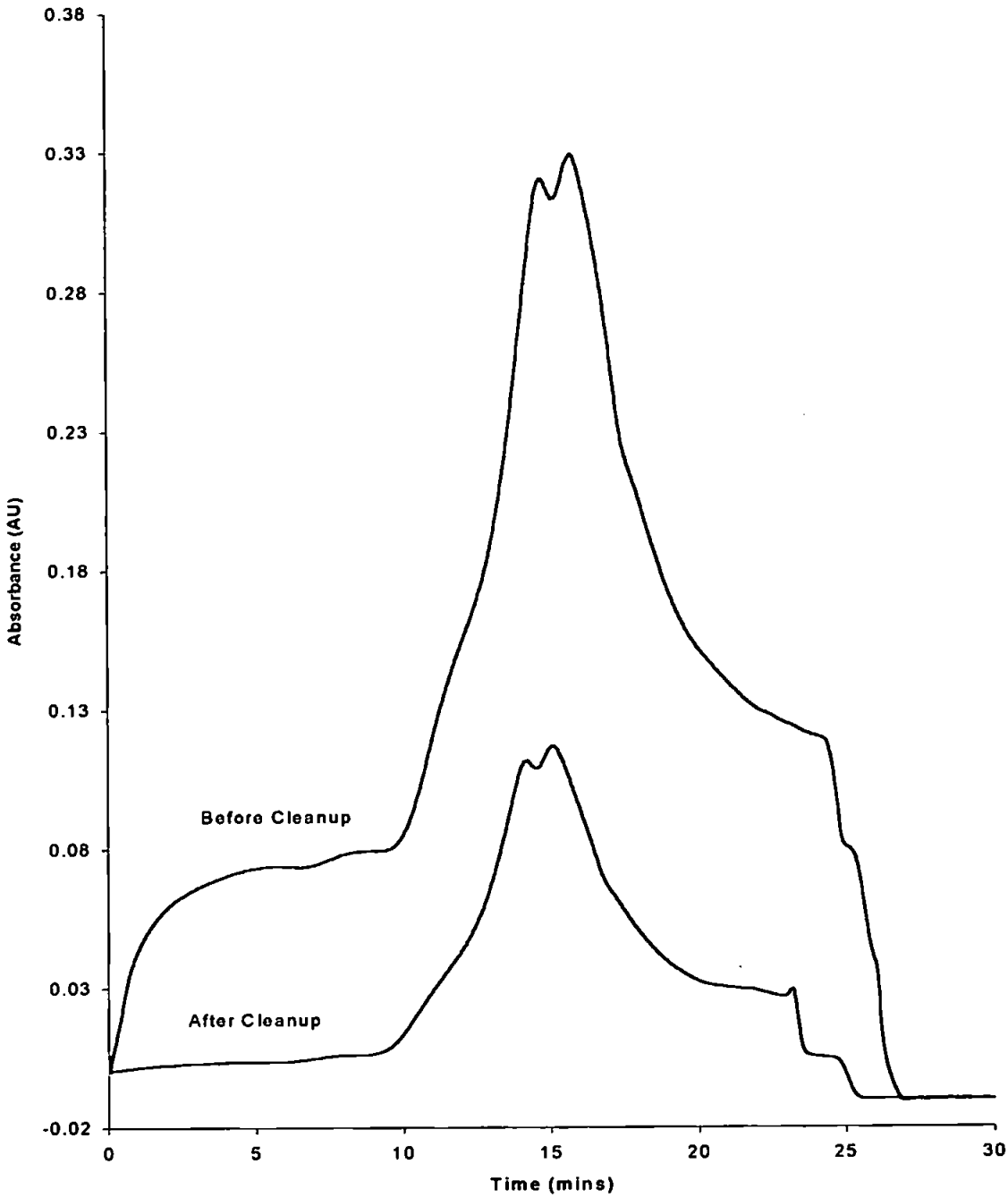

Figure 2.4. Concentration of contaminants present in 1M KNO_3 before and after cleanup at pH9 using a 10cm 5μm PLRP-S column loaded with ATA. Contaminants were eluted using 0.25M HNO_3.

2.3.4.2 Column Capacity.

The capacity of a column is a measure of the amount of dye that is available for chelation. The capacity of a column is calculated from the time taken to the mid-point of an s-shaped breakthrough curve. This breakthrough curve is obtained by pumping a Cu(II) solution ($50mgl^{-1}$ prepared in 1M KNO_3 and buffered to pH 6.5 with ammonium acetate) at $1mlmin^{-1}$ through the column until breakthrough is achieved. Detection is made at 490nm using a PAR PCR and the capacity calculated using the following equation;

$$\text{Capacity} = \text{Adjusted Breakthrough} \times [Cu]$$

Where [Cu] is the concentration of the Cu solution used and the breakthrough time is measured from the injector onwards and is adjusted to subtract the dead time. The capacity is generally quoted *as millimoles of Cu per gram of resin.*

2.3.4.3 Column Activity.

Not all the dye that is impregnated onto the resin is available for chelation. Steric effects can render a potentially large percentage of the dye inactive making it unavailable for chelation. The percentage activity of a column is the amount of dye that is actually available for chelation, compared to the total amount of dye actually loaded. This can be calculated using the following equation;

$$\%Activity = \frac{[Cu]}{DyeLoading} \times 100$$

2.4 Results and Discussion.

The studies reported in this chapter detail the fabrication of a selection of dye impregnated columns and their subsequent use in the analysis of selected heavy and transition metals in highly mineralised waters.

2.4.1 Initial Studies.

As was outlined in Chapter 2.1.4, the aim of this study was to develop an HPCIC system which utilises the unique properties of chelating dyestuffs for the determination of trace metals. Initial studies involved the evaluation of a column made previously and the fabrication of new chelating columns suitable for the required analysis.

2.4.1.1 PLRP-S Resin Loaded with XO.

This column was approximately five years old and was prepared by B Paull [119]. The column was a 100mm x 4.6mm ID PEEK column, which was packed with an 8μm, 100Å PLRP-S resin loaded with XO. The reasons for the use of this column were twofold, firstly to introduce the experimental setup and secondly to evaluate the column's capabilities so as to help in the design of new ones. Paull reported almost baseline resolution between Mn(II) and Cd(II) when using an eluent of pH 3.2 [119]. However, the investigations carried out here showed that in order to obtain similar resolution between these two peaks an eluent of pH 4 - 4.2 is required. Therefore, whilst this columns' capabilities has decreased over time it is still capable of high efficiency separations.

2.4.1.2 Dye Impregnated Columns Prepared.

Table 2.2 shows a list of columns that were prepared for use, though not all of these columns proved suitable for analytical applications. Of the eleven columns prepared only five of them proved suitably efficient for analytical separations namely numbers 1, 7, 8, 10, 11.

2.4.1.3 "Dionex" Columns.

Initially a 9μm, neutral polystyrene based resin, which was supplied by Dionex, was used. This column was packed as described in section 2.3.2 with the exception that the resin was loaded with XO (Sigma) at pH 5.5 as described in section 2.3.1.1. Once the column was conditioned, injections of metal standards produced some broad peaks and so the system parameters were modified in an attempt to reduce this broadening effect. This modification involved shortening some of the tubing and ensuring that, from the injector onwards, all the tubing used was of the same internal diameter. A new T-junction (PEEK, low pressure Tee, 0.8mm thruhole with $^{1}/_{16}$" flangeless fittings) supplied by Alltech was also fitted. Next the PCR coil was modified. The coil being used was determined to be of 0.75mm ID and 194.8cm in length. The internal volume and through time was calculated for coils of various internal diameters ranging from 0.17mm to 1mm as is shown in Table 2.3.

At a flow rate of 1ml min^{-1}, it was decided that the 0.5mm ID tubing offered the best compromise between internal volume and through time and so a two meter coil was used

Table 2.2. Dye Impregnated Columns Prepared.

	Resin Used	Dye Used	Column Length (cm)	Dye Loading ($mmolesg^{-1}$)	Capacity ($mmolesg^{-1}$)	% Active Dye
1	9μm Dionex	XO (Sigma)	10	$2.18x10^{-2}$	$5.62x10^{-3}$	25.78
2	9μm Dionex	XO (Fluka)	25	---	---	---
3	9μm Dionex	XO (Sigma)	25	$2.53x10^{-2}$	$3.73x10^{-4}$	14.7
4	9μm Dionex (depacked)	XO (Sigma)	10	---	---	---
5	9μm Dionex	MTB	10	---	---	---
6	10μm PLRP-S	XO (BDH)	10	$4.20x10^{-2}$	$7.18x10^{-3}$	17.10
7	8μm PLRP-S	XO (BDH)	10	0.1157	$7.39x10^{-3}$	6.39
8	7μm Hamilton	XO (BDH)	10	$4.24x10^{-2}$	$5.35x10^{-3}$	12.62
9	7μm Hamilton	XO (BDH)	25	$8.65x10^{-3}$	$2.25x10^{-3}$	26.01
10	7μm Hamilton	XO (BDH)	25	$3.84x10^{-2}$	$4.20x10^{-3}$	10.94
11	7μm Hamilton	ATA	25	0.151	$2.00x10^{-2}$	13.20

from now on. With the modification of the system now complete, the metal standards were rerun under the same conditions and a slight decrease in peak width was observed. As this

Table 2.3. PCR Coil Residence Time Characteristics (flow rate of $1 ml min^{-1}$).

ID (mm)	Volume ($cm^3 m^{-1}$)	Residence Time for a 1m coil (s)
0.17	0.023	0.68
0.25	0.049	1.47
0.50	0.196	5.88
0.75	0.441	13.23
1.00	0.785	23.55

column's characteristics compared favorably with Paull's column, it was decided to prepare a 25cm column as this should result in a column two and a half times more efficient than the 10cm column. Again the 9μm Dionex resin was used, though this time XO supplied by Fluka was used. Packing, loading and conditioning were carried out as detailed in previous chapters. Due to problems encountered during the conditioning of the column, some of the loaded resin was accidently depacked and as it proved difficult to repack this material it was decided to de-pack the column completely and start over using fresh resin. The second attempt involved XO supplied by Sigma. However this column proved to have a very poor capacity which resulted in very little separating power, with Mn(II) and Cd(II) co-eluting on the solvent front at pH 5 when they should be completely resolved at this pH.

As these results were unexpected, a new 10cm column was prepared, this time with some of the de-packed resin loaded with Fluka XO. Again the capacity was found to be very

poor with a Mn(II) and Cd(II) mixture producing a single peak on the solvent front and Zn(II) showing only slightly greater retention at pH 4. The poor performances of these columns was thought to be as a result of either problems with the instrumentation, dyestuffs or resin. In order to determine if the instrumentation was at fault, Mn(II) and Cd(II) standard solutions were run on the original 10cm Dionex/Sigma column prepared. The results obtained compared favorably with those previously obtained, therefore it was assumed that the instrumentation was not at fault.

A new dyestuff was now investigated. This time methylthymol blue (MTB) was loaded onto the Dionex resin. MTB was chosen as it has very similar chelating characteristics to XO and should therefore produce similar results to those obtained with the original Dionex/Sigma column. In order to prevent any possible photodegradation of the dye, all transparent tubing as well as the flask containing the dye solution was covered with aluminium foil during the loading procedure. However, as with the Fluka column, virtually no retention was found for Zn(II) at pH 4. It was therefore concluded that either all the dyestuffs so far used had "gone off" or the problem lay with the resin.

2.4.1.4 Dye Purity Study.

It was hypothesised that if the dyestuffs had "gone off" then there would be large amounts of impurities present. Therefore, the purity of various dyes was investigated. Commercially available dyestuffs are not 100% pure, in fact the purity of the dye can be as low as 55% with the remaining 45% consisting of various impurities. For XO, the major impurity present is generally Semi-Xylenol Orange (SXO). SXO differs from XO in that it has only one IDA functional group, as is shown in Figure 2.5. If this impurity is present in

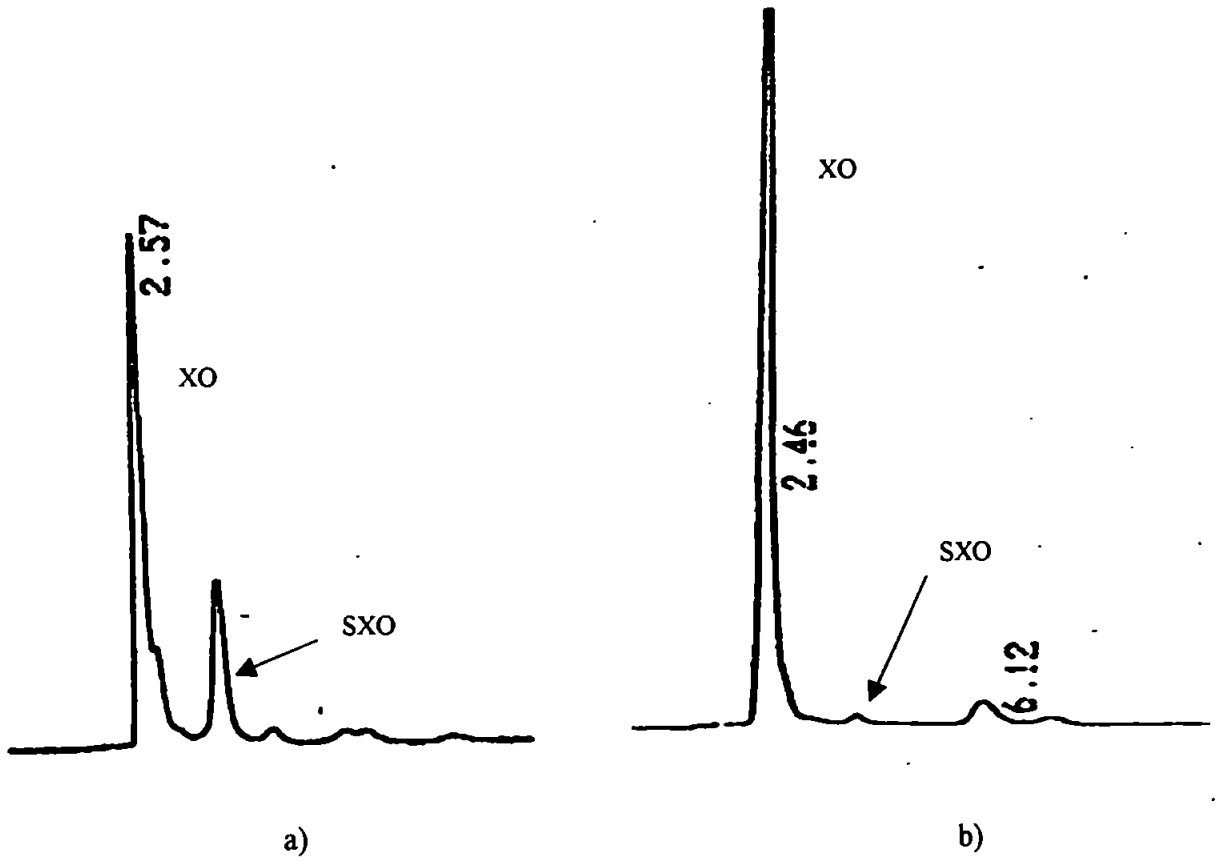

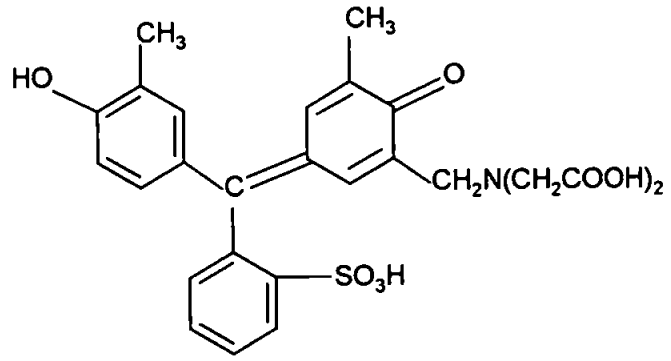

Figure 2.5. Sample chromatograms of a) the v. old XO tested and b) the new XO tested and the structure of SXO.

large enough quantities then the efficiency of the column can be dramatically reduced due to SXO being a much weaker chelating ligand than XO. Therefore, it was suggested that the lack of retention found with the columns so far prepared was due to the presence of high levels of SXO being present.

A selection of XO dyes (supplied by various manufacturers) were tested for their SXO content. This was carried out using a method detailed by Smedes *et al* [163]. This reversed phase HPLC method utilises a 10cm ODS column (5μm particle size) with an eluent containing 0.06M perchloric acid:acetone (4:1 v/v) for the separation of SXO from XO. A Dionex GP40 gradient pump coupled with a Dionex AD20 absorbance detector was used for the analysis. The absorbances were measured at 400nm and the dye solutions contained 10mg of dye in 25mls of eluent. The purity of the XO content of the dyes is given in Table 2.4.

Table 2.4. Purity of XO dyestuffs investigated.

Dyestuff	% XO Purity	Literature Purity
BDH (new)	95.82	>93% [164]
BDH (old)	96.31	>93% [11]
BDH (very old)	69.47	>93% [11]
Sigma	94.52	N/A
Fluka	85.98	N/A
Janssen	82.21	N/A
Aldrich	89.80	~90% [165]

The % XO purity was calculated from the peak areas of the XO and SXO peaks obtained and should only be considered as an approximation of the % purity. The results show that all the dyes previously used are of an acceptable purity and that the SXO content should not have any significant effect on the retention characteristics of the columns. Sample chromatograms of the SXO content of the dyes are given in Figure 2.5. Therefore, it can be concluded that the purity of the dyestuffs were not the cause of the poor performances obtained and therefore, either the resin or procedure was at fault.

2.4.2 "Polymer Laboratory's" Columns.

As it did not appear that the quality of the dyestuffs was at fault, it was decided to try a new resin. This time a range of resins supplied by Polymer Laboratory's were investigated. These resins were all polystyrene based resins (PLRP-S) but of varying particle and pore size.

2.4.2.1 10μm Polymer Laboratory's Column.

The first resin investigated was a 10μm, 300Å PLSP-S resin. The column was prepared as before except that the resin slurry was prepared in >30% methanol due to it's greater hydrophobicity. Also a 0.5% dye solution (at pH 5) was prepared from the new batch of XO supplied by BDH. After conditioning, initial results showed that there was metal retention occurring as shown in Table 2.5 however, it was soon discovered that there was a problem in that peak splitting was occurring. In fact several of the metals investigated showed splitting at specific pH's e.g. Zn(II) at pH 2.5, Co(II) at pH 3 and Cd(II) at pH 3.5. Also several metals produced peaks with shoulders as is shown in Table 2.5. Visual

inspection of the column showed that the top of the column was found to be dark orange in colour whilst the bottom of the column was a pale lemon colour. It is possible that the peak splitting and peak shoulders that were occurring were as a result of an uneven dye coating as indicated by the difference in colour found on the column.

Table 2.5. Retention times (in minutes) for 10cm XO loaded (10μm PLRP-S resin) column (t_0 = 1.26 minutes) before adjustment of ionic strength and pH. Eluent used was 1M KNO_3 buffered with 50mM acetic acid. Detection was with PAR at 490nm.

pH	Mn(II)	Cd(II)	Zn(II)	Pb(II)	Co(II)	Ni(II)	Cu(II)
2.00	1.46	1.53	1.56	1.76	1.57	1.52	~35
2.50	1.47	1.62	1.68/ 2.09	2.56	1.67	1.57	---
3.00	1.49	1.55	2.15	3.99	1.63/ 2.13	1.55	---
3.50	1.50	1.57/ 1.87	3.87	10.16	3.72	1.57	---
4.00	1.57	2.18	11.05	36.37	10.78	>30	---
4.50	1.76	3.68	41.50	---	---	---	---
5.00	2.11	9.44	---	---	---	---	---

2.4.2.2 Dye Impregnation via Ultrasonic Agitation.

In an attempt to solve the problem of the uneven dye coating a new dye impregnation method was developed which utilised ultrasonic agitation during the impregnation of the resin. Wang and Chen [166] reported on the effect of mechanical and ultrasonic agitation on the adsorption rate of PAR with Amberlite XAD-2 resin. This study reported that ultrasonic agitation enhanced the adsorption of PAR by the XAD-2 resin. It was postulated

that this was due to an increased diffusion rate of the dye towards the resin surface rather than an "opening-up" of the resin pores. For this investigation a 15-20μm, 100Å PLRP-S resin was used to see if this method was a viable alternative to the continuous flow impregnation method currently used. Several experimental conditions were investigated which included methanol concentration, dye concentration and pH of the dye solution.

The first parameter investigated was the methanol concentration of the dye solution the results of which are shown in Table 2.6. 5ml of the methanol:MilliQ solution was added to 10mg of resin in a test-tube and mixed for a few seconds on a vortex mixer.

Table 2.6. Wetability of 15-20μm PLRP-S resin.

Weight of resin (mg)	Methanol concentration	Observations
9.92	0%	Completely dry
10.35	10%	Slightly wet
10.40	20%	~90% wet
10.38	30%	Completely wet

As the methanol concentration increases, so does the wetability of the resin. In pure MilliQ water the resin simply floats on the surface while in 30% methanol it sinks to the bottom of the test tube. A methanol concentration of 20% was chosen as a suitable compromise between wetability and desired low methanol concentration. Next the dye concentration required was investigated. The dyestuff used was XO (new from BDH) and prepared in 20% methanol and initially adjusted to pH 5. Table 2.7 shows the conditions investigated.

This study was carried out by sonicating 150mg of resin in 15mls of dye solution in 15ml poly(propylene) centrifuge tubes (Luckman, Life Sciences International, Hampshire, UK) using a Sonicor ultrasonic bath (Sonicor, Copague, NY, USA, Freq; 50-60 Hz, model number: SC-120) at a temperature of between 20-30°C. Samples 1, 2 and 3 in Table 2.7 were initially tested with sample 2 visually determined to offer the best loading. A similar study was being carried out simultaneously by Truscott [167] who found that a 0.2% dye solution in 10% methanol adjusted to pH 3 produced an acceptable loading with very little bleeding of the column. Therefore, samples 4, 5 and 6 were run using the Sonicor ultrasonic bath (Freq: 50-60 Hz, model number: SC52T) as used by Truscott. This bath differed from the one originally used in that it's volume was approximately half. This time sample 4 visually appeared to offer the best loading and so these parameters were used to investigate the effect of mechanical agitiation on adsorption of the dye using a magnetic stirrer (Stuart Scientific, setting 7) and a vortex mixer (Fison's Whirlimixer). Both these samples visually produced disappointing loadings. Therefore, it was determined that the best conditions for XO impregnation by ultrasonic agitation was, per gram of resin, a 100ml solution of a 0.2% dye solution in 10% methanol adjusted to pH 3.

2.4.2.3 8µm Polymer Laboratory's Column.

A new column was now prepared using the ultrasonic loading procedures as described in section 2.3.1.2. A 10cm column was packed with an 8µm, 100Å PLRP-S resin from Polymer Laboratories. This time the column showed a low but acceptable capacity (Table 2.9). Again peak splitting and poor peak shapes in general were found. As these problems

Table 2.7. Samples Used for Sonication Method Development.

Sample	Method of Agitation	Dye Concentration	MeOH Concentration	pH	Time	Observations
1	Sonication 1	0.1%	20%	5	~10 hr	*
2	Sonication 1	0.2%	20%	5	~10 hr	*
3	Sonication 1	0.4%	20%	5	~10 hr	*
4	Sonication 1	0.2%	10%	3	5 hr	#
5	Sonication 1	0.2%	20%	3	5 hr	#
6	Sonication 1	0.2%	10%	5	5 hr	#
7	Magnetic Stirrer	0.2%	10%	3	5 hr	*
8	Vortex Mixer	0.2%	10%	3	5 hr	#

Sonication 1 :- Large Sonic Bath.
Sonication 2 :- Small Sonic Bath.
*:- Took $1^1/_2$ to 2 hours before completely wet.
#:- Mixed with Vortex mixer for a few seconds and wet that much more quickly.

were thought to be due to an uneven dye coating it was supposed that the sonication procedures did not improve the evenness of the dye coating. An alternative reason hypothesised for the peak splitting was that the column was being overloaded. Therefore, a series of standards of decreasing concentration were ran for Cd(II) and Zn(II). As both these metals were producing split peaks on the solvent front it was difficult to distinguish between the peak corresponding to the metal and the peak corresponding to the solvent front disturbance. Therefore the metal standards were prepared in the eluent so as to minimise the baseline distortion of the solvent front. These new standards, adjusted to pH 3, produced a single peak. In fact, all the standards showed a dramatic improvement in peak shape upon being prepared in the eluent. Some metals still produced some shouldered peaks e.g. Zn(II) and Co(II) at pH 2, Cd(II) at pH 4.5, however these shoulders disappeared with the adjustment of the pH of the metal standard to that of the eluent (Table 2.10). An example of this improvement in peak shape is shown in Figure 2.6. Therefore, matrix matching between the eluent and sample is important to the attainment of good peak shapes. This proved true for the 10μm polymer laboratory's column also (Table 2.8).

Table 2.8. Retention times (in minutes) for 10cm XO loaded (10μm PLRP-S resin) column (t_0 = 1.26 minutes) after adjustment of ionic strength and pH. Eluent used was 1M KNO_3 buffered with 50mM acetic acid. Detection was with PAR at 490nm.

PH	Mn(II)	Cd(II)	Zn(II)	Co(II)	Pb(II)	Ni(II)	Cu(II)
2.00	1.51	1.50	1.52	1.52	2.00	1.47	> 60
2.50	1.45	1.50	1.72	1.70	3.23	1.48	---
3.00	1.48	1.63	2.74	2.63	8.73	1.45	---
3.50	1.50	1.93	6.47	6.78	27.03	---	---
4.00	1.56	2.61	14.33	---	---	---	---
4.50	1.52	4.65	---	---	---	---	---

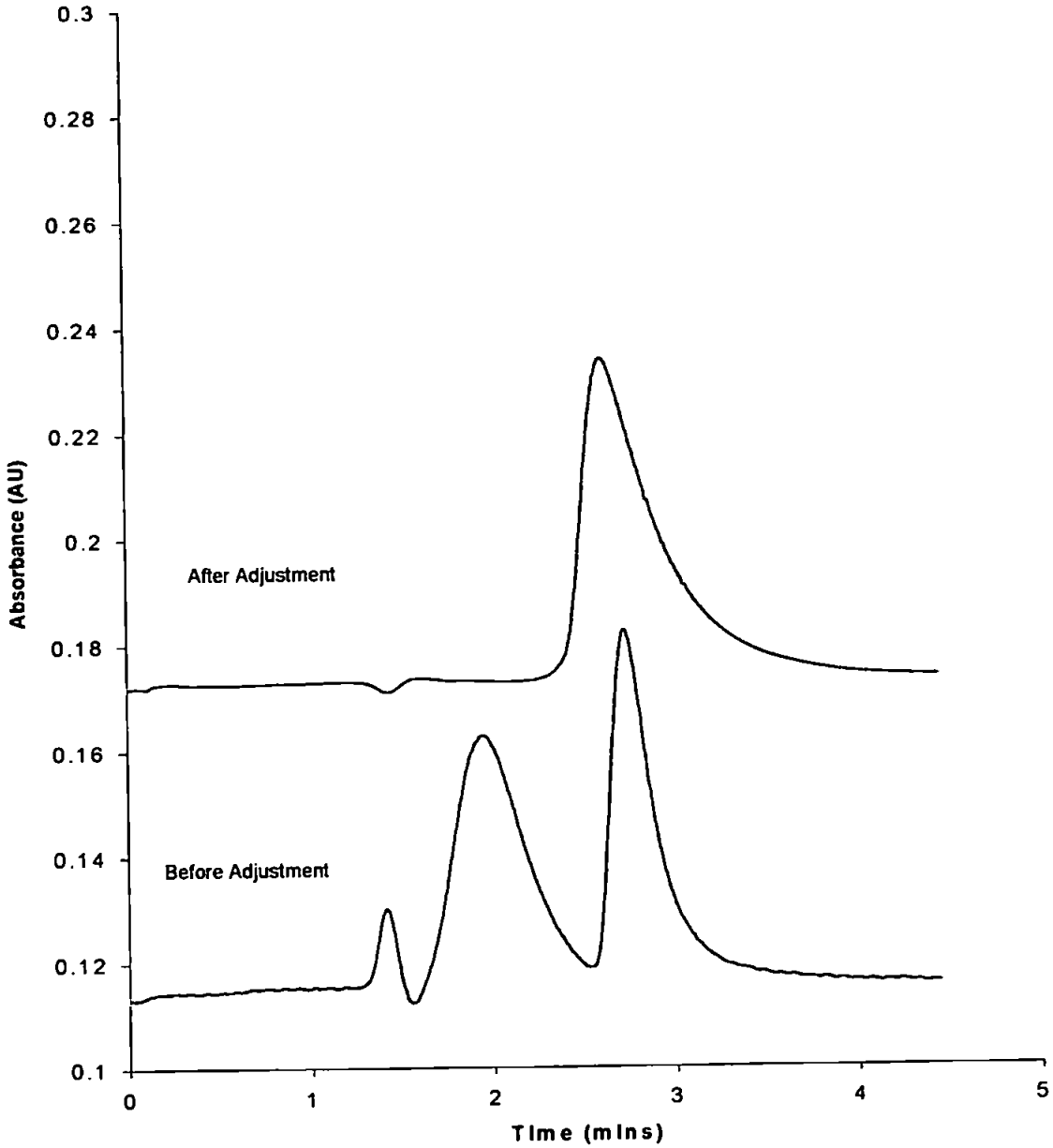

Figure 2.6. A 500µl injection of 20µgl^{-1} Zn(II) on a 10cm XO impregnated column (8µm PLRP-S resin) using a 1M KNO_3 eluent buffered with 50mM acetic acid at pH3 before and after adjustment of ionic strength and pH. Detection was made at 490nm with PAR.

Table 2.9. Retention times (in minutes) for 10cm XO loaded (8μm PLRP-S resin) column (t_0 = 1.20 minutes) before adjustment of ionic strength and pH. Eluent used was 1M KNO_3 buffered with 50mM acetic acid. Detection was with PAR at 490nm.

PH	Mn(II)	Cd(II)	Zn(II)	Co(II)	Pb(II)	Ni(II)	Cu(II)
2.00	1.40	1.43	1.52	1.52	2.05	1.43	>60
2.50	1.40	1.50	1.68/ 2.45	1.67/ 2.43	3.17	1.48	---
3.00	1.47	1.58	1.93/ 2.63	1.92/ 2.55	6.30	1.58	---
3.50	1.47	1.67/ 2.47	10.17	8.92	19.57	1.53	---
4.00	1.53	1.89/ 2.65	14.93	17.33	~50	---	---
4.50	1.87	4.68	~40	>60	---	---	---

Table 2.10. Retention times (in minutes) for 10cm XO loaded (8μm PLRP-S resin) column (t_0 = 1.20 minutes) after adjustment of ionic strength and pH. Eluent used was 1M KNO_3 buffered with 50mM acetic acid. Detection was with PAR at 490nm.

PH	Mn(II)	Cd(II)	Zn(II)	Co(II)	Pb(II)	Ni(II)	Cu(II)
2.00	1.39	1.40	1.43	1.43	2.08	1.44	> 60
2.50	1.47	1.54	1.97	1.93	3.45	1.48	---
3.00	1.43	1.55	2.98	2.98	9.98	1.47	---
3.50	1.43	1.80	6.62	7.33	> 20	---	---
4.00	1.43	2.15	15.67	---	---	---	---
4.50	1.82	4.97	---	---	---	---	---

This also showed that the original continuous flow method of impregnation was not at fault and was, probably, resulting in acceptable peak shapes though this wasn't realised without the pH matching of sample and eluent.

2.4.3. "Hamilton" Columns.

With the problems of poor capacities and poor peak shapes solved, new columns were prepared for analytical applications. This time the columns were prepared using a neutral 7μm polystyrene based resin obtained from Hamilton (Reno, NV, USA). This resin was chosen due to it's commercial availability. Two XO columns, 10cm and 25cm in length as well as a single ATA column, 25cm in length were prepared.

2.4.3.1. XO/Hamilton Columns.

Both these columns were prepared using the sonication procedures as outlined in Chapter 2.3.1.2. The 10cm column prepared was determined to have a capacity of $5x10^{-3}$ mmoles g^{-1} and a dye loading of 0.042mmoles g^{-1} with an active dye percentage of 12.62% whilst the 25cm column showed a capacity of $4.20x10^{-3}$ mmoles g^{-1} with a dye loading of 3.84mmoles g^{-2} and an active dye percentage of 10.94%. As the results for the 25cm column were lower than expected, this column was used principally for eluent clean-up. However, the retention times for this 25cm column are given in Tables 2.11 and 2.12. Table 2.11 shows the retention times for selected transition metals for the first attempt at impregnation though the resulting loading (7.87%) was deemed too low to be of value and therefore the column was stripped and reloaded with fresh dye solution and then repacked

as before. As can be clearly seen there is a marked improvement in retention at the second attempt leading to the conclusion that the ultrasonic loading procedures are effective.

Table 2.11. Retention Times (in minutes) for 25cm XO loaded (7μm Hamilton resin) column. Eluent used was 1M KNO_3 buffered with 50mM acetic acid with detection at 520nm with PAR (1st attempt).

pH	Mn(II)	Cd(II)	Zn(II)	Co(II)	Pb(II)	Ni(II)	Cu(II)
2.00	3.17	3.21	3.30	3.30	3.90	3.20	> 30
2.50	3.21	3.27	3.60	3.60	6.08	3.22	---
3.00	3.21	3.42	5.27	5.30	14.97	3.28	---
3.50	3.25	3.72	9.05	10.00	35.38	---	---
4.00	3.30	4.50	23.87	---	---	---	---
4.50	3.58	7.42	---	---	---	---	---

Table 2.12. Retention Times (in minutes) for 25cm XO loaded (7μm Hamilton resin) column. Eluent used was 1M KNO_3 buffered with 50mM acetic acid with detection at 520nm with PAR (2nd attempt).

pH	Mn(II)	Cd(II)	Zn(II)	Co(II)	Pb(II)	Ni(II)	Cu(II)
2.00	3.23	3.25	3.36	3.35	4.10	3.28	> 60
2.50	3.20	3.30	3.76	3.89	7.07	3.33	---
3.00	3.27	3.58	6.66	7.08	22.87	---	---
3.50	3.31	4.18	14.87	---	---	---	---
4.00	3.43	6.08	---	---	---	---	---
4.50	3.80	11.30	---	---	---	---	---

Initial results from the 10cm column again showed peak splitting and shouldered peaks, though adjustment of sample pH and matrix matching with the eluent again rectified this problem as is shown in Tables 2.13 and 2.14

The initial studies for the 10cm column involved the determination of the retention times of various transition and heavy metals over the pH range of 2-5. This data along with the capacity of the column was used to construct capacity factors or k' plots for the metals of interest. Figure 2.8 shows the resulting k' plots. As expected the k' values and the slopes of the k' plots illustrate that XO chelates more strongly with Pb(II) than it does with Mn(II) which shows very little retention at all and that this chelating strength increases with an increase in pH. Figure 2.8 also shows that Co(II) and Zn(II) coelute over the entire pH range investigated. The elution order for the transition metals investigated was as

Table 2.13. Retention Times (in minutes) for 10cm XO loaded (7μm Hamilton resin) column (t_0 = 1.10 minutes) before adjustment of pH and ionic strength. Eluent used was 1M KNO_3 buffered with 50mM acetic acid with detection at 520nm with PAR.

pH	Mn(II)	Cd(II)	Zn(II)	Co(II)	Pb(II)	Ni(II)	Cu(II)
2.00	1.35	1.40	1.68	1.64	2.18/ 2.48	1.35/ 2.05	> 60
2.50	1.38	1.49	2.24	2.39	5.43	1.38/ 2.50	---
3.00	1.40	1.67	4.33	4.58	16.78	---	---
3.50	1.42	2.02	11.23	12.00	---	---	---
4.00	1.47	3.03	~30	31.23	---	---	---
4.50	1.63	6.23	---	---	---	---	---

Table 2.14. Retention Times (in minutes) for 10cm XO loaded (7μm Hamilton resin) column (t_0 = 1.10 minutes) after adjustment of pH and ionic strength. Eluent used was 1M KNO_3 buffered with 50mM acetic acid with detection at 520nm with PAR.

pH	Mn(II)	Cd(II)	Zn(II)	Co(II)	Pb(II)	Ni(II)	Cu(II)
2.00	1.35	1.37	1.43	1.43	2.03	1.37	> 60
2.50	1.37	1.45	2.19	1.93	5.43	---	---
3.00	1.40	1.67	4.33	4.58	16.78	---	---
3.50	1.51	2.17	8.65	8.10	31.58	---	---
4.00	1.55	3.21	30.00	31.23	---	---	---
4.50	1.63	6.23	---	---	---	---	---

expected, that being Mn(II)<Cd(II)<Zn(II)<Co(II)<Pb(II)<Cu(II). Due to this increase in chelating strength, only three or four metals can be separated isocratically before peak shapes become too broad and/or elution times become too long for any practical purpose. For this reason gradient elution programs were developed for the elution of multiple sets of metals. There is a danger however when using gradient elution programs that the dye coating can be affected. Constantly changing pHs can increase the chance that bleeding of the dye coating may occur thereby resulting in a lower capacity column. However, for the pH gradients used any bleeding that may occur should be negligible. Another problem associated with gradient elutions is changes in the baseline due to changes in the detection pH. Figure 2.7 shows the baseline for Figure 2.11 and the resultant changes that are obtained as the gradient is run. Figures 2.9, 2.10 and 2.11 show the gradient separation of various suites of metals.

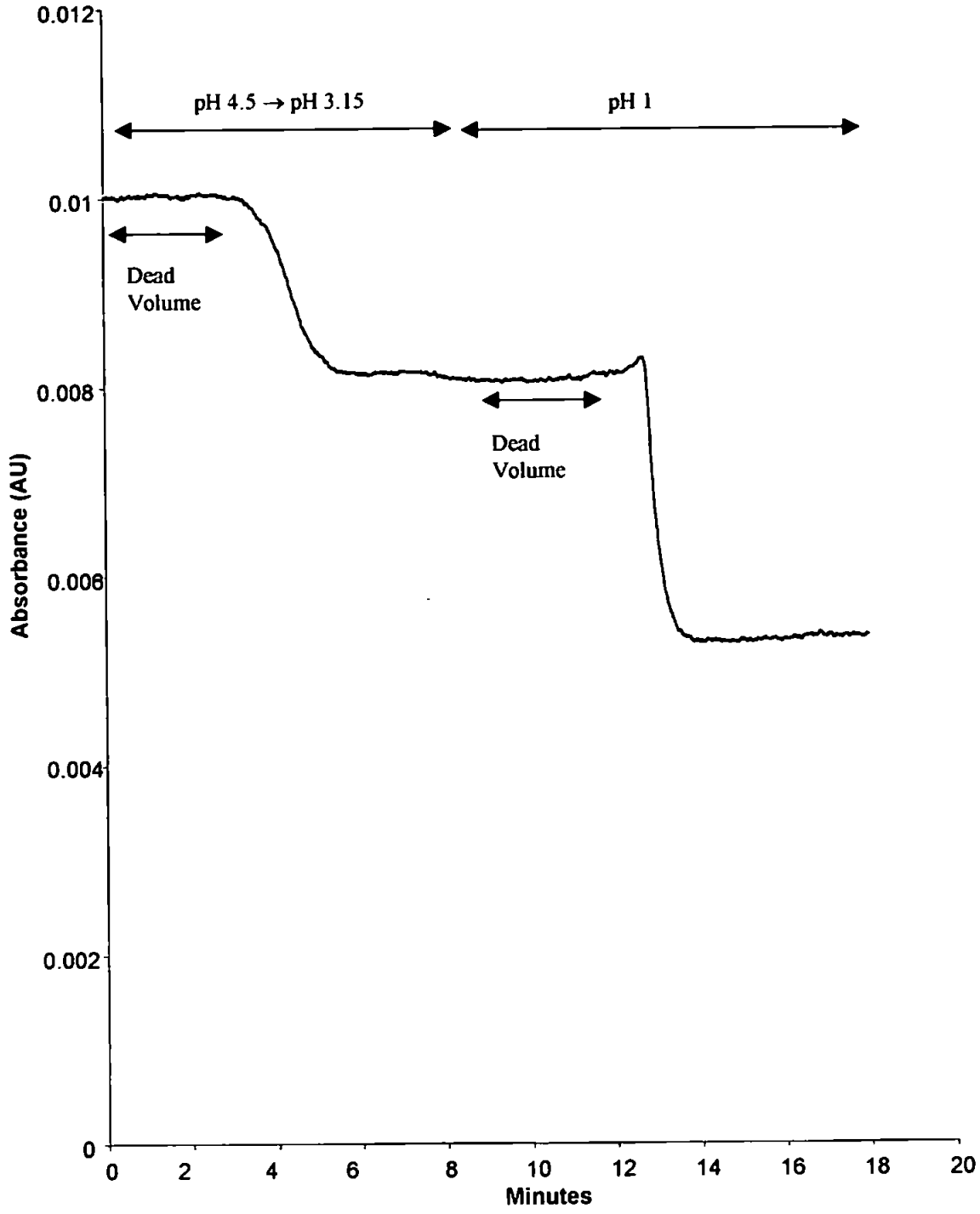

Figure 2.7 Baseline run under same conditions and gradient as for Figure 2.11 showing eluent pH as the gradient is running.

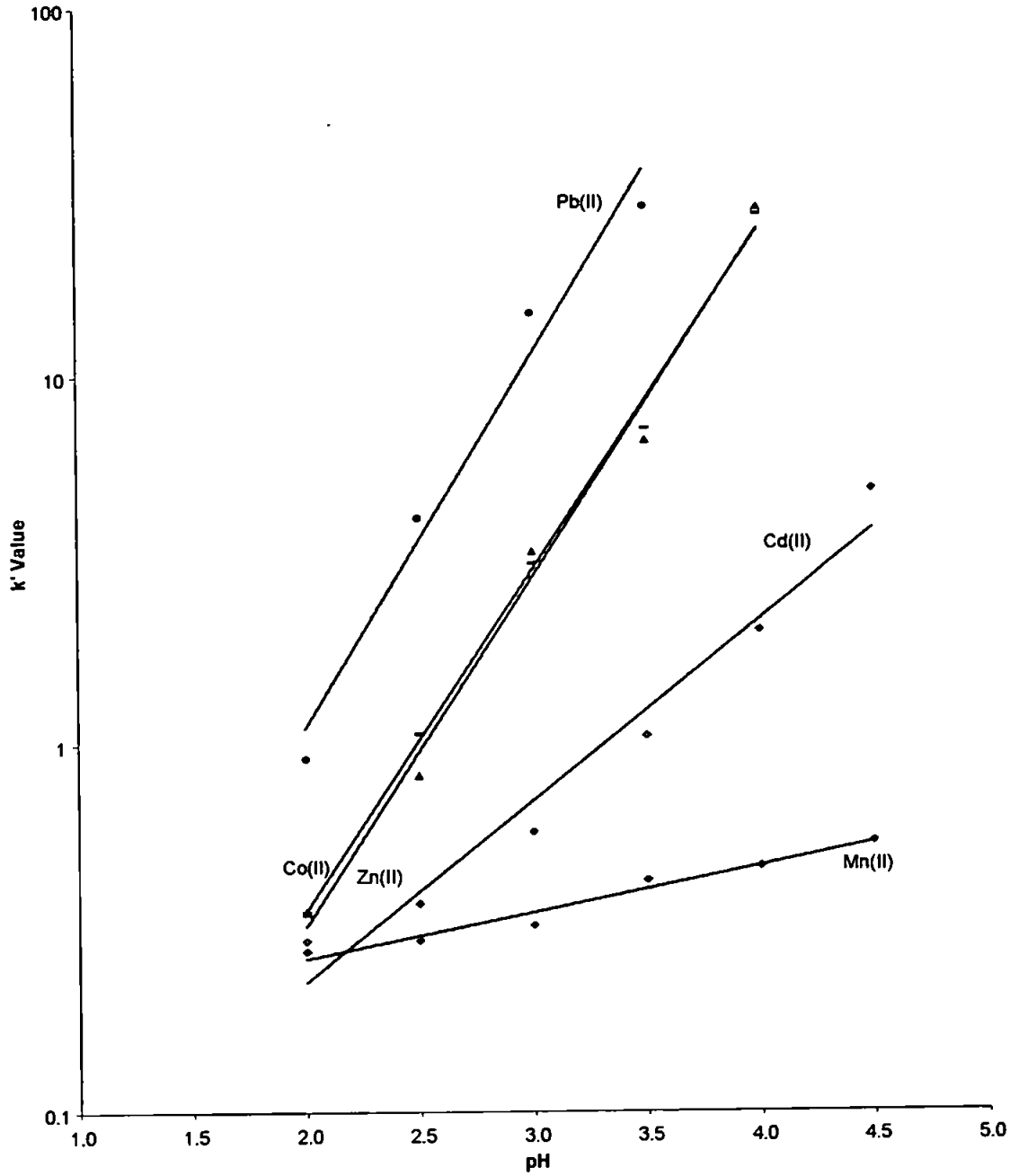

Figure 2.8. The dependence of capacity factors (k') for selected transition and heavy metals on eluent pH with the 10cm XO/7μm Hamilton column. Eluent used was 1M KNO_3 buffered with 50mM acetic acid. Detection was made with PAR/NH_3 at 520nm.

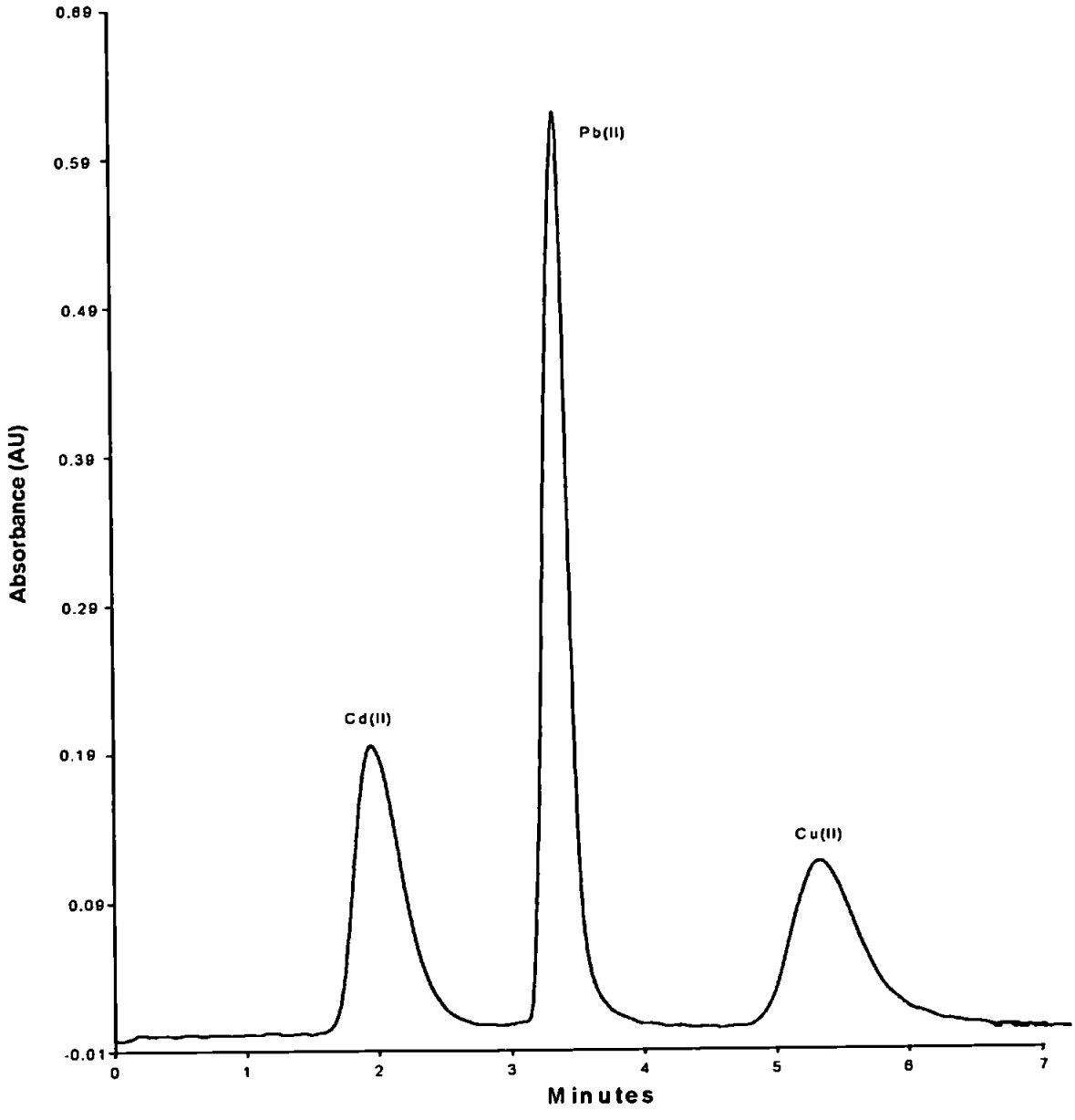

Figure 2.9. Gradient elution of 20mgl^{-1} Cd(II), 10mgl^{-1} Pb(II) and 1mgl^{-1} Cu(II) mixture on the 10cm XO/7μm Hamilton column. A gradient of equilibriating the column at pH 3 then switching to 0.1M HNO_3 for three minutes before the injection was made, was utilised. Eluent used was 1M KNO_3 buffered with 50mM acetic acid. Injection volume used was 100μl with detection at 520nm using PAR/NH_3 PCR.

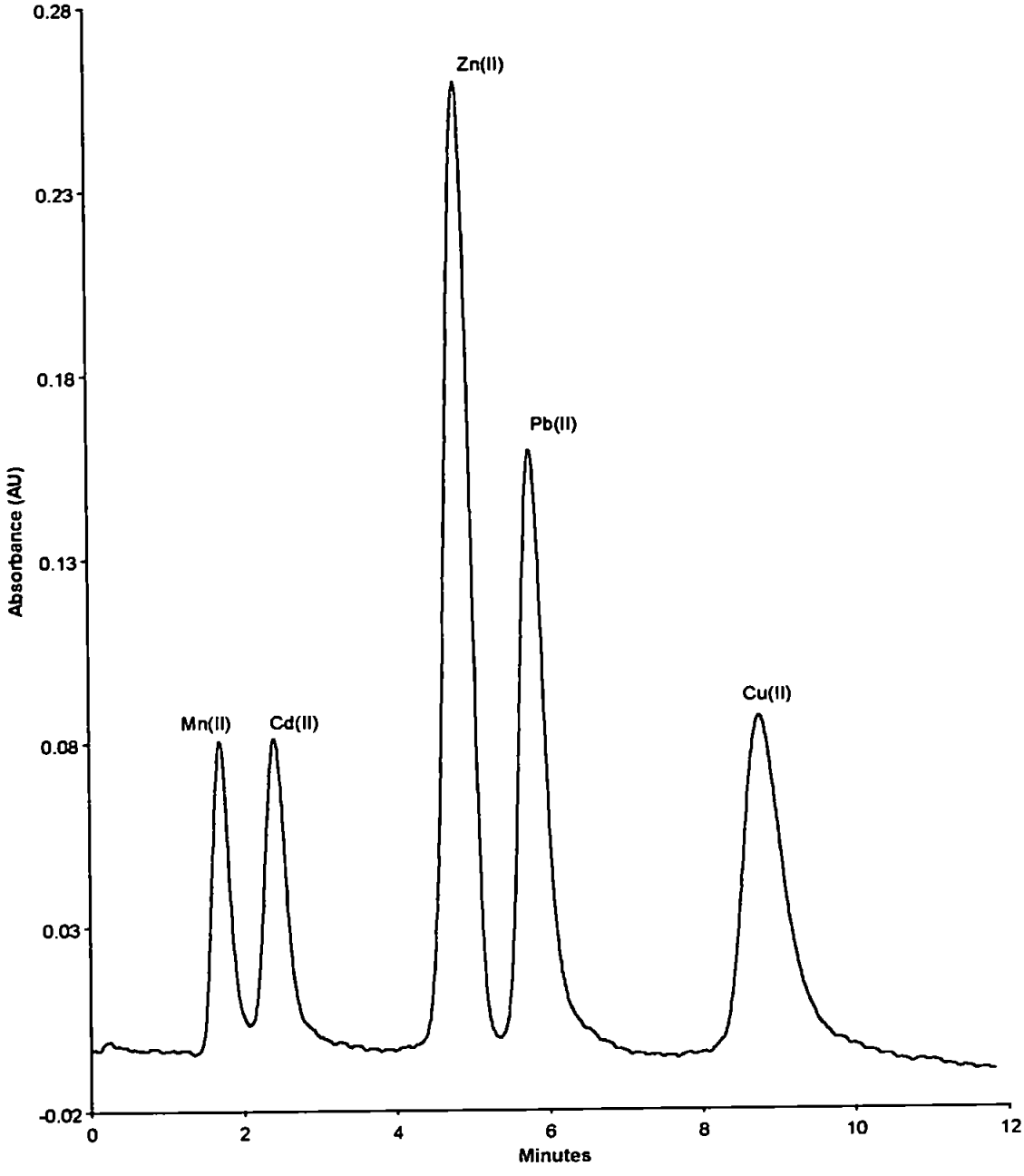

Figure 2.10. Gradient elution of a 0.5mgl^{-1} Mn(II), 20mgl^{-1} Cd(II), 10mgl^{-1} Zn(II), 10mgl^{-1} Pb(II) and 1mgl^{-1} Cu(II) mixture on the 10cm XO/7μm Hamilton column. A gradient of equilibriating the column at pH 3.5 then switching to pH 2 for four minutes before the injection was made then switching immediately to 0.1M HNO_3, was utilised. Eluent used was 1M KNO_3 buffered with 50mM acetic acid. Injection volume used was 100μl with detection at 520nm with PAR/NH_3 PCR.

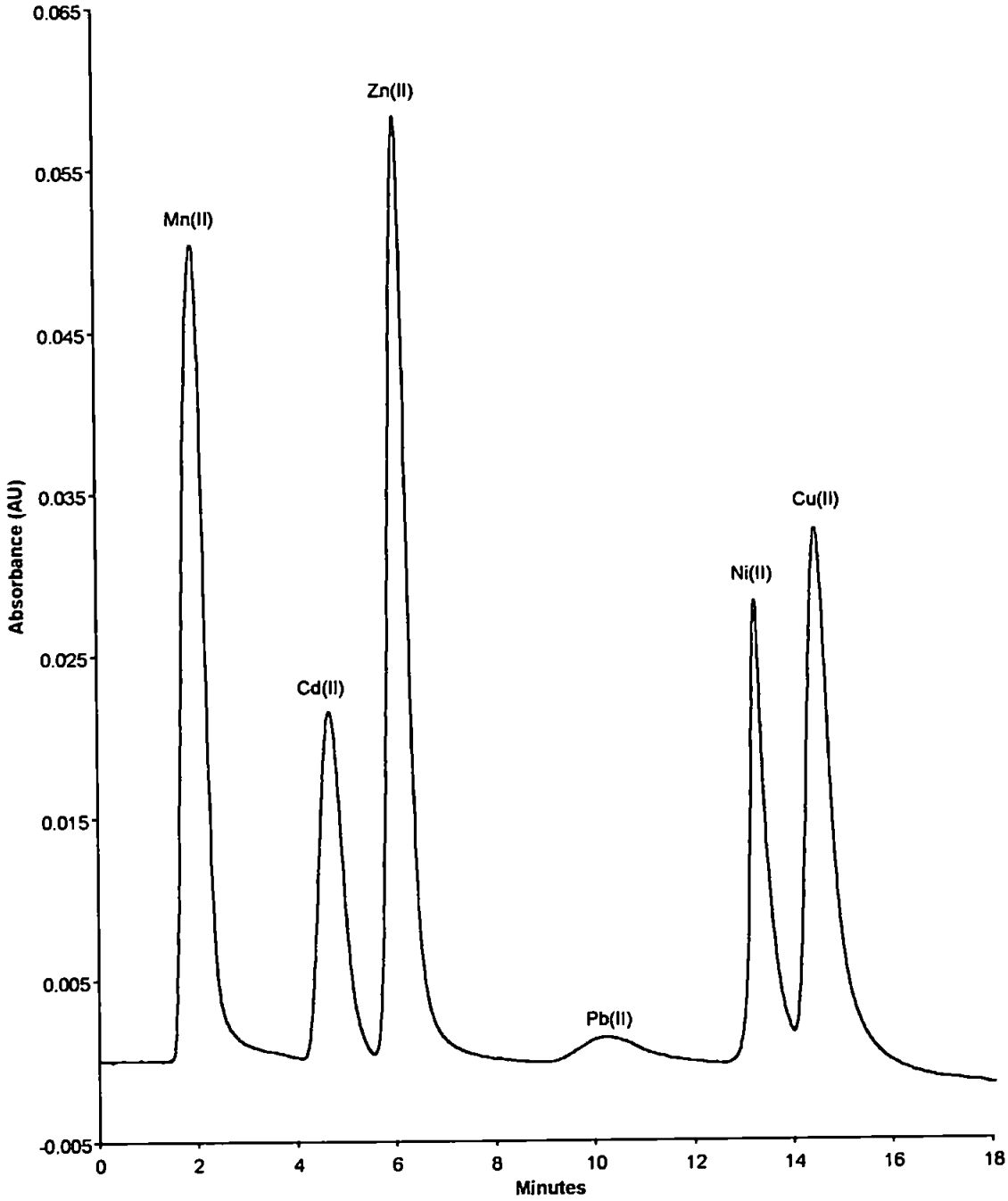

Figure 2.11. Gradient elution of a 100μgl^{-1} mixture of Mn(II), Cd(II), Zn(II), Pb(II), Ni(II) and Cu(II) on the 10cm XO/7μm Hamilton column. A gradient of equilibriating the column at pH 4.5, injecting then switching to pH 3.15 over the following nine minutes before switching to 0.1M HNO_3, was utilised. Eluent used was 1M KNO_3 buffered with 50mM acetic acid. Injection volume used was 500μl with detection at 520nm using PAR/Borate PCR.

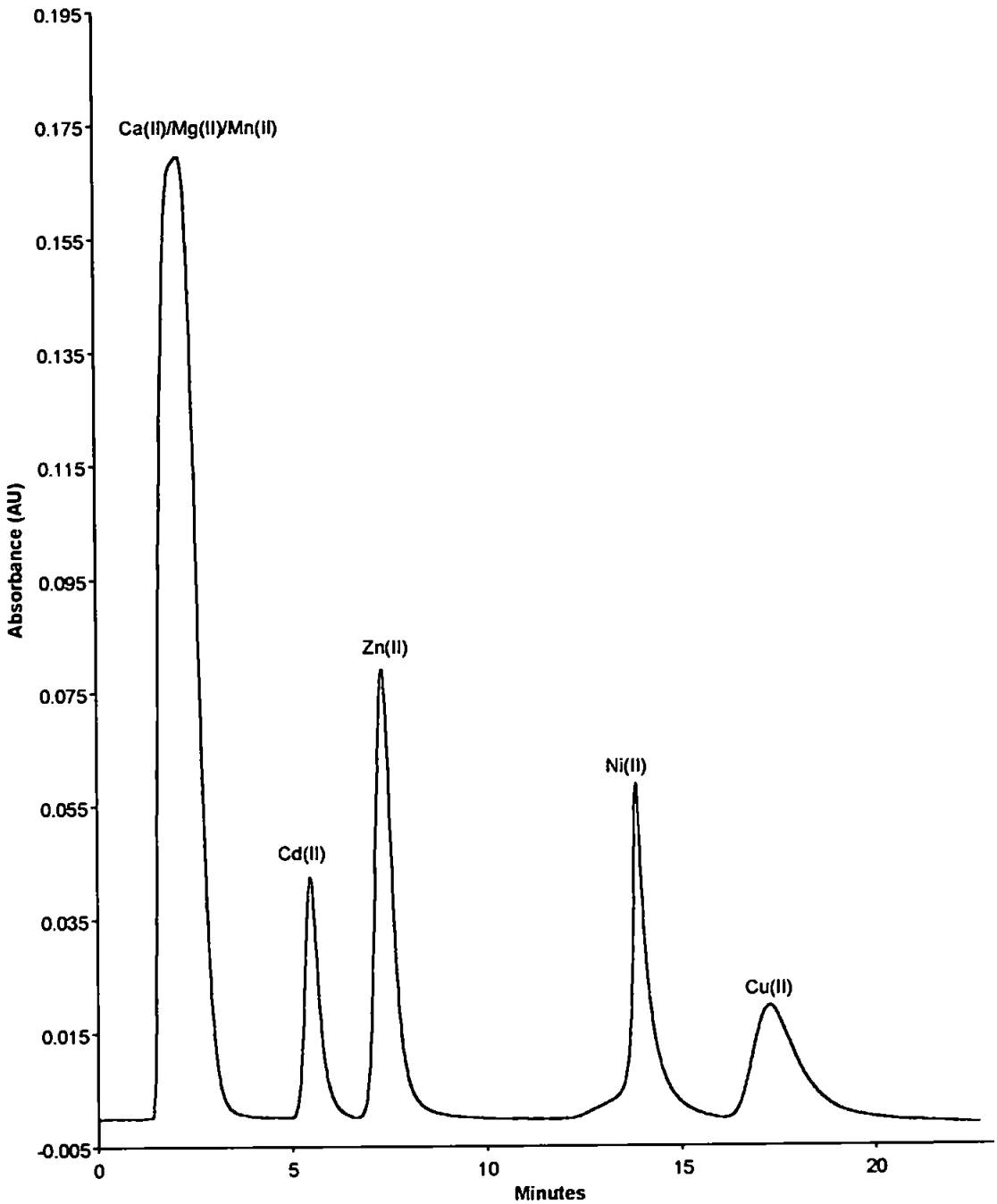

Figure 2.12. Gradient separation of a 100μgl^{-1} mixture of Mn(II), Cd(II), Zn(II), Ni(II) and Cu(II) in the presence of 150mgl^{-1} Mg(II) and 50mgl^{-1} Ca(II) on the 10cm XO/7μm Hamilton column. A gradient of equilibriating the column at pH 4.5, injecting then switching to pH 3 over the following nine minutes before switching to 0.1M HNO_3, was utilised. Eluent used was 1M KNO_3 buffered with 50mM acetic acid. Injection volume used was 500μl with detection at 520nm with PAR/Borate PCR.

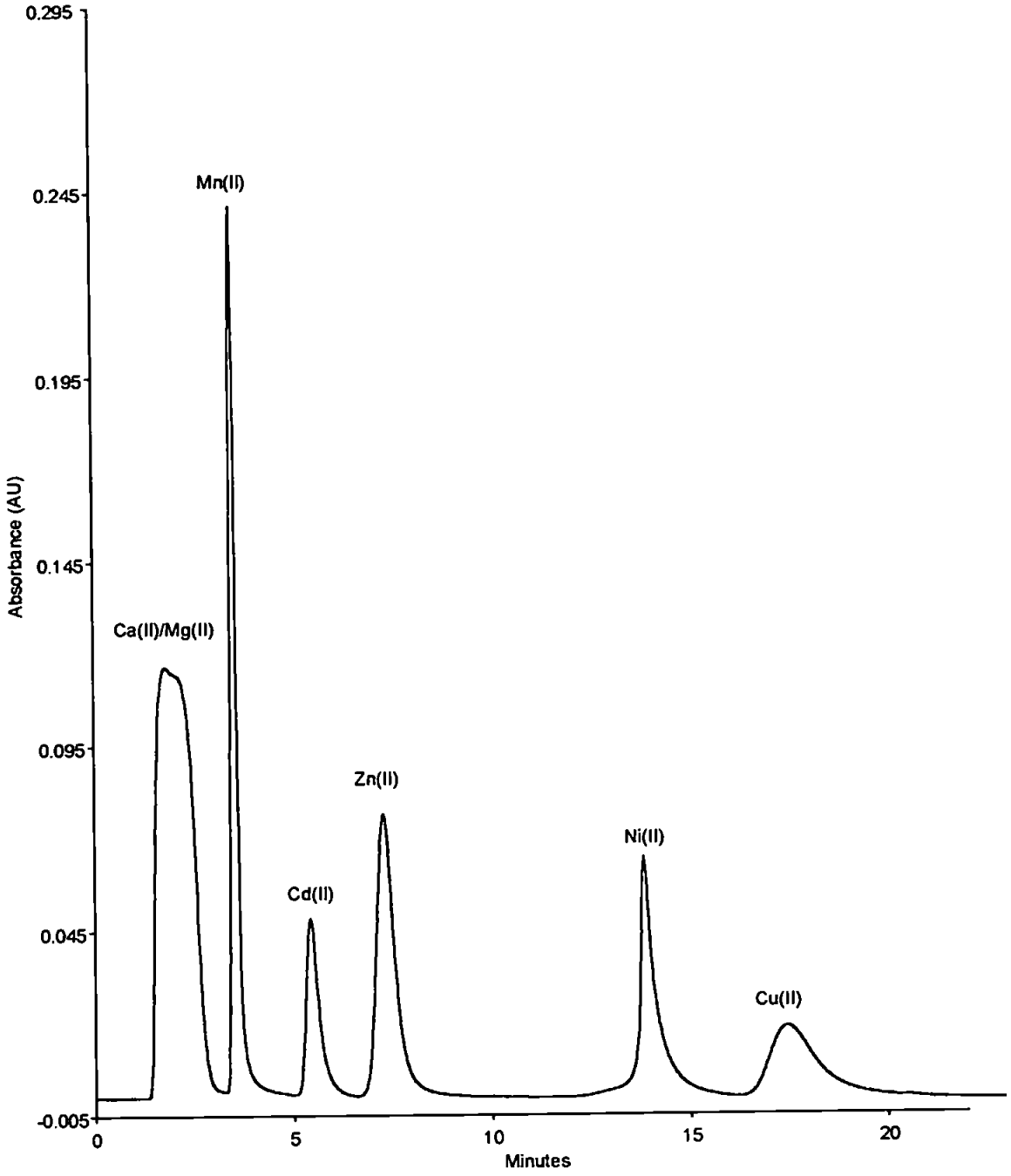

Figure 2.13. Same gradient separation as for Figure 2.11 except sample pH was adjusted to pH6.

For Figure 2.9, a gradient of equilibrating the column at pH 3 then switching to 0.1M HNO_3 for three minutes before the injection was made was used to separate Cd(II), Pb(II) and Cu(II) whereas to separate Mn(II), Cd(II), Zn(II), Pb(II) and Cu(II) as shown in Figure 2.10, a gradient of equilibrating the column at pH 3.5 then switching to pH 2.0 for four minutes before injection and switching immediately to 0.1M HNO_3. For the separation in Figure 2.11 a gradient of equilibrating the column at pH 4.5, injecting and switch to pH 3.15 over the following nine minutes before finally switching to 0.1M HNO_3 was used.

The introduction of Ni(II) into the test mixture dramatically changes the separation profile and has a particular effect upon the elution of Pb(II). Ni(II) produces very poor peak shapes at between pH 2 and pH 3.5 which results in a highly acidic eluent being required to produce a relatively symmetrical peak shape. As a result of this, Pb(II) must be eluted off at approximately pH 2.7 or at a higher pH before the pH can be lowered to approximately pH 1 for the elution of Ni(II) and Cu(II). This results in a much longer run time and a much smaller and broader peak for Pb(II) as is shown in Figures 2.10 and 2.11.

Due to the elution order presented by this column a possible problem that may be found when analysing environmental samples is the presence of the alkali/alkaline-earth metals. These metals, under acidic conditions are eluted together on the solvent front. These metals can be separated, but a pH greater than 8 is generally required when using a XO loaded column [119]. Figure 2.12 shows the effect of relatively large amounts of Ca and Mg under a gradient of equilibrating the column at pH 4.5 then injecting and switching to pH 3 over the next nine minutes before finally switching to 0.1M HNO_3. Even though the combined concentration of the Ca and Mg is two thousand times greater than the concentration of the transition metals present, there is no discernable adverse affect on the

separation except for the co-elution with Mn(II) which can be solved by adjusting the pH of the sample to pH 6 as is shown in Figure 2.13.

Using the gradient elution program as was used for Figure 2.11, calibration curves were constructed for Mn(II), Cd(II), Zn(II), Pb(II), Ni(II) and Cu(II). Both Mn and Cd showed good linearity over a concentration range of 1-100μgl^{-1} and produced regression coefficients of $r^2 = 0.9999$ and 0.9997 respectively while Zn, Ni, Pb and Cu showed good linearity between 5-100μgl^{-1} with regression coefficients of 0.9979, 0.9975, 0.9986 and 1.0000 respectively. Zn, Ni and Cu only show linearity from 5μgl^{-1} due to the presence of underlying contaminant and system peaks which restricted the measurement of peak areas below this concentration. For Pb however, 5μgl^{-1} was the lowest concentration that was detectable.

2.4.3.2. ATA/Hamilton Column.

This column was again prepared as outlined in section 2.3.1.2 i.e by the sonication procedures. Again the 7µm, 100Å resin from Hamilton was used, though a 250 4.6mm ID column was employed with 250ml of a 0.2% dye solution in 20% aqueous methanol being used. After conditioning, the column was determined to have a capacity of 0.02mmolesg^{-1} with a dye loading of 0.151mmolesg^{-1} giving an active dye percentage of 13.2%. The characterisation of the column was carried out in the same manner as for the XO column, that being the repeat injections of transition metal standards over a pH range of 2-4.5. The eluent consisted of 0.1M KNO_3 instead of the 1M KNO_3 as was used for the XO column. The lower ionic strength did not adversely affect the retention characteristics of the column and had the added advantage of lowering the contaminant levels present. Table 2.15 shows

the retention times obtained for this column with Figure 2.14 showing the k' plots for several transition and heavy metals. The k' plot shows a large gap between the slopes for Cd(II) and Pb(II) and between Cd(II) and Ni(II) which illustrates the differences in the resulting retention times of these two metals and confirms the highly selective nature of an ATA impregnated column towards Pb(II) and to a lesser extent towards Cd(II).

Table 2.15. Retention Times (in minutes) for 25cm ATA loaded (7μm Hamilton resin) column (t_0 = 2.35 minutes). Eluent used was 0.1M KNO_3 buffered with 50mM acetic acid with detection at 520nm with PAR.

pH	Mn(II)	Cd(II)	Zn(II)	Co(II)	Pb(II)	Ni(II)	Cu(II)
2.00	3.06	3.08	3.04	3.03	3.14	3.02	4.22
2.50	2.91	3.00	2.93	2.97	3.54	2.95	11.65
3.00	3.37	4.94	3.70	3.61	22.77	3.73	---
3.50	4.43	11.70	5.93	5.54	84.75	5.91	---
4.00	6.77	27.10	10.30	8.82	---	11.00	---
4.50	13.78	---	26.21	17.84	---	27.58	---

Again as with the XO column, it is difficult to separate more than three metals isocratically without getting excessive peak broadening or run times. Figure 2.15 shows the gradient elution of the same suite of metals as was separated on the XO column, though the gradient used was to equilibrate the column at pH 3.3 for fifteen minutes, inject and after a further five minutes switch to pH 2.0 over the following five minutes before switching to 0.25M HNO_3. As can be seen, a completely different retention order is to be found. Pb(II) appears to show a split peak, however this is due to presence of a contaminant peak

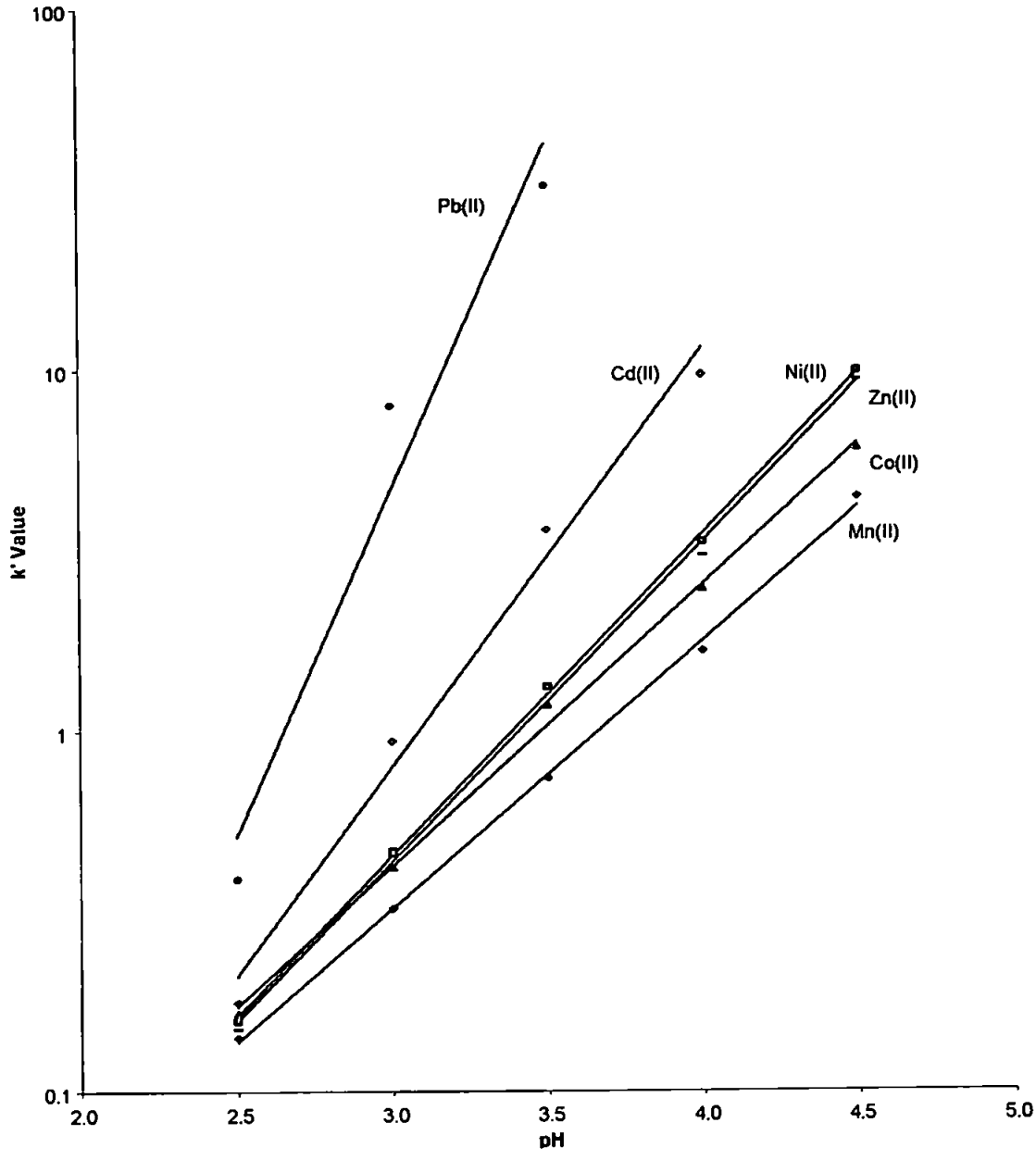

Figure 2.14. The dependence of capacity factors (k') for selected transition and heavy metals on eluent pH with the 25cm ATA/Hamilton column. Eluent used was 0.1M KNO_3 buffered with 50mM acetic acid. Detection was made with PAR/NH_3 at 520nm.

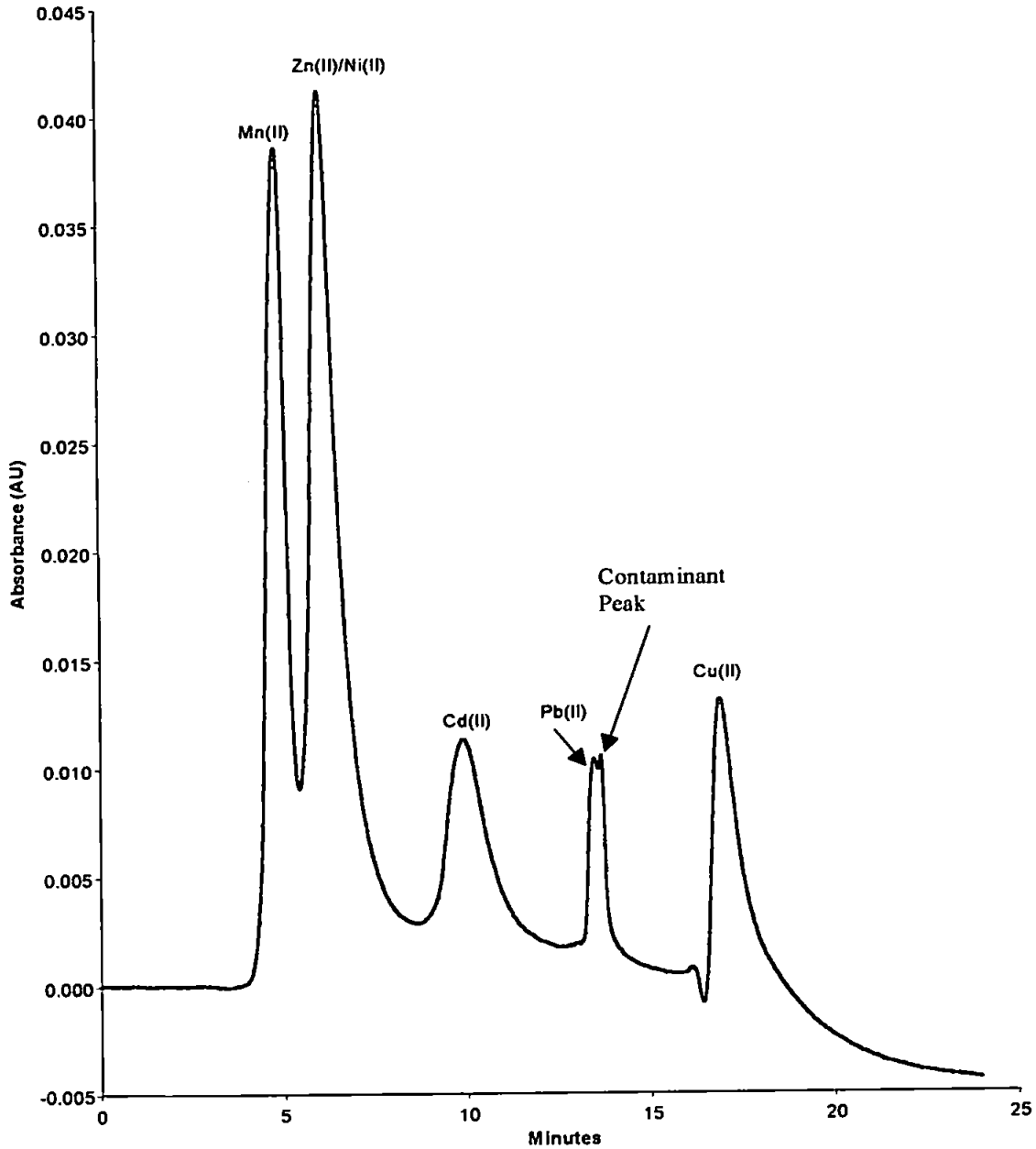

Figure 2.15. Gradient elution of a 100µl mixture of Mn(II), Zn(II), Ni(II),Cd(II), Pb(II) and Cu(II) on the 25cm ATA/7µm Hamilton column. A gradient of equilibriating the column at pH 3.3, injecting then after a further five minutes switching to pH 2 over the following five minutes before switching to 0.25M HNO_3, was utilised. Eluent used was 1M KNO_3 buffered with 50mM acetic acid. Injection volume used was 500µl with detection at 520nm with PAR/Borate PCR. Injection volume used was 500µl with detection at 520nm with PAR/Borate PCR.

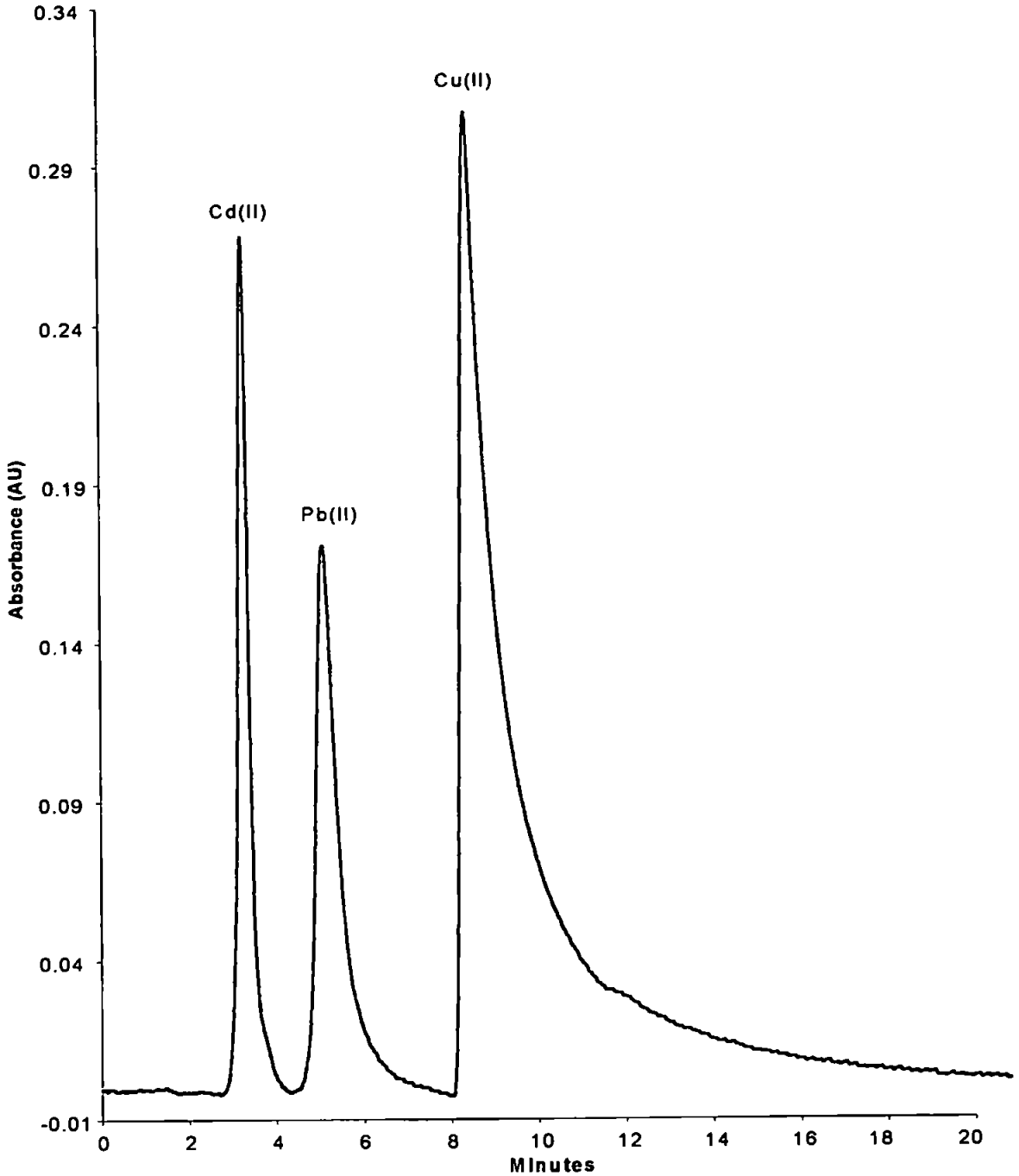

Figure 2.16. Gradient elution of 20mgl^{-1} Cd(II), 10mgl^{-1} Pb(II) and 1mgl^{-1} Cu(II) on the 25cm ATA/7μm Hamilton column. A gradient of equilibriating the column at pH 2.55, injecting then switching to 0.25M HNO_3, was utilised. Eluent used was 1M KNO_3 buffered with 50mM acetic acid. Injection volume used was 100μl with detection at 520nm with PAR/NH_3 PCR.

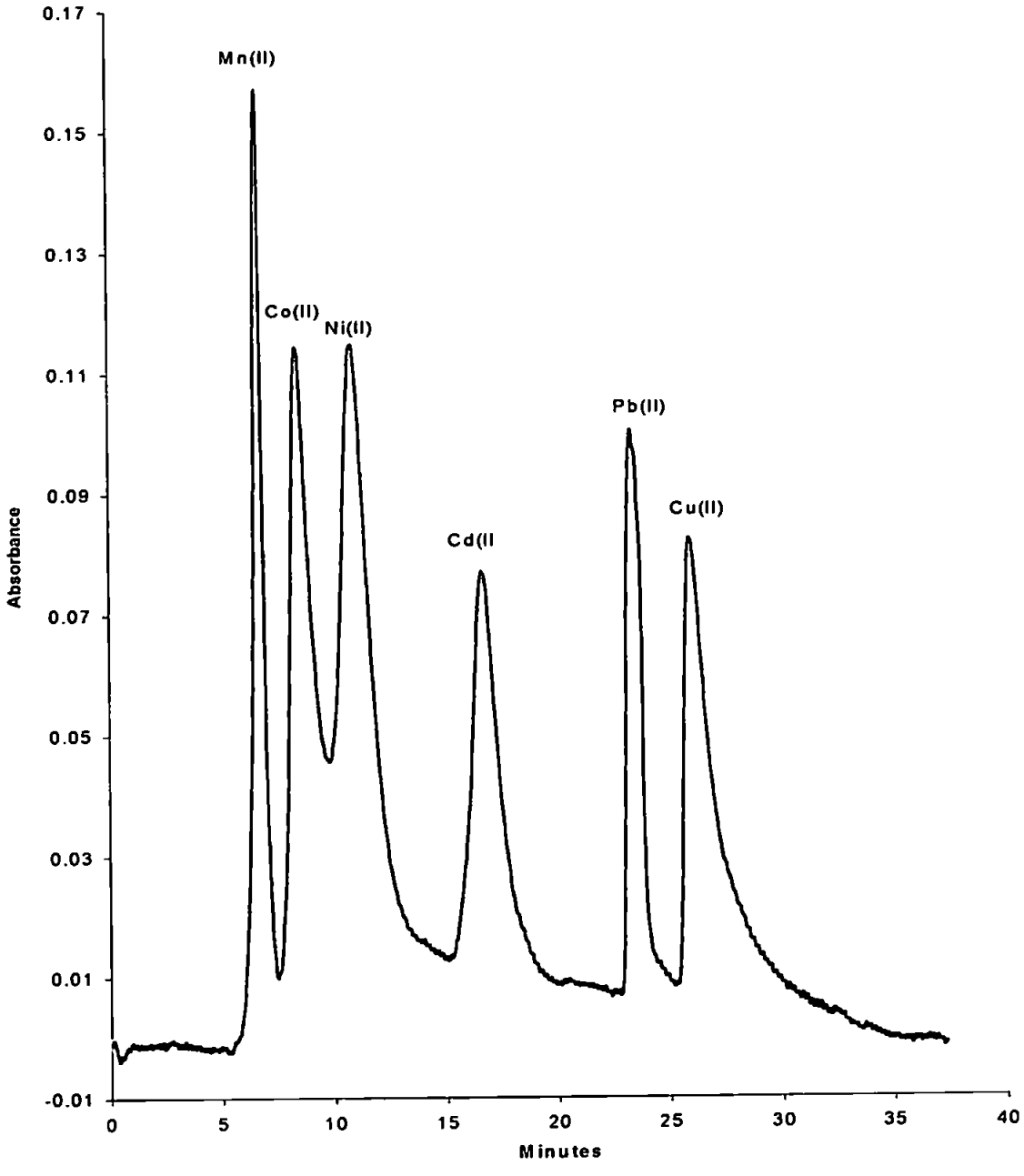

Figure 2.17. Gradient Separation of 1mgl^{-1} Mn(II), 3mgl^{-1} Co(II), 3mgl^{-1} Ni(II), 20mgl^{-1} Cd(II), 5mgl^{-1} Pb(II) and 2mgl^{-1} Cu(II) on the 25cm ATA/7μm Hamilton column. A gradient of equilibriating the column at pH 3.7, injecting then switching to pH 1.8 over the following fifteen minutes. After a further five minutes the eluent was switched to 0.1M HNO_3, was utilised. Eluent used was 0.1M KNO_3 buffered with 50mM acetic acid. Injection volume used was 100μl with detection at 520nm with PAR/NH_3 PCR.

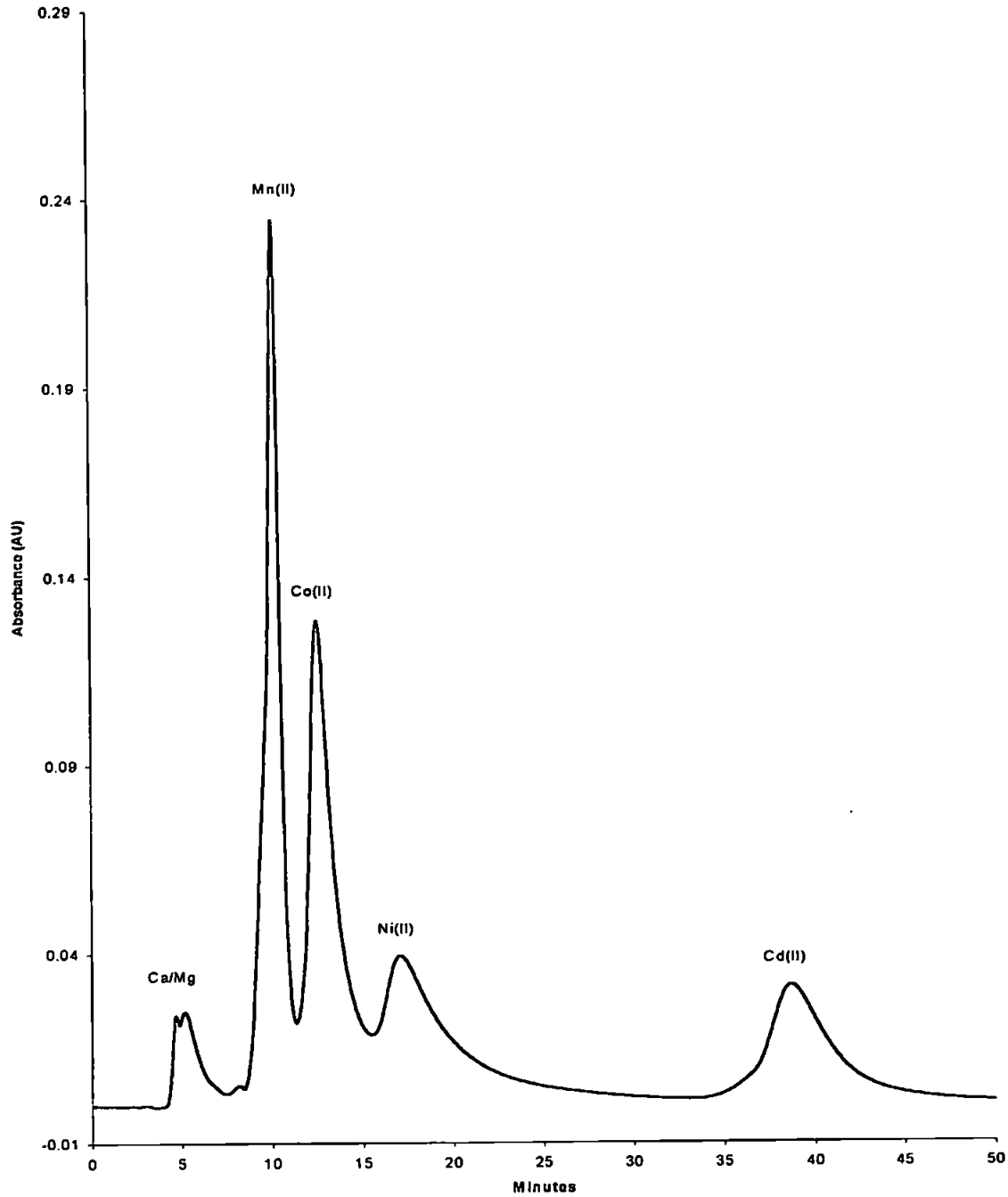

Figure 2.18. Isocratic separation of 1mgl^{-1} mixture of Mn(II), Co(II), Ni(II) and Cd(II) from 150mgl^{-1} Ca(II) and 50mgl^{-1} Mg(II) on the 25cm ATA/Hamilton column at pH3.9. The eluent used was 0.1M KNO_3 buffered with 50mM acetic acid. Injection volume used was 500µl with detection at 520nm with PAR/Borate PCR.

underlying the Pb(II) peak. Zn(II) and Ni(II) are shown to co-elute though they could be separated if a much higher pH was used though excessive run times would be the result. Figure 2.16 uses a gradient of equilibrating at pH 2.55 then injecting and switching to 0.25M HNO_3 whereas the gradient used for Figure 2.17 consisted of equilibrating the column at pH 3.7, injecting and then switching to pH 1.8 over the next fifteen minutes. After a further five minutes the eluent was switched to 0.1 M HNO_3. The presence of Ca and Mg again appears to not affect this column's separating performance. The isocratic elution in Figure 2.18 shows that their presence only results in a little fronting on the Mn(II) peak.

A calibration curve was constructed for Cd(II), Pb(II) and Cu(II) as these were the three metals of principal interest. All three of these metals showed acceptable linearity over the concentration range 5-100μgl^{-1} with regression coefficients of r^2 = 0.9988, 0.9875 and 0.9964 respectively. Once more the presence of contaminant peaks makes it difficult to accurately determine peak areas underneath the Pb and Cu peaks.

2.4.3.3. Comparison of XO and ATA columns.

The most noticeable difference between these two columns is their selectivity towards the transition and heavy metals investigated. For XO the elution order is Mn<Cd<Zn<Co<Pb<Cu whereas for ATA it is Mn<Co<Zn<Ni<Cd<Pb<Cu. Ni is not included in the elution order of XO due to the problems found with its elution, namely the excessive tailing that is obtained at all but the most acidic pHs i.e. <pH 1.5, and its virtually static retention time up to pH3. At pH 3 the tailing that Ni experiences on the XO column is so pronounced that it is barely detectable. However elution under the same

conditions on the ATA column produces a highly symmetrical peak in comparison, as is demonstrated in Figure 2.19. This is thought to be as a result of the difference in functional group of these two dyestuffs. XO is a N, O, O chelator whilst ATA is a O, O chelator and it is theorised that the presence of nitrogen in the IDA functional group of XO is slowing down the kinetics of complex dissociation. An interesting point to note is that Cd(II) is eluted after Zn(II) on the ATA column. This is unusual in that Cd(II) is generally eluted before Zn(II) with only Chrome Azurol-S loaded columns [162] showing a similar reversal in elution order as CAS contains carboxylic acid functional groups. This reversal appears to be a charateristic of O, O chelating molecules.

Another major difference found between these two columns is the greater inherant selectivity of ATA towards Cd(II) and Pb(II). This greater selectivity is shown in the slopes of the k' plots signifying the large difference in the conditional stability constants between these metals and the others investigated. The difference in selectivities becomes even more important when compared to the selectivities of other similar dyestuffs. Studies by Paull [119] and Shaw [120] have shown that the selectivity that XO shows is all but identical to the selectivities of a wide range of dyestuffs, with the dyestuffs that offer O, O chelation the only ones to show significant differences in the retention order for transition and heavy metals. The exception to this appears to be PAR, a N, O, O chelator, which also shows major differences in retention order.

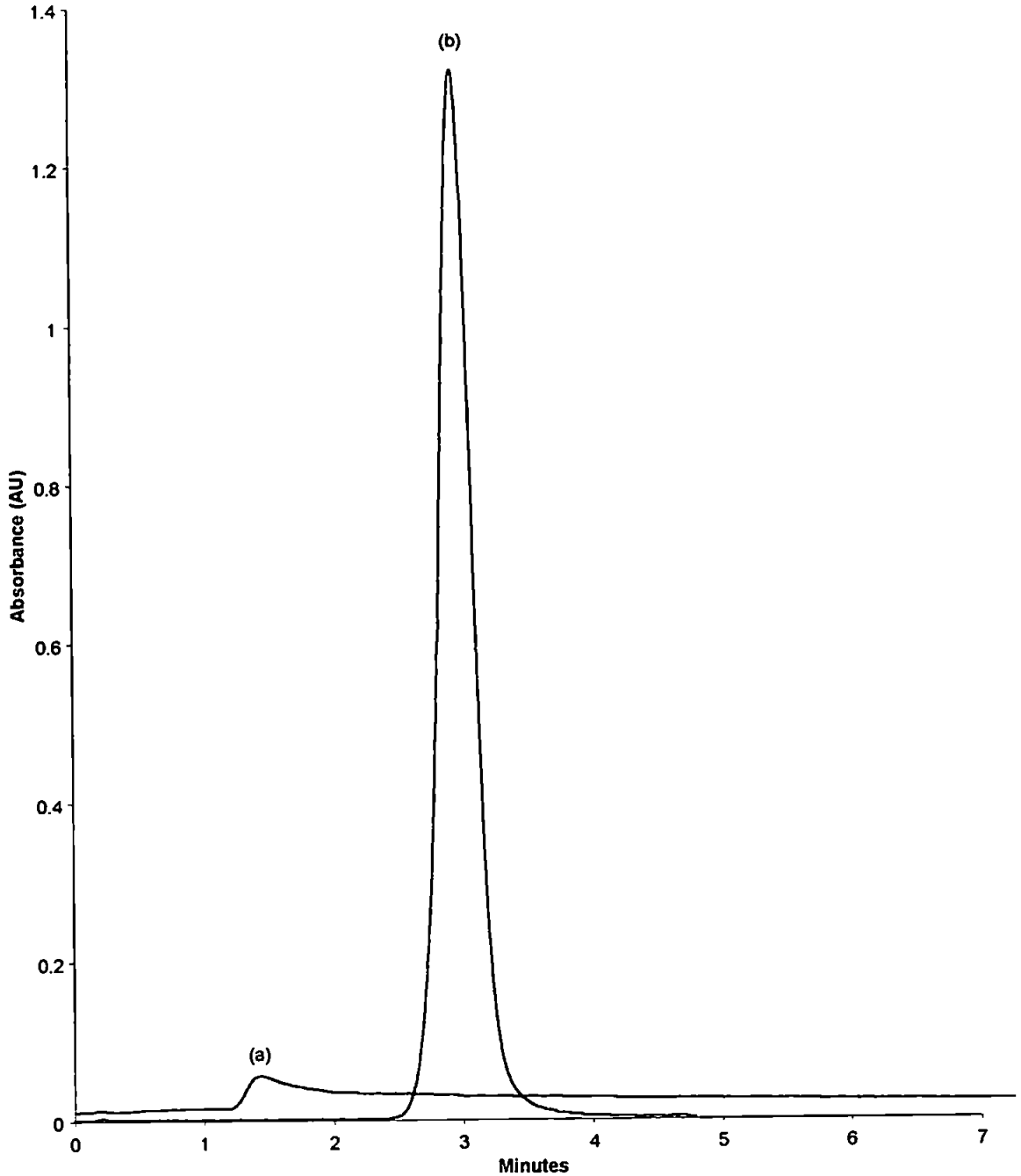

Figure 2.19. The difference in Ni(II) elution at pH3 on the XO/Hamilton column (a) and the ATA/Hamilton column (b).

2.5. Analysis of Transition Metals in Mineral Waters.

2.5.1. Introduction.

The determination of trace metal concentrations in environmental samples is one of the most important areas of analytical chemistry. Two of the most challenging metals to determine are Cd(II) and Pb(II). Cadmium is a silvery metal first discovered by F. Stromeyer in 1817 and has the atomic number 48 and atomic mass of 112.40 [19]. Its abundance in the earth's crust is 0.11ppm and between $1.1x10^{-6}$ and $100x10^{-6}$ ppm in seawaters [169]. It has found use in rechargeable batteries, alloys and pigments though due to its toxicity its use is being phased out. There is no principal ore of cadmium though most cadmium is produced as a by-product of the smelting of zinc. Lead is a soft, weak ductile metal that is dull grey in colour and has the atomic number 82 and an atomic mass of 207.19 [19]. The main ore of lead that is found is Galena which produces silver as a by-product. It has an abundance of 14ppm in the earth's crust and between $1x10^{-6}$ and $30x10^{-6}$ ppm in seawaters [169]. Lead has found use in many areas including batteries, glass and radiation shielding as well as in paints and as an anti-knock agent in petrol.

There are relatively few IC methods for the simultaneous detection of Cd(II) and Pb(II) in real samples. There are several reasons for this, one of which is poor sensitivity. Transition and heavy metals are generally separated as anionic dipicolinic acid complexes on a mixed mode cation and anion exchange column [13]. Pb(II) however, complexes strongly with dipicolinic acid, log k_1 = 5.1 [95] which can interfere with the sensitivity of post column reaction systems involving chromogenic ligands such as PAR. Though weaker complexing agents such as oxalic acid can be used, the resulting detection limits are still too high for practical purposes.

Another problem with ion-exchange separations is their susceptibility towards ionic strength and the presence of matrix metals such as the alkaline-earth metals. For example, Ding et al [170] found that Ca(II) and Mg(II) at concentrations greater than $10mgl^{-1}$ reduced retention times for transition and heavy metals thereby affecting the columns selectivity. HPCIC does not suffer from these problems. The XO and ATA loaded columns previously discussed were used for the development of a method for trace Cd(II), Pb(II) and Cu(II) determinations in highly mineralised waters.

2.5.2. Instrumentation.

The instrumentation used in this study was as described in section 2.2.1. Detection was made at 520nm using the PAR/Borate PCR.

2.5.3. Reagents.

For the studies involving the XO column, the eluent used consisted of 1M KNO_3 buffered with 50mM acetic acid and prepared in MilliQ water then adjusted to the required pH using either conc HNO_3 or 5M NaOH. For the studies involving the ATA column, the eluent used was the same except that only 0.1M KNO_3 was used. The PCR used was PAR which consisted of 0.1mM PAR, 0.125M di-sodium tetraborate adjusted to pH 10.5 with 5M NaOH.

All reagents were from BDH unless otherwise stated and of AnalaR grade. PAR was supplied by Fluka (Fluka, Glossop, UK). Metal standards were prepared from $1000mgl^{-1}$

stock solutions which were diluted to working standards using the eluent and stored in poly(propylene) bottles.

2.5.4. Results and Discussion.

To assess the ability of both the XO and ATA columns to cope with a complex sample matrix, a commercially available highly mineralised water (Badoit, Danone, France) was investigated. This mineral water contained elevated levels of the alkali and alkaline-earth metals with concentrations of 190mgl^{-1} Ca(II), 85mgl^{-1} Mg(II), 150mgl^{-1} Na and 10mgl^{-1} K. Even though the elution orders are different for these two columns with ATA being more selective towards the metals of interest, a gradient elution program had to be developed for both columns. For the XO column, the gradient developed entailed equilibrating the column at pH 4.5 for 15 minutes, injecting the sample and immediately switching to an eluent of pH 3.15 which switches linearly to 0.1M HNO_3 over a period of 9 minutes. For the ATA column, the system was equilibrated at pH 4.5 for 15 minutes, injecting the sample and switching immediately to pH 3.5 for a further 10 minutes before switching to 0.1M HNO_3. Calibration curves were constructed using metal standard solutions to assess the method and are shown in Figures 2.20 and 2.21. All three metals showed good linearity over a concentration range of 1-100μgl^{-1} for the XO column and 5-100μgl^{-1} for the ATA column with Cd(II), Pb(II) and Cu(II) producing regression coefficients of r^2 = 0.9994, 0.9973 and 0.9995 respectively on the XO column and 0.9963, 0.9835 and 0.9989 respectively on the ATA column. The detection limits obtained were good and calculated as twice the baseline noise. Values of 1μgl^{-1}, 5μgl^{-1} and 5μgl^{-1} were recorded for Cd(II), Pb(II) and Cu(II) respectively on both the XO and ATA columns.

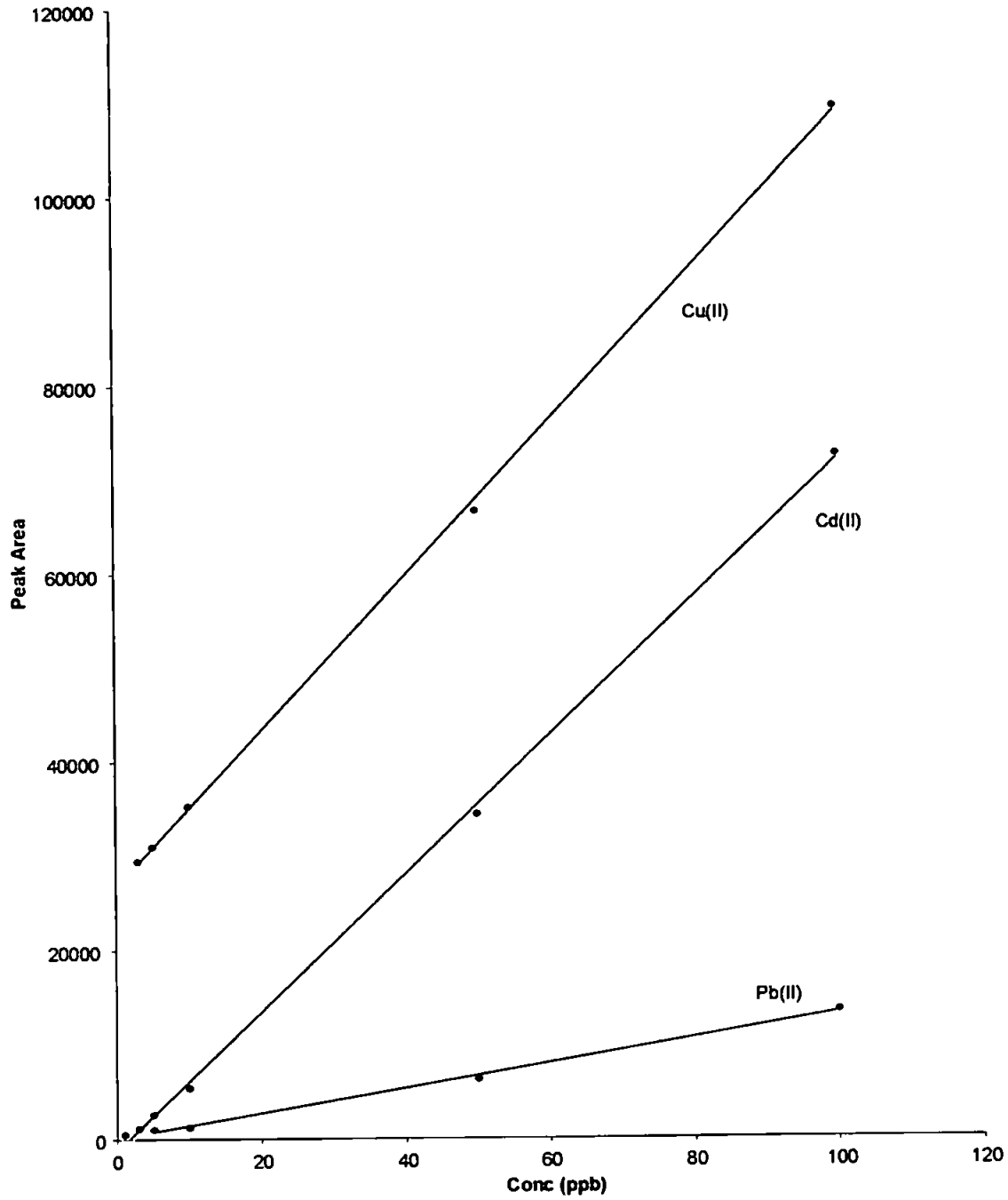

Figure 2.20. Calibration curves for Cd(II), Pb(II) and Cu(II) standards on the 10cm XO/7μm Hamilton column. The eluent used was 1M KNO_3 buffered with 50mM acetic acid. Injection volume used was 500μl with detection at 520nm with PAR/Borate PCR.

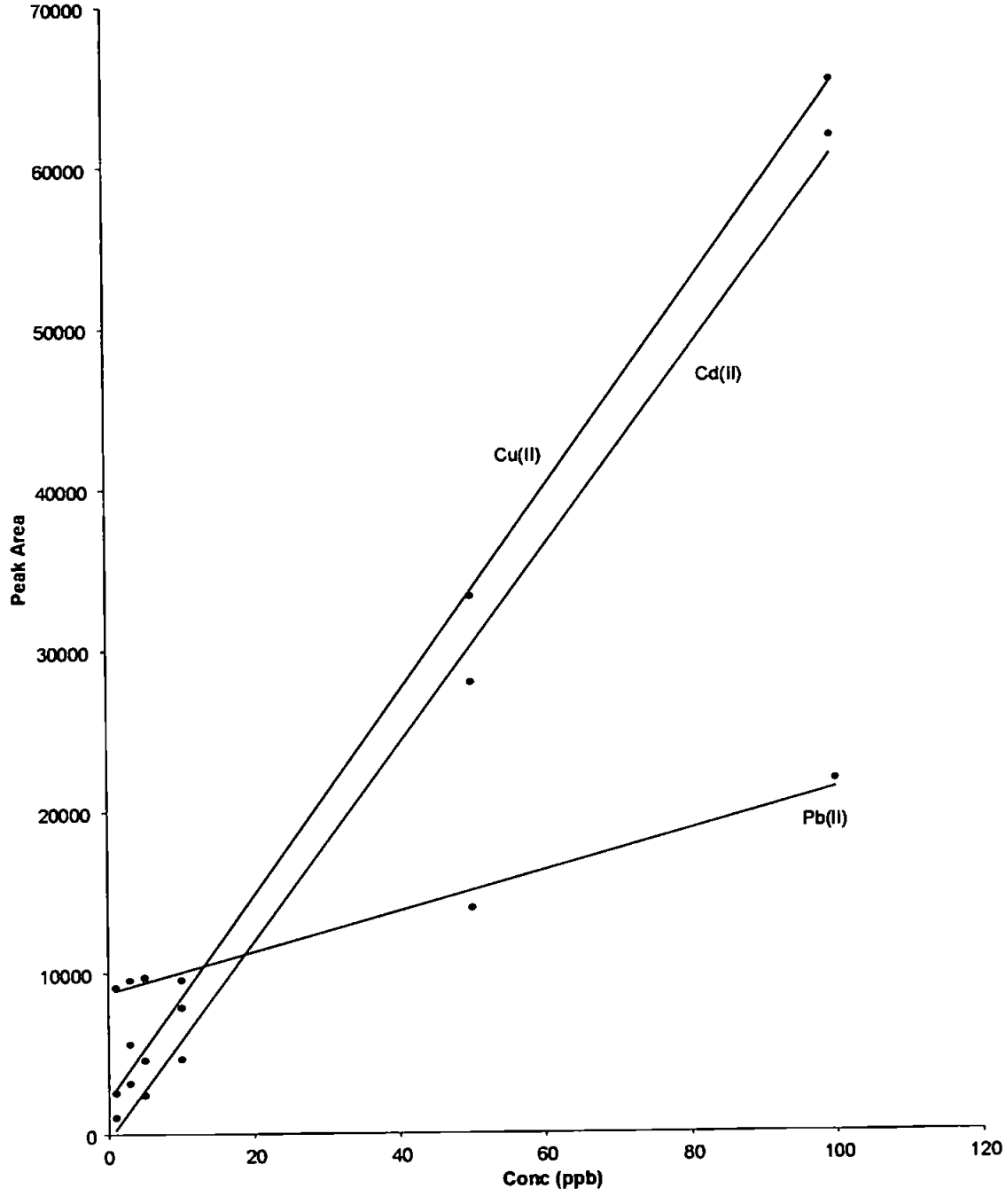

Figure 2.21. Calibration plots for Cd(II), Pb(II) and Cu(II) standards on the 25cm ATA/7μm Hamilton column. The eluent used was 0.1M KNO_3 buffered with 50mM acetic acid. Injection volume used was 500μl with detection at 520nm with PAR/Borate PCR.

The Badoit mineral water had a natural pH of 6.5. This was adjusted to the starting pH of the gradient program used after spiking with known concentrations of Cd(II), Pb(II) and Cu(II). Spiking was carried out as the concentrations of the metals of interest were below the limits of detection for this method though the method could be improved by the use of larger volume injections. Calibration curves were constructed for the spiked mineral water over a concentration range of 1-100μgl^{-1} for the XO column and 5-100μgl^{-1} for the ATA column and are shown in Figure 2.22-2.25.

Again good linearity was found with regression coefficients of r^2 = 0.9958, 0.9967 and 0.9964 for Cd(II), Pb(II) and Cu(II) respectively on the XO column and 0.9942, 0.9959 and 0.9994 respectively on the ATA column. The reproducibility (%RSD) of the method was calculated with repeat injections (n=6) of a mineral water sample spiked with 30μgl^{-1} Cd(II), 80μgl^{-1} Pb(II) and 80μgl^{-1} Cu(II) and determined to be 0.77%, 2.07% and 8.36% for these respective metals on the XO column and 4.5%, 18.5% and 4.79% on the ATA column. The %RSD for Pb(II) on the ATA column is higher due to the presence of a contaminant peak as well as the close proximity of a "gradient peak" both of which makes accurate measurements highly difficult. Figure 2.26-2.29 shows examples of both the spiked and non-spiked Badoit mineral water on both the XO and ATA columns.

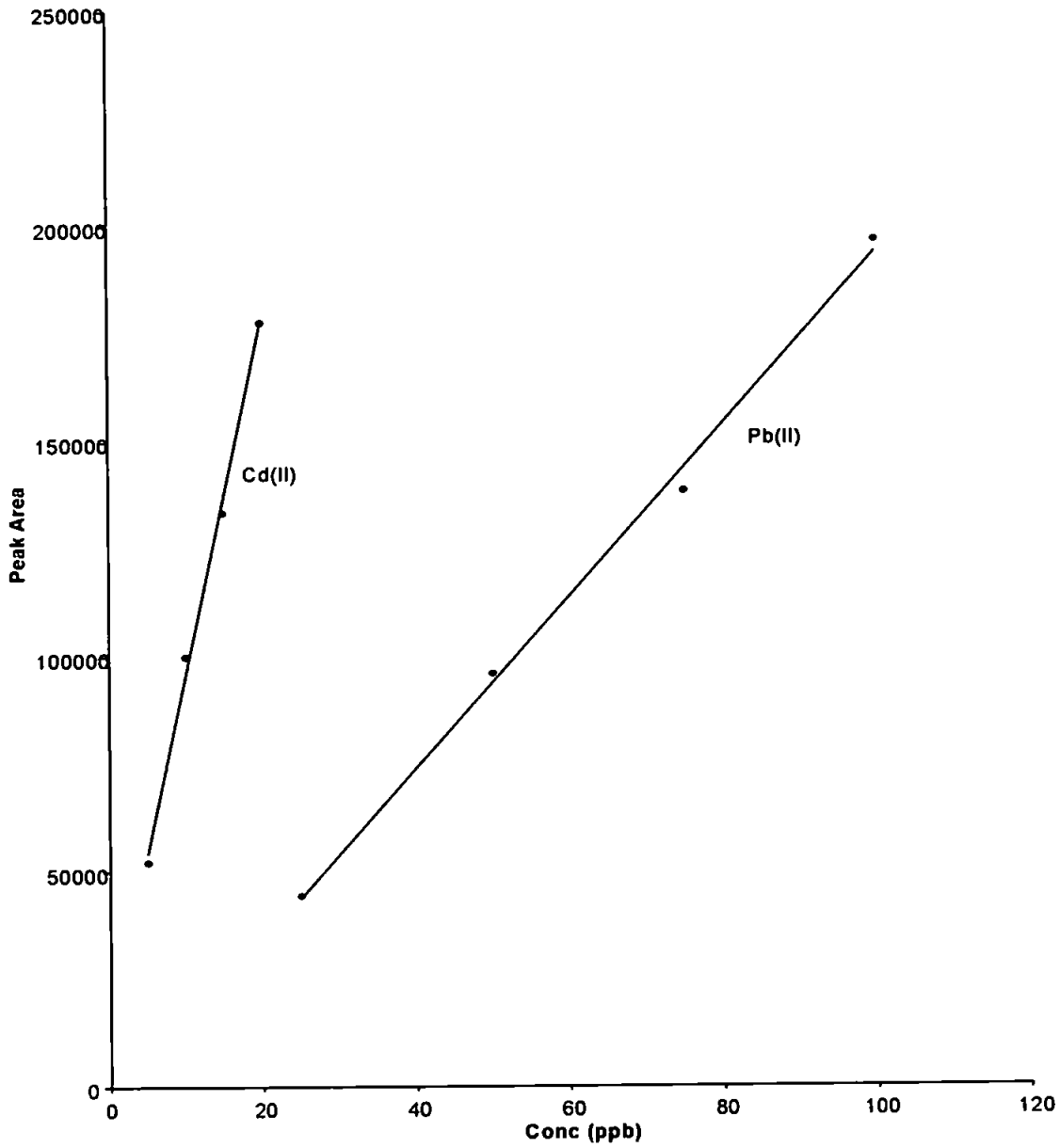

Figure 2.22. Calibration curves for Cd(II) and Pb(II) in spiked Badoit mineral water on the 10cm XO/7μm Hamilton column. The eluent used was 1M KNO_3 buffered with 50mM acetic acid. Injection volume used was 500μl with detection at 520nm with PAR/Borate PCR.

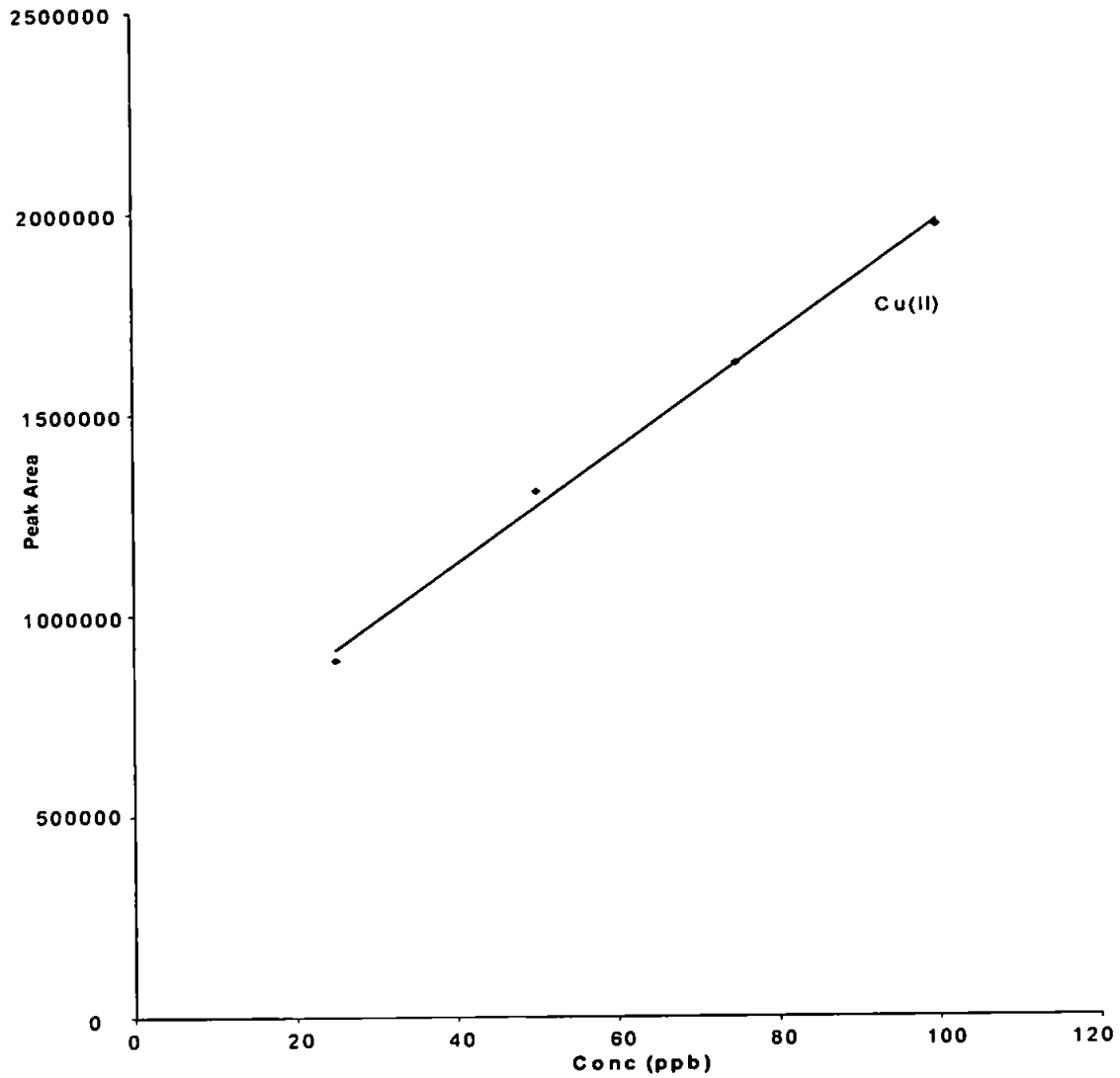

Figure 2.23. Calibration curve for Cu(II) in spiked Badoit mineral water on the 10cm XO/7μm Hamilton column. The eluent used was 0.1M KNO_3 buffered with 50mM acetic acid. Injection volume used was 500μl with detection at 520nm with PAR/Borate PCR.

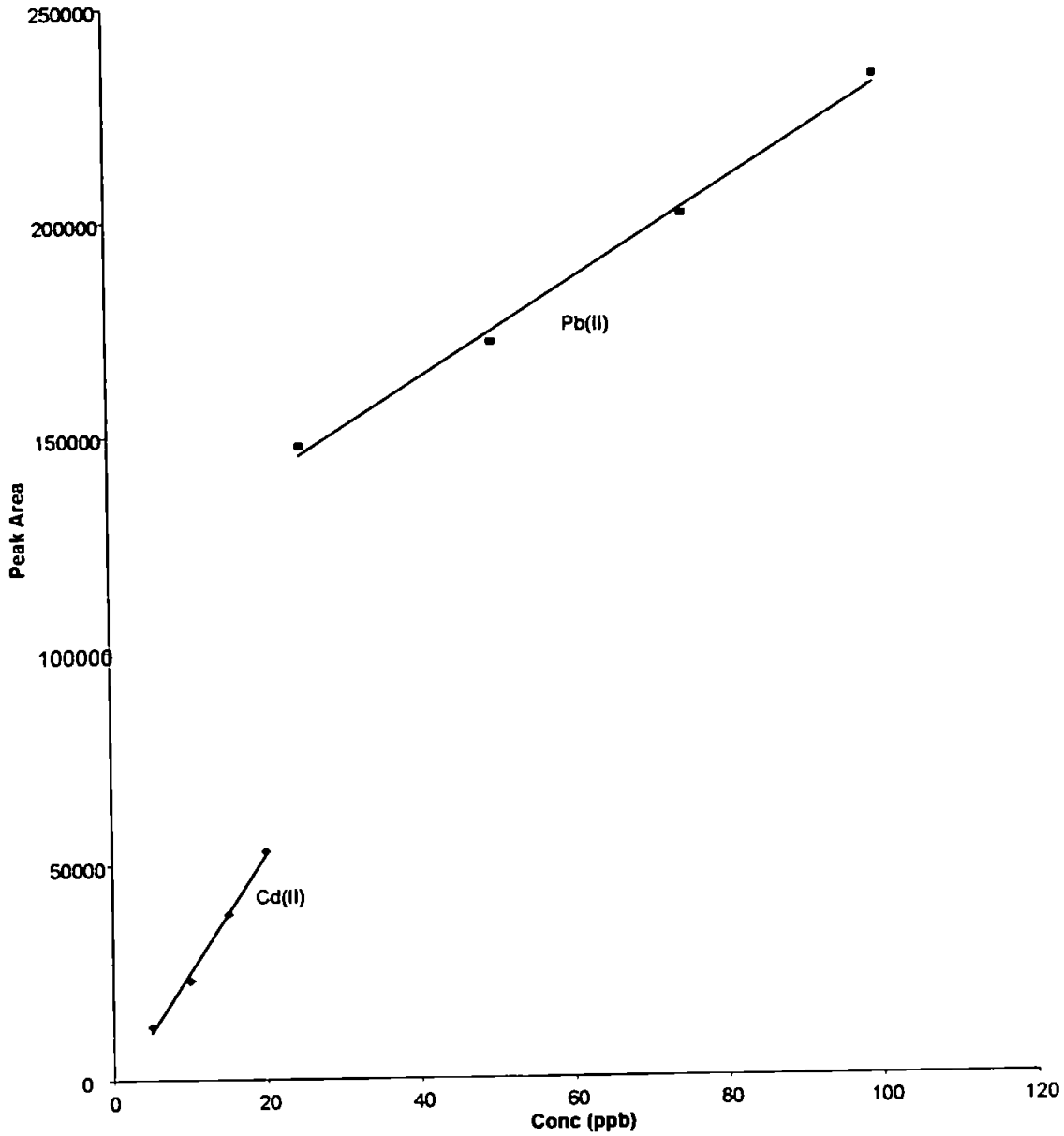

Figure 2.24. Calibration curves for Cd(II) and Pb(II) in spiked Badoit mineral water on the 25cm ATA/7μm Hamilton column. The eluent used was 0.1M KNO_3 buffered with 50mM acetic acid. Injection volume used was 500μl with detection at 520nm with PAR/Borate PCR.

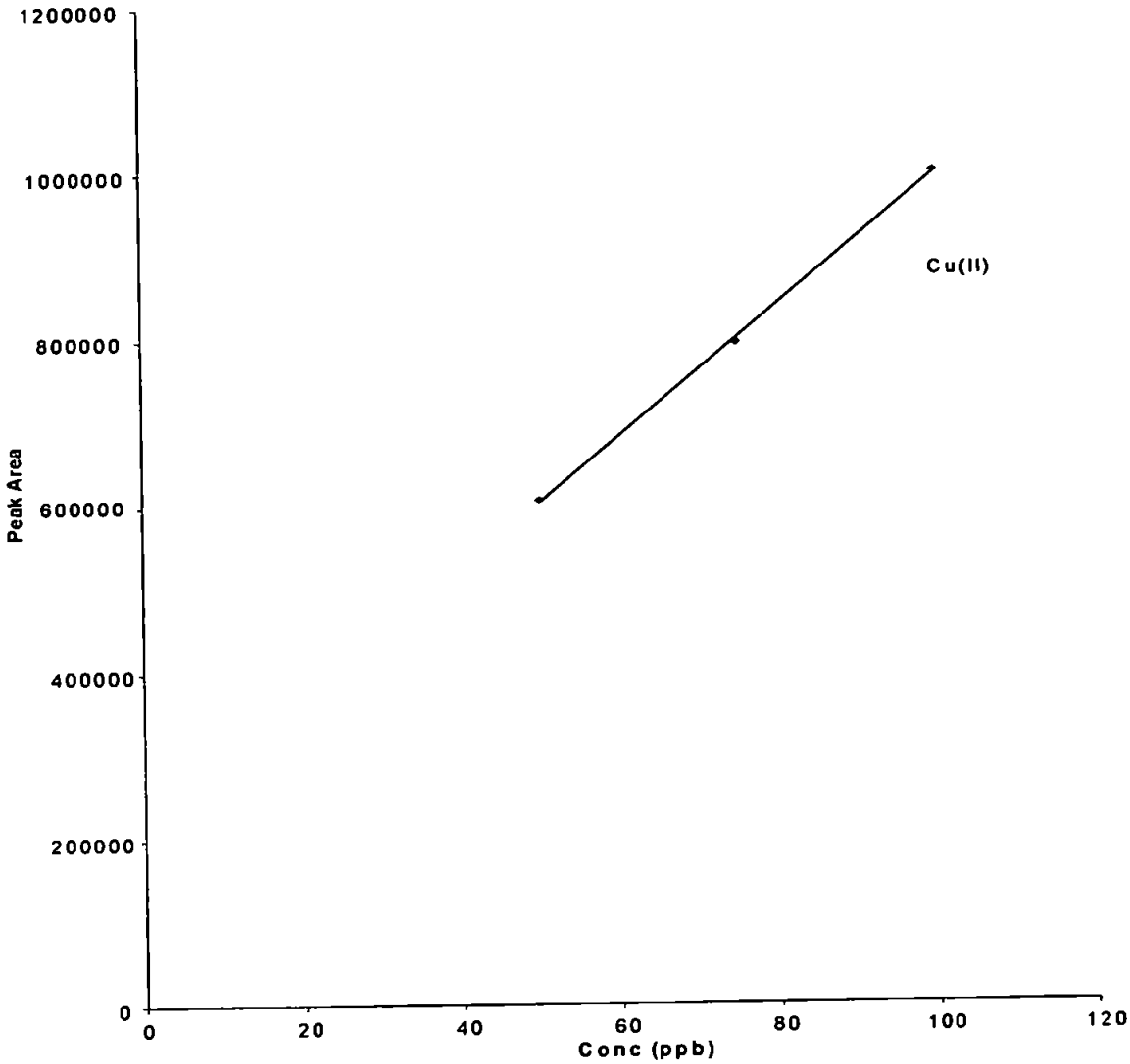

Figure 2.25. Calibration curve for Cu(II) in spiked Badoit mineral water on the 25cm ATA/7μm Hamilton column. The eluent used was 0.1M KNO_3 buffered with 50mM acetic acid. Injection volume used was 500μl with detection at 520nm with PAR/Borate PCR.

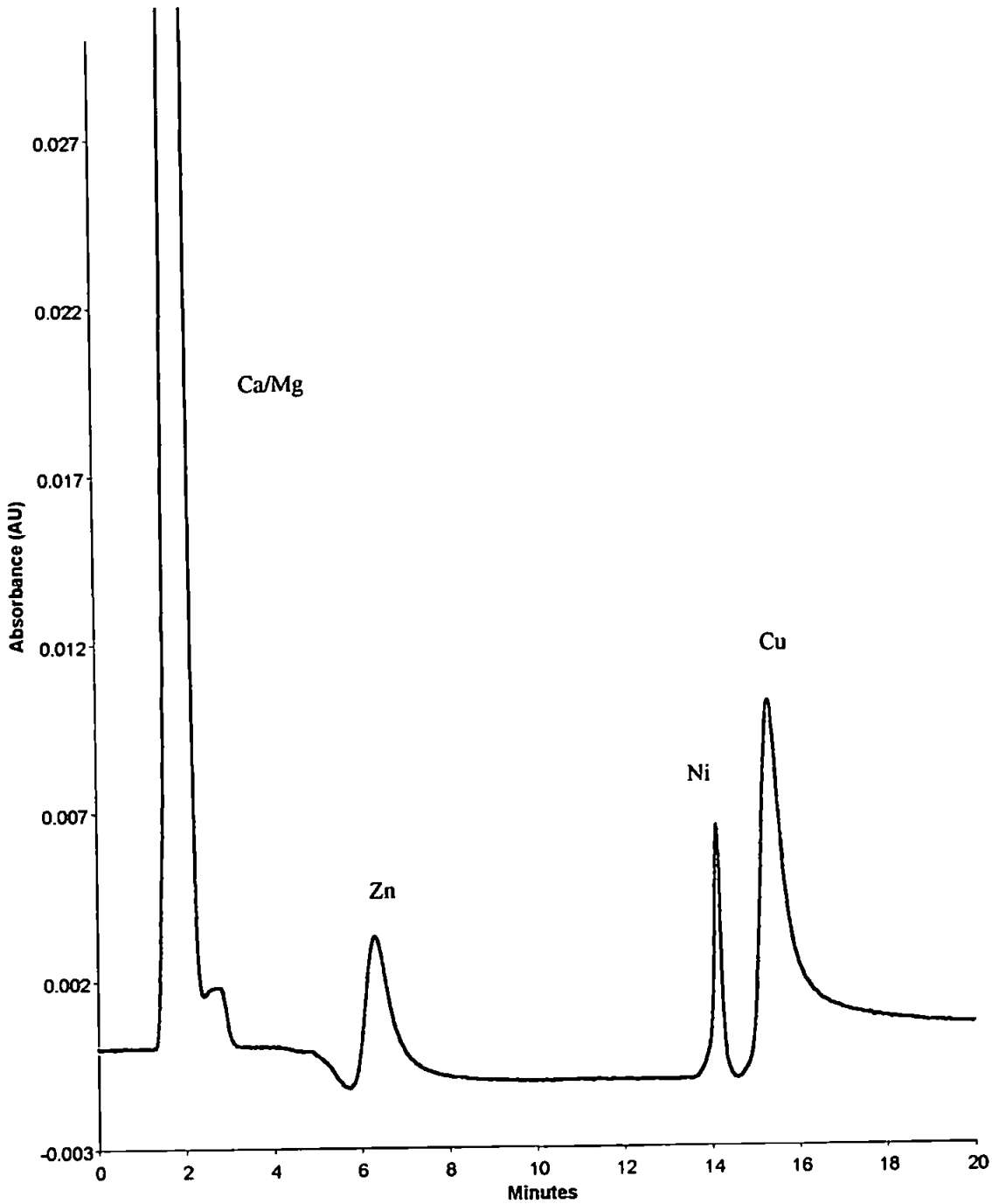

Figure 2.26. Gradient elution of Badoit mineral water on the 10cm XO/7μm Hamilton column. A gradient of equilibriating the column at pH 4.5 for fifteen minutes, injecting then immediately switching to pH 3.15 which switches to 0.1M HNO_3 over the following nine minutes was utilised. Eluent used was 1M KNO_3 buffered with 50mM acetic acid. Injection volume used was 500μl with detection at 520nm with PAR/Borate PCR.

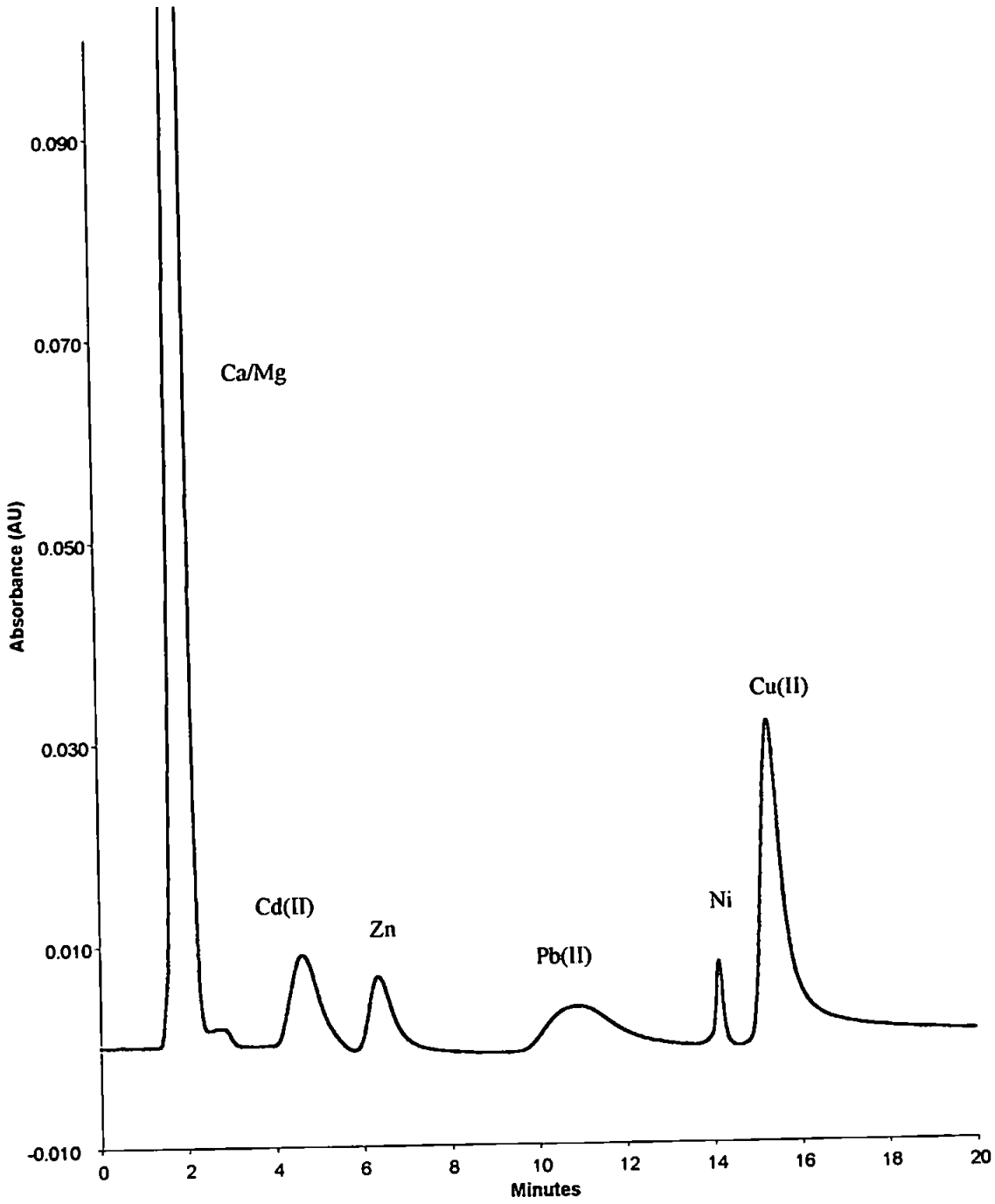

Figure 2.27. Gradient elution of Badoit mineral water spiked with 50μgl^{-1} Cd(II), 200μgl^{-1} Pb(II) and 50μgl^{-1} Cu(II) on the 10cm XO/7μm Hamilton column. Gradient and conditions used were as for Figure 2.26.

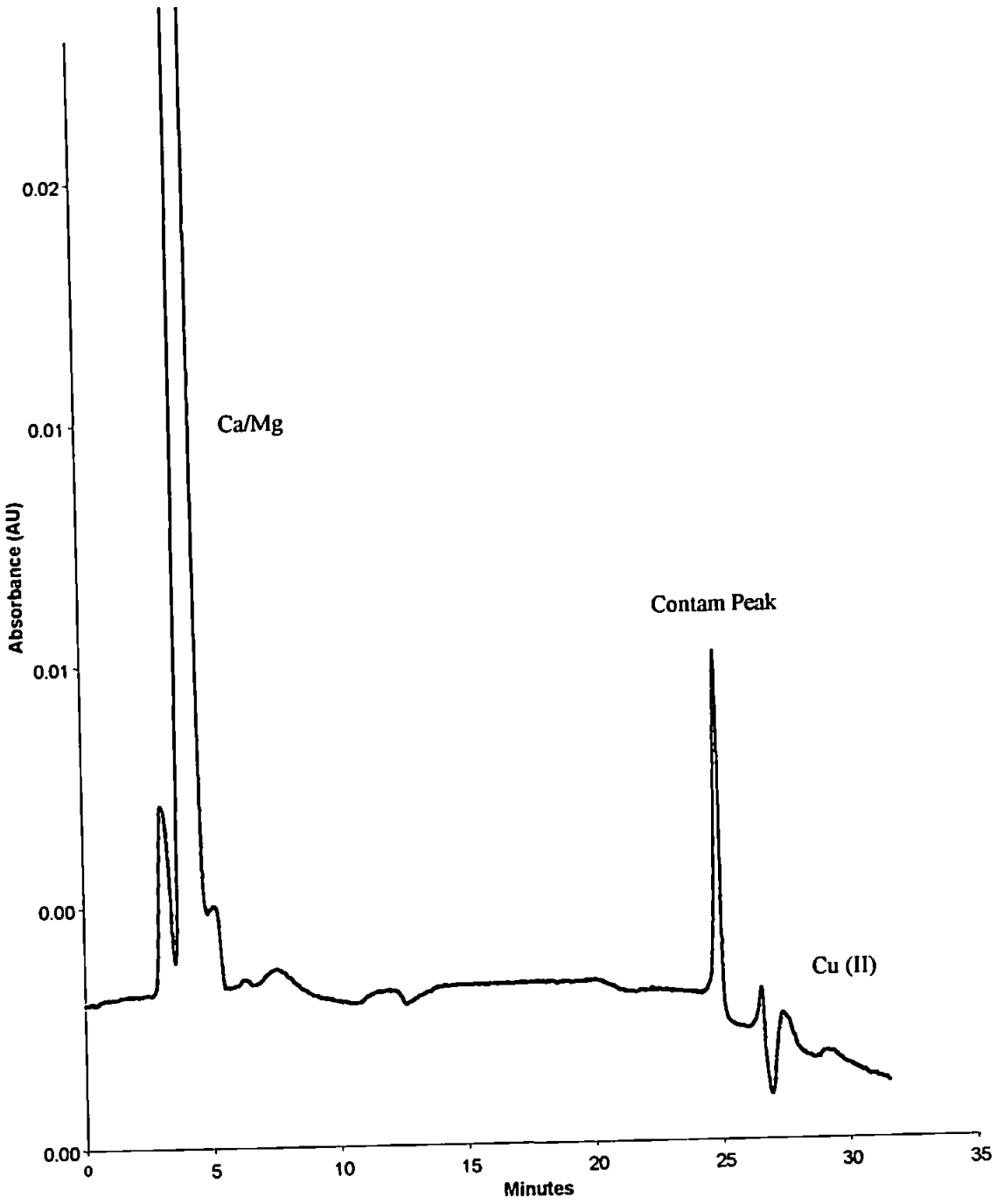

Figure 2.28. Gradient elution of Badoit mineral water spiked on the 25cm ATA/7μm Hamilton column. A gradient of equilibriating the column at pH 4.5 for fifteen minutes, injecting then immediately switching to pH 3.15 for a further ten minutes before switching to 0.1M HNO_3 was utilised. Eluent used was 1M KNO_3 buffered with 50mM acetic acid. Injection volume used was 500μl with detection at 520nm with PAR/Borate PCR.

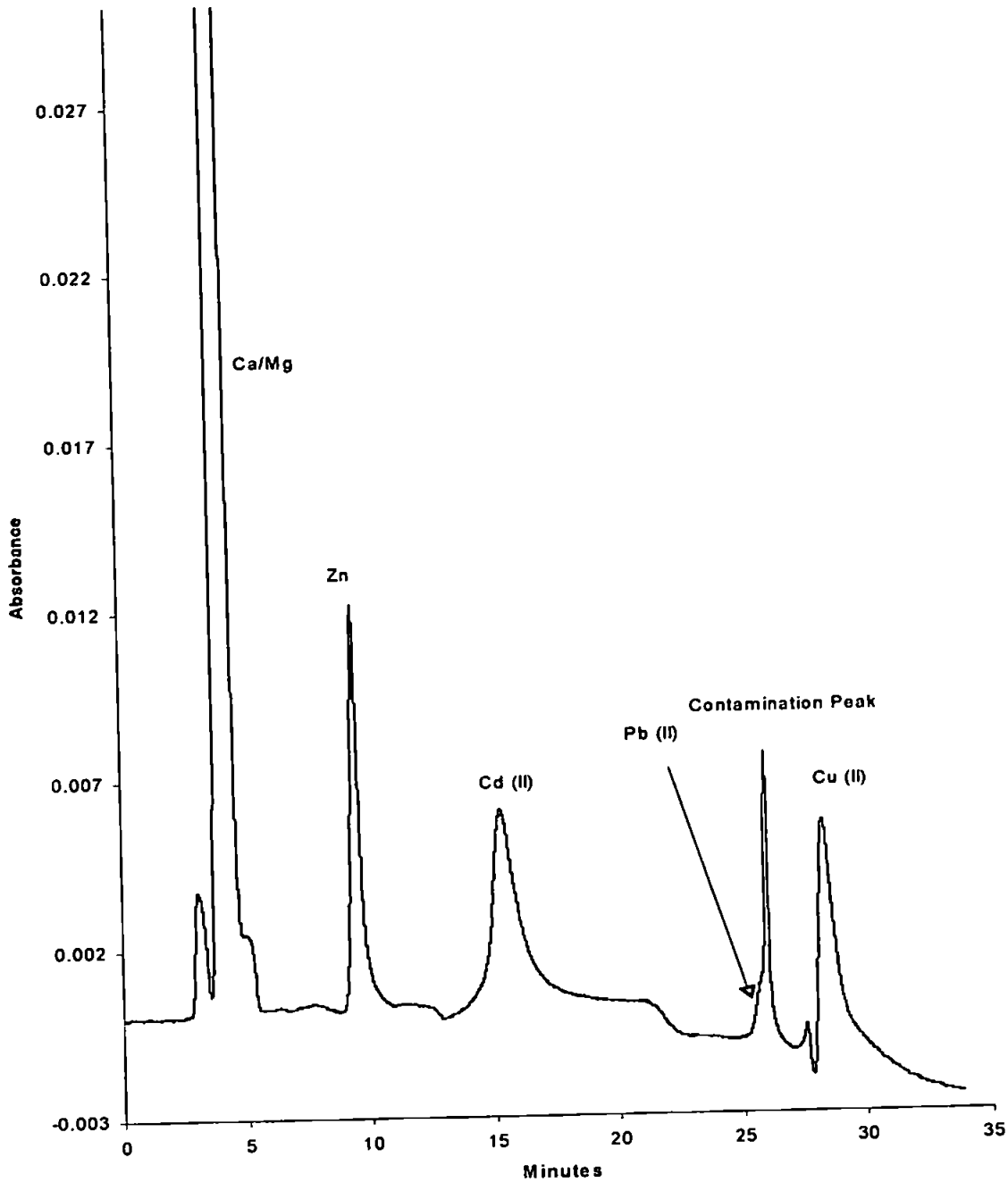

Figure 2.29. Gradient elution of Badoit mineral water spiked with 100μgl^{-1} Cd(II), 50μgl^{-1} Pb(II) and 50μgl^{-1} Cu(II) on the 25cm ATA/7μm Hamilton column. Gradient and conditions used were as for Figure 2.28.

2.6. Summary.

The investigations discussed in this chapter have highlighted the many advantages of high efficiency dye impregnated substrates. Firstly, these dye impregnated columns have shown that they have a considerable working life span. Even after seven years and being allowed to dry out, they can still produce efficient separations of individual metal ions. The 10cm XO/Hamilton column was used continuously over a time frame of one year under potentially damaging gradient elution programs without any decline in column efficiency.

Unlike traditional IC columns, high ionic strength and high concentrations of matrix metals does not adversely affect the retention and separation of transition and heavy metal ions. Matrix matching of the sample with the eluent is important, particularly pH, for the attainment of good peak shapes over the pH range of 2-5.

The differing selectivities offered by the two chelating dyes used, highlights the versatility of HPCIC in that a column, with a suitable capacity, can be fabricated with a dye that can be highly selective towards potentially only the metals of interest. The overall reversal of retention when compared to traditional IC columns is another advantage in that the alkali and alkaline-earth metals are not retained at low pHs and therefore, do not have any discernable affect upon the retention of the transition and heavy metals.

The development of ultrasonic impregnation has resulted in a method which can produce a chelating column of similar if not greater efficiency to one prepared using continuous flow impregnation. Ultrasonic impregnation does offer other significant advantages over the continuous flow method. These include lower conditioning times, upto 3 days in

comparison with upto 5 days for the continuous flow method. Perhaps the most important advantage over the continuous flow method is that the ultrasonic method enables a column to be stripped and reloaded with a fresh dye solution without any adverse affects, as was shown with the column prepared using the 8μm PLRP-S resin. When this is done using the continuous flow method, the resulting column generally shows not only a decrease in efficiency but also poor peak shapes and poor reproducibility.

The analysis of the Badoit mineral water has shown that these dye impregnated columns are perfectly suitable for the analysis of samples of high ionic strength. The presence of high levels (>1000x) of Mg^{2+} and Ca^{2+} relative to the metals of interest does not have any adverse affect on the retention or peak shapes of the metal ions under analysis. If the Mg^{2+} and Ca^{2+} levels were at vastly increased levels or if the Zn^{2+} concentration was much greater, the ATA column appears to offer a slight advantage for the determination of the transition metals investigated, particularly for Cd^{2+} due to its greater retention and change in the retention order on this column. Even though the metals of interest were not readily detectable or not at all in the case of Cd(II), this could be solved by using a greater sample injection volume for example 1000μl instead of the 500μl injection used. This would have the added advantage of producing peaks of greater size that would be not only more easily detectable but would have much more easily determinable areas and therefore be masked less by contaminant peaks.

Chapter 3:- Detection Systems in HPCIC

3.1 Introduction.

The ability to perform a high efficiency separation of multiple metal ions is of little use if the metal ions in question cannot be detected. The absence of a universal detector for liquid chromatography (LC) is considered its weakest link. As discussed in section 1.5, there are numerous ways to detect metals in solution when using LC. For these studies, a direct spectrophotometric method utilising the post-column complexation of the metal ion(s) under analysis with a chelating agent, containing a chromophore which absorbs strongly in the visible region of the spectrum, was used.

3.1.1 Post Column Reaction Systems.

The post column reaction systems involving the formation of a metal chelate offers several advantages which makes this method highly attractive and are listed below:

i. Many of the metal chelates formed, strongly absorb in either the UV or visible region of the spectrum which allows for the use of commonly found absorbance detectors.
ii. Selectivity can be varied by careful choice of reagent and/or the use of masking agents.
iii. The formation of a metal chelate is generally fast with very little mixing required thereby reducing the effect of peak broadening.

As stated, the PCRs used for the detection of metals are chelating molecules that contain a chromophore, that is an unsaturated group such as C=C, C=O, C=S or N=O. This group is responsible for the electronic energy absorption of the molecule. This absorption of energy results in the transition of electrons from the ground state to an excited state and corresponds to the increase in absorption of the UV/VIS spectrum. Detection using post column reagents is carried out by introducing the PCR into the column effluent with the two solutions being mixed together in a t-piece and reaction coil, before entering the UV/VIS detector.

There are potentially hundreds of post column reagents suitable for the detection of metal ions though perhaps the three most common PCRs found are PAR, PAR containing Zn-EDTA and Arsenazo III.

PAR is the most highly used PCR for the detection of transition and heavy metals. As it is such a broad based reagent it can also be used in the detection of the alkaline-earth metals and selected lanthanide and actininde elements. The applications of PAR have been reviewed in Chapters 1 and 2. PAR containing Zn-EDTA is the most commonly used PCR for the alkaline-earth metals. For example, Mg(II) and Ca(II) react with PAR but only form very weakly absorbing complexes at the pHs investigated. When Zn-EDTA is added to the PAR solution, the alkaline-earth metals will displace the Zn which will readily complex with PAR to form a strongly absorbing complex. This displacement reaction is shown below.

$$M^{2+} + Zn(EDTA)^{2-} + 2PAR^{2-} \rightarrow M(EDTA)^{2-} + Zn(PAR)_2^{2-}$$

Arsenazo III is the most commonly used PCR for the detection of both lanthanide and actinide elements. The application of its use will be reviewed in Chapters 4 and 5. Many other chelating dyes have found use as post column reagents but have shown no particular advantage over the ones used here.

3.1.2 Aim of this Study.

The aim of this study was to obtain fully optimised post column reaction systems particularly with regard to sensitivity that are suitable for the detection of a variety of selected transition, heavy and high valency metals. The post column reagents investigated were 4-(2-pyridylazo) resorcinol (PAR) for the transition and heavy metals and Arsenazo III and Pyrocatechol Violet (PCV) for selected high valency metals. Techniques to improve the sensitivity of these systems, including a noise reduction system and large volume injections were also investigated.

3.2 Experimental.

3.2.1 Instrumentation.

The HPCIC instrumentation used for these studies is as described in section 2.2.1. UV/VIS spectral analysis was carried out using a HP 8453 spectrophotometer (Hewlett Packard, OR, USA).

3.2.2 Reagents.

All reagents were obtained from BDH (BDH, Poole, UK) and of AnalaR grade unless otherwise stated. PAR was supplied by Fluka (Glossop, UK), Arsenazo III by ICN and PCV supplied by BDH.

The chromatographic and spectrophotometric investigations carried out for the PAR based PCRs utilized an eluent of 1M KNO_3 with 50mM acetic acid made up to 1 litre with MilliQ water and adjusted to the required pH. The column used for these studies was a 100 x 4.6mm ID PEEK column packed with the 7μm resin supplied by Hamilton and loaded with XO. For the studies involving the Arsenazo III and PCV post column reagents, the eluents used consisted of 1M KNO_3 prepared in dilute HNO_3 with 0.1mM dipicolinic acid. The spectrophotometric analysis used the same eluent though no dipicolinic acid was used. The column used for these studies was a 100 x 4.6mm ID PEEK column packed with 5μm PLRP-S resin from Polymer Laboratories.

3.3 Results and Discussion.

3.3.1 4-(2-pyridylazo) resorcinol (PAR).

As previously stated, PAR is a broad based reagent which has been used to detect a wide variety of metal ions but principally the transition and heavy metals. It is a heterocyclic azo dye with its structure shown in Figure 1.10. Depending upon the acidity, it can exist as one of the following six species [171];

$$\underset{(90\%\ H_2SO_4)}{H_5L^{3+}} \rightleftharpoons \underset{(50\%\ H_2SO_4)}{H_4L^{2+}} \rightleftharpoons \underset{pH<2}{H_3L^{+}} \rightleftharpoons \underset{pH2.1\text{-}4.2}{H_2L} \rightleftharpoons \underset{pH4.2\text{-}7}{HL^{-}} \rightleftharpoons \underset{pH>10.5}{L^{2-}}$$

The complexes formed by PAR involve the replacement of the hydrogen of the *ortho* OH group with the metal and bonding between the metal and both the pyridine and azo nitrogens [171]. Table 3.1 shows the log stability constants of selected metal ions with PAR.

Table 3.1. Log equilibrium constants of metal ions with PAR [95]. 0.1M Ionic strength.

M^{n+}	K_1	M^{n+}	K_1
Mn^{2+}	9.7	Pb^{2+}	11.2
Co^{2+}	10	Cd^{2+}	10.5
Ni^{2+}	13.2	In^{3+}	9.3
Zn^{2+}	11.9	Al^{3+}	11.5
Cu^{2+}	11.7	UO_2^{2+}	12.5

The relative response of three different PAR solutions to selected metals was investigated, the constituents of which are given in Table 3.2. The reason for the reduction or removal of NH_3 from the reagent was to evaluate its effect on the sensitivity of detection because NH_3 is known to complex strongly with certain metals.

Table 3.2. PAR based detection systems investigated.

PAR System	Components
Original NH_3 System	3.5M NH_3, 0.8M HNO_3, $1.2x10^{-4}$M PAR
Reduced NH_3 System	0.35M NH_3, 0.8M HNO_3, $1.2x10^{-4}$M PAR
Borate System	0.125M Borate, $1x10^{-4}$M PAR

3.3.1.1. NH_3 Buffer System.

The PAR solution used initially consisted of $1.2x10^{-4}$M PAR and buffered with 3.5M NH_3 and 0.8M HNO_3 made up to 1 litre in MilliQ water though these concentrations are in effect halved upon dilution with the eluent. As PAR complexes with such a wide range of metals, it is unfortunate that it does not produce similar responses for each of these metals. In fact the difference in ε_{max} values can vary dramatically from, for example, $5.5x10^{-3}$ for Co(III) at 510nm to $86.5x10^{-3}$ for Mn(II) at 496nm [171]. This is dependent, to an extent, upon the complex ratio formed as well as the pH and wavelength at which the complex is being detected at. However, some of the transition metals investigated, Cd(II) in particular, showed a very poor response which could not be explained by either the complex ratio formed , pH or wavelength of detection.

As can be seen in Figure 3.1, Cd(II) appears to produce a peak approximately half the size of the Mn(II) peak however, the concentration of the Cd(II) is twenty times greater than the concentration of Mn(II). It was concluded that this low response was due to the presence of

some species that was inhibiting the complexation of Cd(II) and PAR. This species was thought to be the NH_3 present in the buffer of the PAR solution. Reduction of the NH_3 concentration should therefore result in a greater response for Cd(II). Figure 3.2 shows the same six element mixture ran using a PAR solution containing $1.2x10^{-4}$M PAR, 0.35M NH_3 and 0.8M HNO_3. As can be seen, the response for Cd(II) has increased dramatically along with an increase in Zn(II) and Ni(II). Pb(II) however, does not show any increase. This would be expected if the presence of NH_3 was inhibiting the response for Cd(II). This is because Cd(II) complexes with NH_3 in preference to the PAR. Pb(II) however, complexes much more weakly with NH_3 and therefore reduction of the NH_3 concentration will not affect the obtained response. Figure 3.3 shows the UV/VIS spectrum of the PAR/NH_3 system with selected transition metals.

3.3.1.2. Borate Buffer System.

Due to the adverse affect that the presence of NH_3 has on the sensitivity of the Cd(II) determinations, a new buffer system for the PAR solution was investigated. This new system utilized the buffering capabilities of di-sodium tetraborate. This system was chosen as it has a natural pH of 9.15 for a 0.05M solution and does not complex readily with the metals under investigation. The difference in log stability constants for selected metal ions with ammonia and boric acid is shown in Table 3.3. An optimization of this system was carried out to determine the borate concentration required to produce no change in pH (or as small a change as possible) when the PAR solution is mixed with the eluent.

Table 3.3. Log Equilibrium constants of selected metals with ammonia and boric acid [95]

M^{n+}	Log K_1 (NH_3)	Log K_1 $B(OH)_3$
Cu^{2+}	4.18	3.48
Cd^{2+}	2.80	1.42
Zn^{2+}	2.14	0.9

The initial conditions used were a 1 x 10^{-4} M PAR solution buffered with 0.05M borate. This borate concentration produced a pH of 9.15 for the PAR system; however upon a 1:1 dilution with 0.1M HNO_3 the pH dropped to approximately 6.60. It was decided to adjust the pH of the PAR/Borate solution using 1M NaOH and then mix with a pH2 eluent (in a 50:50 ratio) to determine the pH drop that would be expected. The results obtained in Table 3.5 showed that adjustment of the PAR/Borate solution to pHs greater than 10.5 would result in an unacceptably large pH drop. Runs one and two from Table 3.4 were then investigated further.

Table 3.4. Conditions investigated for 0.05M borate buffer.

Run	Adjusted pH	50:50 pH (with pH2 eluent)
1	10.00	8.75
2	10.50	9.00
3	11.25	9.10
4	11.50	9.15

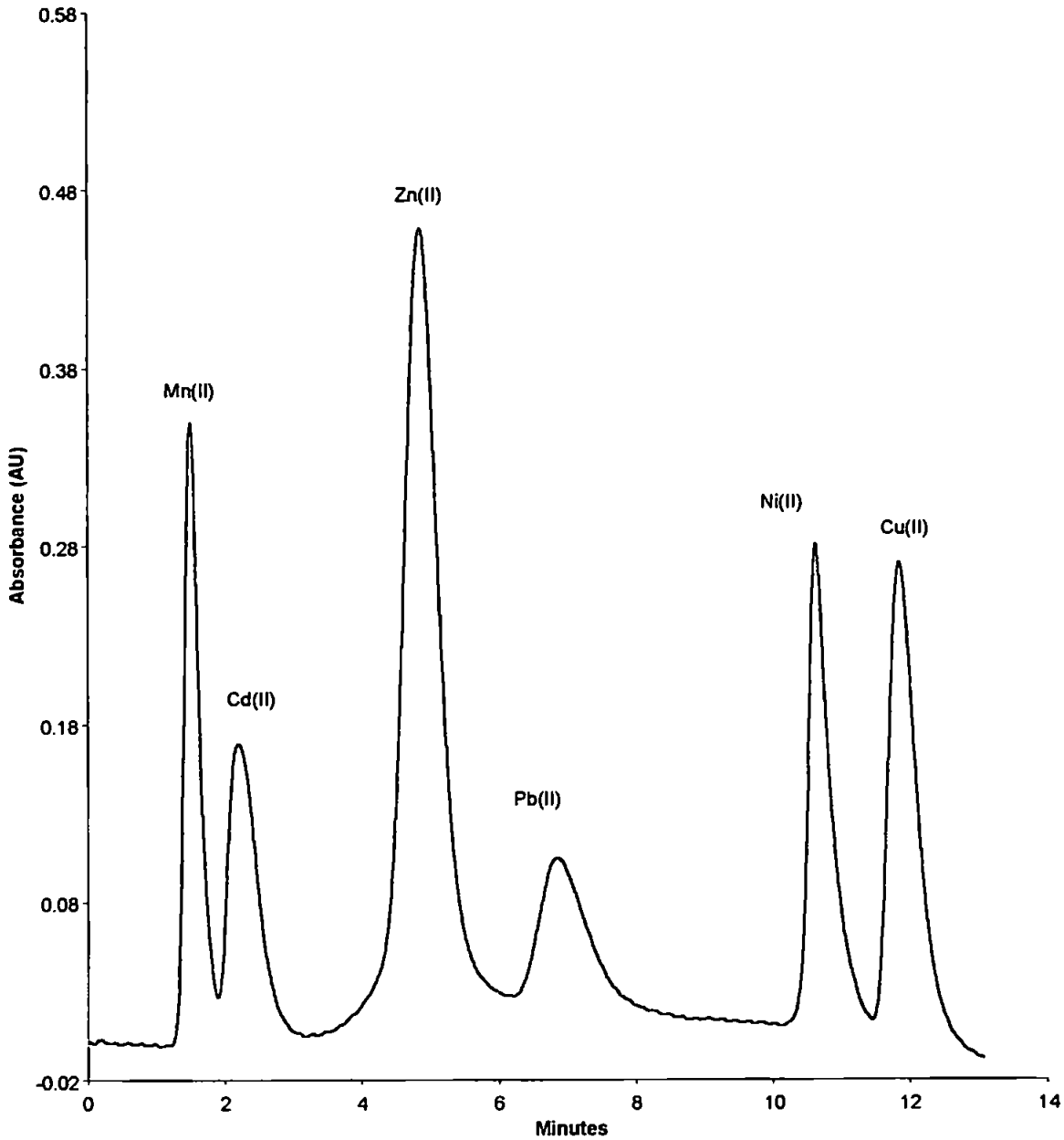

Figure 3.1. Gradient separation of 1mgl^{-1} Mn(II), 20mgl^{-1} Cd(II), 3mgl^{-1} Zn(II), 5mgl^{-1} Pb(II), 3mgl^{-1} Ni(II) and 2mgl^{-1} Cu(II) on the 10cm XO/7μm Hamilton column. Eluent used was 1M KNO_3 buffered with 50mM acetic acid. Injection volume used was 100μl with detection at 520nm with PAR/NH_3 PCR.

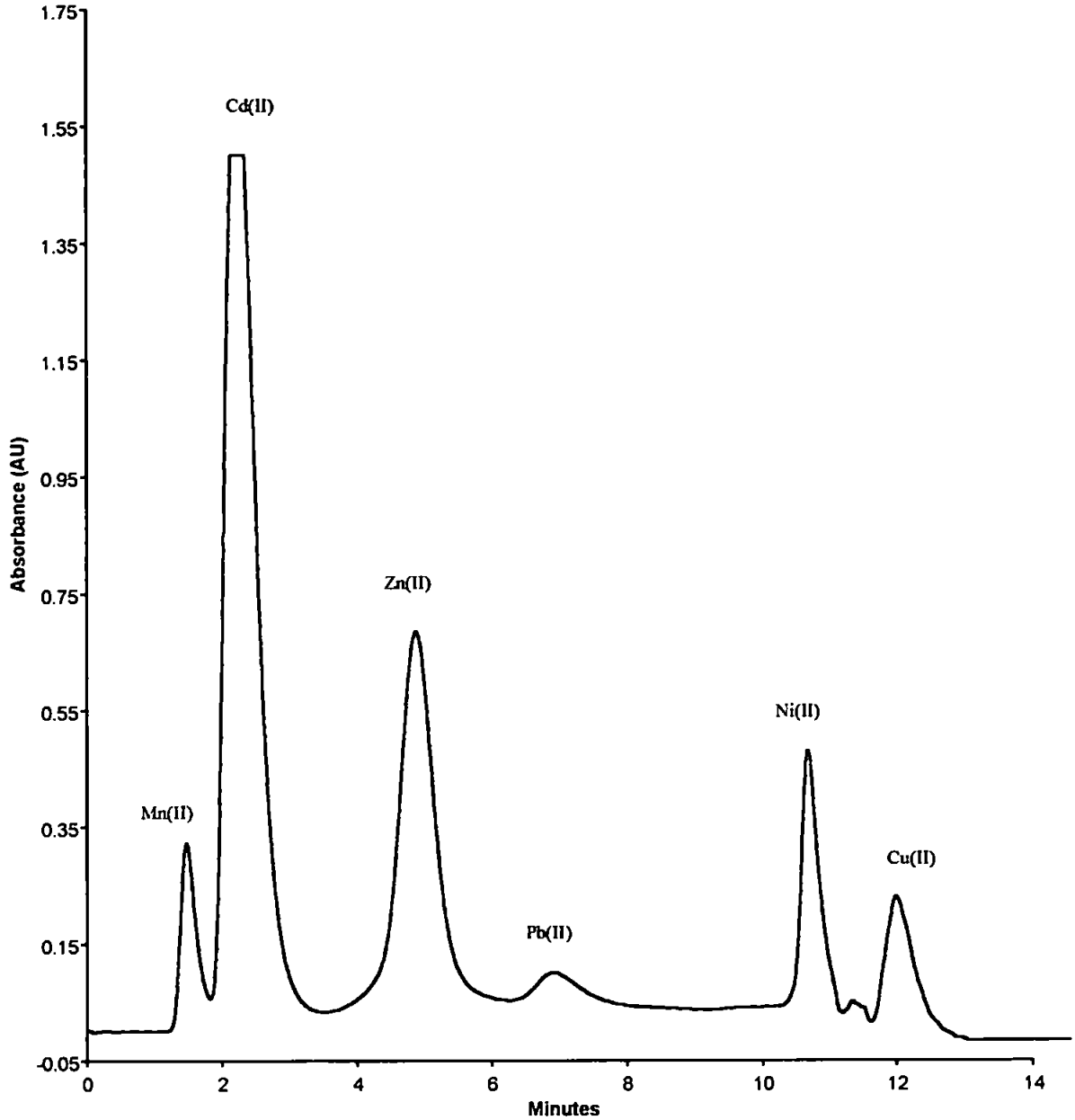

Figure 3.2. Gradient separation of 1mgl^{-1} Mn(II), 20mgl^{-1} Cd(II), 3mgl^{-1} Zn(II), 5mgl^{-1} Pb(II), 3mgl^{-1} Ni(II) and 2mgl^{-1} Cu(II) on the 10cm XO/7μm Hamilton column. Eluent used was 1M KNO_3 buffered with 50mM acetic acid. Injection volume used was 100μl with detection at 520nm with PAR/Reduced NH_3 PCR.

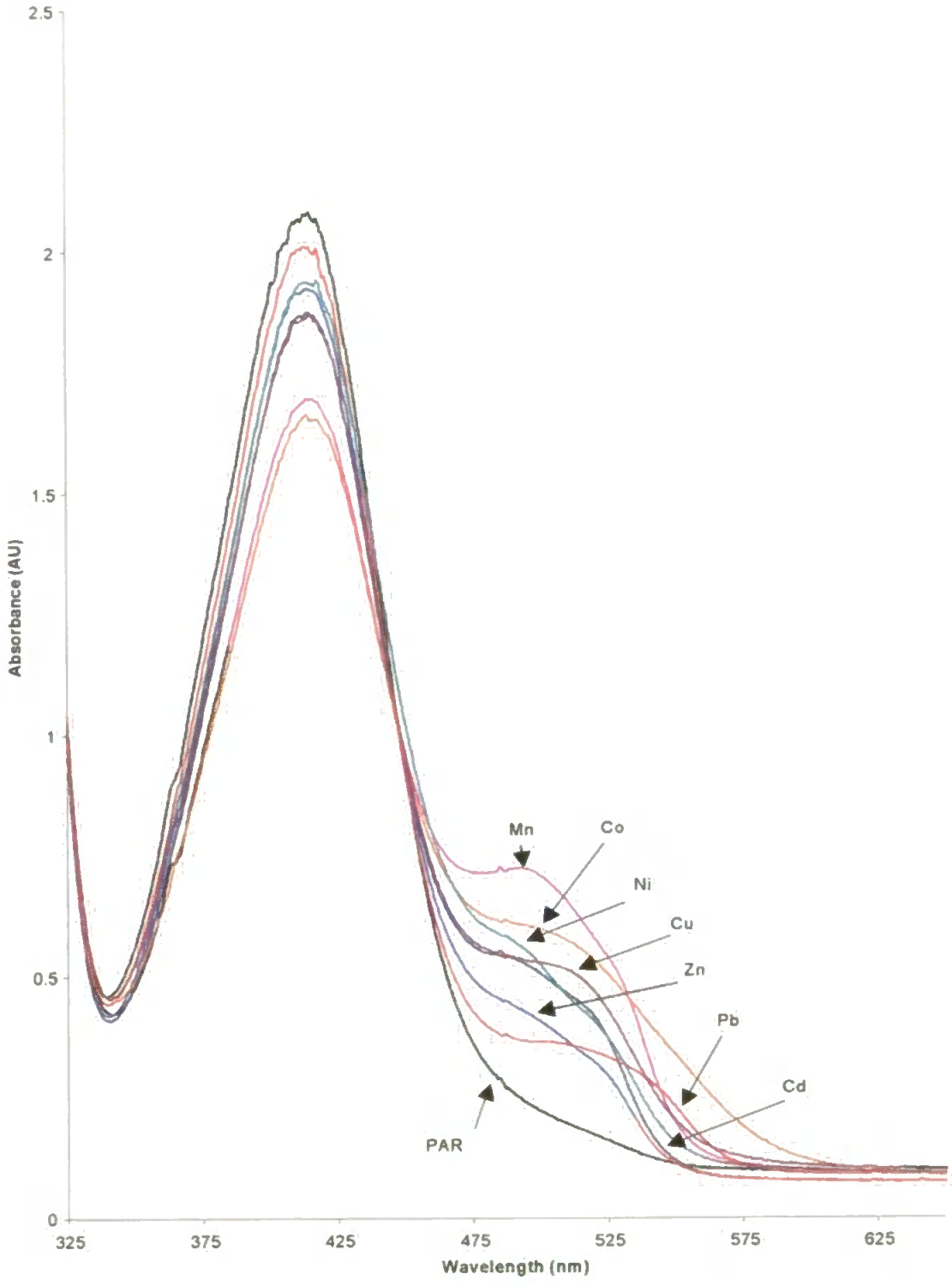

Figure 3.3. UV/VIS spectra of PAR/NH_3 PCR with selected transition and heavy metals.

A comparitive study between the original NH_3 containing PAR system and the PAR/Borate system was carried out by injecting the transition metals of interest at pH2. This pH was chosen as all the metals would elute on the solvent front and therefore produce the maximum peak size possible. From the results shown in Table 3.5 and in Figure 3.4 it can be clearly seen that there is an increase in peak height for Mn(II), Zn(II), and Co(II) as well as a substantial increase (approx twelve times greater) for Cd(II) with the PAR/Borate system. However both Pb(II) and Ni(II) showed no increase.

Table 3.5. Average peak heights (in Absorbance Units) for NH_3 containing PAR and Borate containing PAR Solutions.

	Mn(II)	Cd(II)	Zn(II)	Co(II)	Pb(II)	Ni(II)
Orig PAR	0.320	0.017	0.112	0.219	0.051	0.034
Run 1	0.337	0.194	0.472	0.300	0.051	0.028
Run 2	0.385	0.206	0.481	0.296	0.054	0.029

Clearly the borate system produced much better results so it was decided to try increasing the concentration of the borate in an attempt to try to keep the PAR:eluent pH as constant as possible at approximately pH 10 (as for the PAR/NH_3 system) for the maximum possible response. This time however, the pH was checked upon the addition of the eluent at pH4 as well as upon the addition of 0.1M HNO_3 (again both in a 50:50 ratio). These pHs were chosen as the gradient elution programs used for the multi-element separations on the XO loaded column used for this study generally started at approximately pH4 and finished at pH1. The results obtained are shown in Table 3.6.

It was decided that a 0.125M borate concentration adjusted to pH 10.50 with 5M NaOH offered the most practicable system. One problem noted though was that when the borate concentration was greater than 0.1M, over two hours was required for the borate to dissolve at room temperature. Therefore, the borate had to be heated until complete dissolution was obtained before addition of the PAR and allowed to cool back down to room temperature before the pH was adjusted. A maximum concentration of 0.15M could be used as at greater concentrations the borate precipitates out of solution at room temperature. Figure 3.5 shows the UV/VIS spectrum of the PAR/Borate system with selected transition metals

Table 3.6. Concentrations and pH Investigated for optimisation of PAR/Borate system.

Borate Conc (M)	Run	Adjusted pH	50:50 pH4	50:50 pH1
0.1	1	9.25	8.90	8.40
	2	10.00	9.55	9.20
	3	10.50	~9.82	9.50
	4	11.00	10.00	~9.65
0.125	1	9.35	~8.93	8.56
	2	10.00	9.55	9.27
	3	10.50	9.95	9.60
	4	11.00	10.2	9.80
0.15	1	9.30	8.95	8.65
	2	10.00	9.60	9.27
	3	10.50	10.00	9.71
	4	11.00	10.25	9.90

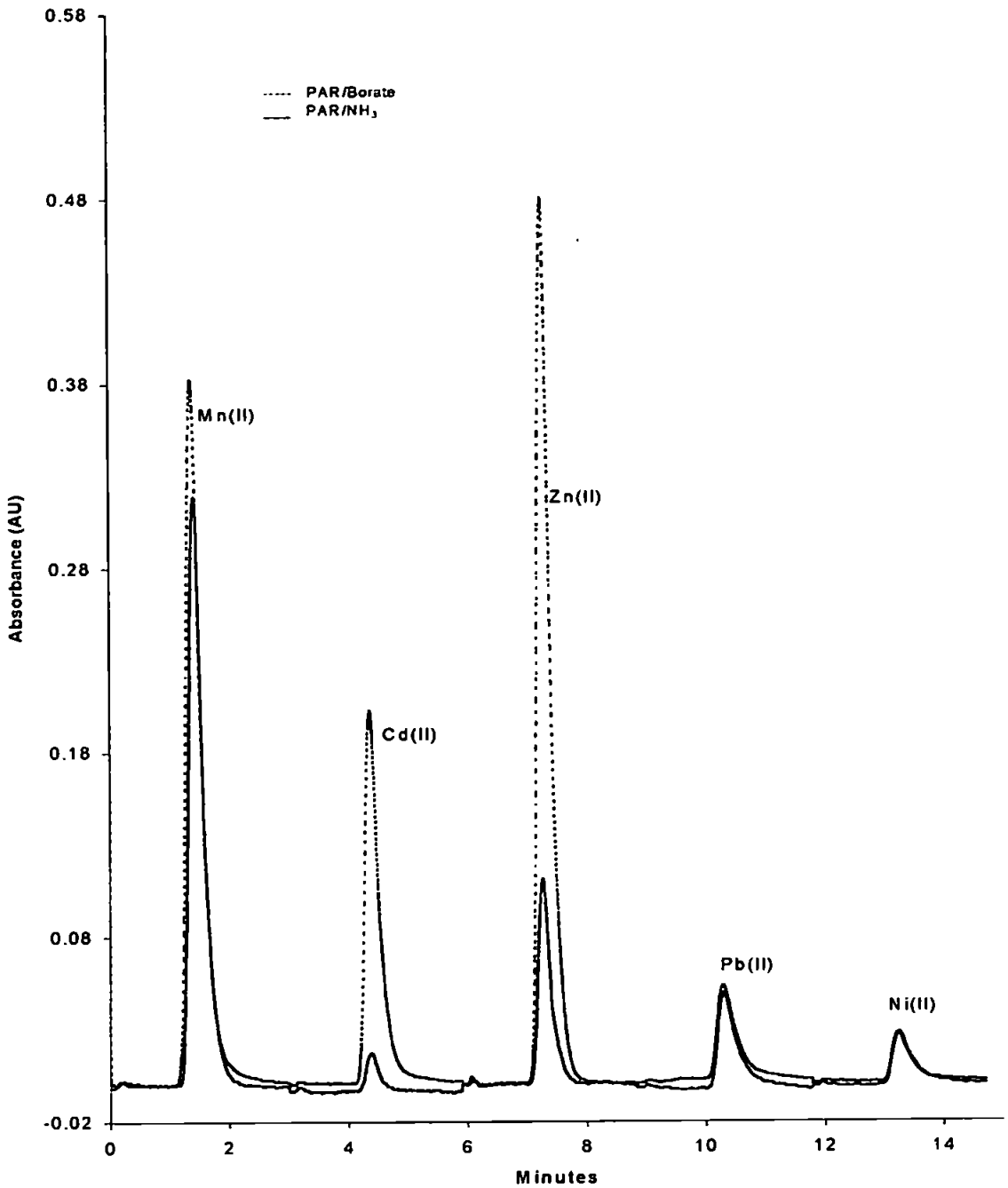

Figure 3.4. Difference in absorbance for Mn(II), Cd(II) and Zn(II) for the PAR/NH_3 and PAR/Borate PCRs. Eluent used was 1M KNO_3 buffered with 50mM acetic acid. Detection was at 520nm.

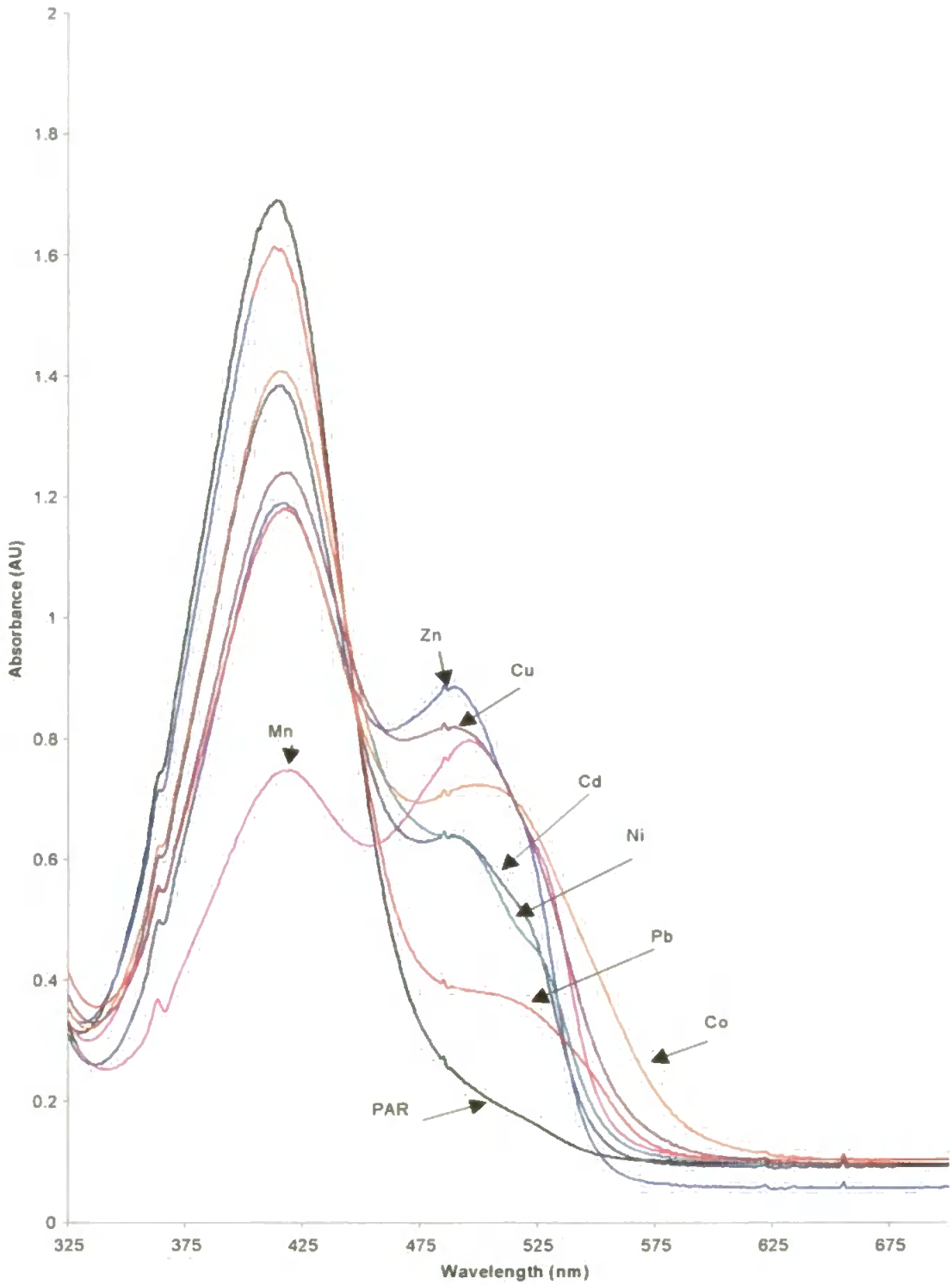

Figure 3.5. UV/VIS spectra of PAR/Borate PCR with selected transition and heavy metals.

3.3.2. Arsenazo III.

The azo dye, Arsenazo III was chosen for its wide selectivity for high valency metals such as U(VI) and Th(IV). It can form 1:1 complexes with +2 and +3 metal cations, for example UO_2^{2+} and La^{3+} and can form either 1:1 or 1:2 complexes with quadruply charged metal cations such as Hf(IV) and Zr(IV) [171]. This reagent is particularly useful for U(VI) determinations as it will readily complex over an acid range of 0.01-10M HCl. Also, decreasing the pH increases the selectivity towards U(VI) thereby reducing interference from other ions and increasing the sensitivity for U(VI). The Arsenazo III solution used was initially based upon a system developed by Shaw [120].

This solution consisted of 0.15mM Arsenazo III with 10mM Urea prepared in 1M HNO_3. With the exception of the studies reported in Chapter 5, the HNO_3 concentration was varied depending upon the HNO_3 concentration of the eluent being used. This entailed adjustment of the Arsenazo III HNO_3 concentration so that the combined pH of the Arsenazo III and eluent was pH0 (1M HNO_3). The urea was removed from the Arsenazo III solution as it appeared to make no difference to the obtained absorbance.

A major problem experienced with Arsenazo III however, was a constantly increasing baseline. Figure 4.4 in section 4.3.4.1 illustrates this problem. After a preliminary investigation of Arsenazo III spectra with time there appeared to be no discernable reason as to why this change in the baseline absorbance occurred, and particularly as to why the change increased after the elution of certain metals.

In an attempt to minimize this effect, the parameters of the Arsenazo III solution were optimized prior to the studies carried out in Chapter 5. This optimization entailed measuring the baseline drift at different Arsenazo III concentrations as well as the concentration of HNO_3 added to the Arsenazo III solution for pH adjustment was studied over a nine minute time period, the results of which are shown in Tables 3.7 and 3.8.

Table 3.7. Variation of Baseline Drift with Arsenazo III concentration.

Arsenazo III Concentration (mM)	Baseline Drift (AU)
0.05	0.0003
0.075	0.0005
0.1	0.001
0.15	0.0018
0.3	0.013

Table 3.8. Variation of baseline drift with HNO_3 concentration added to Arsenazo III solution for pH adjustment.

HNO_3 Concentration (M) added to A III for pH adjustment	Baseline Drift (AU)
0	0.00027
0.5	0.00025
1	0.0003
1.5	0.0003

For the results shown in both Table 3.7 and 3.8, an eluent of 1M HNO_3 with 0.1mM dipicolinic acid was used. From these results, an optimum Arsenazo III concentration of 0.05mM was used to determine an optimum HNO_3 concentration of 0.5M HNO_3. While this optimization did not solve the problem of the increasing baseline absorbance it did appear to minimize the drift. Figure 3.6 shows the UV/VIS spectrum of Arsenazo III with selected high valency metals.

3.3.3. Pyrocatechol Violet (PCV).

Not all of the high valency metals investigated produced a suitable (if any) response with the Arsenazo III. As a result of this, Sn(IV), V(IV), V(V) and Ti(IV) were all determined using Pyrocatechol Violet (PCV) as the post-column reagent. The structure of PCV is shown in Figure 1.10 with the UV/VIS spectrum of PCV with selected high valency metals given in Figure 3.7. In solution, PCV forms the following species [171];

$$H_4L \xrightarrow{\sim pH1} H_3L^- \xrightarrow{\sim pH7} H_2L^{2-} \xrightarrow{>pH10} HI^{3-}, L^{4-}$$

Again the PCV solution used was based on a system developed by Shaw [120] and contained 40mgl^{-1} PCV buffered with 2M hexamine at pH 6.

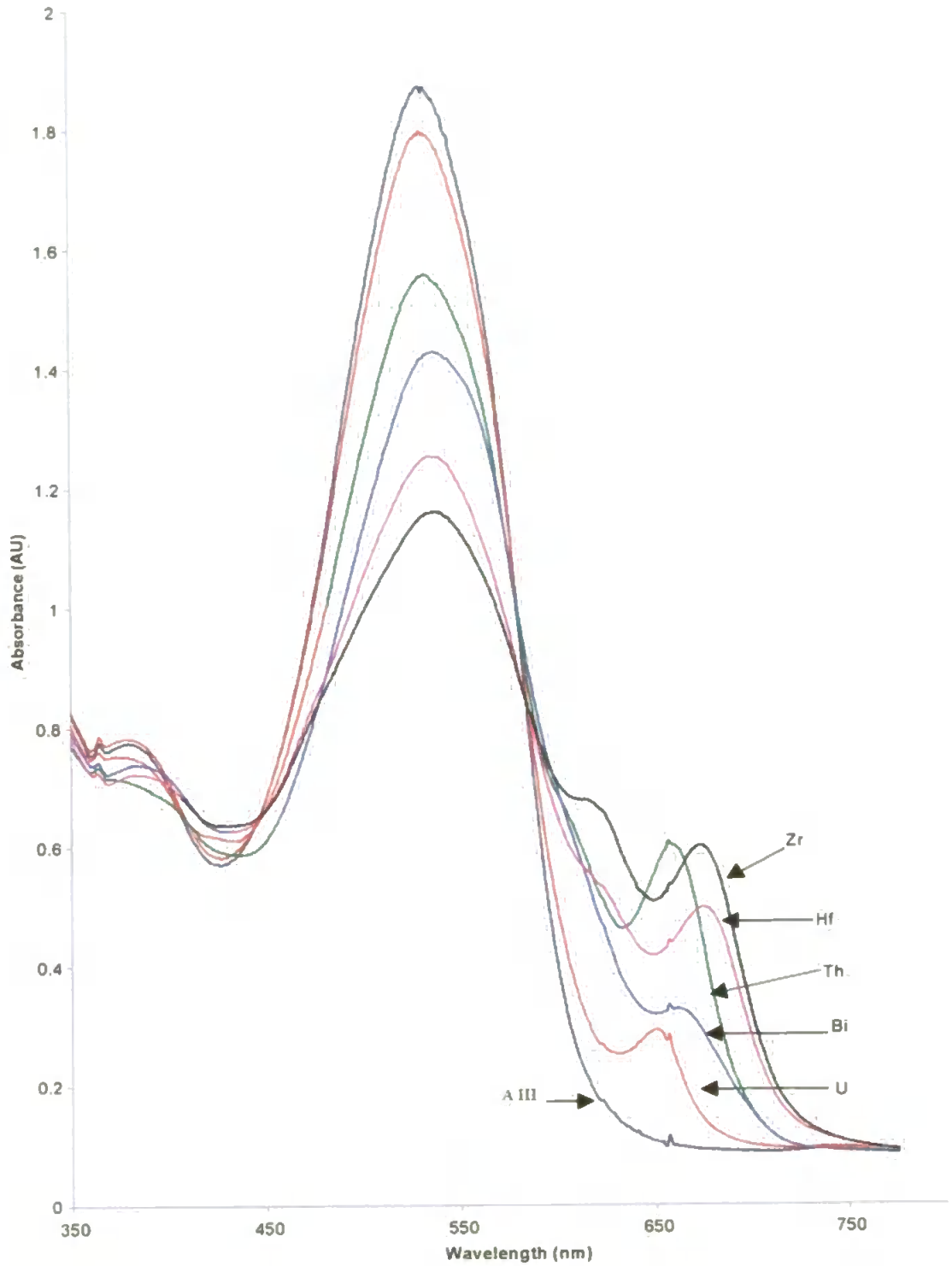

Figure 3.6. UV/VIS spectra of Arsenazo III PCR with selected high valency metals.

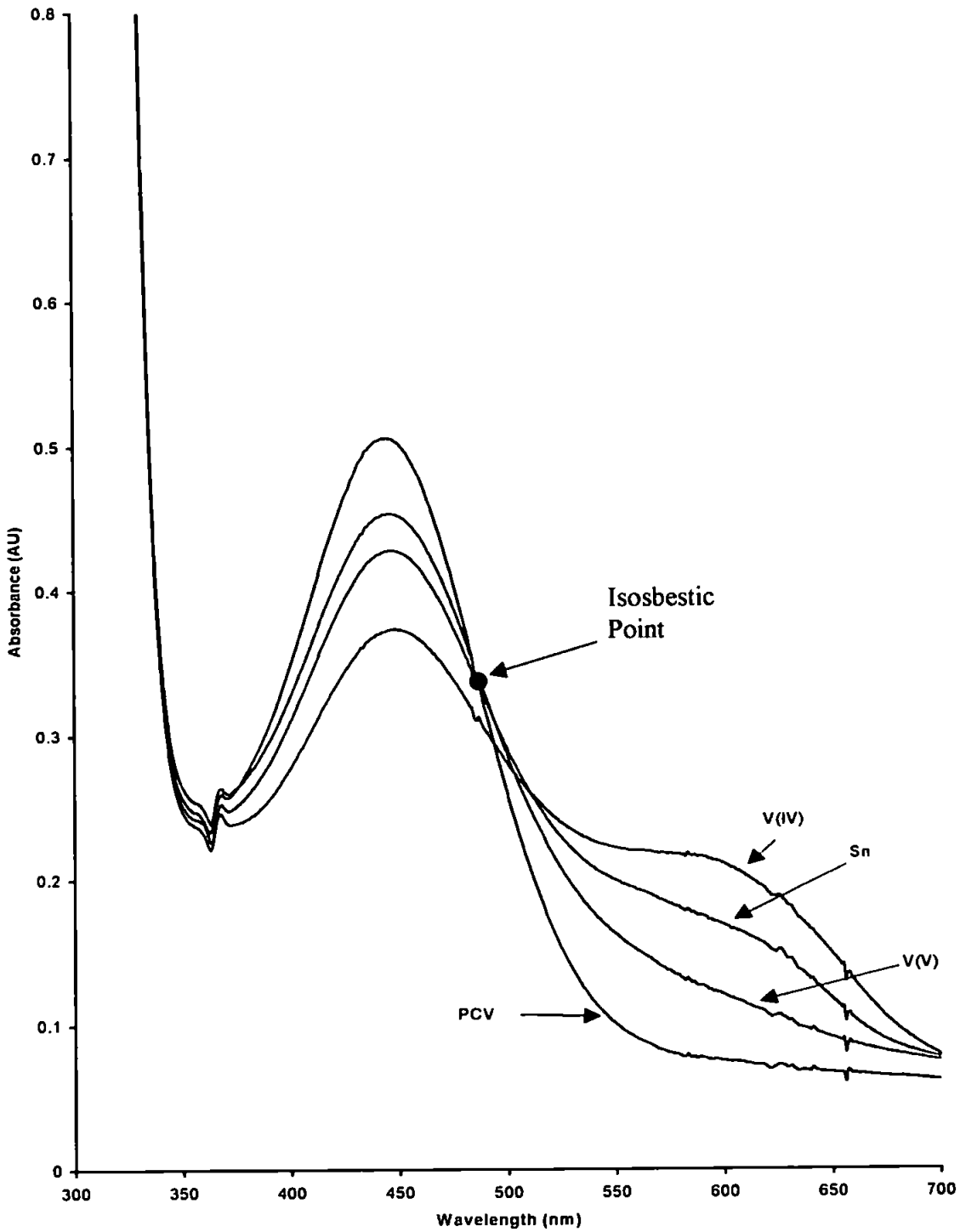

Figure 3.7. UV/VIS spectra of PCV PCR with selected high valency metals.

3.4. Sensitivity Enhancement.

There are several ways to enhance the sensitivity of post column reagents. Already discussed are the optimizations on both the PAR and Arsenazo III PCRs. Other ways to enhance the sensitivity of the detection system include lowering the baseline noise levels or increasing the amount of sample loaded onto the column.

3.4.1 Noise Reduction System.

One way to improve the sensitivity of the post column reaction system is to lower the baseline noise levels. There are in fact three distinct types of baseline noise that can be encountered. These are short term noise, long term noise and drift. *Short term noise* entails electronic noise and possible pump noise and has a frequency much higher than the analyte peak width. This type of noise can be removed using smoothing techniques as well as electronic filtering and mechanical dampening. *Long term noise* has a frequency that is comparable to the analyte peak width and is generally associated with slower pump variations such as fluctuations in pump speed due to the presence of air bubbles. This type of noise cannot be removed without also removing the analyte peak of interest. The third type of noise that is found is *drift*. This is generally a long term increase or decrease in the baseline and can be removed with appropriate computer software. Therefore, both short and long term noise are the main causes of decreases in the sensitivity and have to be eliminated. If this can be achieved then the signal to noise ratio will be greatly improved and thereby allow for lower concentrations to be detected. In order to achieve this, a noise reduction system developed by Jones [172] was employed.

This system involves the simultaneous recording of two chromatograms at two different wavelengths. The first wavelength used is the detection wavelength normally used for the detection of the metal ions, for example 490 or 520nm when using a PAR post column reagent. The second wavelength used is called the compensating wavelength and it is the wavelength at which the isosbestic point is found. This is shown in Figure 3.7. With the addition of a metal ion to the PAR solution, an increase in absorbance is observed at the detection wavelength. However, there is no increase or decrease in the absorbance at the isosbestic point. Due to this characteristic, a chromatogram recorded at this wavelength will only show fluctuations or changes in the baseline that are as a result of pump noise or irregularities and not the metal-PAR complex. As these baseline changes are also recorded at the normal detection wavelength, subtraction of the chromatogram recorded at the compensating wavelength from the chromatogram recorded at the normal detection wavelength will result in a third chromatogram. This new chromatogram should show only the changes in the baseline that correspond to the metal-PAR chelates.

This noise reduction system can produce at least a ten fold decrease in the baseline noise levels and can allow for the detection of peaks which may be "hidden" away under fluctuations in the baseline caused by pumping irregularities or pump noise. An example of the noise reduction system is shown in Figures 3.8. Note the much lower absorbance scale in Figure 3.8b.

The noise reduction system will therefore also allow for calibrations to lower concentrations to be carried out. For example, Figures 3.9 and 3.11 show the calibration curves for Mn(II) and Pb(II) using the 10cm Hamilton/XO column before the noise reduction system is used. Mn(II)

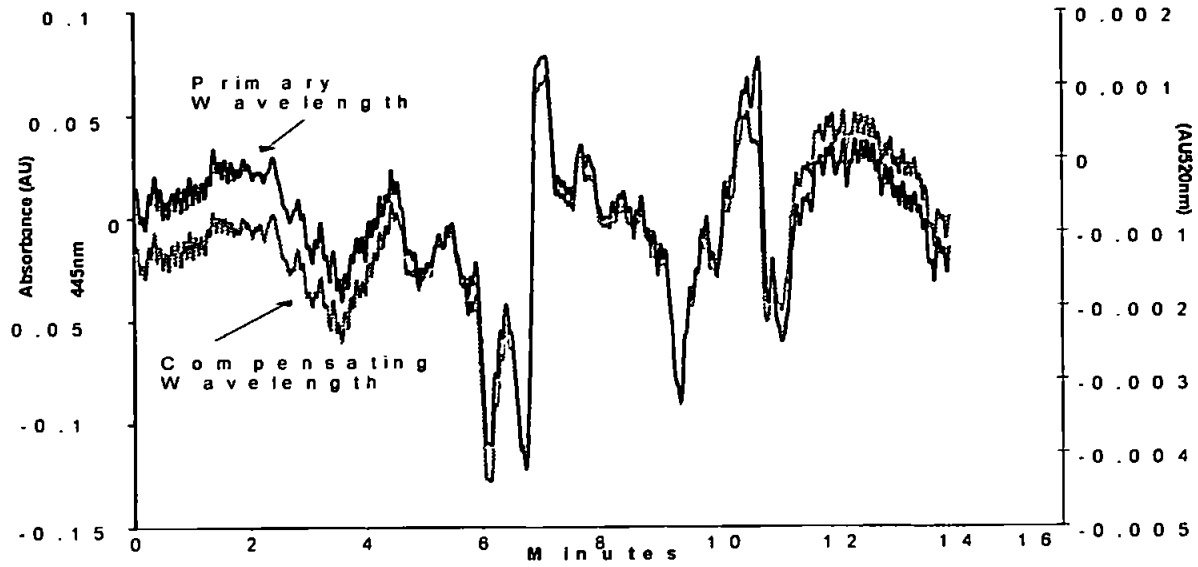

a)

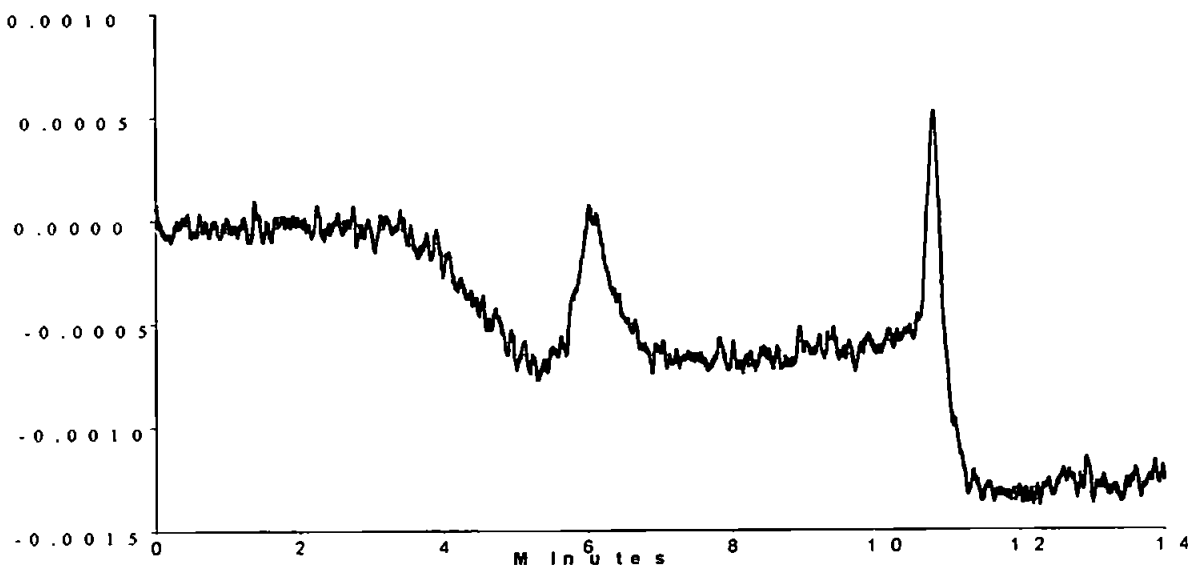

b)

Figure 3.8. Example of a) detection (520nm) and compensating (445nm) wavelengths and b) the resulting chromatography after wavelength subtraction for a baseline run on the 10cm XO/7μm Hamilton column run under gradient and conditions used for Figure 2.11.

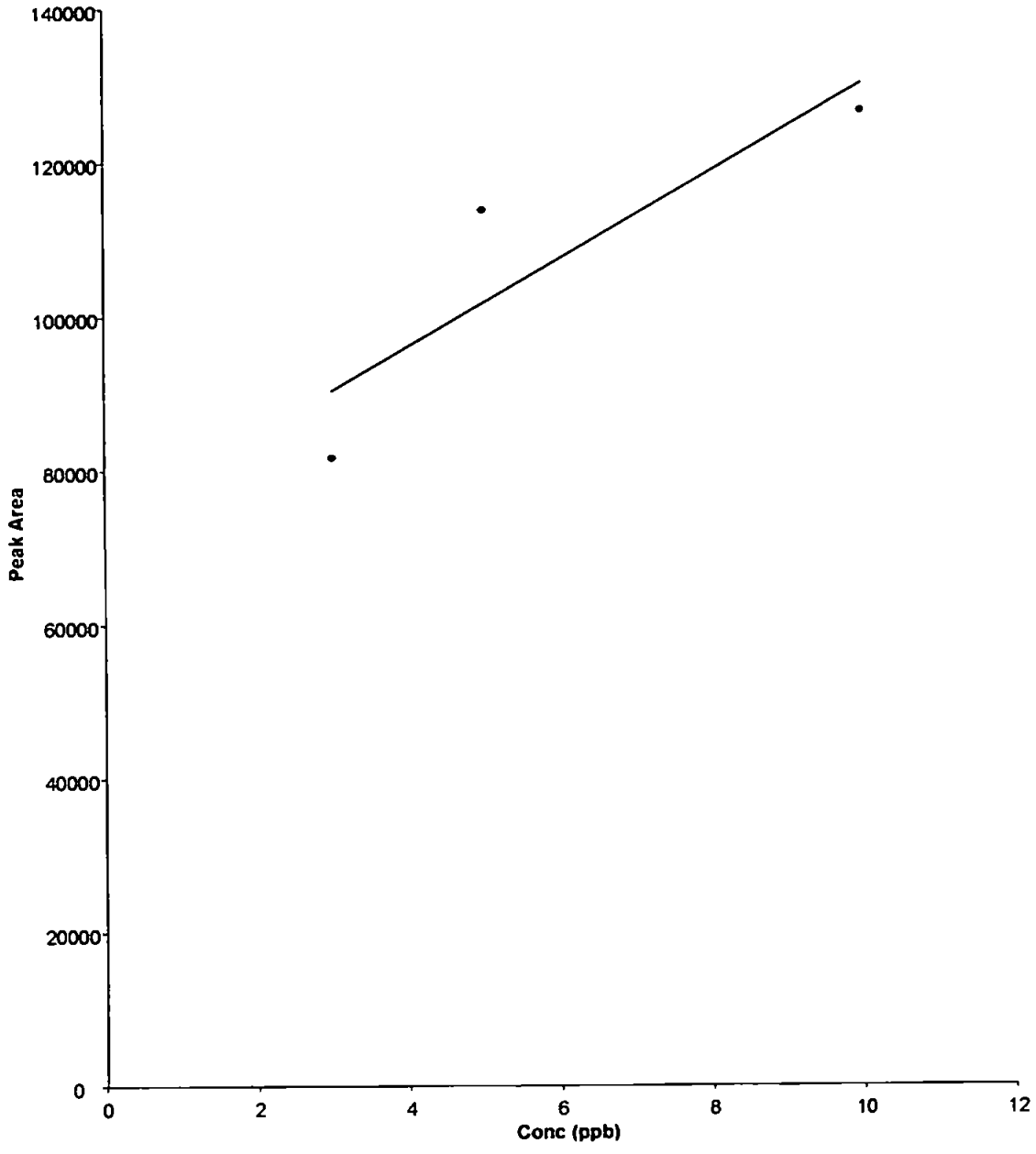

Figure 3.9. Mn(II) calibration before noise reduction on the 10cm XO/7μm Hamilton column. Gradient and conditions used were as for Figure 2.11.

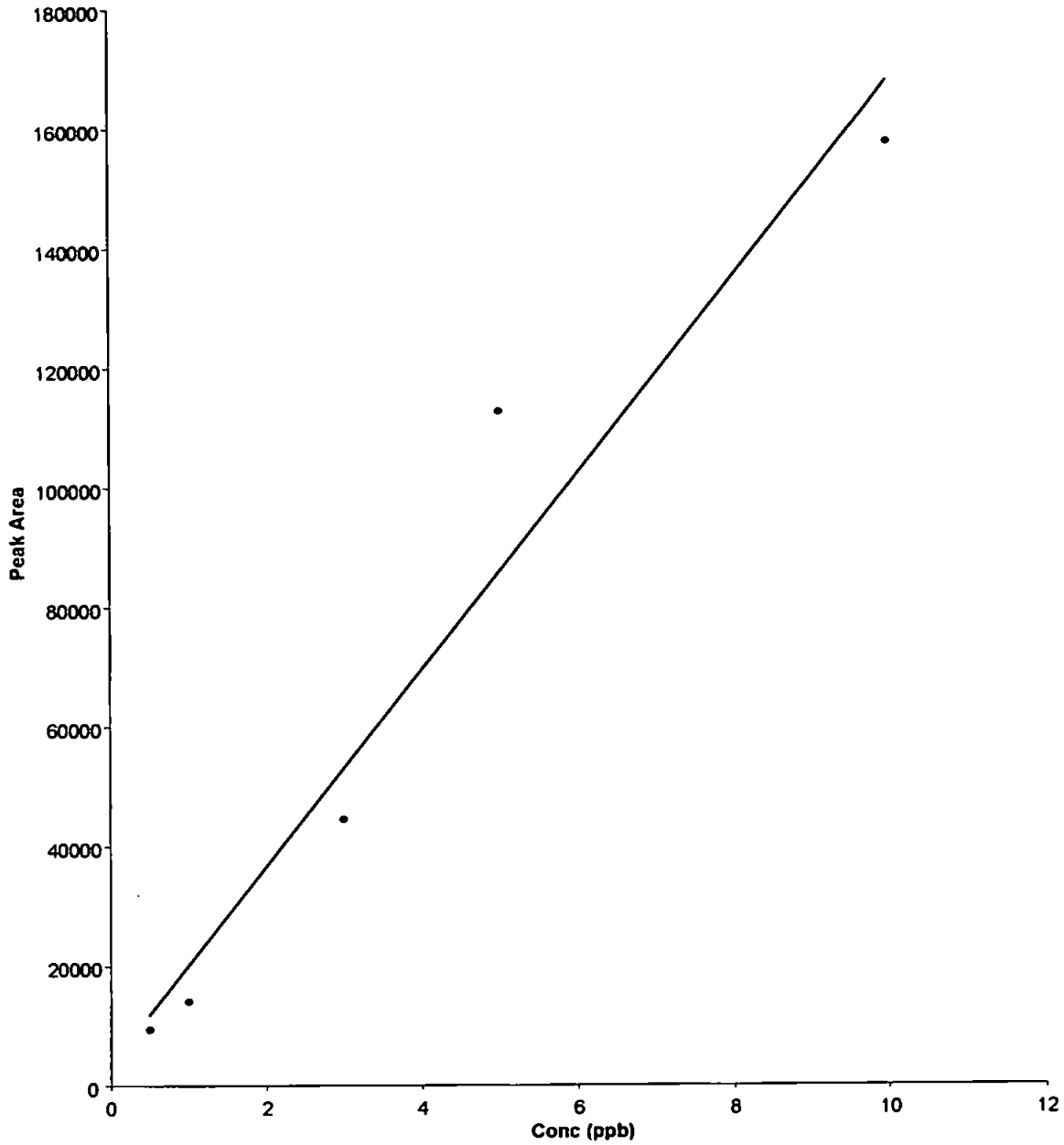

Figure 3.10. Mn(II) calibration after noise reduction on the 10cm XO/7μm Hamilton column. Gradient and conditions used were as for Figure 2.11.

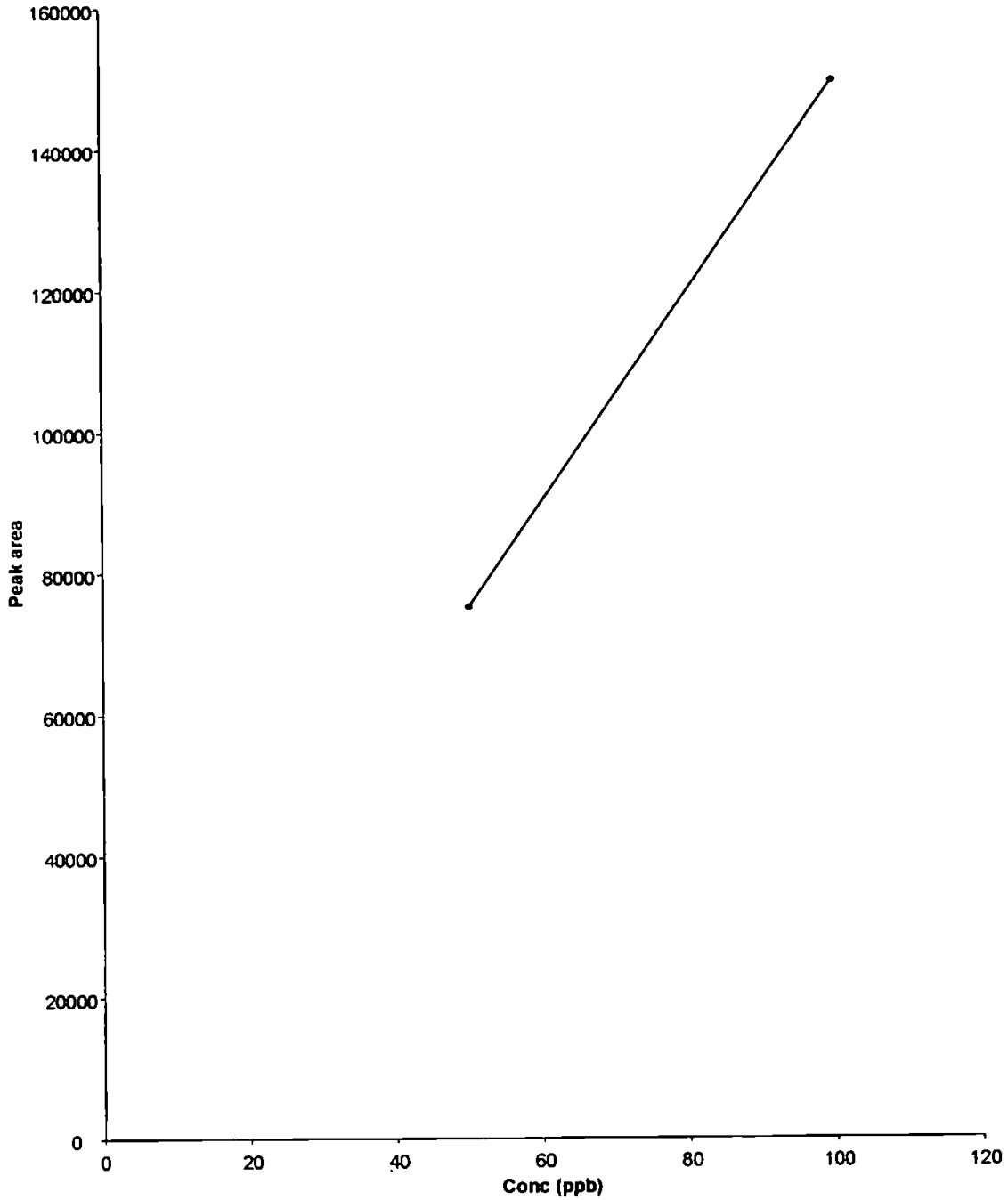

Figure 3.11. Pb(II) calibration before noise reduction on the 10cm XO/7μm Hamilton column. Gradient and conditions used were as for Figure 2.11.

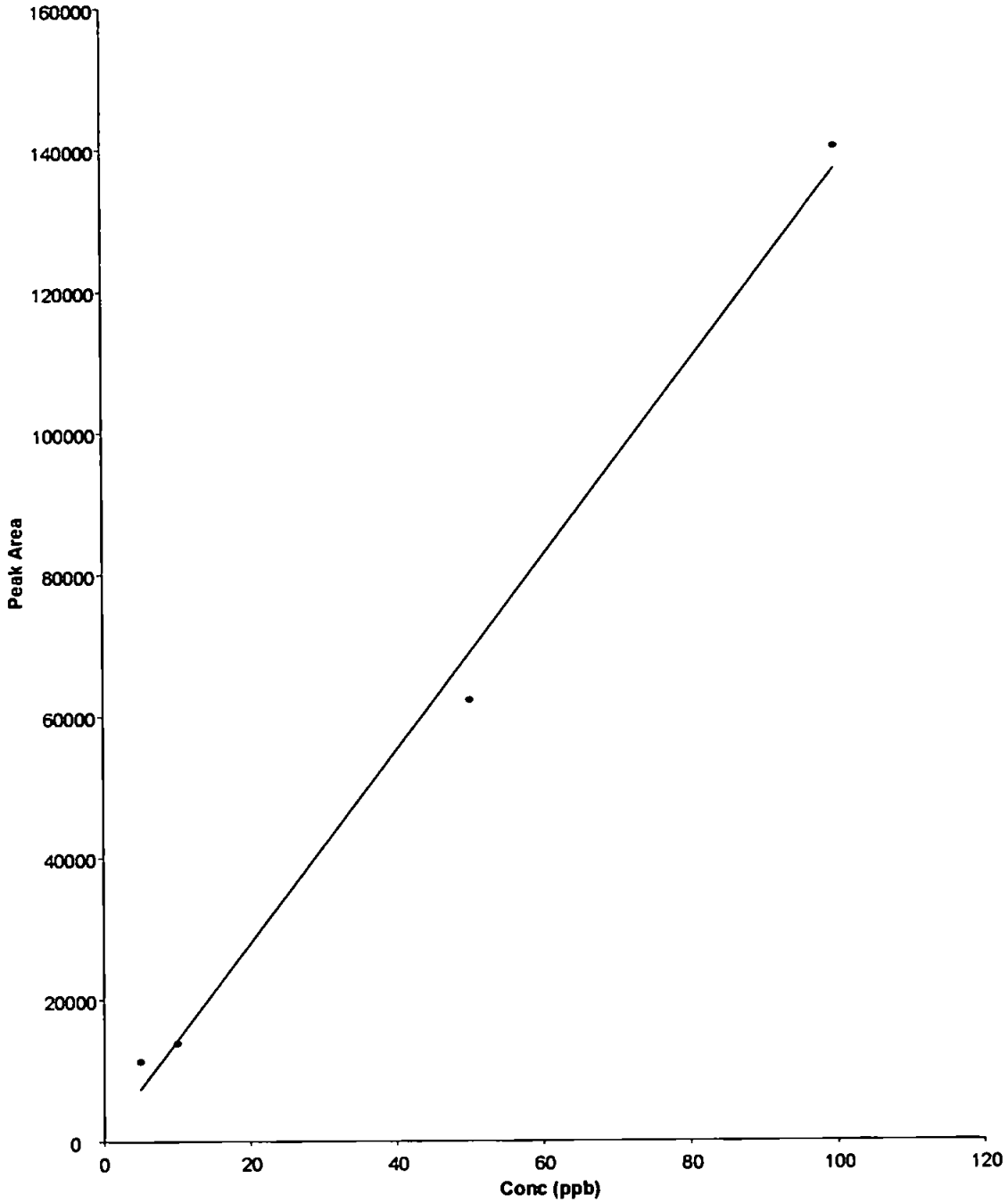

Figure 3.12. Pb(II) calibration after noise reduction on the 10cm XO/7μm Hamilton column. Gradient and conditions used were as for Figure 2.11.

shows a calibration range of 3-10μg l^{-1} with an $r^2 = 0.78$ whereas Pb(II) only shows a 2 point calibration between 50-100μg l^{-1}. After applying the noise reduction system, the Mn(II) calibration range is extended to 0.5-10μg l^{-1} with an $r^2 = 0.944$ and Pb(II) now shows a 4 point calibration over the concentration range 5-100μg l^{-1} with an $r^2 = 0.9938$. These new calibrations are shown in Figures 3.10 and 3.12.

It is important to note however, that the compensating wavelength used is only an approximate wavelength as the isosbestic point can be different for each individual metal as shown in Figure 3.3, 3.5-3.7 and for each PCR system. The compensating wavelengths used were 445nm for the PAR based PCR, 585nm for Arsenazo III and 371nm for the PCV PCR.

3.4.2 Large Volume Injections.

Another way to increase the sensitivity of the detection system is to increase the amount of sample injected onto the column. Again this increases the signal to noise ratio and thereby increases the sensitivity of the system. Figure 3.13 shows repeat injections of 100μg l^{-1} Cd(II) standard on the 10cm Hamilton/XO column using increasing sample volumes. As can be seen, a constant increase in peak size is obtained. However an additional problem caused by large volume injections is the increase in peak broadening that is encountered. Again this is shown in Figure 3.13 with the peak corresponding to the 1000μl injection broadening out sufficiently to cause a much smaller peak height than would be expected i.e. twice the height of the 500μl injection. This can lead to a loss in peak resolution particularly between peaks close to the solvent front however. Nevertheless, careful manipulation of the sample pH can reduce this

peak broadening quite significantly. However there is a limit to the sample size that this will work for, with this limit decreasing the closer the peak is to the solvent front.

3.5 Baseline Problems.

The combination of the noise reduction system and large volume injections, while providing increased sensitivity also produced several unexpected problems.

The first of these problems was in fact discovered originally when using the NH_3 containing PAR system though the seriousness of it was not fully realised until the increased sensitivity was attained. This problem was and still is 'contamination peaks' which was discussed in Chapter 2.3.3. This is such a major problem that the increase in sensitivity due to the use of the noise reduction system could not be fully exploited due to these elevated blank levels.

Even though the contaminant levels can be reduced 100 fold by the method discussed in Chapter 2.3.3, the improved sensitivity afforded by the noise reduction system means that the low levels that remain still cause problems when attempting to determine similar or lower levels of these metals. As the size of the contamination peaks is dependent upon the length of time that the contaminated eluent is being pumped through to bring the column to equilibrium i.e. its preconcentration time. Shortening the time required to reach equilibrium would cause a decrease in the contaminant levels. This can be done by increasing the buffering capacity of the eluent i.e. increasing the acetic acid concentration in the eluent. While this shortens the

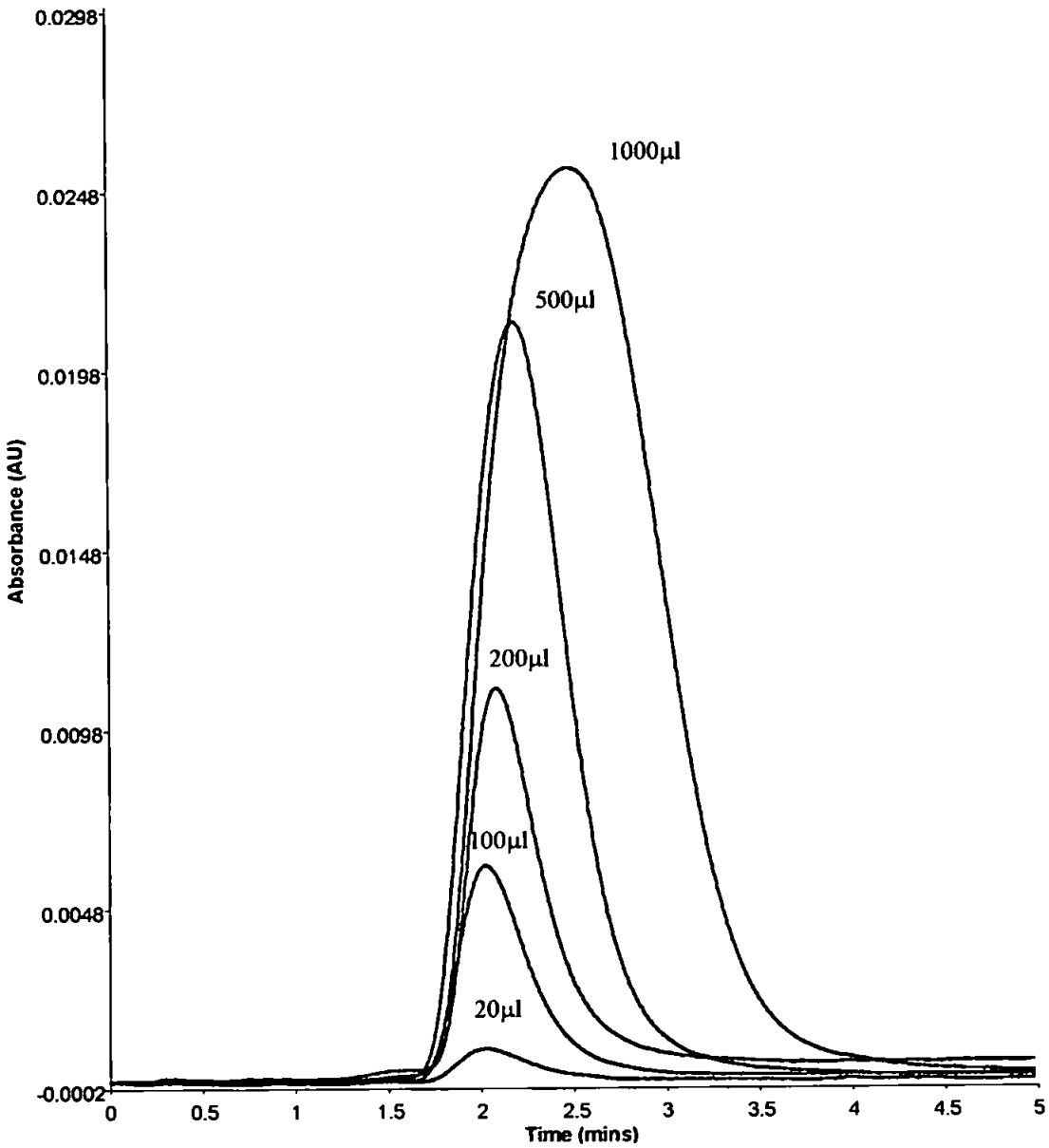

Figure 3.13. Repeat injections of a 100µgl^{-1} Cd(II) standard of increasing volume on the 10cm XO/7µm Hamilton column. Eluent used was 1M KNO_3 buffered with 50mM acetic acid at pH 2. Detection was made at 520nm with PAR.

equilibrium time required it makes worse another problem which already exists, namely changes in the baseline (see Fig 3.8b).

These changes are believed to be caused by the differences in pH found when the PAR solution mixes with the eluent. By its very nature, the absorbtion spectra of PAR is pH dependent (see Figure 3.14). As the pH of the 50:50 PAR:eluent mixture changes over a gradient, the absorbance of the PAR will change and therefore the baseline absorbance level will change. The reason that these baseline changes are a problem, small as they are, is that they generally occur at the same time as one (or more) of the metals under analysis are being eluted thereby "hiding" the peak(s). The noise reduction system coupled with baseline subtraction can help to "reveal" the peak in question but this can be a time consuming and laborious process. The most effective way of combating this is either to use a more concentrated borate solution or use another buffer system in place of the borate system to hold the detection pH more constant.

A 0.2M borate system was tried and this produced, upon adjustment to pH 10.5, a pH difference of 0.05 of a pH unit between the addition of eluent at pH4.5 and 0.1M HNO_3. However, a 0.2M concentration exceeds the solubility of di-sodium tetraborate at room temperature and therefore it slowly crystalises back out at room temperature. If an increase in the temperature of the PAR solution does not have an adverse affect on the system's response then this may provide an acceptable solution to this problem.

Another new buffer system was also quickly looked at. This involved using 3-cyclohexylaminopropan sulphonic acid (CAPS) (Sigma-Aldrich) in place of the di-sodium

tetraborate. CAPS is a biological buffer with a pH range of 9.7-11.1. Concentrations of up to 0.6M proved to be not strong enough to hold the detection pH constant between the addition of eluent at pH 4.5 and 0.1M HNO_3.

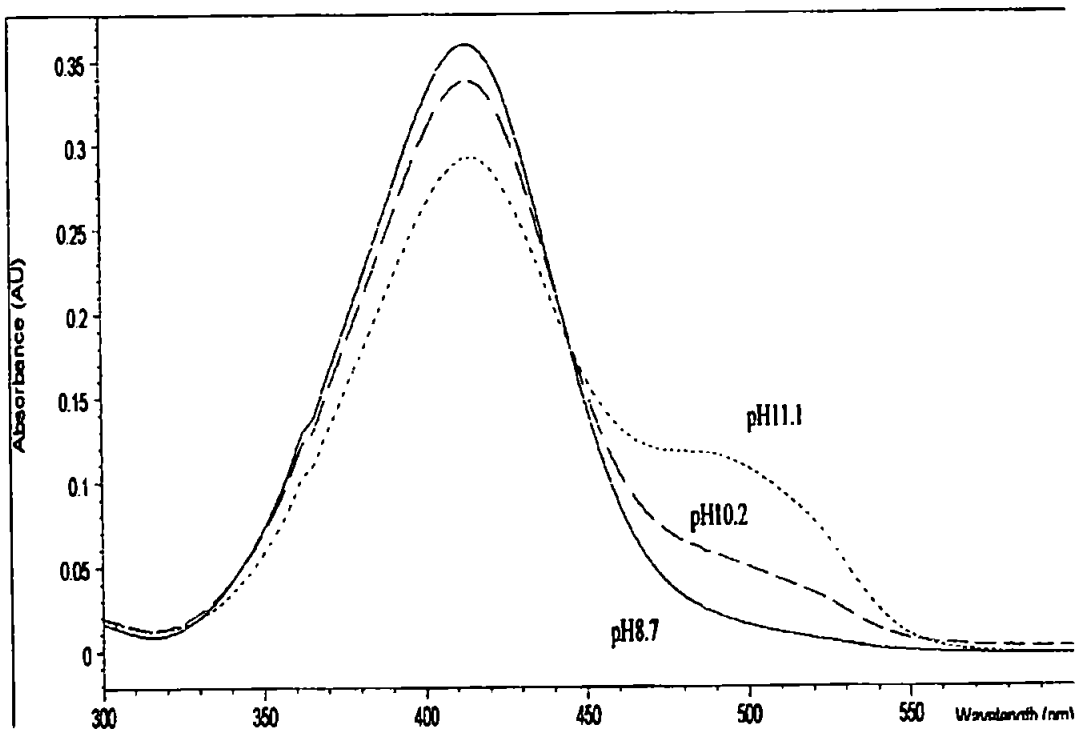

Figure 3.14. UV/VIS Spectrum of PAR at varying pHs.

One final factor that was investigated was the adjustment of the eluent's buffer concentration. As already stated, this itself can cause changes in the baseline. It may be possible however to use the baseline changes caused by adjusting the eluent's buffer concentration over a gradient

run to cancel out the baseline changes caused by the change in pH over the gradient run. For this to work, highly accurate pH control would be required, as the baseline changes experienced are very small, irrespective of the cause. However, it is unlikely that a buffer system could be found which would keep the pH change to virtually zero.

3.6 Summary.

Several post column reaction systems have been developed and optimized for the detection selected transition and high valency metals. The use of the borate buffer system and the employment of a noise reduction system has provided much greater sensitivities than would be normally attained as well as allowing the true baseline to be seen. The problems of baseline fluctuations reported here can be solved though the procedures required to do so are relatively time consuming. More details on the actual post column detection systems used are given in the appropriate chapters.

Chapter 4 :- Development of Dynamically Modified Chelating Substrates.

Part 1:- Investigation of Small Organic Chelating Molecules.

4.1 Introduction.

The investigations so far discussed have dealt with the physical, essentially permanent, impregnation of a chelating molecule onto a high efficiency substrate. As mentioned in Chapter 1.4.1, another way to fabricate a chelating substrate is to dynamically modify the resin with a chelating molecule. This is accomplished by having the ligand of choice present in the mobile phase. In Chapter 2.1.3, the use of metallochromic ligands in this manner was discussed, however these are not the only ligands that can be used. Small organic molecules such as carboxylic acids have also found use in this dynamic modification of substrates.

Shaw [120, 173] investigated the suitability of several small organic molecules including picolinic, dipicolinic, 4-chlorodipicolinic and quinaldic acids as well as L-tryptophan and 2-hydroxyhexadecanoic acid for this use on both PS-DVB and silica based substrates for the separation of selected transition and high valency metals. Shaw used a 7μm PS-DVB resin dynamically modified with 4-chlorodipicolinic acid for the isocratic separation of 7 transition and heavy metals [174] as well as dynamically modifying this resin with dipicolinic acid for the determination of U(VI) in certified reference waters and sediment samples [175]. Elchuk *et al* [176] used an eluent containing mandelic acid for the separation of transition metals, lanthanides, uranium and thorium on a C_{18} silica column whilst Merly *et al* [102] used an oxalic acid containing eluent for the separation of Ni(II),

Cd(II), Pb(II) and Cu(II) on a porous graphitic carbon column. Though neither of these authors reported their findings as chelation-exchange, the elution orders and response to pH changes suggests that a sorbed layer of either mandelic or oxalic acid was present. Hao *et al* [177] used an eluent containing glycolic or mandelic acid for the separation of Th(IV) and U(VI) on a reversed phase C_{18} column. Hao *et al* [178] also reported on the addition of mandelic acid to the sample matrix for the preconcentration of U(VI) and Th(IV) on a short C_{18} concentrator column before elution with an eluent of α-hydroxyisobutyric acid and 10% methanol whilst Nesterenko *et al* [179, 180] used picolinic and quinaldic acids to modify silica columns for the separation of transition metals. With the exception of Shaw and Nesterenko none of the above authors reported the formation of chelating surface on the stationary phase. However, when using small organic carboxylic acids in the eluent, a chelating surface can readily form on a neutral substrate.

The investigations detailed in this chapter discuss the retention behavior of selected transition and high valency metals on dynamically modified high efficiency PS-DVB substrates. For the high valency metals investigated, Bi(III) and U(VI) will be discussed in Chapter 5 whilst the remaining metals investigated, namely Th(IV), V(IV), V(V), Hf(IV) and Zr(IV) will be discussed in this chapter. The ability to determine the concentration of all of these metals in environmental, industrial and biological samples is of increasing importance. A lot of studies have been carried out on these high valency metals since the 1950's using mainly classical ion-exchange resins. Few however, involve the use of high performance separations though lately reverse phase systems using C_{18} columns have been used. The following discussion shows selected recent representation studies on the elements under study.

The first of the metals, Th(IV), was first discovered in 1829 by J. J. Berzelius who named it after Thor, the Norse god of war. Thorium (atomic number 90, atomic mass 232.0381 [19]) is one of the only two actinide elements, the other being uranium, which is naturally occurring in the environment. This is due to the long half life of the ^{232}Th radioisotope, approximately $1.4x10^{10}$ years [169]. It is a soft, ductile silvery metal, the chief ores of which are thorianite and monazite. It has a natural abundance of 12mg kg^{-1} in the earth's crust and $9.2x10^{-6}$ mg l^{-1} in seawater [169] and has found use in refractory materials, nuclear fuel elements and incandescent gas mantles. Thorium compounds are moderately toxic but the main danger is posed by its radiotoxicity.

Th(IV) is usually separated in the presence of U(VI). Dev *et al* [91] preconcentrated and separated Th(IV) from U(VI), La(III), Nd(III) and Tb(III) on Amberlite XAD-4 resin functionalised with Bicine ligands whilst Jain *et al* [181] also used XAD-4 resin but this time functionalised with o-vanillinsemicarbazone for the preconcentration and separation of La(III), Ce(III), Th(IV) and U(VI) followed by detection with atomic spectrometry. Pavon *et al* [182] used Dowex 50-X8 resin for the preconcentration of Th(IV) and U(VI) followed by their determination by flow injection followed by UV/VIS detection with Arsenazo III.

Vanadium was first discovered in 1801 by the Mexican chemist Manuel del Rio who named it 'erythronium'. In 1830, N. G. Selfstrom who named it vanadium after Vanadis, the Norse god of beauty, rediscovered it. It is a shiny, silvery metal with an atomic number of 23 and an atomic mass of 50.941 [19]. Its principle ores are carnotite, descloizite, patronite and vanadinite with a natural abundance of 160mg kg^{-1} in the earth's crust and an average of $1.35x10^{-3}$ mg l^{-1} in surface seawaters [169]. It is used mainly in alloys due to its

corrosion resistance and it is also an essential element for cell growth at μg l^{-1} levels though is toxic at higher concentrations [183]. The toxicity of vanadium is dependant upon its oxidation state with V(V) being more toxic than V(IV) [184]. As V(V) is the more toxic of the two oxidation states, the ability to separate and quantify this species is of great importance.

Bagur *et al* [185] selectively preconcentrated V(V) as its complex with *N*-phenylbenzohydroxamine acid (PBHA) on a Superspher Si60 normal phase column. Elution was with an eluent of trichloromethane/methanol and the method applied to V(V) determinations in clam tissue. Wuillond *et al* [186] used Amberlite XAD-7 resin to preconcentrate V(IV) and V(V) as their complexes with 5-Br-PADAP followed by detection with ICP-AES for vanadium in drinking water whilst flow injection ICP-MS was used by Willie *et al* [187] for vanadium determinations in seawater. Strelow [188] determined trace amounts of V(IV) in Molybdenum metal using an AG50W-X8 cation exchange resin. Detection was made using PAR in the presence of cyclohexanediaminetetraacetic acid (CDTA). Tomlinson *et al* [189] used a CS5 column for the separation of V(IV) and V(V) using an eluent containing PDCA followed by detection by ICP-MS whilst Gong *et al* [190] used an epoxy-dicyandiamide chelating resin for the preconcentration and separation of V(V), Sn(IV), Ti(IV), Bi(III), Ga(III) and In(III) before detection by ICP-AES.

Hafnium (atomic number 72, atomic mass 178.49 [19]) was first discovered in 1923 by D. Coster and G. C. von Hevesey while zirconium (atomic number 40, atomic mass 91.22 [19]) was first discovered in 1789 by M. H. Klaproth and first isolated in 1824 by J. J. Berzelius. Both are lustrous, silvery metals that are resistant to corrosion. They have

found use in alloys, ceramics and nuclear reactors with hafnium being used in the control rods of nuclear reactors [169]. Both metals are relatively non-toxic. The chief mineral of hafnium is known as hafnon and has an abundance of 5.3 mg kg^{-1} in the earth's crust and $7x10^{-6}$ mg l^{-1} in seawater [169]. The principle ores of zirconium are baddeleyite and zircon and has an abundance of 190mg kg^{-1} and $9x10^{-6}$ mg l^{-1} in the earth's crust and seawater respectively.

The simultaneous determination of hafnium and zirconium can be extremely difficult due to the similarities between their physical properties. Oszwaldowski *et al* [191] used reversed phase HPLC for the simultaneous separation of ternary Hf(IV) and Zr(IV) fluoride/5-Br-PADAP complexes with spectrophotometric detection as well as the detection of fluoride by this same method [192]. Yang and Pin [193, 194] used an Amberchrom CG-71m, polymethacrylate resin functionalised with either Aliquat 336 or N-benzoyl-N-phenylhydroxylamine (BPHA) for the preconcentration of Hf(IV) and Zr(IV) in basaltic rocks with detection by ICP-AES. Trubert *et al* [195] used a Bio-Rad AG-MP1 anion exchange resin to separate Hf(IV) and Zr(IV) from Nb(V), Ta(V) and Pa(V) in chloride-fluoride media whilst Queshi *et al* [196] reported the quantitative separation of Zr(IV) and Hf(IV) on Dowex 50 W-X8 resin in formic acid media. Purohit and Devi [197] used a variety of chelating resins including 8-hydroxyquinoline and hydroquinone for the preconcentration of trace quantities of Zr(IV) with spectrophotometric detection with XO at 535nm.

Of the studies reviewed most of then resulted in low efficiency separations commonly with eluents containing concentrated acids. The aim of this study is to produce high efficiency

separations of the metals of interest using more "user friendly" eluents that contain lower acid concentrations.

4.2 Experimental.

4.2.1 Instrumentation.

The instrumentation used for these studies was as described in Chapter 2.2.1 with the exception that a Dionex GP40 (Dionex, Sunnyvale, CA, USA) gradient pump was used to deliver the eluent.

4.2.2 Reagents.

All reagents used for these investigations were obtained from BDH and of AnalaR grade unless otherwise stated. The eluents used in this study contained 1M KNO_3 and the requisite amount of chelating ligand adjusted to the required pH with conc HNO_3. The transition and heavy metals were determined at 520nm with the PAR/Borate PCR ($1x10^{-4}$ M PAR, 0.125M di-sodium tetraborate made up to 1 litre and adjusted to pH10.5 with 5M NaOH). The determination of the high valency metals was carried out using either Arsenazo III (ICN) at 654nm (0.15mM Arsenazo III in 1M HNO_3 with the HNO_3 concentration being adjusted so that the mixing pH was pH0) or Pyrocatechol Violet (PCV) (BDH) at 555nm ($40mgl^{-1}$ PCV, 2M hexamine) as the PCR. Compensating wavelengths (Chapter 3.4.1) of 445, 585 and 371nm were used respectively.

Metal standards were prepared from $1000mgl^{-1}$ Spectrosol metal stock solutions with the exception of V(IV), V(V) and Ti(IV). V(V) was prepared by dissolving ammonium

vanadate in 1M HNO_3 to produce a stock solution of 2800mgl^{-1}. The V(IV) stock solution was prepared by addding an excess of ascorbic acid to the V(V) solution and allowing to stand for 5 minutes before use. A 1000mgl^{-1} stock solution of Ti(IV) was prepared by dissolving titanium oxysulfate in 1M HNO_3. All working standards were made up to the required volume in dilute HNO_3 of the same pH as the eluent being used. All standards were stored in poly(propylene) bottles.

4.2.3 Preparation of the Mobile Phase.

The required amount of ligand was added to 50ml of MilliQ water in a covered glass beaker and stirred using a magnetic stirrer and, if necessary, heated until complete dissolution was obtained. This solution was then made up to the required volume with 1M KNO_3 and adjusted to the required pH using HNO_3.

4.3 Results and Discussion.

4.3.1 Measurement of Dynamic Loading.

As previously discussed, dynamically modified substrates can be readily attained by adding a chelating ligand to the mobile phase. As the mobile phase is pumped through the column, the chelating ligand is adsorbed onto the substrate. This results in an equilibrium being formed between the sorbed layer of ligand and that which remains in the mobile phase. Increasing or decreasing the amount of chelating ligand in the mobile phase will result in a corresponding increase or decrease in the concentration of ligand in the sorbed layer which will change the equilibrium thereby affecting the selectivity of the column.

For a separation of metal ions to occur, the sorbed layer of ligand has to be of a significantly higher concentration than that remaining in the eluent. A simple experimental method which can provide an indication of the amount of chelating ligand that will be sorbed is the determination of the capacity factor of the ligand. As with capacity factor determinations of metal ions on the dye impregnated columns, the capacity factor of the chelating ligand is derived from its retention time when a discrete amount is injected onto an unmodified substrate. The greater the k' value, the greater the amount of ligand that will be sorbed relative to the amount remaining in the eluent.

4.3.2 Factors Affecting Dynamic Loading.

There are several factors which can influence the extent of the dynamic modification of a substrate. Firstly, the particle size of the substrate would be expected to greatly affect the extent of dynamic loading. As particle size decreases, a greater dynamic loading would be expected due to the increased number of pores and therefore increased surface area available for the sorption of the ligand. Decreasing the substrate's particle size should also increase the resin's hydrophobicity thereby resulting in a greater attraction for these hydrophobic molecules. Studies carried out by Shaw [120] have shown that these suppositions are reasonably correct and that the k' value for a chelating ligand will generally increase with a decrease in particle size.

An experimental parameter which can also affect the dynamic modification of a substrate is temperature. As dynamic modification is an equilibrium condition involving partitioning between the mobile and stationary phases, a change in the temperature of the system would be expected to affect the equilibrium and therefore the sorbed layer on the

substrate and thereby change the retention times of the metal ions under analysis. Shaw [120] reported that neutral resins dynamically modified with dipicolinic acid are suited to the separation of high valency metals such as U(VI), Th(IV) and Bi(III). Repeat injections of a U(VI) standard on a column modified with dipicolinic acid showed an almost linear decrease in retention time with an increase in temperature between 15-30°C, the average ambient temperature of the laboratory. Table 4.1 shows a 2.1 minute decrease in the retention time of U(VI) and this change was considered sufficiently large enough to warrant thermostating the column. This was attained by placing the column in a water bath set at 30°C which resulted in a constant retention time of approximately 7.9 minutes.

Table 4.1. Variation of U(VI) retention time with temperature on 5μm PLRP-S resin dynamically modified with dipicolinic acid. Eluent used was 0.5M HNO_3 with 0.1mM dipicolinic acid. Injection volume was 500μl with detection made at 654nm with Arsenazo III.

Temperature (°C)	Retention Time (min)
16	10.05
18	9.91
19	9.54
21	9.20
22	8.92
23	8.73
24	8.71
25	8.58
30	7.90

4.3.3 Reproducibility of Dynamic Systems.

One significant advantage of dynamically modified substrates over dye impregnated substrates is the ease with which the bare substrate can be recovered. With dye impregnated resins a small amount of the dye is, for all intents and purposes, permanently impregnated onto the resin. Even though the ultrasonic loading procedures allow for the reimpregnation of dye columns it is advisable to use the same dyestuff i.e. use a fresh XO dye solution to reimpregnate a XO loaded column. The small organic molecules that are used for dynamic modification can be much more readily and completely removed from the substrate thereby allowing the bare resin to be used for other purposes. Even after several reloadings of the column over a period of several months, the retention times obtained remained relatively constant. This consistency was found not only with the dipicolinic column but also with all the other ligands investigated. Table 4.2 shows the retention times of U(VI) after several reloadings of the column using an eluent containing 1M HNO_3 and 0.1mM dipicolinic acid. The slight differences in retention shown are due to slight differences in the sample concentration, sample pH and injection volume.

Table 4.2. Reproducibility of dynamic loading on 5µm PLRP-S resin dynamically modified with dipicolinic acid. Eluent used was 1M HNO_3 with 0.1mM dipicolinic acid. Injection volume was 500µl with detection made at 654nm with Arsenazo III.

Loading	U(VI) Retention Time (min)
1	4.70
2	4.65
3	4.85
4	4.90

4.3.4 Column Characteristics.

There are potentially hundreds if not thousands of small organic chelating compounds that could be potentially used for the dynamic modification of a substrate. For these investigations, four small carboxylic acids were investigated, dipicolinic acid, 2-chloromandelic acid, 4-chloromandelic acid and 4-chlorophenylalanine. The reasons for these choices were that dipicolinic acid complexes strongly at low pHs with a wide selection of metal ions as well as offering reasonably fast kinetics. The chloromandelic acid was chosen as it is a weaker complexing agent and also is an O, O chelator rather than a N, O chelator as is dipicolinic acid. 4-chlorophenylalanine was chosen as an amino acid functional group had not been investigated before. The structures of these compounds are given in Figure 4.1.

4.3.4.1 Dipicolinic Acid.

2,6-pyridinedicarboxylic acid or dipicolinic acid (99%, Aldrich, Dorset, UK) is a widely used complexation reagent that offers N, O, O chelation. The structure of dipicolinic acid is given in Figure 4.1. It has found extensive use as an eluent complexing agent for enhanced IC selectivity and separations. The column used for this study was a 100 x 4.6mm ID PEEK column packed with a 5μm, 100Å PLRP-S resin supplied by Polymer Laboratories. Sutton [118] and Shaw *et al* [120] have reported studies involving the investigation of transition and heavy metals on columns dynamically modified with dipicolinic acid and so these metals were not investigated. These studies also reported on the highly specific nature of dynamically modified dipicolinic columns towards uranium.

The retention characteristics of a selection of high valency metal ions including U(VI), Th(IV), Bi(III), Hf(IV), Zr(IV), V(IV), V(V), Sn(IV), and Ti(IV) were investigated. Zr(IV) and Hf(IV) were investigated due to the wide spread use of Zr(IV) in the nuclear industry. Also a high efficiency separation of these two metals remains problematic in less concentrated acids due to the similarities in the properties of these two metals. V(IV) and V(V) were of interest due to vanadium being an essential eluent for cell growth at trace levels though becomes more toxic at higher concentrations with V(V) being more toxic than V(IV) [183, 184].

Two different post column reagents were used in this study. Pyrocatechol Violet (PCV) was used for the determination of V(IV), V(V), Sn(IV) and Ti(IV) whilst Arsenazo III was used for the determination of the remaining metals. An elution order of Th(IV) < V(V) < Bi(III) < U(VI) < Hf(IV) < Zr(IV) was found at pH1, though as the k' plots in Figure 4.2 show the elution order of Bi(III) and V(V) reverses at approximately pH1.5. V(IV), Sn(IV) and Ti(IV) all showed no retention over the pH range 0-2. The retention times of these metals are given in Table 4.3.

The k' plots of the high valency metals can be explained by the complicated relationship that exists between the sorbed layer of dipicolinic acid and the dipicolinic acid in the mobile phase. If metal chelation on the surface of the substrate was the only factor involved in the retention and separation of the metals, then linear k' vs pH plots would be expected. This is thought to be due to the increase in stability constants with pH.

a)

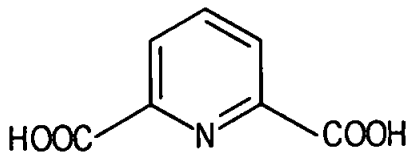

b)

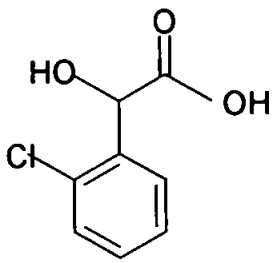

c)

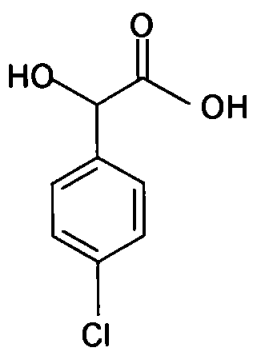

d)

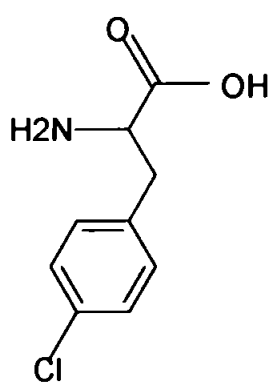

Figure 4.1. Structure of a) Dipicolinic acid, b)2-Chloromandelic acid, c) 4-chloromandelic acid and d) 4-Chlorophenylalanine.

Table 4.3. Retention times (in minutes) for 10cm Dipicolinic/5μm PLRP-S column (t_0 = 1.36 minutes). Eluent used was 1M KNO_3 with 0.1mM dipicolinic acid. Injection volume was 500μl with detection made at 654nm with Arsenazo III.

pH	Th(IV)	Bi(III)	U(VI)	Zr(IV)	Hf(IV)	V(V)
-0.3	1.44	2.27	2.06	6.77	6.07	---
-0.17	1.52	2.48	2.66	7.77	6.97	---
0	1.58	3.15	4.81	9.69	8.67	1.59
0.3	1.67	3.60	7.67	12.24	10.99	1.98
1	1.88	5.31	12.37	15.98	14.01	4.54
1.3	1.96	4.71	12.66	16.43	14.62	5.04
2	3.27	3.43	14.98	18.90	15.76	5.04

However, as the pH increases, complexation in the mobile phase becomes more important. It is theorised that this is due to the formation of the more stable 1:2 metal:dipic complex in the eluent with the 1:1 metal:dipic complex being the principle complex found on the surface of the substrate. It is assumed that steric effects will prevent or at least minimise the formation of these more stable 1:2 complexes on the surface of the substrate regardless of pH. An additional factor which will reinforce the increased competition in the mobile phase is the steadily decreasing amount of dynamically loaded dipicolinic acid with an increase in pH as is shown in the k' plot of dipicolinic acid itself (Figure 4.3). The lack of stability constant data for dipicolinic acid complexes of high valency metals makes this retention behavior difficult to interpret fully. Nevertheless the complex k' plots do offer some unusual selectivity control, for example Bi(III) can be eluted either before or after

V(V) depending upon the pH used. Figures 4.4-4.7 show the separation of selected metals on this dynamically modified column.

Figure 4.4 shows the separation of Bi(III) and U(VI) at pH 0. This chromatogram shows the major problem experienced with the Arsenazo III PCR, that being a steadily increasing baseline. The separation of six metal species at pH0.3 (0.5M HNO_3 eluent) is given in Figure 4.5. Fe(III) was added to the metal mixture to show the exact position of the solvent front and to highlight to very slight retention of Th(IV) that was experienced. An interesting point to note is the wide range of metal ion concentrations shown (0.5-20mg l^{-1}) which indicates the wide range of sensitivities experienced with the Arsenazo III. Figure 4.6 shows the separation of the same suite of metals but this time at a flow rate of 0.5ml min^{-1}. As can be seen, there is greater resolution between Hf(IV) and Zr(IV) however the run time, as well as peak width, has doubled without any increase in peak height or resulted in any adverse affect on the separation. Zr(IV) and Hf(IV) are sufficiently separated on this column to allow quantification by peak height though if column efficiency increases proportionately with column length then increasing the column length to, for example 25cm, this should result in the baseline resolution of these two peaks. As V(IV) shows no retention on this column, V(V) can be readily separated from V(IV) as is shown in Figure 4.7. This is in fact the reverse of what would be expected for a cation exchange separation in acid media [188].

The dipicolinic acid loaded column shows a lot of potential for the separation and determination of high charged metal species. This was investigated further and is described in Chapter 5.

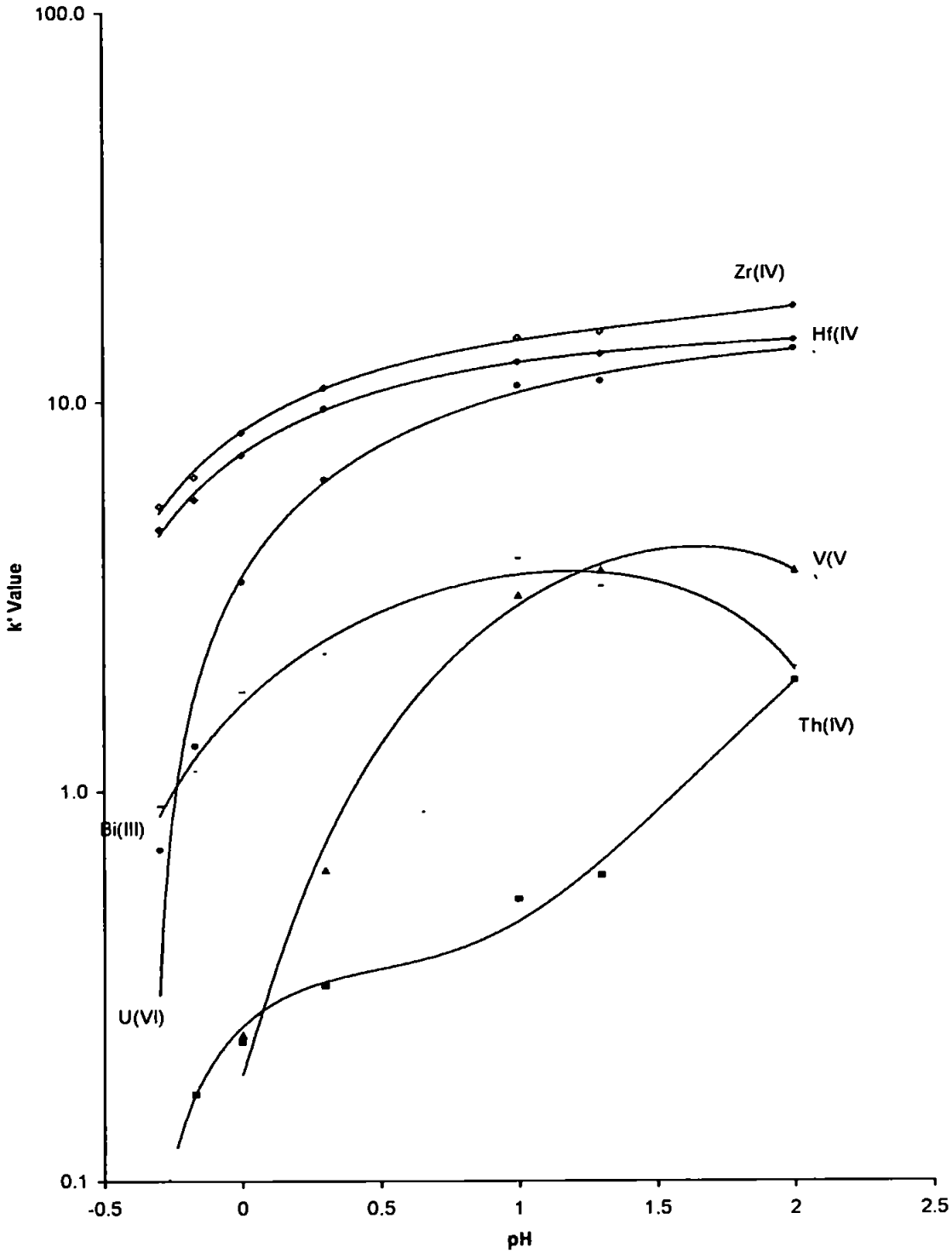

Figure 4.2. The dependence of capacity factors (k') for selected high valency metals on eluent pH with dipicolinic acid modified 5μm PLRP-S column. Detection made at 654nm with Arsenazo III.

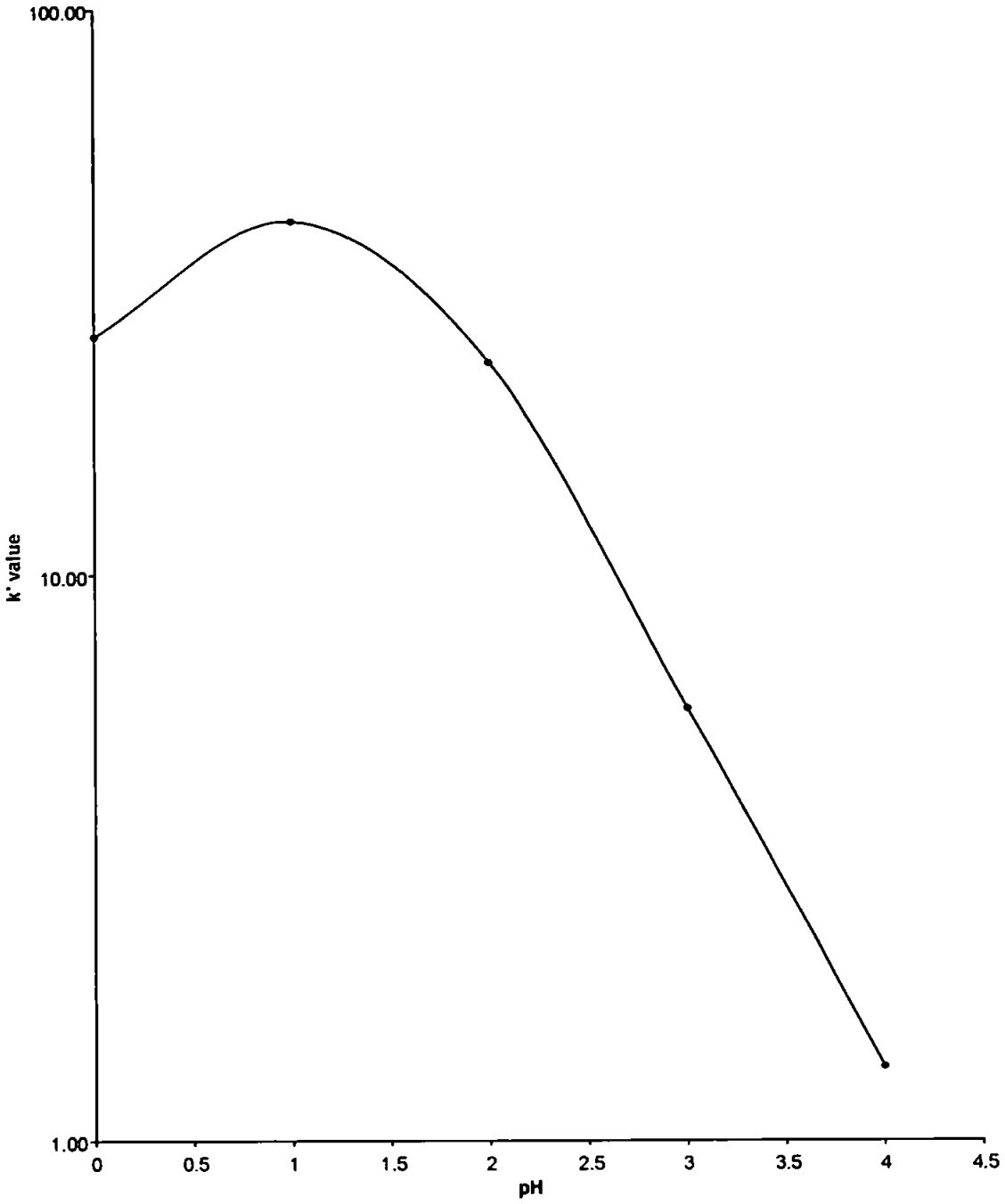

Figure 4.3. k' plot of dipicolinic acid injected onto 10cm 5μm PLRP-S column. Injection volume was 500μl with detection made at 270nm.

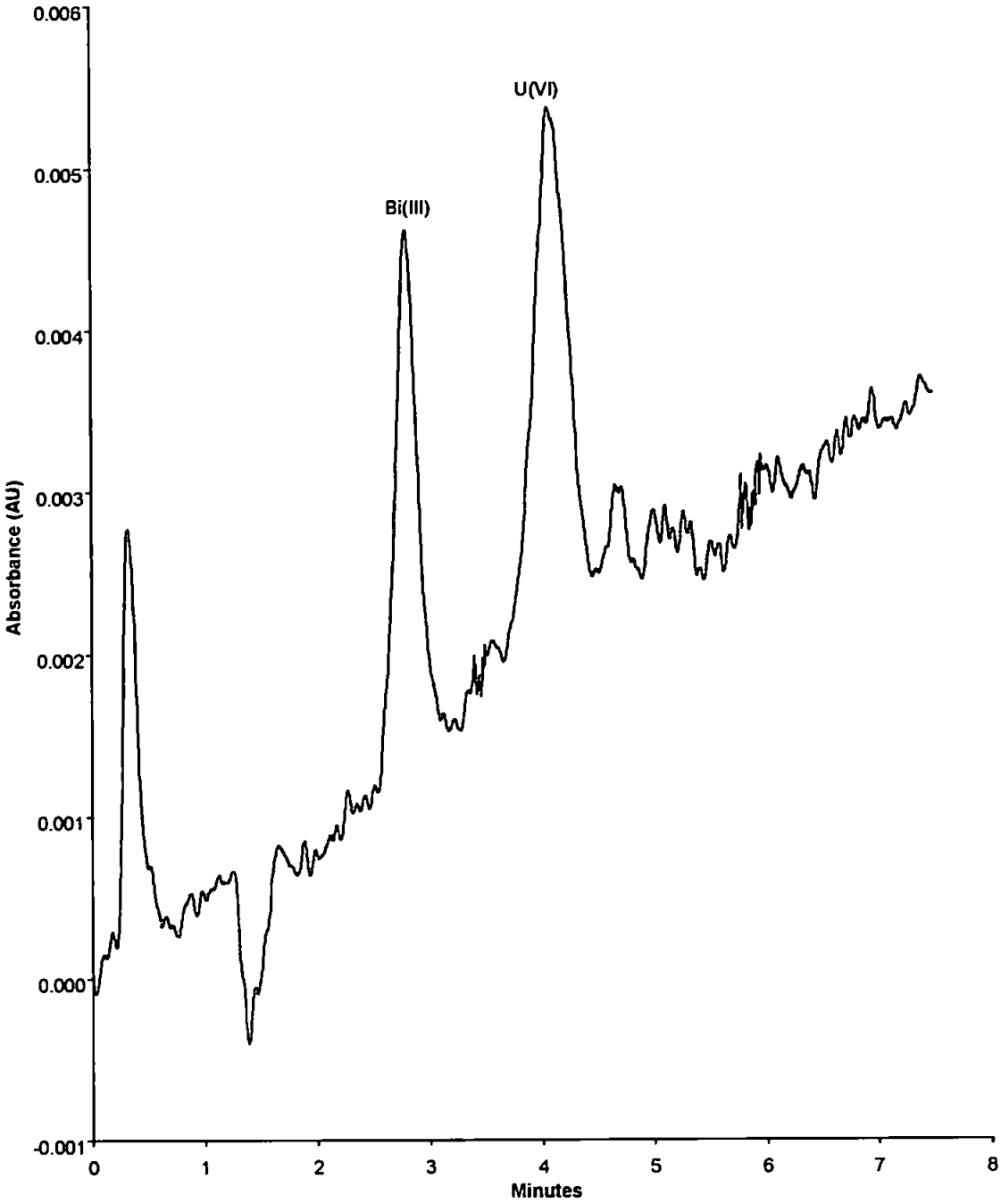

Figure 4.4. Isocratic separation of 20mgl^{-1} Bi(III) and 0.5mgl^{-1} U(VI) on 10cm dipicolinic modified 5μm PLRP-S column at pH 0. Eluent used was 1M HNO_3, 0.1mM dipicolinic acid with an injection volume of 100μl with detection at 654nm with Arsenazo III PCR.

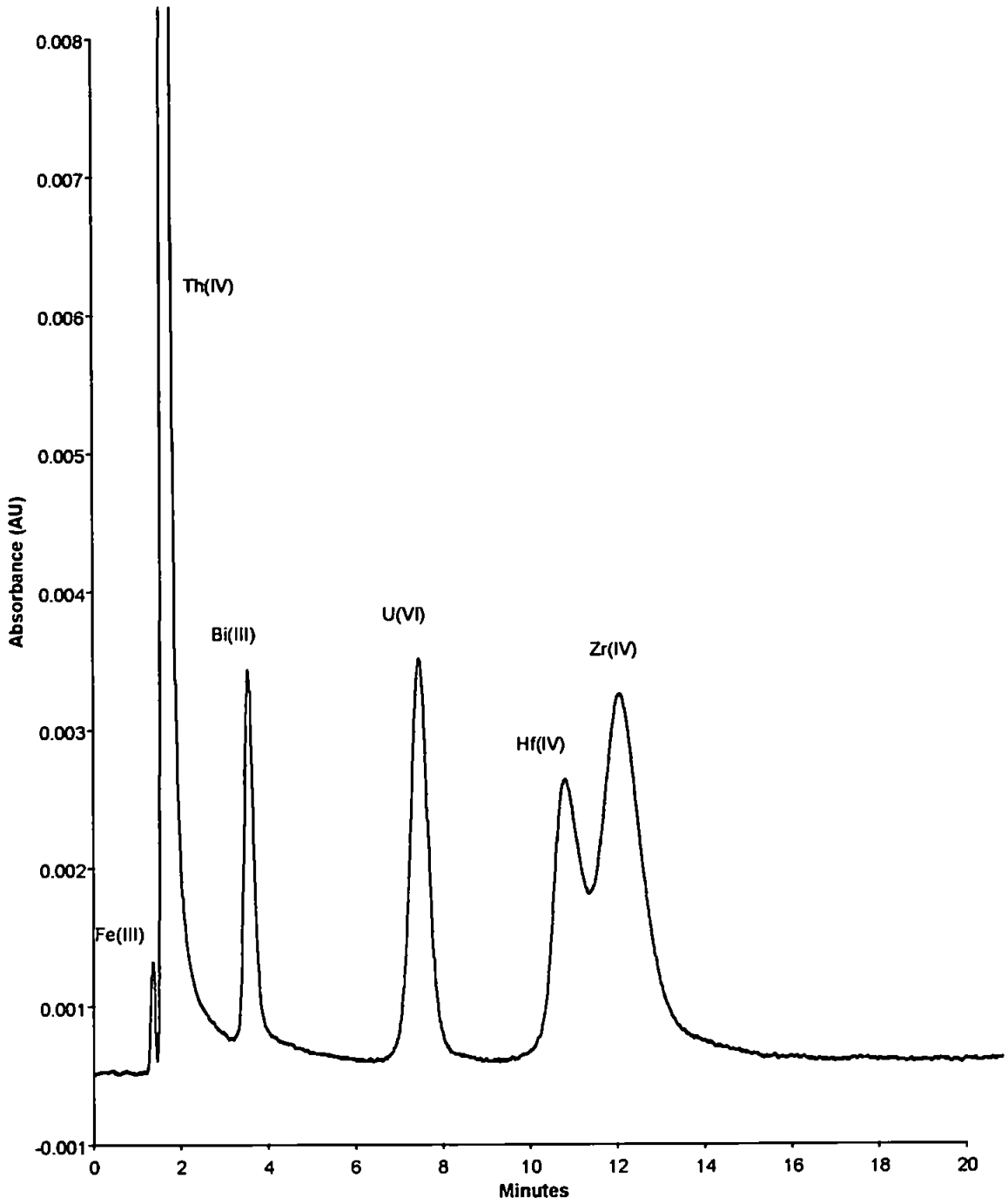

Figure 4.5. Isocratic separation of 20mgl^{-1} Fe(III), 0.5mgl^{-1} Th(IV), 20mgl^{-1} Bi(III), 0.5mgl^{-1} U(VI), 25mgl^{-1} Hf(IV) and 5mgl^{-1} Zr(IV) on the 10cm dipicolinic/5μm PLRP-S column. Eluent used was 1M HNO_3, 0.1mM dipicolinic acid with an injection volume of 100μl and detection at 654nm with Arsenazo III.

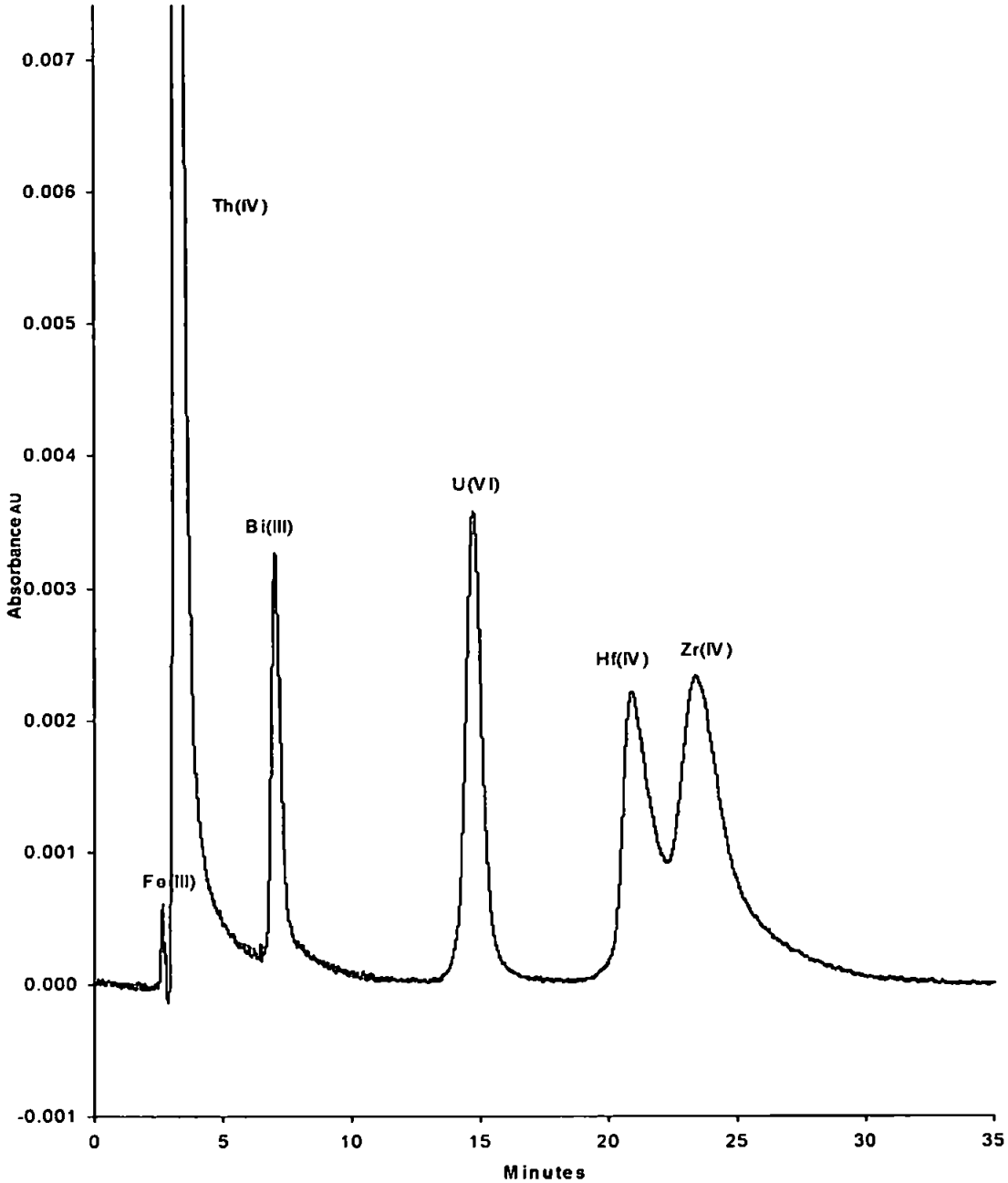

Figure 4.6. Same separation and conditions as for Figure 4.5 with the exception that a flow rate of 0.5mls/min rather that 1ml/min was used.

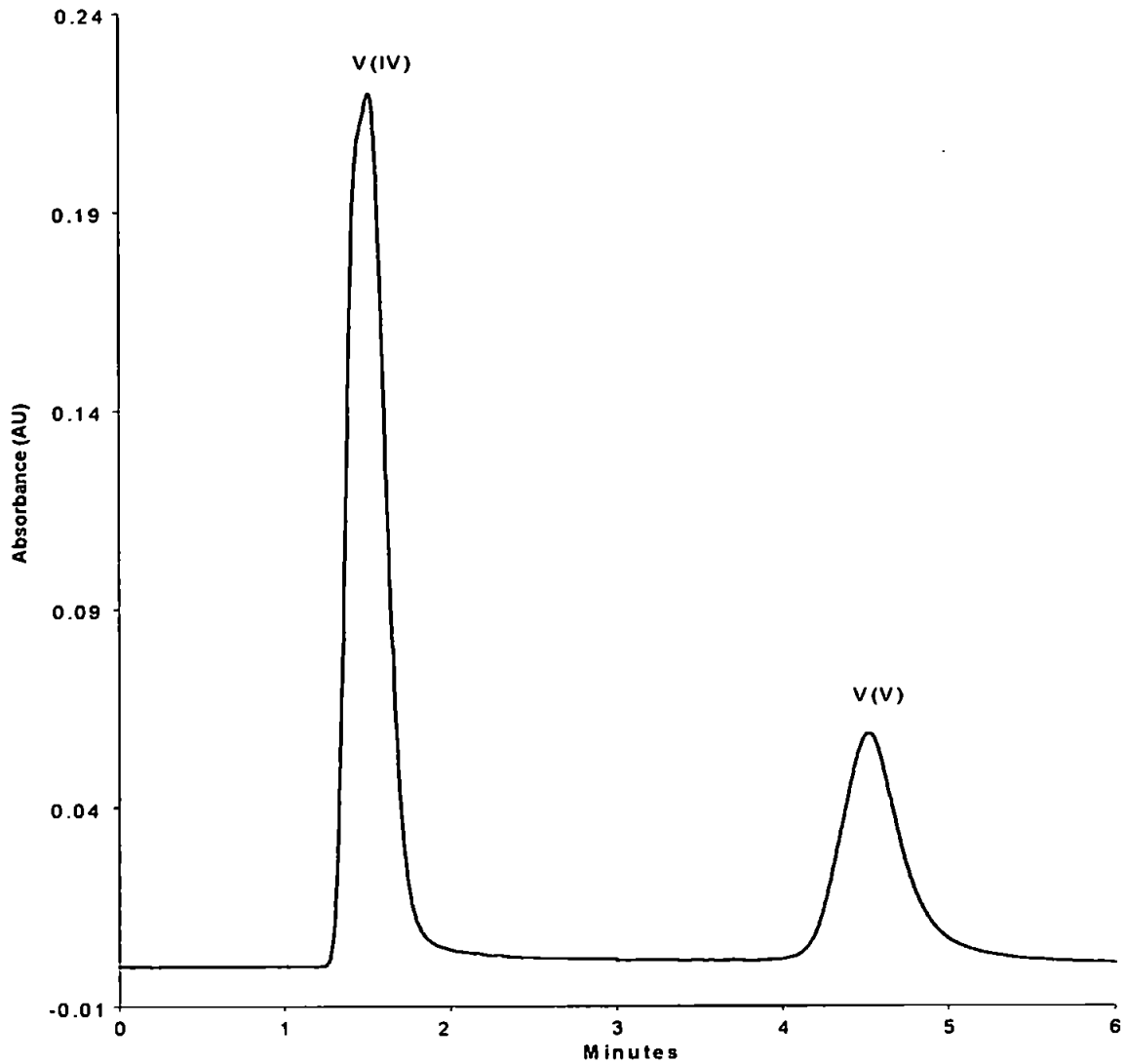

Figure 4.7. Isocratic separation of V(IV) and V(V) on 10cm dipicolinic/5μm PLRP-S column. Eluent used was 0.1M HNO_3, 0.1mM dipicolinic acid with an injection volume of 100μl and detection at 555nm with PCV.

4.3.4.2 2-Chloromandelic Acid.

2-Chlorophenylhydroxyacetic acid or 2-chloromandelic acid (98%, Acros Organics, Leicestershire, UK), the structure of which is shown in Figure 4.1 is an O, O chelator which is a derivative of mandelic acid. Past studies [120, 174] have shown that under certain conditions e.g. high pH, the dynamically sorbed layer of ligand can become insufficient and unstable which leads to poor peak resolution. Also competition from the ligand present in the mobile phase increases making it more difficult to provide an explanations for the separations occurring.

One way to improve this is to either use a more hydrophobic chelating ligand which has the same functional group or improve the stability of the dynamically sorbed layer, either of which should increase the concentration of the sorbed layer relative to that in the mobile phase. For these reasons a chlorinated derivative of mandelic acid was used, namely 2-chloromandelic acid. The presence of the chlorine group means that this compound is not only more hydrophobic than its parent molecule but also produces a more stable dynamic layer. The π-electron donating properties of PS-DVB matrices are well documented [198] and therefore, with the introduction of a molecule with a π-electron acceptor functional group the π-π interactions between PS-DVB matrix and the chelating molecules will be much stronger. This will result in an increased capacity. As the chelating molecule coordinates preferably on the flat outer surface of the substrate, it will also increase the accessibility of the chelating functional groups to the metal ions which, altogether, will result in a more stable chelating stationary phase of enhanced performance.

Initial studies using this ligand to modify the 5µm PLRP-S resin proved disappointing with poor retention of both the transition and high valency metals. The use of this ligand also resulted in the formation of an unstable system with constantly changing retention times. 4-chloromandelic acid (98%, Acros Organics) was also investigated but this provided results similar to those obtained with the 2-chloromandelic acid. It was hypothesised that there might be sufficient quantities of the 4-chloromandelic acid present in the 2-chloromandelic acid and vice versa and this could possibly be the cause of the poor results being obtained. In order to determine if this was the case, both of these chlorinated derivatives were analysed by Liquid Chromatography - Mass Spectrometry (LC-MS).

4.3.4.2.1 LC-MS Analysis.

Mr P. McCormack, of the University of Plymouth, UK, kindly performed this analysis.

This analysis was carried out using a Finnigan MAT LCQ-MS detector (Finnigan MAT, San Jose, CA, USA). An eluent of 80:20 methanol:MilliQ water with 0.1% formic acid was delivered by a Dionex GP40 gradient pump at a flow rate of 1ml min^{-1}. The column used was the 100 x 4.6mm ID column packed with the 5µm PLRP-S resin. The results of this analysis showed that there was indeed trace levels of the 4-chloromandelic acid in the 2-chloromandelic acid and vice versa. However, the levels present were deemed insufficient to cause the poor results obtained from this column.

4.3.4.3 4-Chlorophenylalanine.

Another small organic molecule that was investigated was DL-4-chlorophenylalanine (99%, Aldrich) this time a N, O chelator. Again a chlorinated derivative was investigated rather than the parent molecule. Figure 4.1 shows the structure of this molecule.

The 100 x 4.6mm ID PEEK column packed with the 5μm PLRP-S resin as used previously was again used for these studies. Figure 4.8 shows the k' plot of the 4-chlorophenylalanine on this column at varying ionic strengths. The 4-chlorophenylalanine shows maximum absorption at 265nm and as the nitrate ion also shows very strong absorption at this wavelength ionic strength was provided by KCl rather than KNO_3 with conc HCl used for pH adjustments instead of conc HNO_3. The k' plots were obtained at low (0.01M), medium (0.1M) and high (1M) ionic strengths. As is shown in Figure 4.8 the greater the ionic strength the greater the retention of the 4-chlorophenylalanine and therefore, the greater the dynamic loading. It was decided to investigate selected transition, heavy and high valency metals on a column dynamically modified with 1mM 4-chlorophenylalanine.

Figure 4.9 shows the k' plot of selected transition and heavy metals with Table 4.4 showing the corresponding retention times at an ionic strength of 1M KNO_3. Except for Cu(II) none of these metals showed any significant retention until pH4.5-5 was reached when an eluent containing 1mM 4-chlorophenylalanine was used. The elution order found

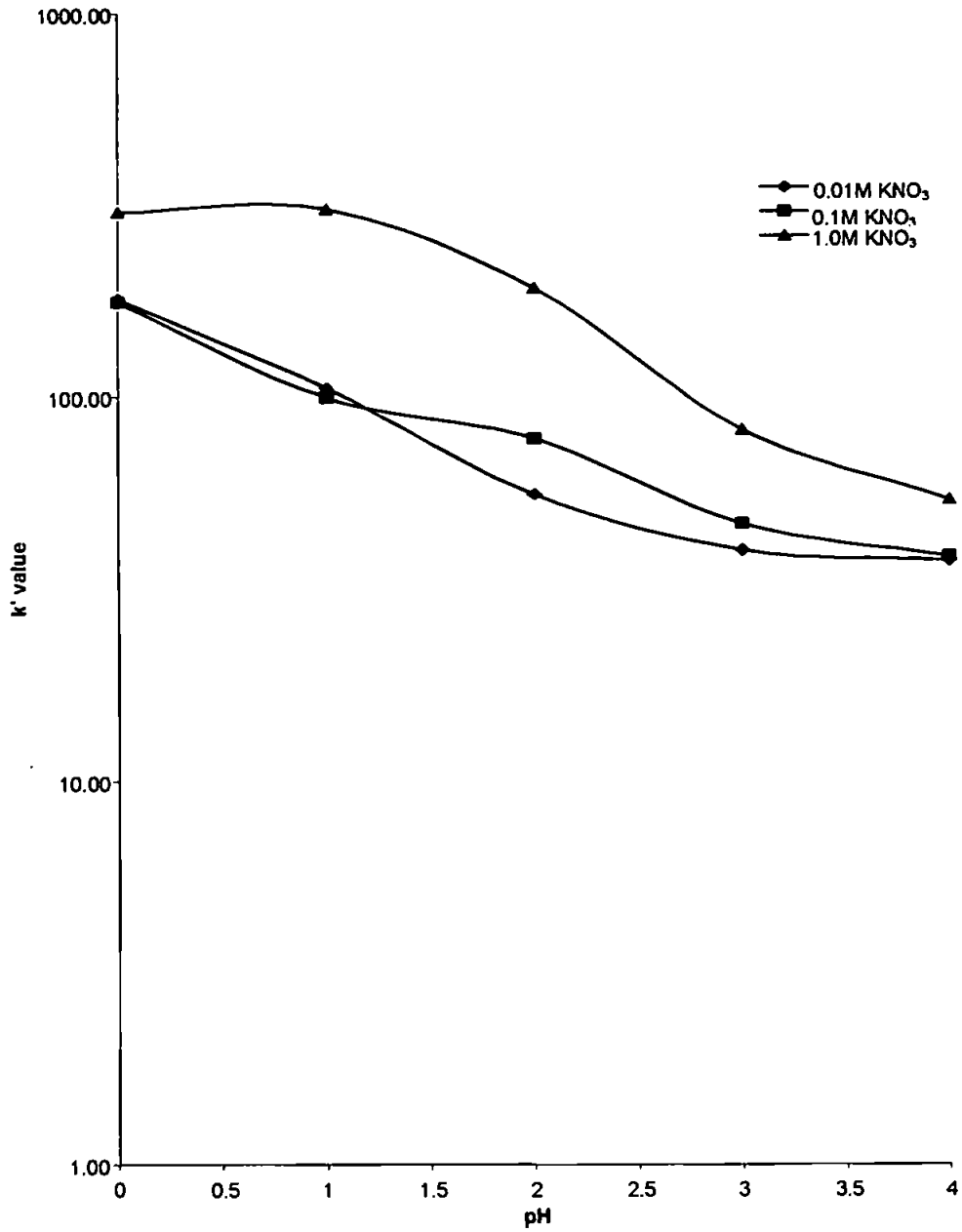

Figure 4.8. k' of 4-chlorophenylalanine on 10 5µm PLRP-S column at various ionic strengths. Injection volume was 500µl with detection at 280nm.

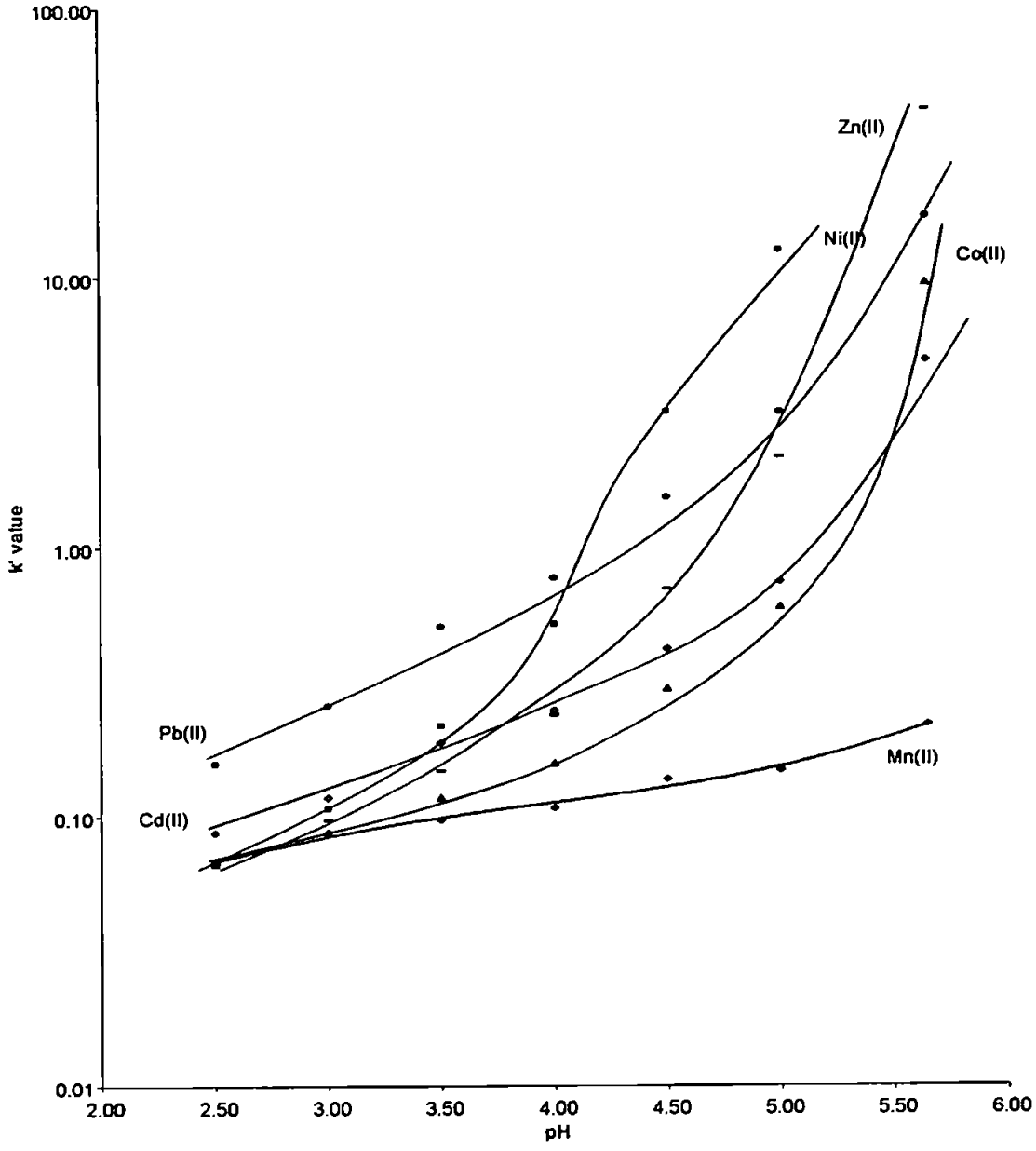

Figure 4.9. The dependence of capacity factors (k') for selected transition and heavy metals on eluent pH with 4-chlorophenylalanine modified 5μm PLRP-S column. Eluent used was 1M KNO_3 with an injection volume of 500μl. Detection was made at 520nm with PAR.

at pH 5 was Mn(II) < Co(II) < Cd(II) < Zn(II) < Pb(II) < Ni(II) < Cu(II) however this changed to Mn(II) < Cd(II) < Co(II) < Pb(II) < Zn(II) < Ni(II) < Cu(II) at pH 5.65. The separation of some selected transition and heavy metals is shown in Figures 4.10-4.12.

Table 4.4. Retention times (in minutes) for transition metals on a 10cm 4-chlorophenylalanine/5μm PLRP-S column (t_0 = 1.45 minutes). Eluent used was 1M KNO_3 with an injection volume of 500μl. Detection was made at 520nm with PAR.

pH	Mn(II)	Cd(II)	Zn(II)	Pb(II)	Co(II)	Ni(II)	Cu(II)
2.50	1.42	1.44	1.42	1.51	1.42	1.42	14.20
3.00	1.44	1.47	1.45	1.61	1.44	1.46	95.80
3.50	1.45	1.54	1.50	1.86	1.47	1.57	---
4.00	1.46	1.60	1.59	2.12	1.51	1.87	---
4.50	1.49	1.77	2.05	2.88	1.65	4.53	---
5.00	1.50	2.09	3.50	4.50	1.95	13.89	---
5.65	1.57	6.23	43.00	18.00	10.98	---	---

As can be seen in Figures 4.10 and 4.11, peak shapes are reasonably symmetrical with the exception of Pb(II) which shows some tailing. Ni(II) produces a symmetrical but very broad peak. Overall the efficiency of this system was not very good with, it appears, a limited pH range for obtaining a multi-element separation. This could be explained by the strong protonation of the NH_2 group until this pH is reached inhibitinf complex formation with these metal cations until this pH is reached.

The high valency metals also showed very little retention until pH2 at which point U(VI), Zr(IV) and Hf(IV) all started to show some retention, the retention times of which are given in Table 4.5. This column did prove however to be more selective towards Th(IV) than the dipicolinic acid column. In fact the elution of Th(IV) and U(VI) was reversed when using this system. Also, it appeared to be very selective towards Bi(III) as a 200mgl^{-1} standard was not detected after 80minutes at pH2. The peak shapes obtained were reasonable though some tailing was experienced with all the metals. Zr(IV) and Hf(IV) both showed a split peak at pH1, the reasons for which are not known. An elution order of Hf(IV) < Zr(IV) < U(VI) < Th(IV) < Bi(III) was found at pH2 with Sn(IV), Ti(IV), V(IV) and V(V) showing no retention at all. Figure 4.12 shows a separation of U(VI) and Th(IV) using this chelating ligand.

Table 4.5. Retention times (in minutes) of High Valency Metals on 4-chlorophenylalanine 5µm PLRP-S column (t_0 = 1.45 minutes). Eluent used was HNO_3 with an injection volume of 500µl. Detection was made at 654nm with Arsenazo III.

pH	U(VI)	Bi(III)	Th(IV)	Zr(IV)	Hf(IV)	V(IV)	V(V)
1.00	1.47	1.84	1.54	1.72/3.62	1.51/2.65	1.43	1.44
1.50	1.50	2.99	1.71	1.63	1.58	1.43	1.46
2.00	3.10	>80	15.30	2.90	2.45	1.57	1.58/3.53

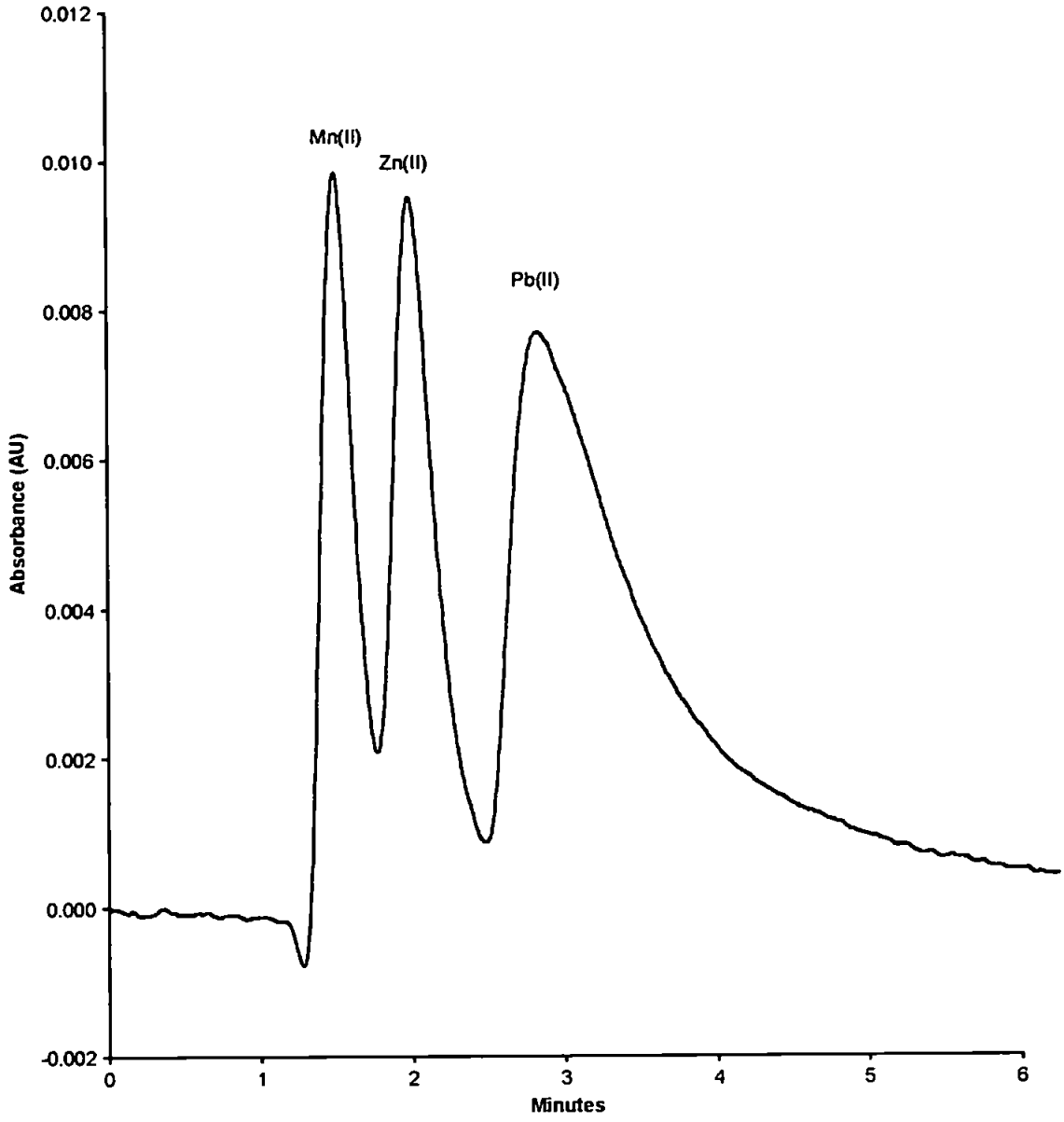

Figure 4.10. Isocratic separation of 50μgl^{-1} Mn(II), 50μgl^{-1} Zn(II) and 1mgl^{-1} Cu(II) at pH4.5 on the 10cm 5μm PLRP-S resin modified with 4-chlorophenylalanine. Injection volume was 100μl with detection at 520nm with PAR/Borate PCR.

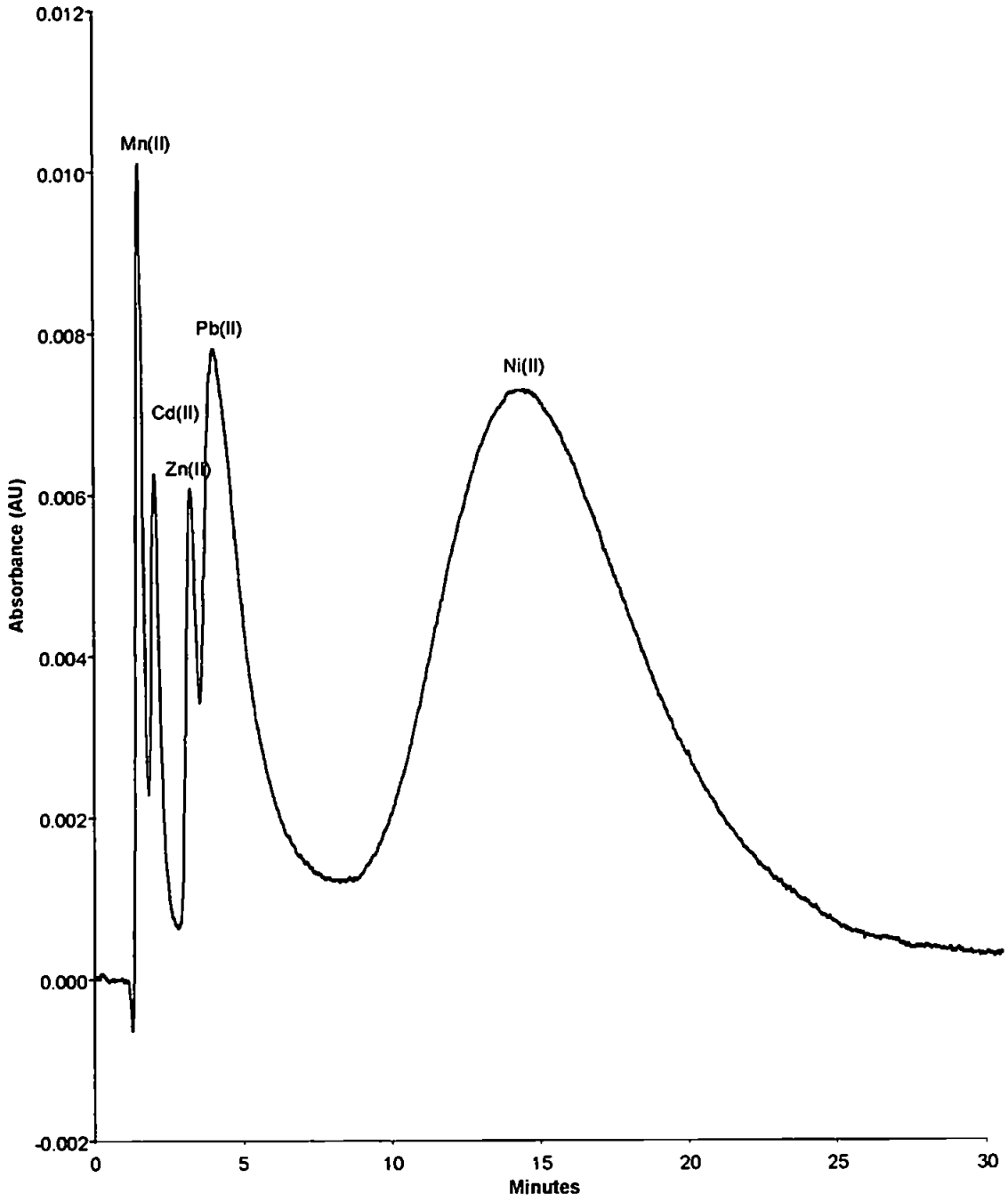

Figure 4.11. Isocratic separation of 50μgl^{-1} Mn(II), 50μgl^{-1} Zn(II), 50μgl^{-1} Cd(II),1.5mgl^{-1} Pb(II) and 1mgl^{-1} Ni(II) at pH5 on the 10cm 5μm PLRP-S resin modified with 4-chlorophenylalanine. Injection volume was 100μl with detection at 520nm with PAR/Borate PCR.

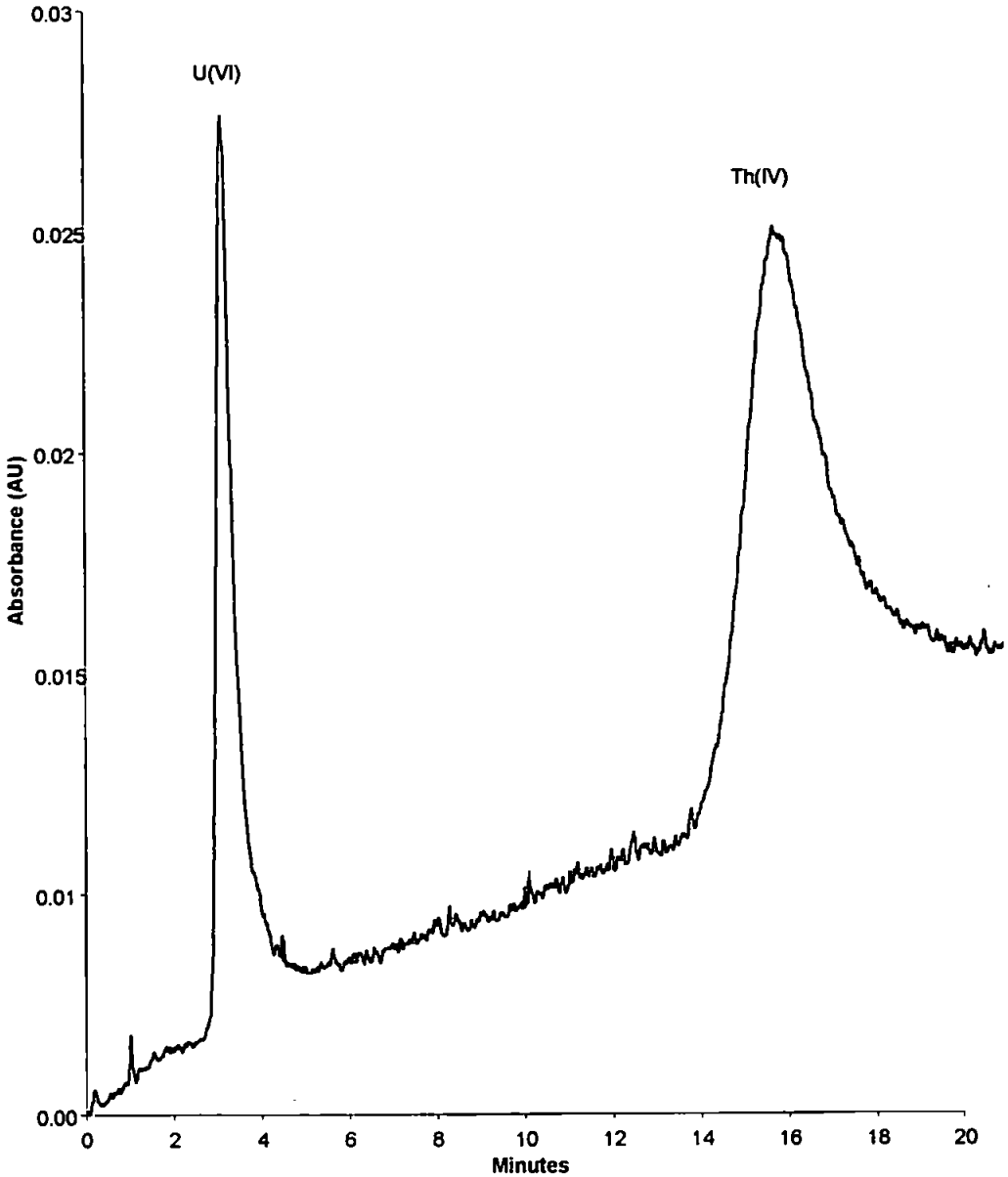

Figure 4.12. Isocratic separation of 4mgl^{-1} U(VI) and 4mgl^{-1} Th(IV) at pH2 on the 10cm 5μm PLRP-S resin modified with 4-chlorophenylalanine. Injection volume was 100μl with detection at 654nm with Arsenazo III PCR.

Part2:- Investigation of a Hypercrosslinked Polystyrene Resin for Dynamic Modification.

4.4 Introduction.

All the studies so far reported in this thesis have entailed the use of PS-DVB resins which have an average of approximately 8% DVB crosslinking. This is the most common form of PS-DVB resins to be found, though some PS-DVB resins have a much greater degree of crosslinking. Increasing the degree of crosslinking will result in a resin of greater density with fewer pores. However there is a type of PS-DVB resin that has a high degree of crosslinking (>40%) but still retains an open pore structure. These types of resins are known as hypercrosslinked resins and were first developed by Davankov and Tsyurupa [199-202]. These resins contain a large network of macroreticular pores which, in addition to the intrinsic micro porosity of the polymer, gives rise to a much greater surface area of greater than $1000m^2g^{-1}$ in comparison to an area of $20\text{-}300m^2g^{-1}$ for normal macroporus resins. Several manufacturers produce commercially available resins of this type. Purolite (Purolite, Pontyclun, Wales, UK) produce a series of resins with the prefix "MN" which are available in both neutral and charged forms. These resins are readily wetable and are very rigid due to their high degree of crosslinking. Penner *et al* [198] carried out a detailed investigation of some of the physical and chemical properties of hypercrosslinked polystyrene resins from Purolite to determine their suitability for use as a stationary phase in HPLC. Sutton *et al* [203] reported the use of dye coated MN200 resins for the determination of trace bismuth in lead as well as the use of MN200 dynamically modified with dipicolinic acid for U(VI) and Th(IV) determinations [204]. The resin used for this

study was a neutral 9μm MN200 resin supplied by Dr Pavel Nesterenko of Moscow State University.

4.5 Experimental.

4.5.1 Instrumentation.

The instrumentation used for these studies was as described in Chapter 2.2.1 with the exception that a Dionex GP40 (Dionex, Sunnyvale, CA, USA) gradient pump was used to deliver the eluent.

4.5.2 Reagents.

All reagents used for these investigations were obtained from BDH and of AnalaR grade unless otherwise stated. The eluents used in this study contained 1M KNO_3 and the requisite amount of chelating ligand adjusted to the required pH with conc HNO_3. The transition and heavy metals were determined at 520nm with the PAR/Borate PCR with 445nm used as the compensating wavelength. Both the eluent and PCR were delivered at a flow rate 1ml min^{-1}.

Metal standards were prepared from 1000mgl^{-1} Spectrosol metal stock solutions and made up to the required volume in dilute HNO_3 of the same pH as the eluent being used and stored in poly(propylene) bottles.

4.6 Results and Discussiuon.

4.6.1 Initial MN200 Investigations.

Sutton [118] showed that "bare" MN200 resin had some unexpected metal retaining characteristics. Therefore, the bare resin was investigated briefly using a 50 x 4.6mm ID column packed with the 9μm MN200 which was thoroughly washed with methanol before use. Selected transition and heavy metals showed no retention on this column with the exception of Pb(II) which showed only the slightest of retention and Cu(II) which showed retention at approximately 7 minutes using an eluent of pH3. Sutton [118] also reported that columns containing dye impregnated MN200 resin showed greater loadings and capacities than those obtained for dye impregnated PS-DVB resins with lower degrees of crosslinking.

It was decided to dynamically modify the MN200 resin with dipicolinic acid on the supposition that not only would a column of greater capacity be produced, but that some of the dipicolinic acid may be irreversibly retained by the MN200 thereby negating the need for the dipicolinic acid in the eluent or at least dramatically lowering the amount required in the eluent.

4.6.2 Dynamic modification of MN200.

Figure 4.13 shows the k' plot of dipicolinic acid on the 5cm column packed with MN200. Comparing Figures 4.3 and 4.13 it can be clearly seen that the retention of dipicolinic acid on this column is much greater than its retention on the 10cm column packed with the 5μm PLRP-S resin and should therefore result in a column of much higher capacity.

As we were attempting to produce a column that contained some permanently retained dipicolinic acid, the column was saturated with a 20mM dipicolinic acid solution at pH1 then the excess was bled off over time using a high ionic strength eluent adjusted to pH1 till a steady system was obtained. This was monitored by repeat injections of Th(IV) over several hours. Figure 4.14 shows the bleed profile for two different systems on a 10cm column packed with the MN200 resin. The nitrate system consisted of a 1M KNO_3 eluent prepared in 0.1M HNO_3 and the chloride system consisted of 1M KCl prepared in 0.1M HCl. The chloride system was investigated as the NO_3^- ion is retained by this resin and to see if this retention adversely affects the sorption of the dipicolinic acid by the resin. As can be seen in Figure 4.14, the retention of the nitrate ion does appear to have an adverse affect on the initial uptake of the dipicolinic acid. Initially the chloride system shows approximately 2.5 times the retention for dipicolinic acid than the nitrate system does, though this drops to approximately 2 times the retention after 10 hours. It was decided to continue using the nitrate system as it was hypothesised that after a sufficient period of time, the amount of dipicolinic acid adsorbed would be approximately the same for both systems. As the slopes of these two plots are starting to flatten out it was concluded that some dipicolinic acid would be permanently retained or have a very high retention time i.e. days. However, it was concluded that the amount of dipicolinic acid that would be permanently retained would be too little to allow for analytical separations to be carried out on this column.

Figure 4.15 shows the k' plot for selected transition and heavy metals on a 1.5 cm column loaded with 0.5mM dipicolinic acid. Table 4.6 shows the corresponding retention times. As with the k' plots of the high valency metals on the dipicolinic/polymer laboratories

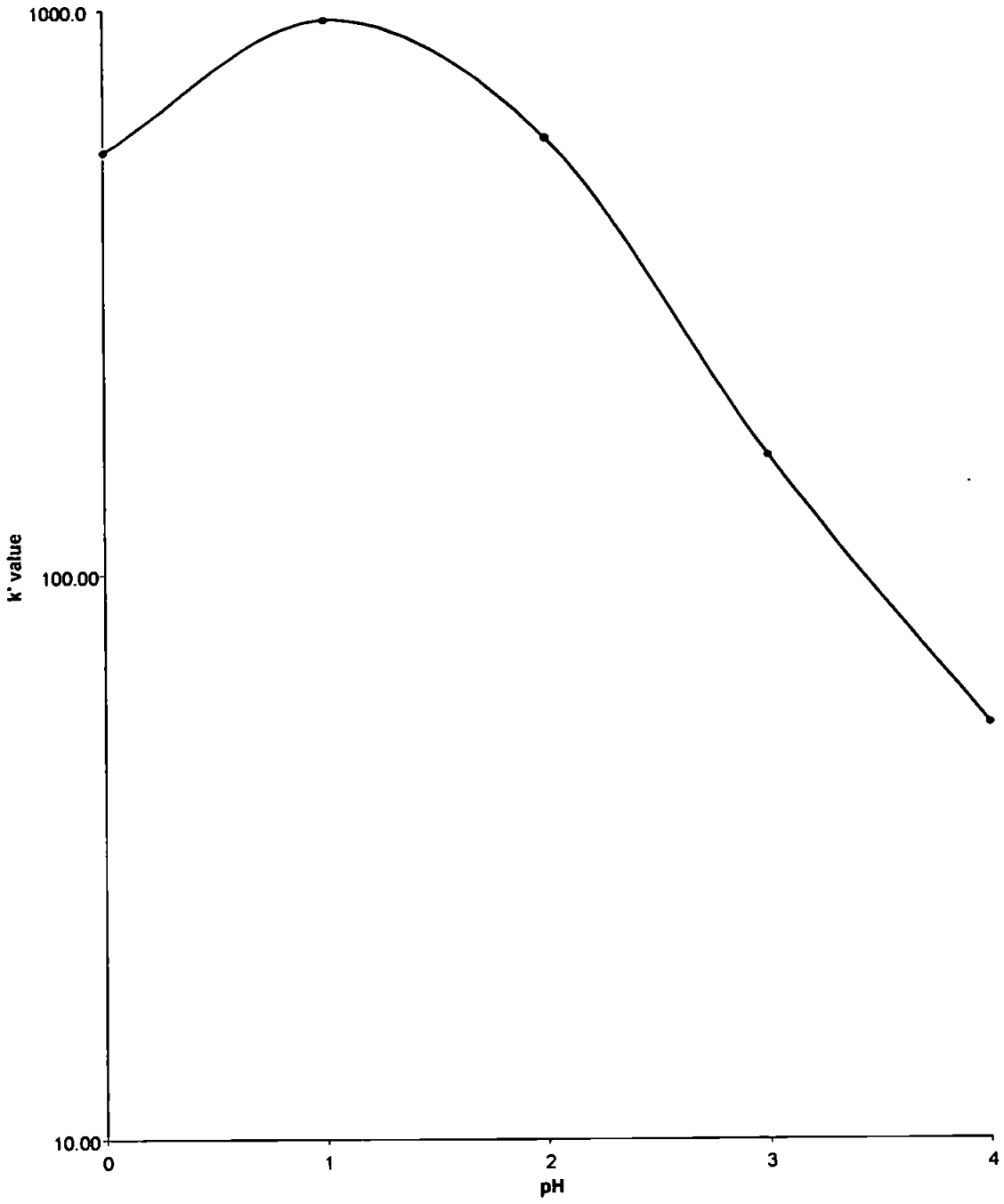

Figure 4.13. k' plot of dipicolinic acid on 1.5cm 9µm MN 200 column. Injection volume was 500µl with detection made at 270nm.

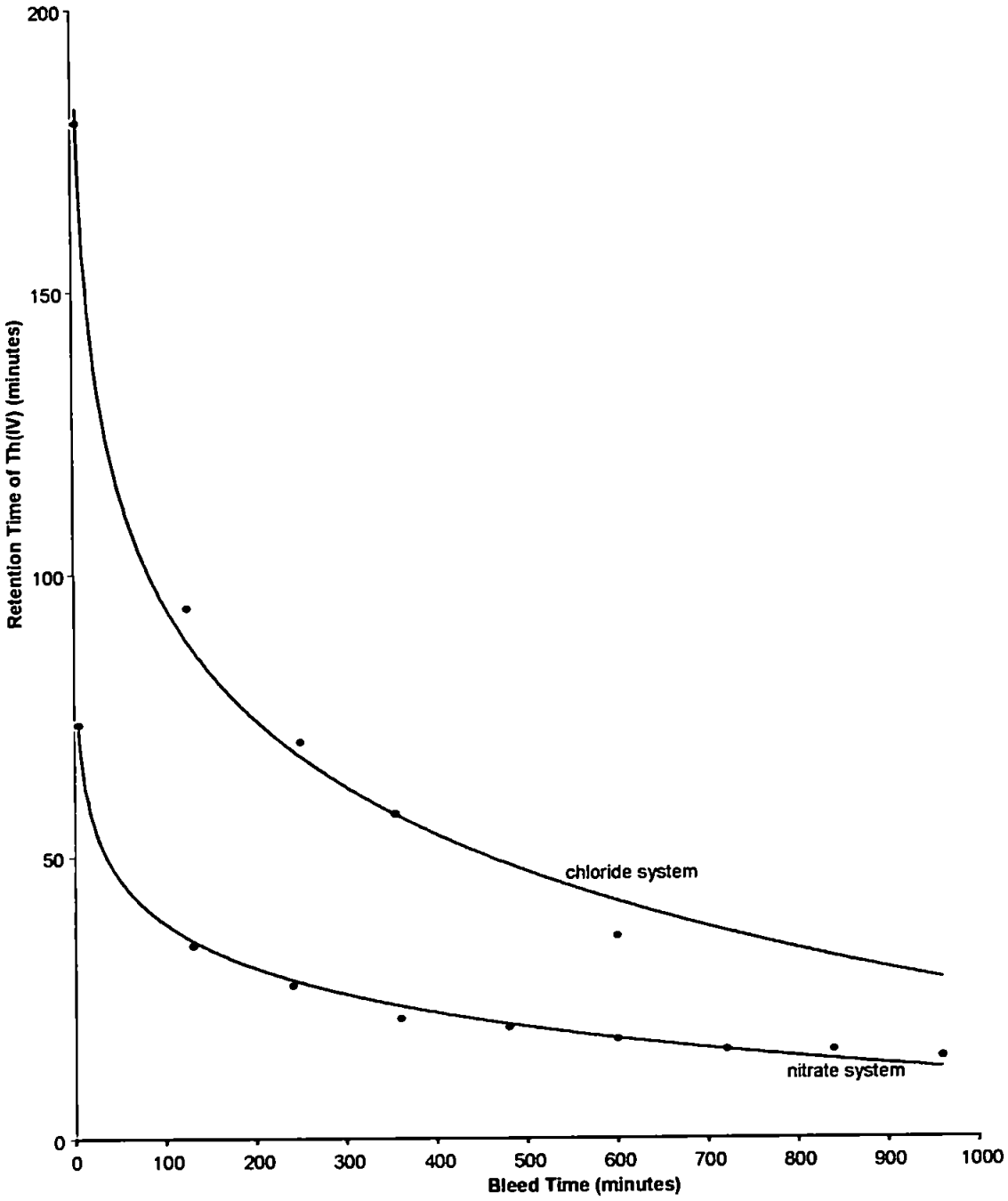

Figure 4.14. Bleed profile of dipicolinic acid at pH1 on 9μm MN 200 in a KNO_3 containing eluent and a KCl containing eluent monitored by repeat injections of Th(IV).

column the k' plots are not linear. In fact all the plots, except Mn(II), show a steady increase then decrease in the k' value. Again this is thought to be due to the increased competition from the low level (relative to the substrates surface) of dipicolinic acid still present in the mobile phase for the reasons discussed in section 4.3.4.1. Comparison of the k' plots in Figure 4.15 with those obtained by Shaw [120] on an 7μm PLRP-S resin for the same transition metals shows almost identical trends. The only difference between these two sets of plots is the actual k' values obtained. Those reported in Figure 4.15 are much greater than those reported by Shaw at similar pHs.

Table 4.6. Retention times (in minutes) of transition metals on 1.5cm Dipicolinic/9μm MN200 column (t_0 = 0.14 minutes). Eluent used was HNO_3 with 0.5mM dipicolinic acid. Injection volume was 100μl with detection at 520nm with PAR.

pH	Mn(II)	Cd(II)	Zn(II)	Co(II)	Pb(II)	Ni(II)	Cu(II)
0.50	1.22	3.49	1.24	1.25	10.43	1.26	34.70
1.00	1.35	5.32	1.97	1.38	23.00	1.38	75.50
1.50	1.47	8.36	4.26	2.02	23.88	2.47	---
2.00	1.63	11.20	10.94	2.66	23.60	3.49	22.00
2.50	2.10	10.09	6.40	3.63	21.75	2.65	6.71
3.00	2.67	9.11	4.48	3.53	22.40	2.36	4.09

These greater values allow for the increase in retention of the transition metals at similar pHs as well as increasing the selectivity of the system at lower pHs and thereby allowing for the separations in Figures 4.16 and 4.17 to be obtained. It is interesting to note that while it was not possible to obtain a column, of sufficient capability, with irreversibly retained dipicolinic acid, the separating capability of this column is much greater at the

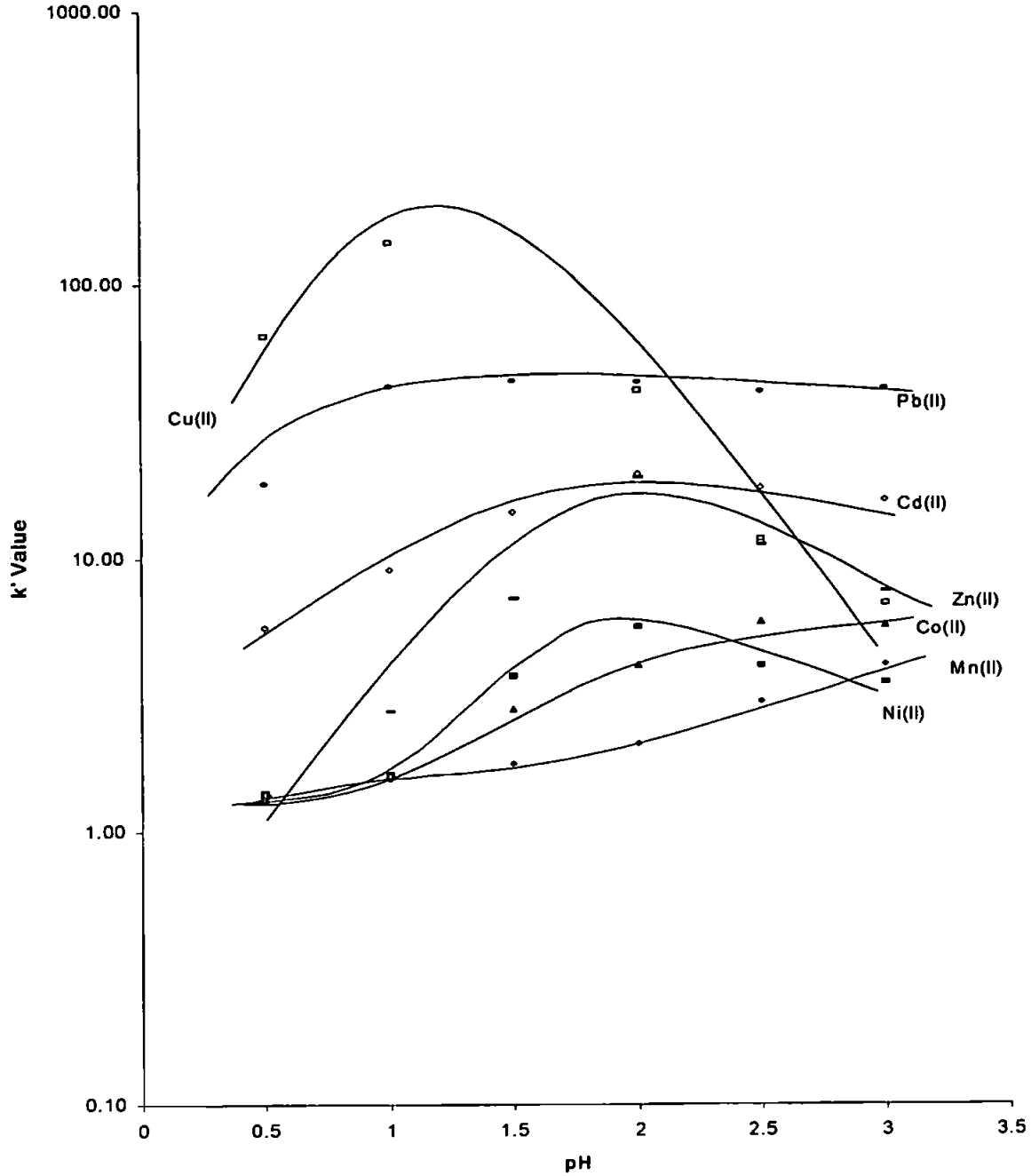

Figure 4.15. The dependence of capacity factors (k') for selected transition and heavy metals on eluent pH with a 1.5cm 9μm MN 200 column modified with dipicolinic acid. Eluent used was HNO_3 with 0.5mM dipicolinic acid. Injection volume was 100μl with detection at 520nm with PAR.

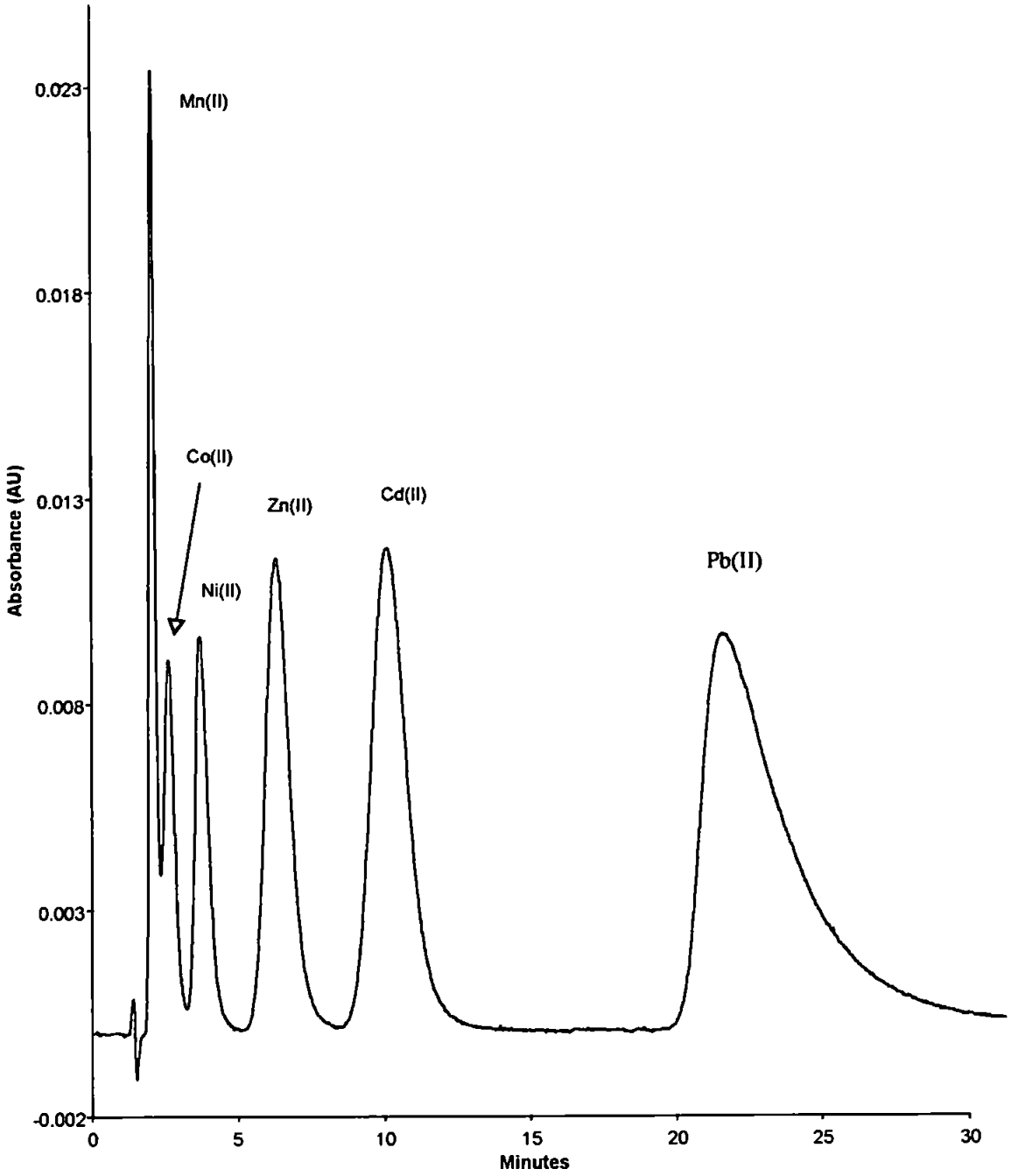

Figure 4.16. Isocratic separation of 0.1mgl^{-1} Mn(II), 0.1mgl^{-1} Co(II), 3mgl^{-1} Ni(II), 0.2mgl^{-1} Zn(II), 0.5mgl^{-1} Cd(II) and 10mgl^{-1} Pb(II) at pH2.5 on a 1.5cm column containing MN 200 dynamically modified with 0.5mM dipicolinic acid. Injection volume used was 100µl with detection at 520nm with PAR/Borate PCR.

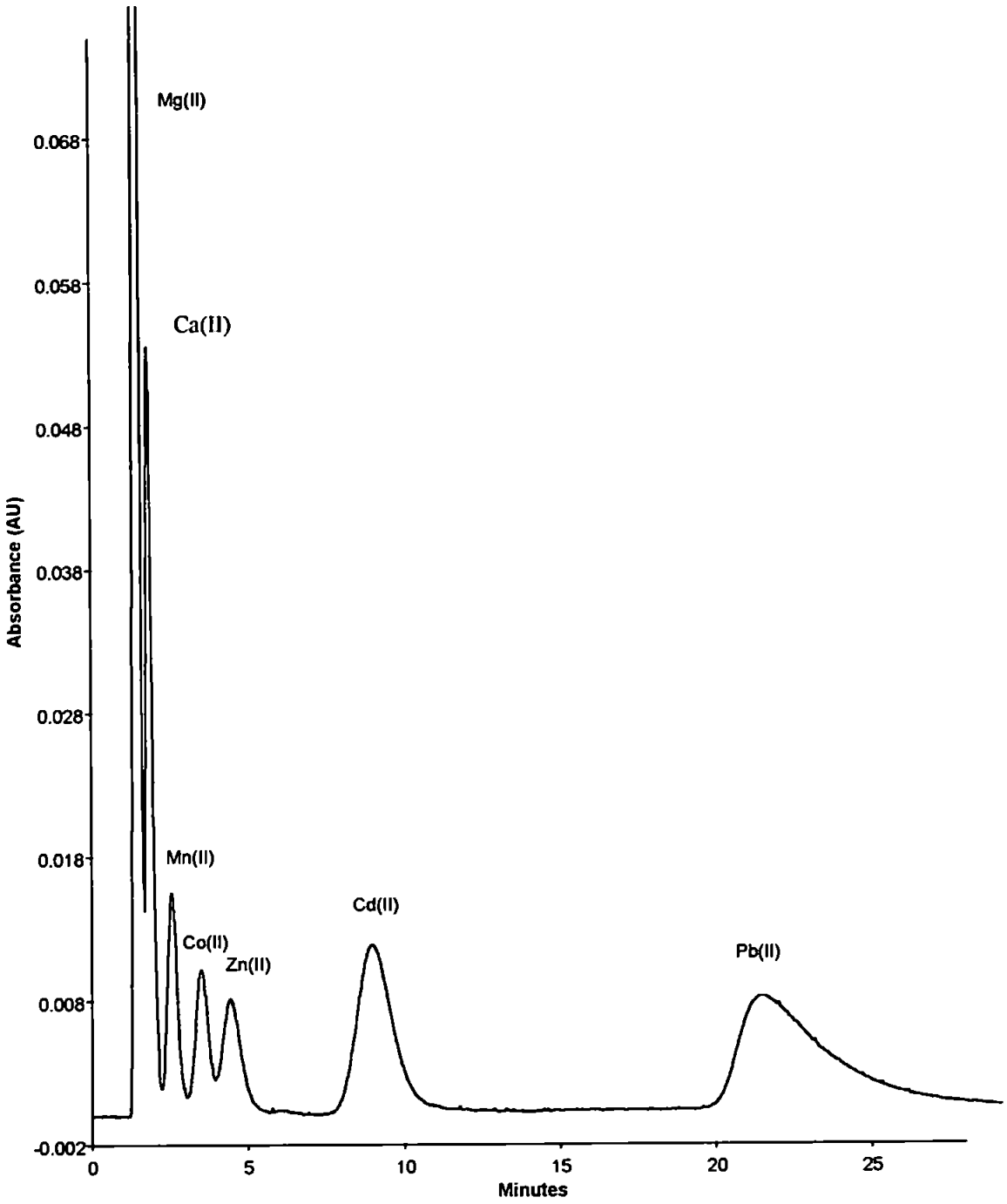

Figure 4.17. Isocratic separation of 240mgl^{-1} Mg(II), 160mgl^{-1} Ca(II), 0.1mgl^{-1} Mn(II), 0.1mgl^{-1} Co(II), 0.1mgl^{-1} Zn(II), 0.5mgl^{-1} Cd(II) and 10mgl^{-1} Pb(II) at pH3 on a 1.5cm column containing MN 200 dynamically modified with 0.5mM dipicolinic acid. Injection volume used was 100µl with detection at 520nm with PAR/Borate PCR.

same pH than any of the dye loaded or dynamically modified columns used in this thesis. This is illustrated in Figures 4.16 and 4.17, which show the isocratic separation of up to seven metals. With all the other systems discussed in this work the maximum number of metals that can be isocratically separated in this time frame is only three or four. Even though not all the metals are 100% resolved, Figure 4.17 does show the partial resolution of Mg(II) and Ca(II) at pH3 which is impossible with any of the other dye impregnated of dynamically modified systems previously described at this pH.

4.7 Summary

This study has shown that chelating substrates can be produced with relative ease by the dynamic modification of neutral PS-DVB resins with low molecular weight organic molecules. Substrates of suitable efficiency can be prepared quickly for the analysis of selected transition, heavy and high valency metals. The ease with which these chelating substrates can be formed allows for the resin to be temporarily loaded with the chelating ligand of choice for the required analysis then removed and reloaded with another ligand for a different set of analysis.

The concentration of the ligand used is a key factor in the attainment of the required metal separation. The greater the amount of ligand added to the mobile phase, the greater the ratio of the ligand in the mobile phase to that of the sorbed layer and therefore the greater the competition between these two phases for the metal ions. While this leads to increased metal retention times it will also decrease the pH range that retention will occur in as is shown by the studies on the MN200 column. The MN200 column produced more highly efficient separations than did any of the dye impregnated or dynamic systems previously

discussed. This is demonstrated with the 6 and 7 metal isocratic separations shown in Figures 4.16 and 4.17.

Of the ligands used, dipicolinic acid has shown itself to be highly suitable for the dynamic modification of neutral substrates whereas the 2- and 4-chloromandelic acid resulted in an unstable system that would be unacceptable for the analysis of metal ions. The 4-chlorophenylalanine offered some promising results though the pH range in which separations could be carried out was rather high i.e. >pH4.5 for the transition and heavy metals and >pH2.0 for the high valency metals investigated. This system did however show some interesting results with respect to U(VI) and Th(IV), that being the reversal in elution order of these two metals with respect to the dipicolinic acid system. This reversal could prove highly useful if Th(IV) is the principle metal ion of interest.

Multi-element separations can also be performed on these substrates under isocratic conditions and within an acceptable time, unlike with the dye impregnated substrates discussed in Chapter 2. The application of these dynamically modified substrates to the analysis of real samples in a variety of complex matrices is given in the Chapter 5.

Chapter 5:- Determination of Trace Metals in Environmental Samples using HPCIC.

Part 1:-Determination of Uranium in Environmental Waters using Dynamically Modified Chelating Substrates.

5.1 Introduction.

Uranium belongs to the group of elements known as the actinides, that is those elements whose atomic number is greater than 89 [19]. It is the only actinide element, apart from thorium, that is naturally occurring in the earth's crust. This is because all the actinides are radioactive in nature with only certain isotopes of uranium and thorium, namely ^{235}U, ^{238}U and ^{232}Th, having a sufficiently long half-life to allow for their continued existence.

Uranium is the fourth member of this series of elements with an atomic number of 92, an atomic mass of 238.029 and oxidation states ranging from +3 to +6 [19] with the most common state being +6. The earth's crust contains approximately 2.7$\mu g g^{-1}$ of uranium with the principal ore being *uranite*, an oxide of composition UO_2. In aquatic systems, the amount of uranium present in ocean water is approximately 2.5$\mu g l^{-1}$ (for a salinity of 35%) with a residence time of $5x10^5$ years and 0.04$\mu g l^{-1}$ in riverine waters and thought to be in the form of dissolved $UO_2(CO_3)_3^{4-}$ [3].

Uranium consists of two naturally occurring isotopes, ^{235}U ($T_{1/2} = 7.04x10^8$ years) and ^{238}U ($T_{1/2} = 4.46x10^9$ years) which decay to the stable lead isotopes of ^{206}Pb and ^{207}Pb respectively [205]. The natural abundance of these isotopes is 99.28% for ^{238}U and 0.72% for ^{235}U [15]. The ^{235}U isotope is of special importance as this is the only natural occurring

nucleus which undergoes nuclear fission when bombarded with neutrons. Because of this unique property the separation of ^{235}U and ^{238}U is rather important. There are several methods with which this separation can be obtained though the most common method is gaseous effusion [15]. This can lead to the production of up to 99% enriched ^{235}U.

Due to its fissionable characteristics, the main use of uranium is as a nuclear fuel and as the principal explosive component in nuclear weapons. It has however found some safer uses as, for example, ships ballast, aircraft counterweights, sea shells and in glass colourings. The radioactive nature of uranium with its decay products and its use in the nuclear industry means that monitoring of the environment for contamination is of vital importance. Not only is it a highly toxic metal, it can readily complex with the mineral matrix of bone as well as bind to various biomolecules including proteins [205]. This can lead to various problems for human health including renal damage, acute arterial lesions and death. Due to its potentially lethal nature, emissions during mining and processing are closely monitored and even though emission levels are low they can lead to significant increases in local aquatic systems due to an accumulative input from waste streams. Also improper storage of disposed waste resulting in leaching into the local environment has lead to stricter environmental monitoring with a number of improved chromatographic techniques developed to monitor this pollutant in our environment, some of which are discussed below.

Barkley *et al* [206] used a reversed phase column for the selective separation of U(VI) and Th(IV) from bacterial leachings of uranium ores. These metals were retained as their α-hydroxyisobutyric acid (HIBA) complexes and this allowed for their selective separation from the transition and rare earth metals. Detection was made using the post-column

reagent Arsenazo III at a wavelength of 658nm. Jackson *et al* [207] again used this system for Th(IV) and U(VI) determinations in mineral sands. This method was also used by Hao *et al* [177, 178] to study the retention behaviour of Th(IV) and U(VI) on a C_{18} reversed phase column and their subsequent determination in a saline solution spiked in seawater whilst Harrold *et al* [208] used a MetPac CC-1 IDA chelating column to preconcentrate Th(IV) and U(VI) from NASS-2 open ocean seawater before separation on a CS2 cation exchange column. Paull and Haddad [209] used a methylthymol blue impregnated column for trace UO_2^{2+} determinations in saturated saline samples. A CS10 strong cation exchange column was used by Al-Shawi and Dahl [210] for the determination of Th(IV) and U(VI) in phosphate rocks used in the production of fertilisers while Merdivan *et al* [211] used a phosphonate derivatised PS-DVB resin for the retention and separation of Th(IV) and U(VI) along with selected transition metals. This study and all of the studies mentioned above utilised post column detection with Arsenazo III.

Byerley *et al* [212] used both CS2 and CS5 cation exchange columns for the separation of U(VI) in process liquors with PAR as a post column reagent. Truscott *et al* [113] used a Tru-Spec column for the preconcentration U(VI) and Th(IV) for a variety of different sample types followed by detection using ETV-ICP-MS. Thermal Ionisation Mass Spectrometry (TIMS) was used by Goodall and Lythgoe [213] to determine U(VI) and Pu(IV) in fission products after separation on an alkyl phosphonate PS-DVB (U/TEVA) column with eluents containing oxalic and ascorbic acids. Yokoyema *et al* [214] also used a U/TEVA column followed by detection with TIMS for the separation of Th(IV) and U(VI) from silicate rock samples. This U/TEVA column was also used by Carter *et al* [215] followed by alpha spectrometry for U(VI) and Th(IV) determinations in geological materials. Lee *et al* [216] used a PS-DVB resin impregnated with TAR for the selective

separation of U(VI) in geological materials with detection being made with ICP-AES. Rollin *et al* [217] used a CG10 cation ion exchange column coupled to an ICP-MS detector for the separation and subsequent detection of U(IV) and U(VI). Mann and Wong [218] used a Chelex-100 column to selectively preconcentrate and separate 'strongly bound' uranium marine waters whilst Nakashima *et al* [219] used Bio-Rad AG1-X2 anion exchange resin to determine U(VI) in seawater by ion-exchanger phase absorptiometry with Arsenazo III.

This method offers the ability to not only preconcentrate but to perform analytical separations on a single column whereas Byerley required a dual column system. It also has the advantage of the relative insensitivity towards high ionic strengths which can cause problems with the various form of atomic spectrometry that is generally used for this type of analysis. The application of a dynamically modified high efficiency substrate to the determination of uranium in a selection of different matrices is discussed in the following chapter. This study involved the use of several certified reference materials (CRMs) along with a 'real' seawater sample obtained from the Tamar estuary.

5.2 Experimental.

5.2.1 Instrumentation.

The HPCIC instrumentation used for this study is as described in Chapter 2.2.1 with the exception that a Dionex GP40 gradient pump was used to deliver the eluent and that a 1 or 2ml sample loop was used. The column used was a 100 x 4.6mm ID PEEK column packed with 5μm PLRP-S resin supplied by Polymer Laboratories and dynamically modified with dipicolinic acid.

5.2.2 Reagents.

All reagents used for these investigations were obtained from BDH (BDH, Poole, UK) and of AnalaR grade unless otherwise stated. The eluent used for these investigations contained 1M KNO_3 with 0.1mM dipicolinic acid (99% purity Aldrich, Gillingham, UK) for all samples investigated. The post column reagent used consisted of 0.05M Arsenazo III (Avocado, Lancashire, UK) in 0.5M HNO_3 with detection being made at 654nm. Both the eluent and PCR were delivered at a flow rate of $1 ml min^{-1}$. $1000 mg l^{-1}$ metal stock solutions were diluted to working standards using dilute HNO_3 to obtain the required pH and stored in poly(propylene) bottles.

5.2.3 Sample Pretreatment.

None of the samples were pretreated with the exception of the Devil's Point samples which were collected from the mouth of the Tamar estuary, SW England and filtered through 0.45μm, 47mm cellulose acetate filters three times to remove any particulate matter present. They were then acidified to pH 1.6 with conc. HNO_3 so as to be comparable with the NASS-4 certified reference material and stored in poly(propylene) bottles. Metal standard solutions were adjusted to pH 0.3 when analysing the drinking water certified reference material and pH 1.6 when analysing the TMDA-54.2 and NASS-4 reference materials.

5.3 Results and Discussion.

The sample reference materials chosen for this study represent a wide range of uranium concentrations to be found in various sample matrices. A "real" seawater sample was also analysed to show that the system is suitable for handling the complex sample matrices that are actually found in the environment.

5.3.1 Drinking Water CRM.

The first certified reference material that was investigated was a High Purity Standards (HPS) certified reference material for trace metals in drinking water (Lot number 904020, High Purity Standards, Charleston, SC, USA). This CRM contained $10\mu gl^{-1}$ +/- $0.05\mu gl^{-1}$ of U(VI). This CRM was certified by spectrometric analysis against an independent source which is traceable to National Institute of Standards and Technology, standard reference material number 3100 series and checked by ICP prior to shipping.

A calibration for U(VI) over a concentration range of 5-$5000\mu gl^{-1}$ was carried out using metal standard solutions to ascertain the analytical capability of the system. The calibration, shown in Figure 5.1, produced good linearity with a regression coefficient of r^2 = 0.9999 calculated from the peak area. A detection limit of approximately $2.5\mu gl^{-1}$ was calculated for U(VI) as twice the baseline noise. Using peak areas, a second calibration was carried out, this time using spiked drinking water samples and is given in Figure 5.2. A concentration range of 5-$30\mu gl^{-1}$ was used and the mean concentration (n = 6) of U(VI) in the CRM was calculated to be 9.38 +/- $0.13\mu gl^{-1}$. The reproducibility of the method was

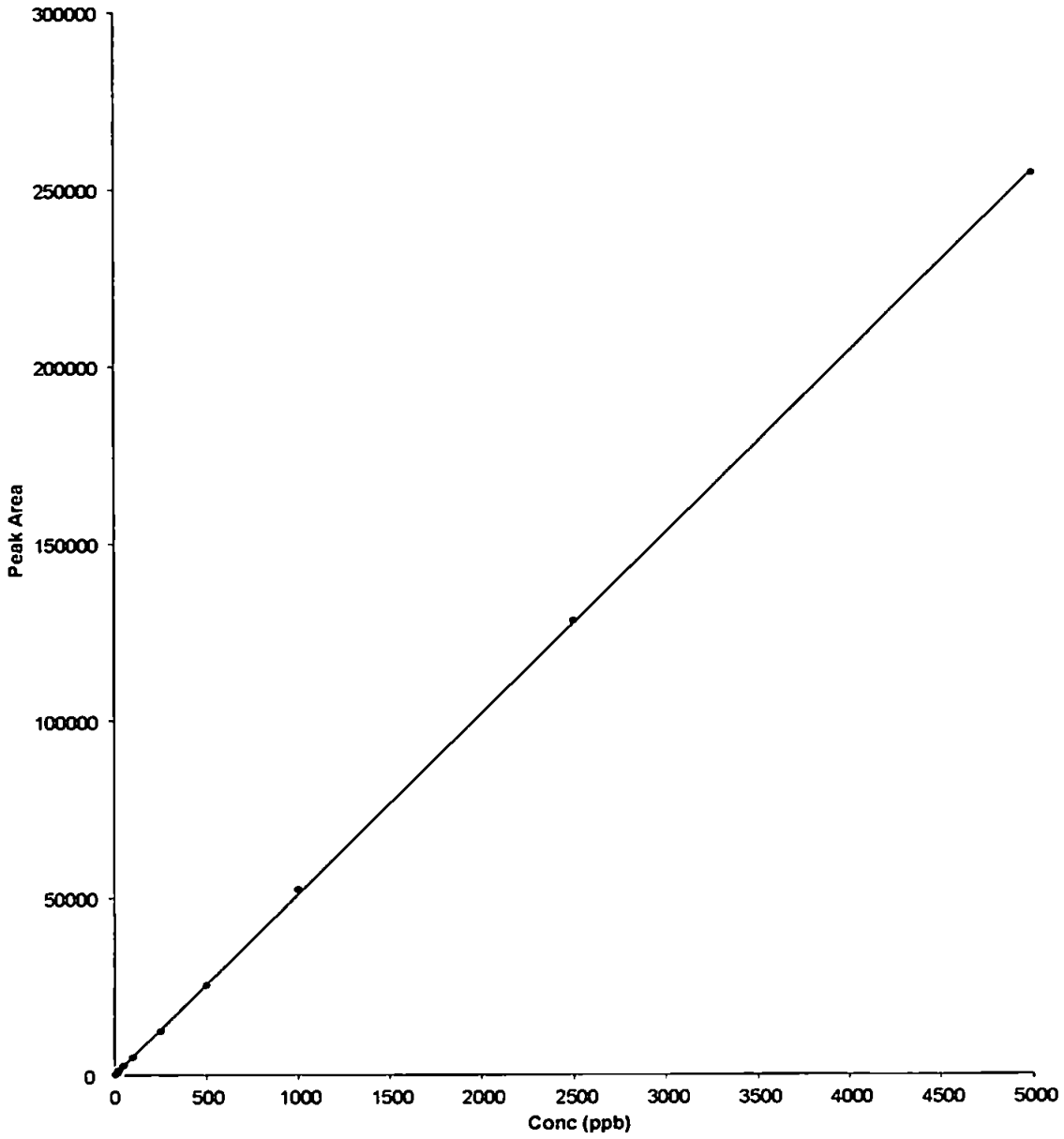

Figure 5.1. Method linearity calibration for U(VI) in drinking water CRM on a 10cm 5µm PLRP-S column dynamically modified with dipicolinic acid. Eluent used was 1M HNO_3 with 0.1mM dipicolinic acid with sample pH 0.3. Injection volume was 1ml with detection at 654nm with Arsenazo III.

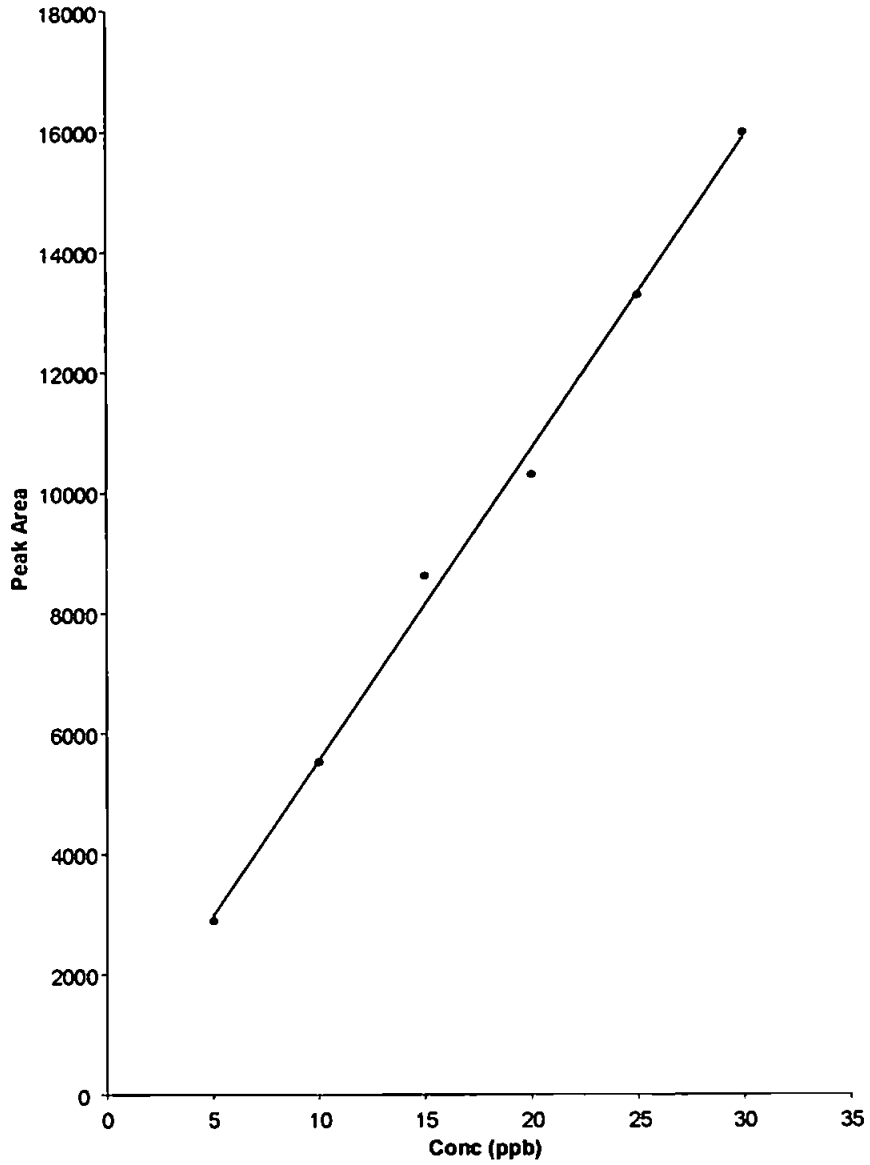

Figure 5.2. U(VI) calibration for drinking water CRM on a 10cm 5μm PLRP-S column dynamically modified with dipicolinic acid. Eluent used was 1M HNO_3 with 0.1mM dipicolinic acid with sample pH 0.3. Injection volume was 1ml with detection at 654nm with Arsenazo III.

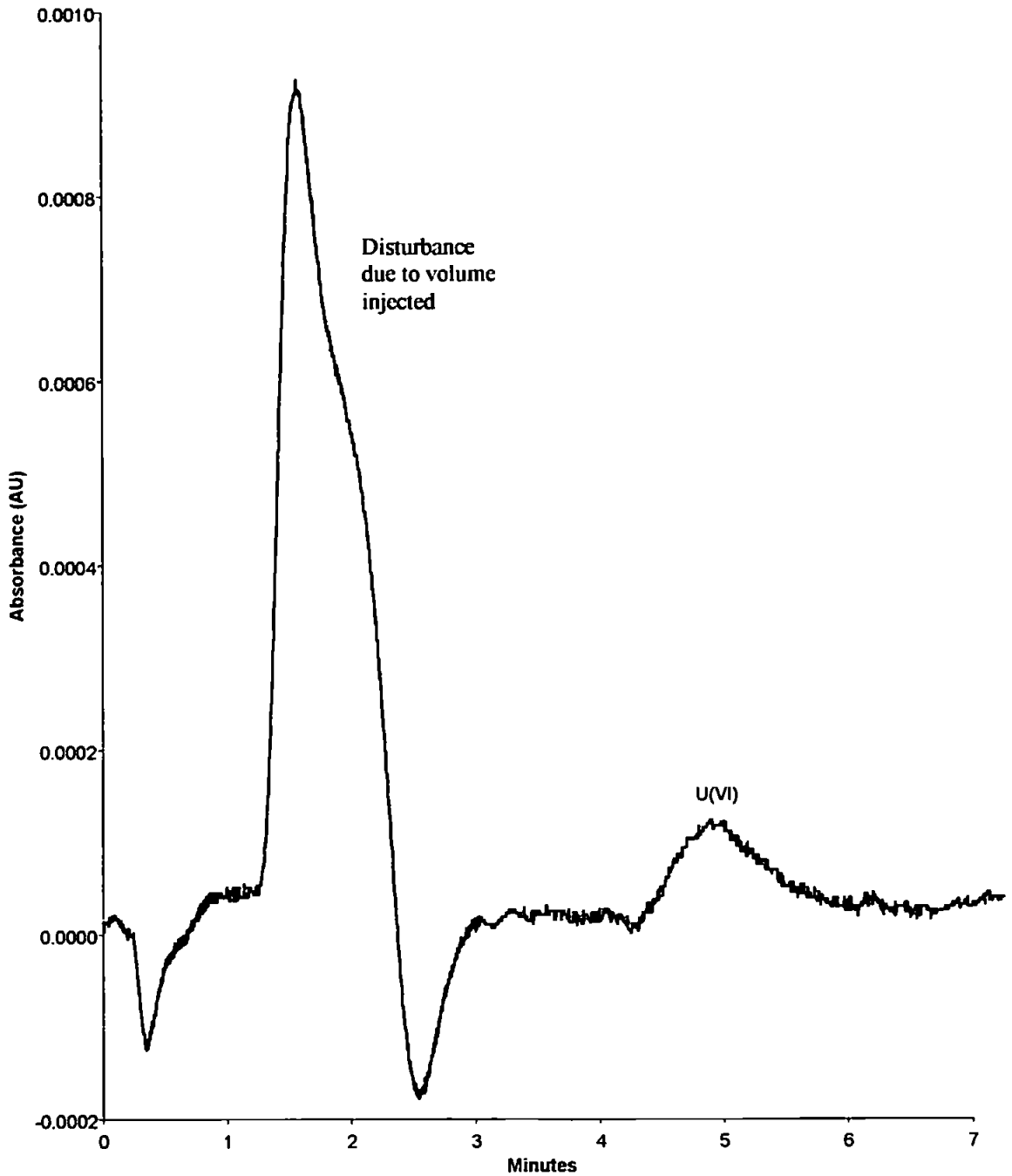

Figure 5.3. U(VI) in drinking water CRM eluted on 10cm PLRP-s column modified with 0.1mM dipicolinic acid. Injection volume used was 1ml with detection at 654nm with Arsenazo III.

calculated from repeat injections (n = 7) of a 20μgl^{-1} U(VI) standard and found to be 3.49%. Figure 5.3 shows an example of U(VI) in the drinking water CRM.

5.3.2 TMDA-54.2.

The second certified reference material investigated for uranium was the National Water Research Institute (NWRI) fortified soft water sample TMDA-54.2 and contained 62.3 +/- 13.1μgl^{-1} of U(VI).

The method used for the determination of uranium was the same method as was used for the previous HPS drinking water CRM with the exception of the sample pH which was pH 1.6 instead of pH 0.3. Figure 5.4 shows the calibration curve obtained for uranium over a concentration range of 50-90μgl^{-1} and produced good linearity with a regression coefficient of $r^2 = 0.9954$. A mean result (n = 6) of 62.8 +/- 0.8μgl^{-1} was obtained which falls well within the certified concentration range of the sample. Reproducibility (%RSD) of the method was determined to be 1.29% using the peak area of repeat injections (n = 7) of a 70μgl^{-1} metal standard. Figure 5.5 shows an example of uranium in this sample.

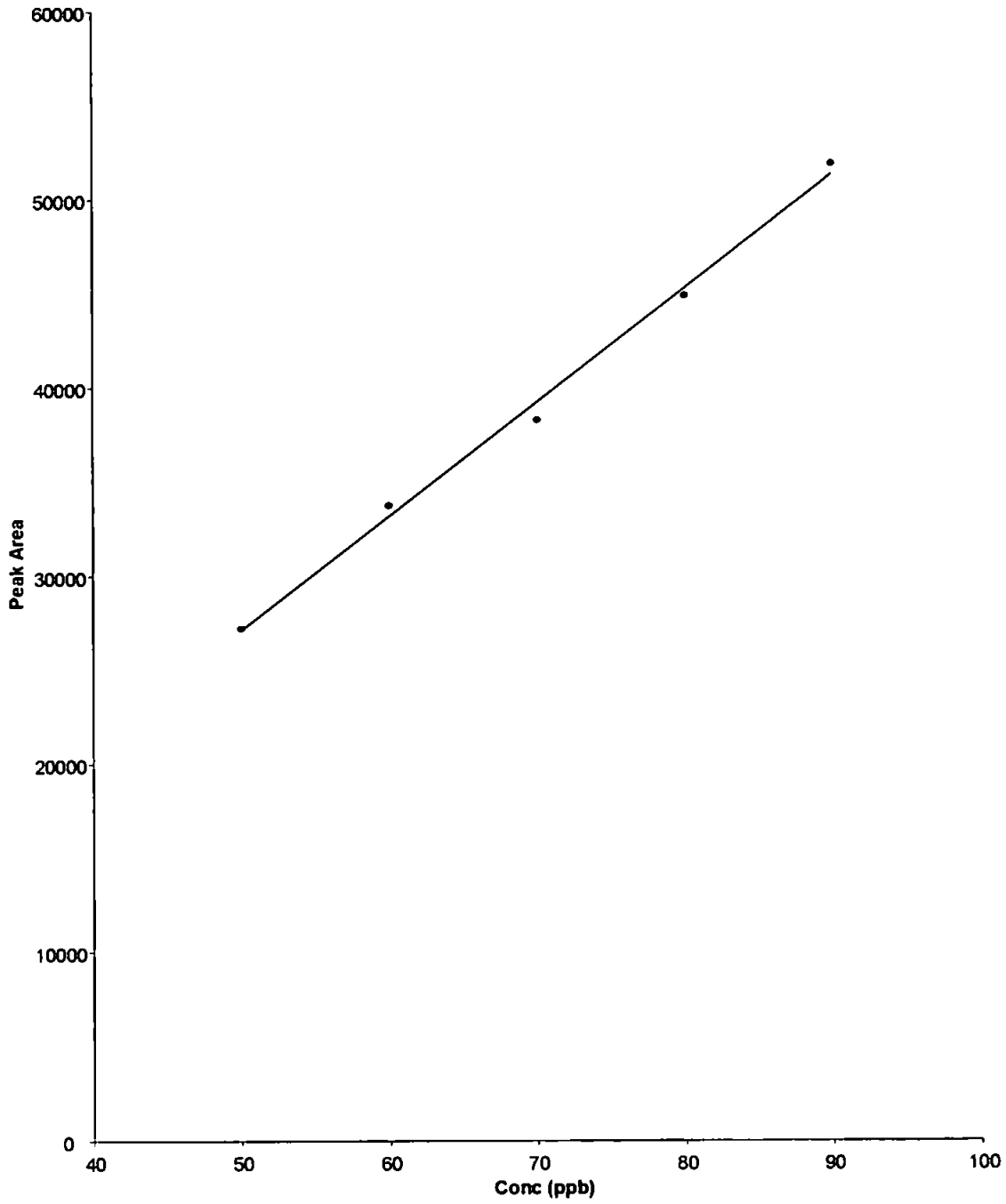

Figure 5.4. U(VI) calibration for TMDA-54.2 fortified soft water CRM on a 10cm 5µm PLRP-S column dynamically modified with dipicolinic acid. Eluent used was 1M HNO_3 with 0.1mM dipicolinic acid with sample pH 1.6. Injection volume was 1ml with detection at 654nm with Arsenazo III.

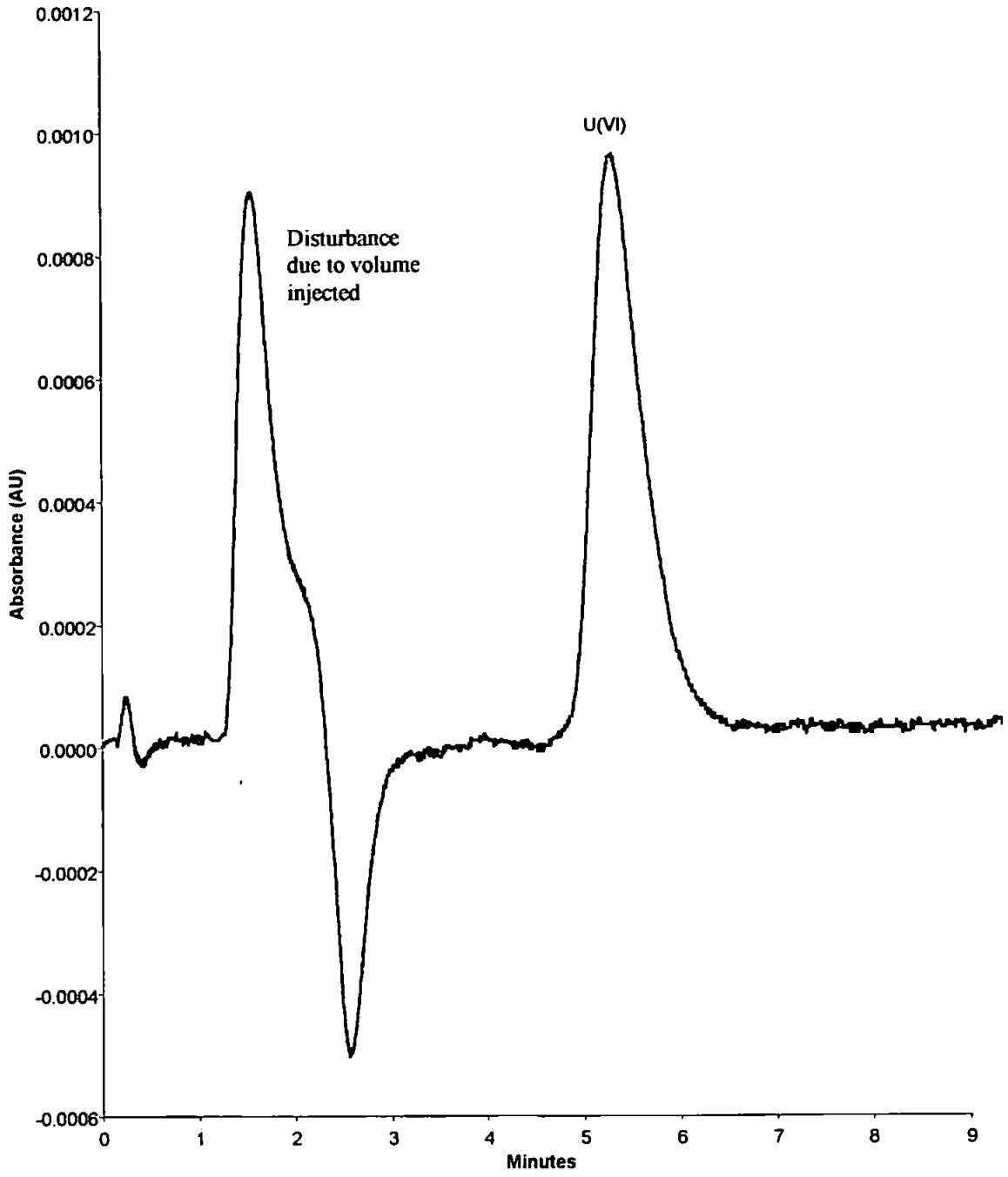

Figure 5.5. U(VI) in TMDA-54.2 fortified soft water CRM eluted on the 10cm PLRP-S column modified with 0.1mM dipicolinic acid. Injection volume used was 1ml with detection at 654nm with Arsenazo III.

5.3.3 NASS-4.

This reference material was a National Research Council Canada (NRCC) open ocean seawater sample. This reference material contained 2.64 +/- 0.12μgl^{-1} U(VI).

The method used for this analysis was again the same as was used for both the HPS drinking water and TMDA-54.2 CRMs with the exception that a 2ml sample loop was used. The calibration carried out for the method, as shown in Figure 5.6, produced good linearity over a concentration range of 1.5-1000μgl^{-1} with a regression coefficient of r^2 = 0.9986. The detection limit for U(VI) with this method was calculated to be 1.0μgl^{-1} as twice the baseline noise with a reproducibility of 7.56% calculated from repeat injections (n = 7) of a 15μgl^{-1} uranium standard solution. A mean uranium concentration (n = 5) of 2.59 +/- 0.1μgl^{-1} was obtained from the calibration shown in Figure 5.7 for a concentration range of 1.5-25μgl^{-1} and compares favourably with the certified value of 2.64 +/- 0.12μgl^{-1}. An example of uranium in the NASS-4 reference material is given in Figure 5.8.

5.3.4 Devil's Point.

The analysis of the NASS-4 seawater CRM shows that this method is suitable for uranium determinations in highly complex sample matrices of high salt content and ionic strength. To confirm this suitability, a "real" seawater sample was also analysed. The sample was collected from the mouth of the Tamar estuary, South West England, at a location known as "Devil's Point". Two samples were collected, the first from the water's edge and the second from a pool on the beach which is constantly refilled with fresh seawater at high tide.

The previous calibrations for the NASS-4 reference material showed the linearity and reproducibility of this method and so a three point calibration (Figure 5.9) was deemed sufficient for uranium determinations. This calibration produced a regression coefficient of $r^2 = 0.985$ from which the uranium concentration was determined to be $2.37\mu gl^{-1}$ and $2.50\mu gl^{-1}$ for the samples taken at the water's edge and pool respectively. Figure 5.10 shows the resulting chromatogram for the Pool sample. From this chromatogram, the retention time for uranium is slightly greater (approximately 30 seconds) than was obtained for the NASS-4, however Figure 5.11 shows the water's edge sample spiked with $10\mu gl^{-1}$ of uranium confirming its retention.

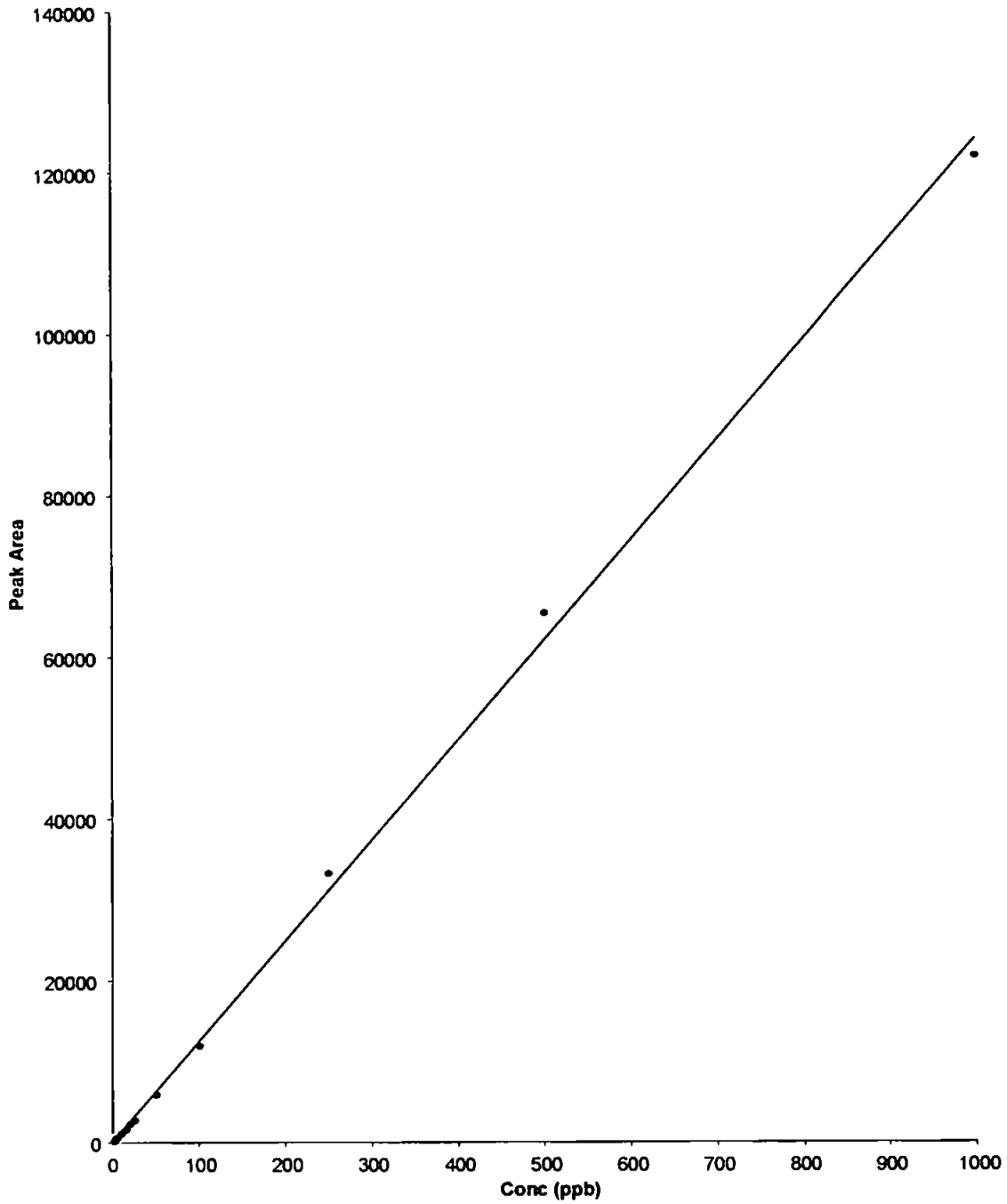

Figure 5.6. Method linearity calibration for U(VI) in NASS-4 seawater CRM on a 10cm 5μm PLRP-S column dynamically modified with dipicolinic acid. Eluent used was 1M HNO_3 with 0.1mM dipicolinic acid with sample pH 1.6. Injection volume was 2ml with detection at 654nm with Arsenazo III.

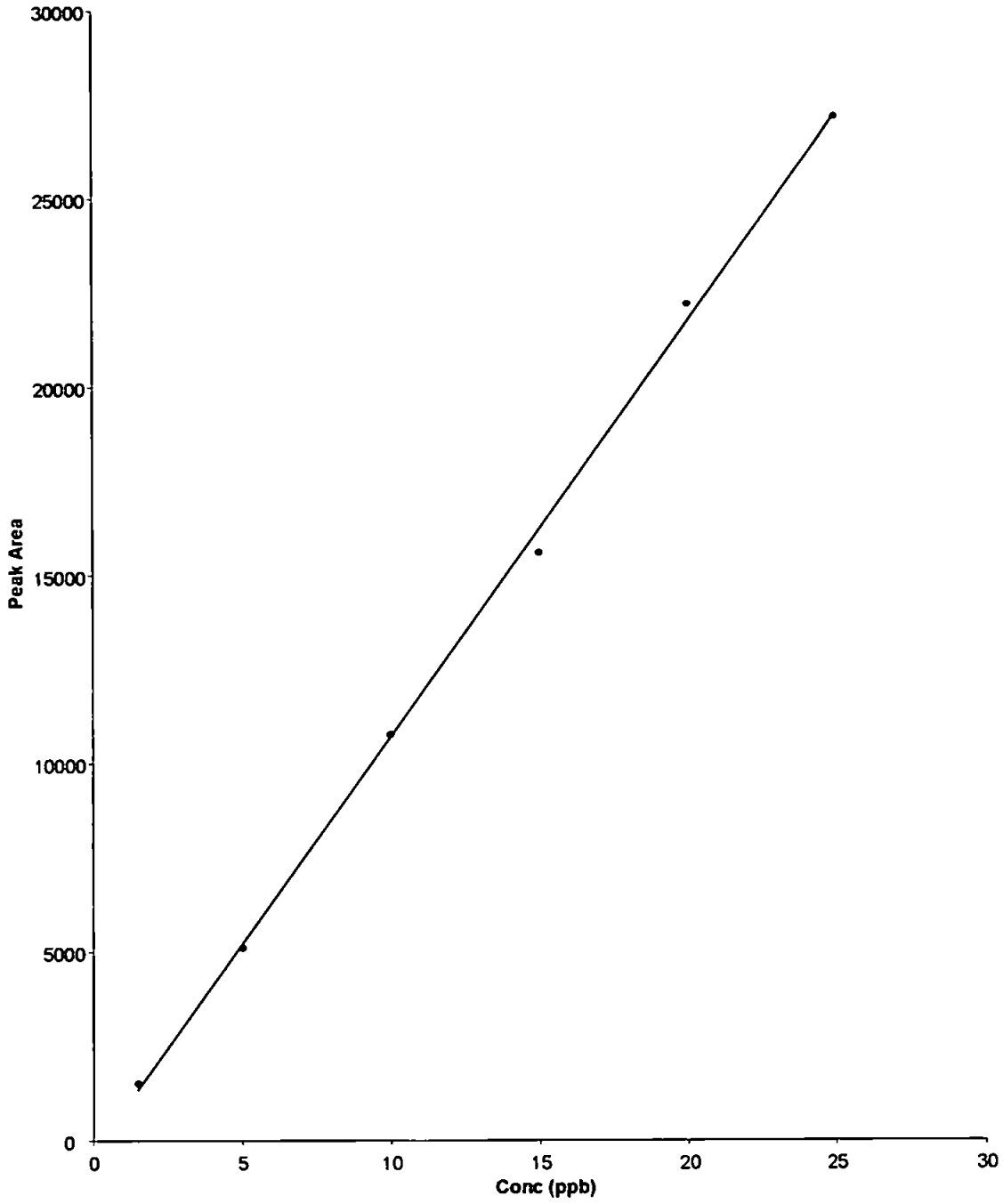

Figure 5.7. U(VI) calibration for NASS-4 seawater CRM on a 10cm 5μm PLRP-S column dynamically modified with dipicolinic acid. Eluent used was 1M HNO_3 with 0.1mM dipicolinic acid with sample pH 1.6. Injection volume was 2ml with detection at 654nm with Arsenazo III.

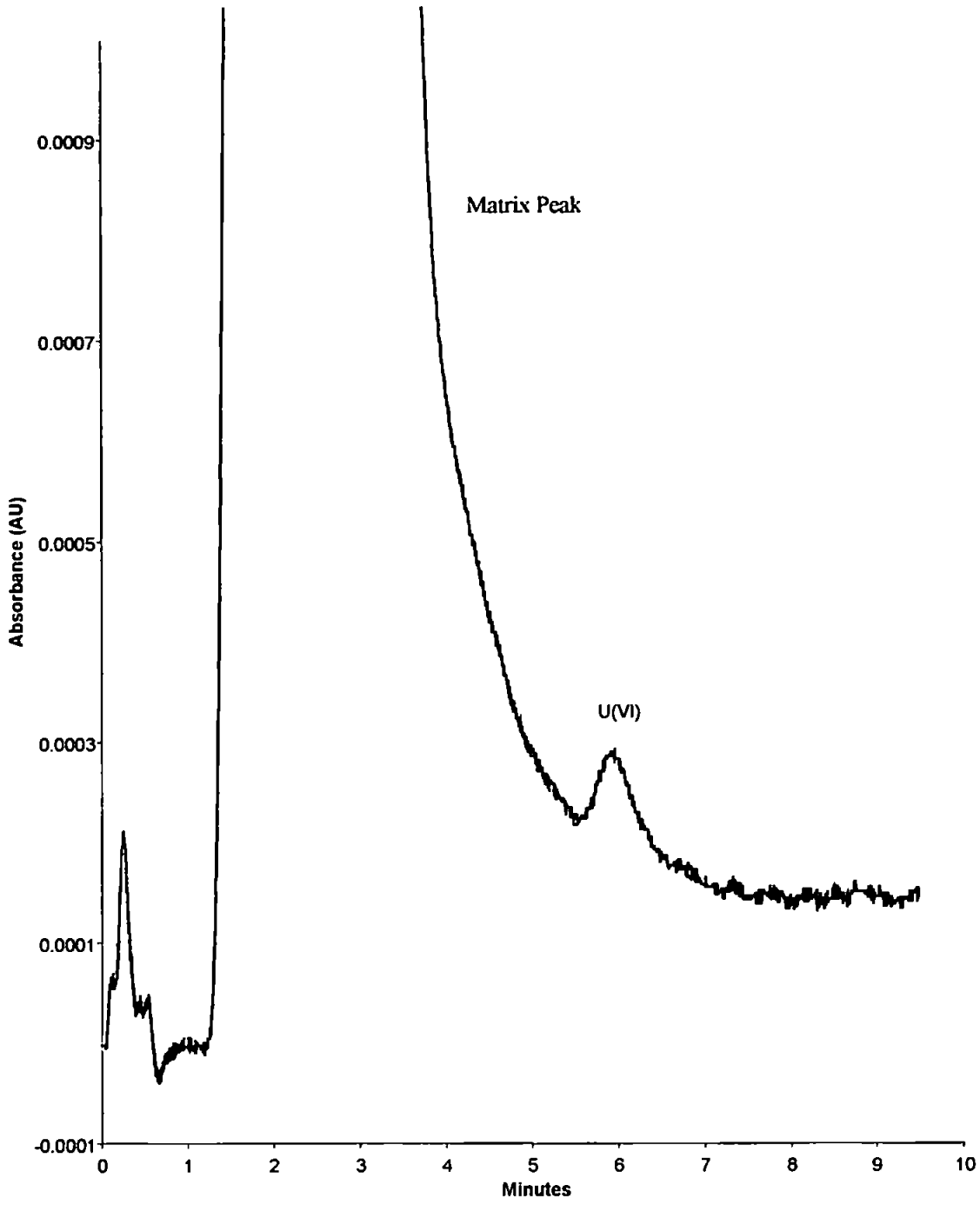

Figure 5.8. U(VI) in NASS-4 seawater CRM eluted on the 10cm PLRP-S column modified with 0.1mM dipicolinic acid. Injection volume used was 2ml with detection at 654nm with Arsenazo III PCR.

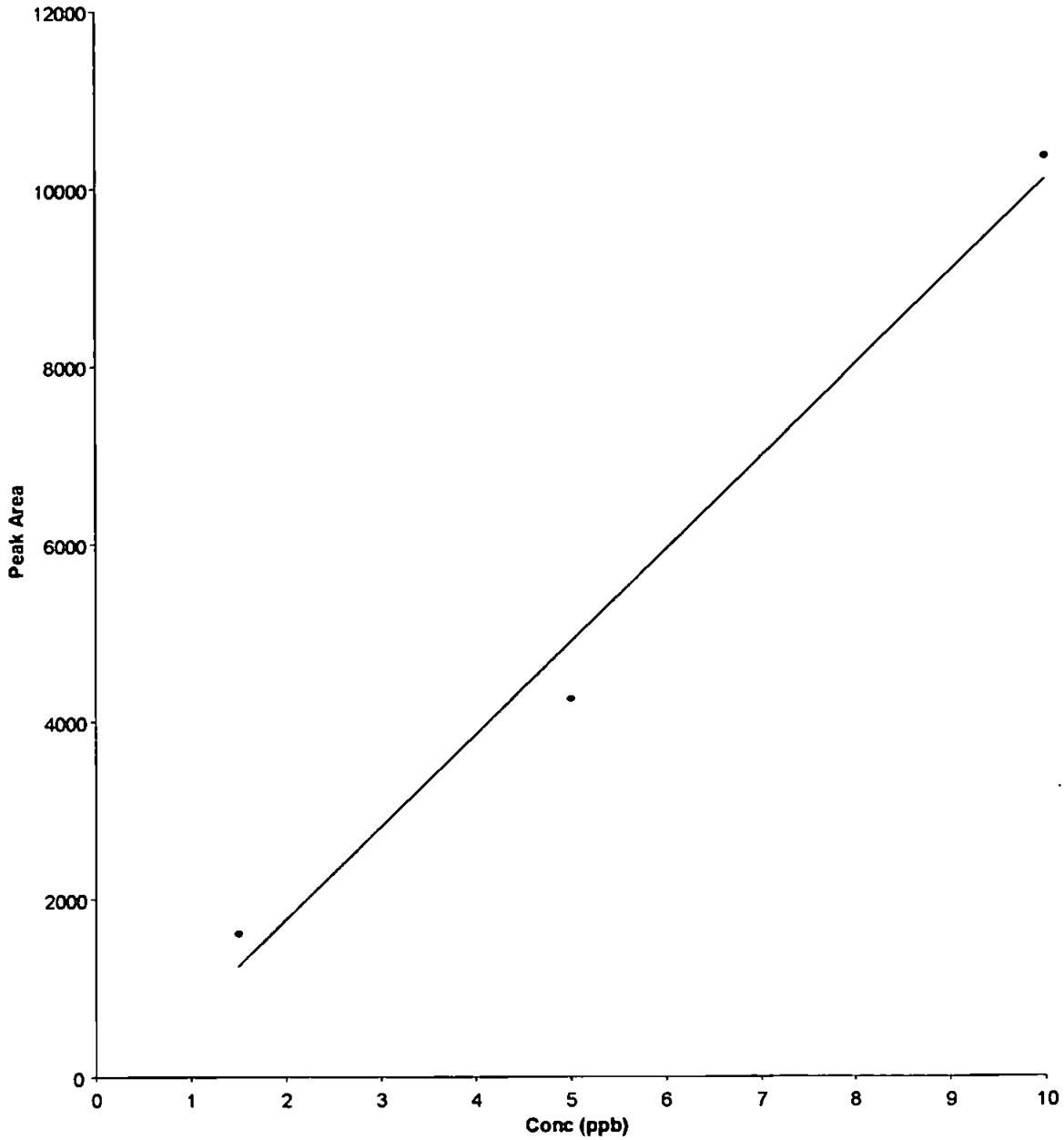

Figure 5.9. U(VI) calibration for Devils Point sample on a 10cm 5μm PLRP-S column dynamically modified with dipicolinic acid. Eluent used was 1M HNO_3 with 0.1mM dipicolinic acid with sample pH 1.6. Injection volume was 2ml with detection at 654nm with Arsenazo III.

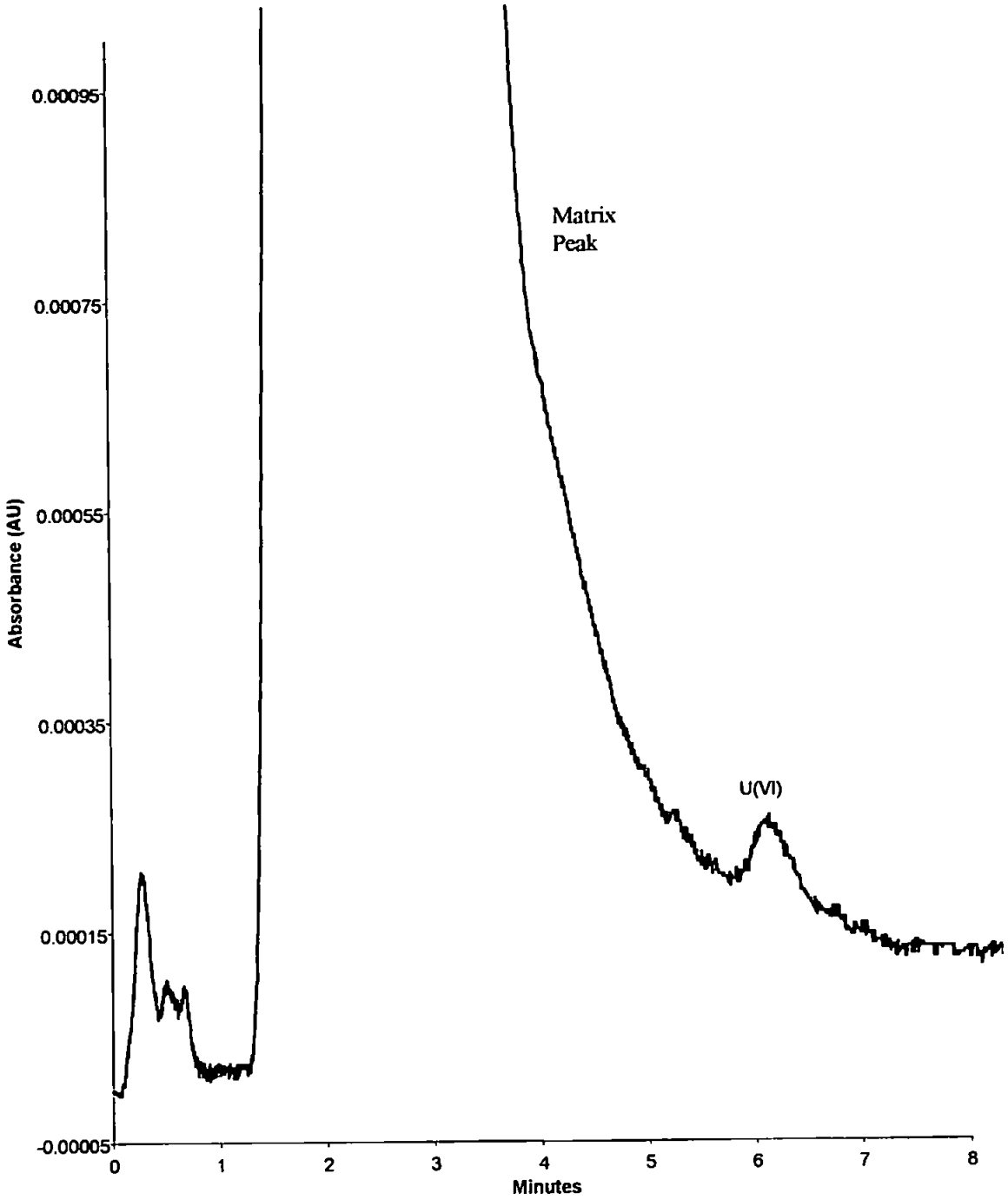

Figure 5.10. U(VI) in Devils Point sample eluted on the 10cm PLRP-S column modified with 0.1mM dipicolinic acid. Injection volume used was 2mls with detection at 654nm with Arsenazo III.

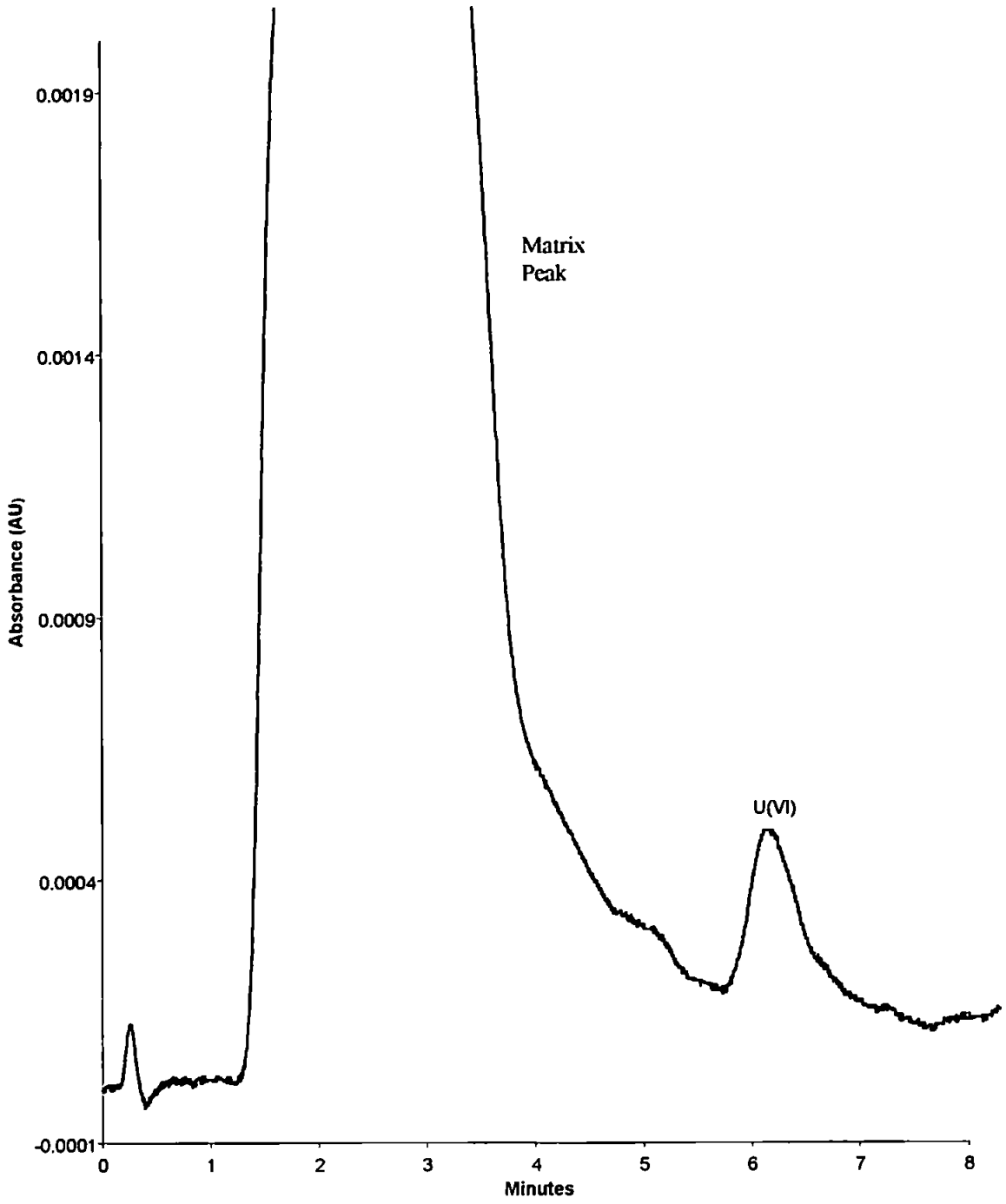

Figure 5.11. Devils Point (water's edge) sample spiked with 10µgl^{-1} U(VI) on a 10cm 5µm PLRP-S column dynamically modified with dipicolinic acid. Eluent used was 1M HNO_3 with 0.1mM dipicolinic acid with sample pH 1.6. Injection volume was 2ml with detection at 654nm with Arsenazo III.

Part 2:- Determination of Bi(III) and U(VI) in Soils and Sediments using a Dynamically Modified Substrate.

5.4 Introduction.

Bismuth belongs to the group VB(15) elements of the Periodic Table. It has an atomic number of 83 with an atomic mass of 208.9804 [19] and is a brittle, reddish-white element. In aqueous solutions, bismuth favours the +3 oxidation state however the metal ion is only to be found in highly acidic media as it will readily precipitate as an insoluble basic salt in water. A concentration of $0.17\mu gg^{-1}$ is to be found in the earth's crust while in aquatic systems a concentration of $2x10^{-2}\mu gl^{-1}$ (for a salinity of 35%) is documented for ocean waters with a residence time of $4.5x10^{4}$ years [3].

Bismuth occurs naturally as the basic oxide Bi_2O_3 in sulphide ores and is reduced by carbon, after roasting, to form the elemental bismuth. It is also found in basaltic and granitic rocks and is a by-product of lead refining. Uses for bismuth include alloys, electronics, catalysts, cosmetics and pigments. Also as it is one of the least toxic heavy metals it has also found use in medicines for stomach upsets though an excess can cause mild kidney damage [169]. Some of the methods and techniques used for the separation and determination of Bi(III) in a variety of sample types is discussed below.

Gong *et al* [220] used a novel chelating resin of macroporous epoxy-dicyandiamide for the preconcentration and separation of B(III) and various lanthanides and transition metals in waters and mineral samples using ICP-OES as the detection method. Gong [221] also reported the use of a novel polyacrylacylaminourea chelating fiber for the preconcentration

of the same suite of metals before detection by ICP-AES. A polyurethane foam loaded with dithiocarbamate was used by Arpadjan *et al* [222] as a preconcentration method for As, Bi, Mg, Sb, Se and Sn from waters while El-Shahawi and Al-Mehrezi [223] used polyurethane foams loaded with either 1,2-di-(2-fluorophenyl)-3-mercaptoformazan or dithizone for the selective detection and quantitative collection of Bi(III) from water.

Kuroda *et al* [224] used the anion exchange resin Bio-Rad AG1,X-4 for the selective separation of Bi(III) in several environmental reference materials including a pool sediment with detection by GF-AAS. Pozebon *et al* [225] used a C_{18} bonded silica column to preconcentrate Bi(III), Se(IV) and selected transition and heavy metals as their respective complexes with the ammonium salt of *O,O*-diethyldithiophosphoric acid from seawaters. An anion exchange column utilising polyaniline was used for the selective preconcentration of Bi(III) from the reference stream sediment GBW07312 as well as high purity antimony and copper plate by Sahayam [226] whereas Amberlite XAD-7 was used by Moyano *et al* [227] for the preconcentration of Bi(III) in human urine followed by detection with HG-ICP-AES.

Strelow [228] used a macroporous cation exchange resin, AGMP-50, for the selective separation of trace Bi(III) from gram amounts of Tl(III), Au(III), Hg(II) and Pt(IV) before detection with AAS. Uehara *et al* [229] used reverse phase HPLC for the separation of Bi(III), Cd(II), Co(II), Cu(II), Ni(II) and Fe(III) using a precolumn chelating reagent called picolinaldehyde-4-phenyl-3-thiosemicarbazone (PAPT).

In Part 1 of this chapter, the application of a column dynamically modified with dipicolinic acid for the determination of uranium in waters was discussed. In this part of the chapter,

this same column will be used for not only uranium determinations in soils and sediments but also for the determination of bismuth and zirconium in these sample matrices.

5.5 Experimental.

5.5.1 Instrumentation.

The instrumentation used was as described in Chapter 2.2.1 with the exception that a Dionex GP40 gradient pump was used to deliver the eluent and that a 500µl sample loop was used. The column used for these studies was a 150 x 4.6mm ID PEEK column packed with the 5µm PLRP-S resin from Polymer Laboratories.

5.5.2 Reagents.

All reagents used were supplied by BDH (BDH, Poole, UK) and of AnalaR grade unless otherwise stated. The eluent used consisted of 1M KNO_3 with 0.1mM dipicolinic acid (99% purity, Aldrich, Gillinham, UK) prepared in 1M HNO_3 for the attainment of the required pH. The PCR used consisted of 0.05M Arsenazo III (Avocado, Lancashire, UK) in 0.5M HNO_3 with detection made at 654nm. Both the eluent and the PCR were delivered at 1ml min^{-1}. Metal standard solutions were diluted from 1000mgl^{-1} stock solutions with dilute HNO_3 for the attainment of the required pH and stored in poly(propylene) bottles.

5.5.3 Sample Pre-treatment.

Mr D. Henon, of the University of Plymouth, UK, kindly performed the standard reference digestions.

The stream sediment sample and both the soil samples were prepared using hydrogen fluoride digestion. The fluoride ion complexes only weakly with uranium in solutions of high acidity so will not interfere with the separation and detection systems. For the digestion procedure, a known amount of accurately weighed sample (approximately 0.5 g) was added to a PTFE vessel together with 10 ml HNO_3, capped and left on a hot-plate (120°C) for 24 hrs. 2 ml of HF was added and left on the hot-plate for a further 48 hrs. The vessel was uncovered, 4 ml HNO_3 added, and the HF and HNO_3 evaporated at 120°C. Another 10mls of HNO_3 was added and evaporated at 70°C. This step was repeated twice more then the residue was transferred to a volumetric flask with small quantities of 0.5M HNO_3 (AristaR), 0.9 g boric acid (AristaR) added to dissolve any insoluble fluorides, and then made up to a final volume of 25 ml using 0.5M HNO_3 (AristaR).

5.6 Results and Discussion.

Three sample reference materials were chosen for this study and were supplied by LGC (LGC, Middlesex, UK). They were chosen so as to represent a range of concentrations for the metals of interest, namely Bi(III) and U(VI) in various sample matrices. Zr (IV) is also included in some of the chromatograms shown in order to show the ability of this system to separate Zr(IV) from the rest of the sample matrix. However, calibrations for Zr(IV) were not carried out for the samples themselves due to poor peak area reproducibility. The peak areas obtained proved to be much smaller than the peak areas obtained from corresponding Zr(IV) standard solutions. ICP-MS analysis carried out by Mr D. Henon confirmed that the concentrations determined for the samples matrices were lower than the certified values quoted. It was hypothesised that this may be as a result of the presence of the boric acid used in the digestion procedure complexing with the Zr(IV) over time. This was theorised

as the excess of boric acid used was white in colour upon completion of the digestion but this slowly darkened over time to a dark brown/black colour.

5.6.1 Stream Sediment GBW07311.

The first reference material investigated was a National Research Center for Certified Reference Materials (NRCCRM) stream sediment sample GBW07311. Both Bi(III) and U(VI) were looked at in this reference material which contained 50 +/- 5μgg^{-1} of Bi(III) and 9.1 +/- 1.3μgg^{-1} of U(VI).

In order to ascertain the system's performance, calibrations for both Bi(III) and U(VI) for the concentration ranges of 0.5-100μgg^{-1} and 14.8-1000μgg^{-1} respectively were constructed. These calibrations produced regression coefficients of $r^2 = 0.9999$ for Bi(III) and 0.9995 for U(VI) using peak area. The reproducibility (%RSD) of the method was calculated from repeat injections of metal standard solutions and determined to be 4.89% for a 2.5μgg^{-1} Bi(III) standard (n = 8) and 1.73% for a 180μgg^{-1} U(VI) standard (n = 8).

A second calibration was carried out for the determination of both these metals in the above reference material. This time regression coefficients of $r^2 = 0.9999$ for a Bi(III) concentration range of 0.5-10μgg^{-1} and $r^2 = 0.982$ for a U(VI) concentration range of 160-200μgg^{-1}. These calibrations produced a mean result of 47.6 +/- 4.4μgg^{-1} for Bi(III) (n = 3) and 8.8 +/- 0.02μgg^{-1} for U(VI) (n = 3) both which compared favourably with the certified values. All of the above calibrations are shown in Figures 5.12-5.14 with a sample chromatogram of this reference material in Figure 5.15.

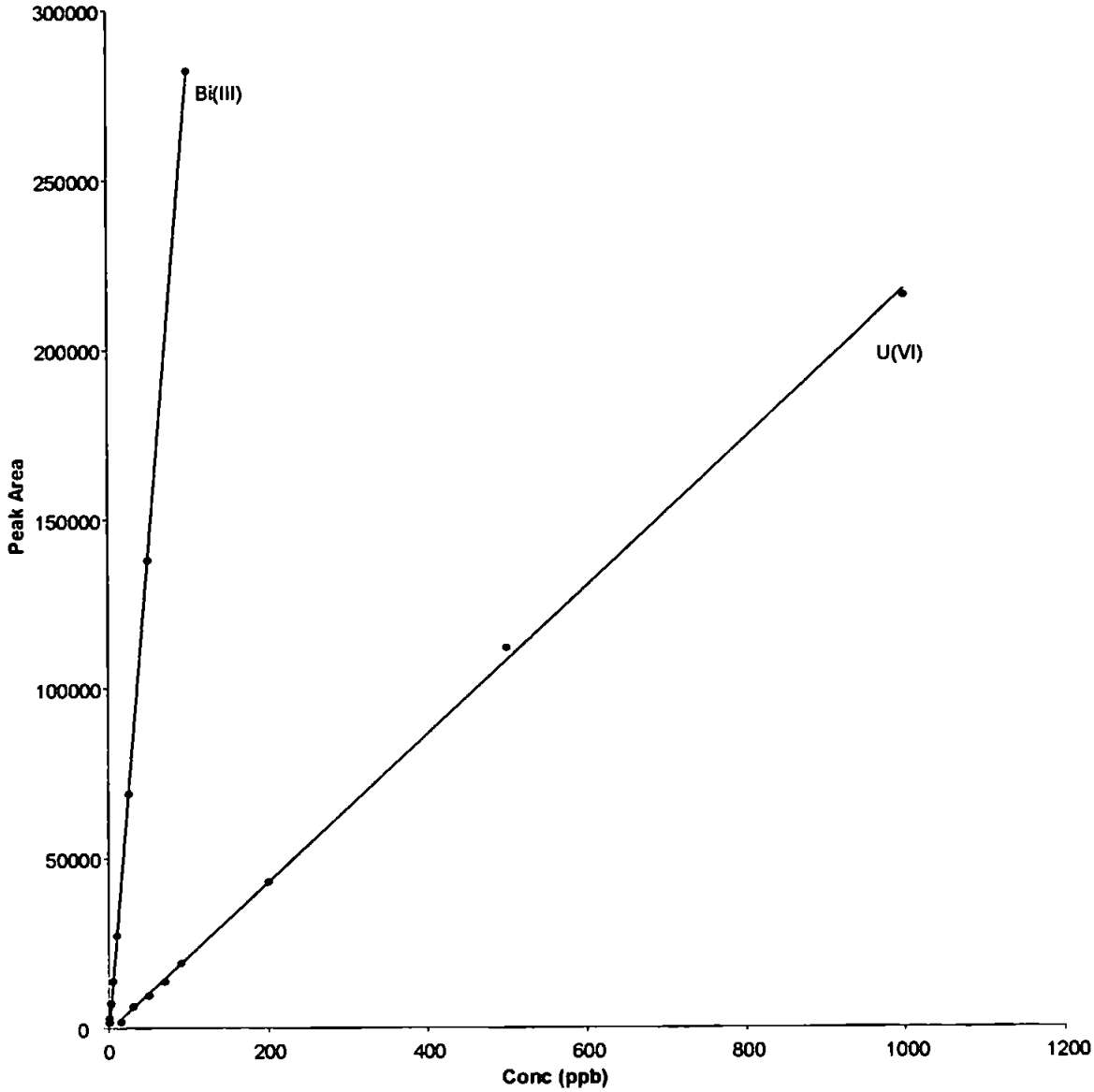

Figure 5.12. Method linearity calibrations for Bi(III) and U(VI) on a 15cm 5µm PLRP-S column dynamically modified with dipicolinic acid. Eluent used was 1M KNO_3 with 1M HNO_3 and 0.1mM dipicolinic acid. Injection volume was 500µl with detection at 654nm with Arsenazo III.

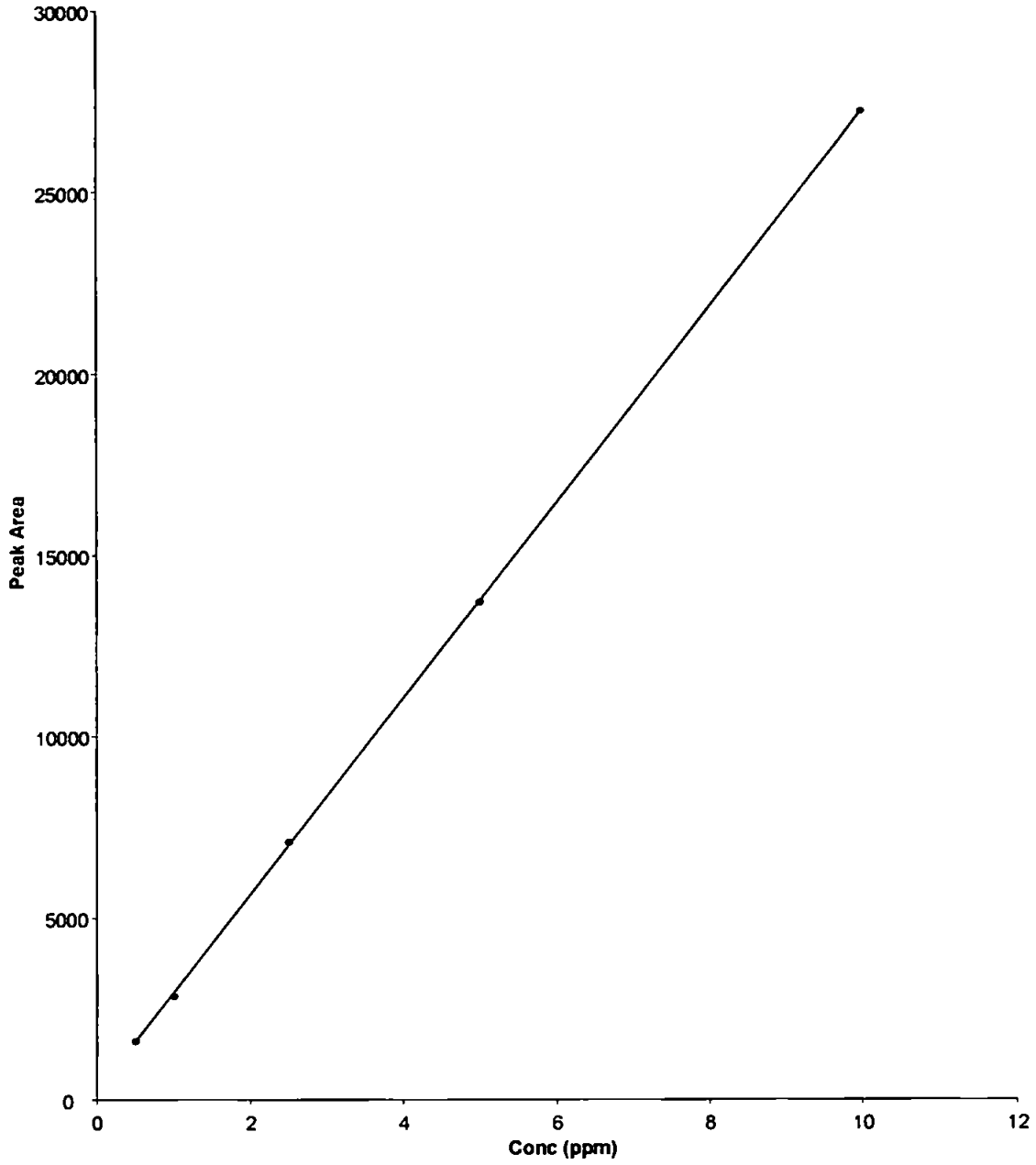

Figure 5.13. Bi(III) calibration for stream sediment CRM GBW07311 on a 15cm 5µm PLRP-S column dynamically modified with dipicolinic acid. Eluent used was 1M KNO_3 with 1M HNO_3 and 0.1mM dipicolinic acid. Injection volume was 500µl with detection at 654nm with Arsenazo III.

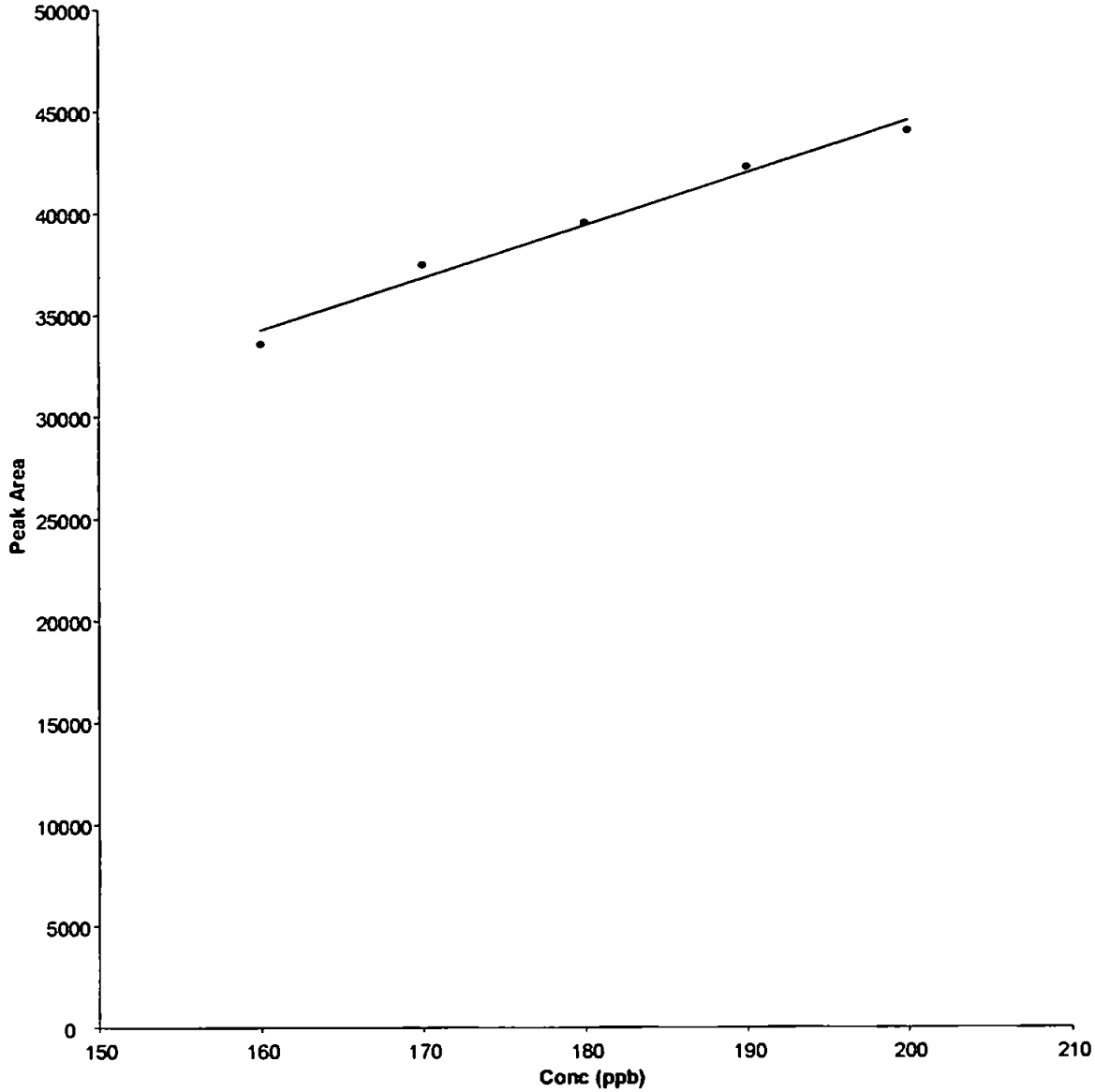

Figure 5.14. U(VI) calibration for stream sediment CRM GBW07311 on a 15cm 5µm PLRP-S column dynamically modified with dipicolinic acid. Eluent used was 1M KNO_3 with 1M HNO_3 and 0.1mM dipicolinic acid. Injection volume was 500µl with detection at 654nm with Arsenazo III.

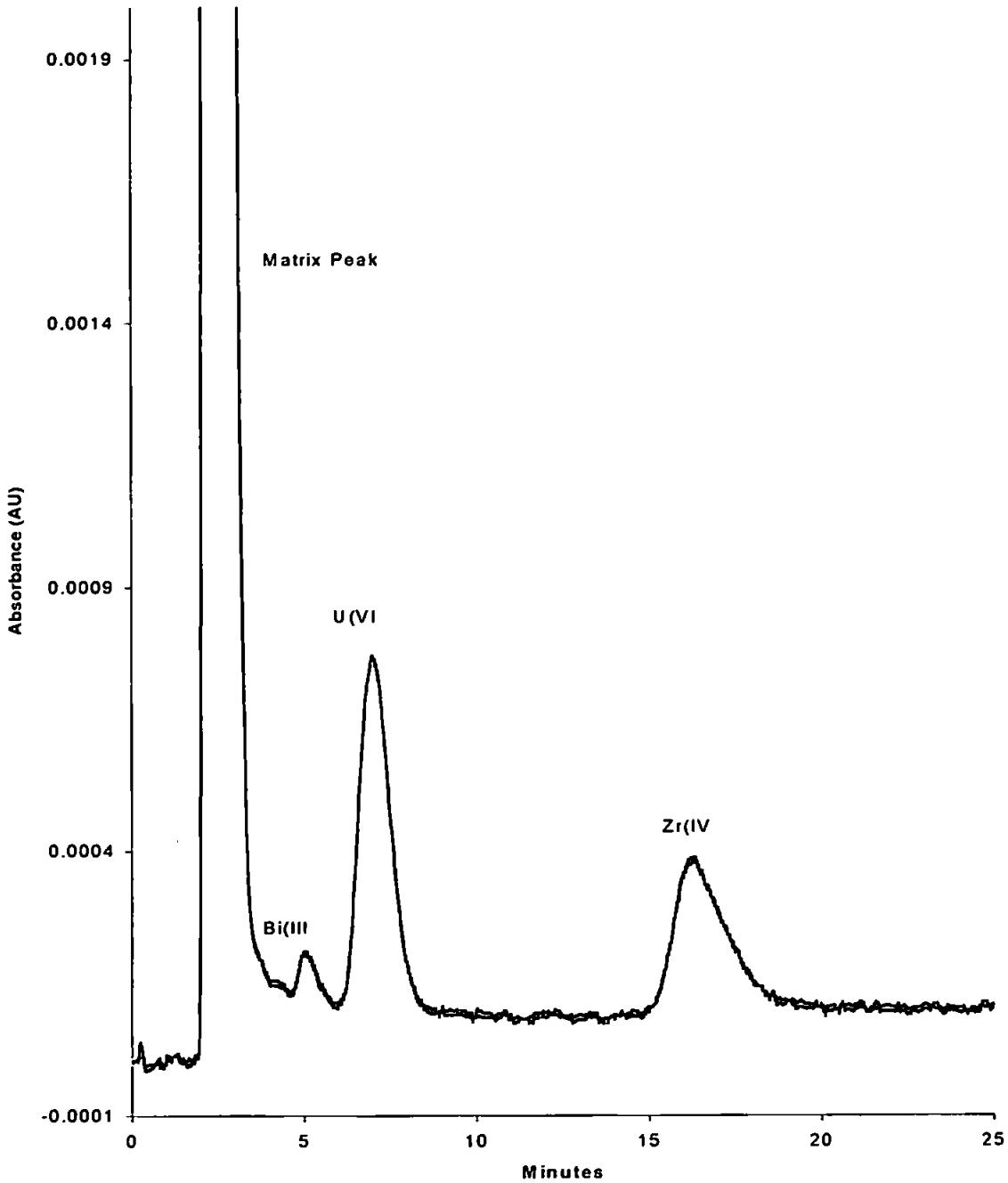

Figure 5.15. Isocratic separation of Bi(III), U(VI) and Zr(IV) in GBW07311 at pH0 on the 15cm PLRP-S column dynamically modified with 0.1mM dipicolinic acid. Injection volume used was 500µl with detection at 654nm with Arsenazo III PCR.

5.6.2 Soil GBW07401.

The reference material investigated this time was a NRCCRM soil sample GBW07401. Only U(VI) was investigated as the Bi(III) concentration was too low to determine by this method. This sample contained a certified concentration of 3.3 +/- 0.3μgg^{-1} U(VI).

The same method as was used for GBW07311 was used for this reference material. That is an isocratic elution utilising an eluent of 1M KNO_3 with 0.1mM dipicolinic acid prepared in 1M HNO_3 with a 500µl injection. A calibration for U(VI) over the concentration range 14.8-90μgg^{-1} was constructed which showed good linearity with a regression coefficient of $r^2 = 0.9906$ using peak area. The average U(VI) concentration (n = 3) was determined to be 3.0 +/- 0.1μgg^{-1} which falls within the certified range. Figure 5.16 shows the calibration curve constructed while Figure 5.17 shows an example of U(VI) in this reference material.

5.6.3 Soil GBW07403.

The third reference material was again a NRCCRM soil sample GBW07403. This differed from GBW07401 only in that the metals present were in lower concentrations. Again only U(VI) was determined due to the lack of sensitivity of this method for Bi(III). The certified concentration of U(VI) in this sample was 1.26 +/- 0.18μgg^{-1}.

Again the method used was as for GBW07311 and GBW07401 with the U(VI) calibration curve constructed for GBW07401 being used as well. This sample's average U(VI) concentration (n = 3) was determined to be 1.09 +/- 0.01μgg^{-1} which again corresponds

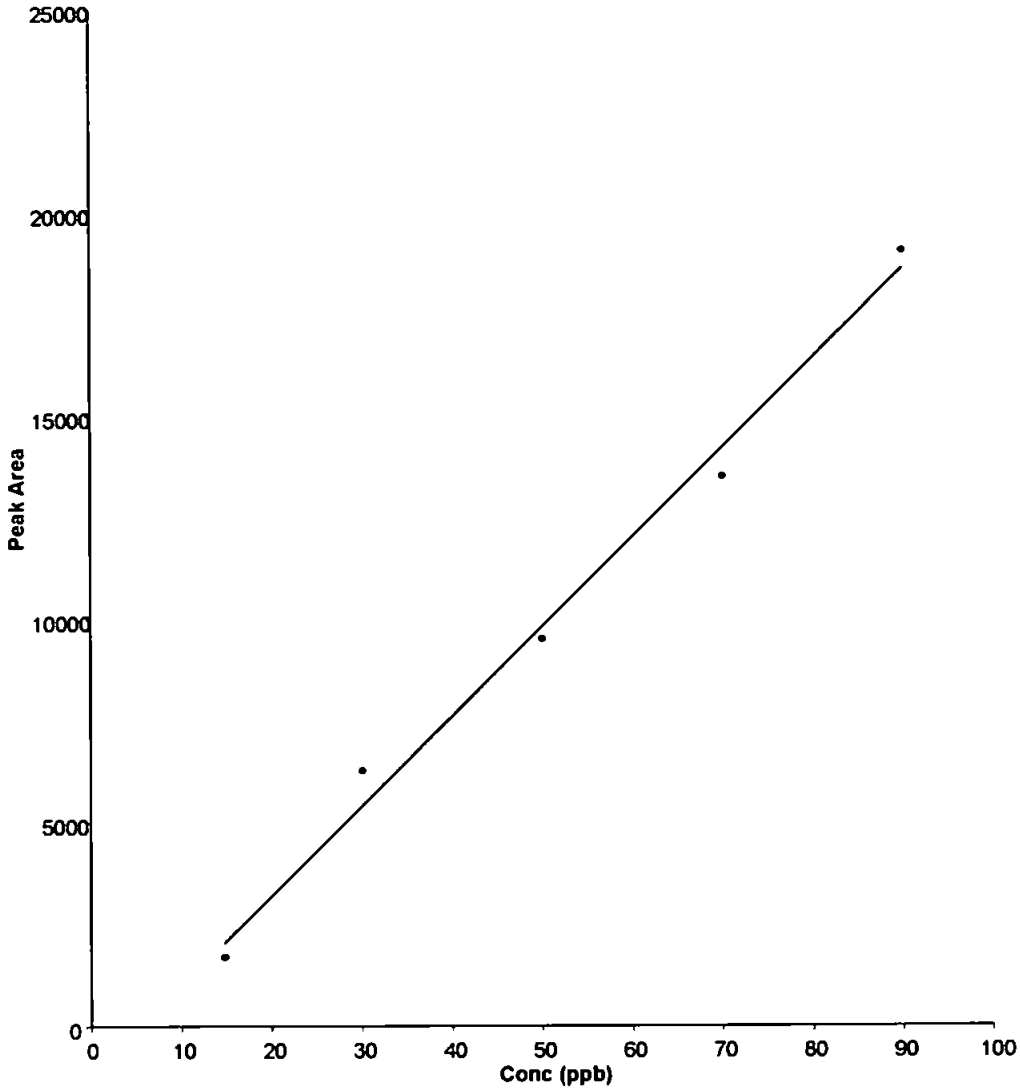

Figure 5.16. U(VI) calibration for stream sediment CRM GBW07401 and GBW07403 on a 15cm 5μm PLRP-S column dynamically modified with dipicolinic acid. Eluent used was 1M KNO_3 with 1M HNO_3 and 0.1mM dipicolinic acid. Injection volume was 500μl with detection at 654nm with Arsenazo III.

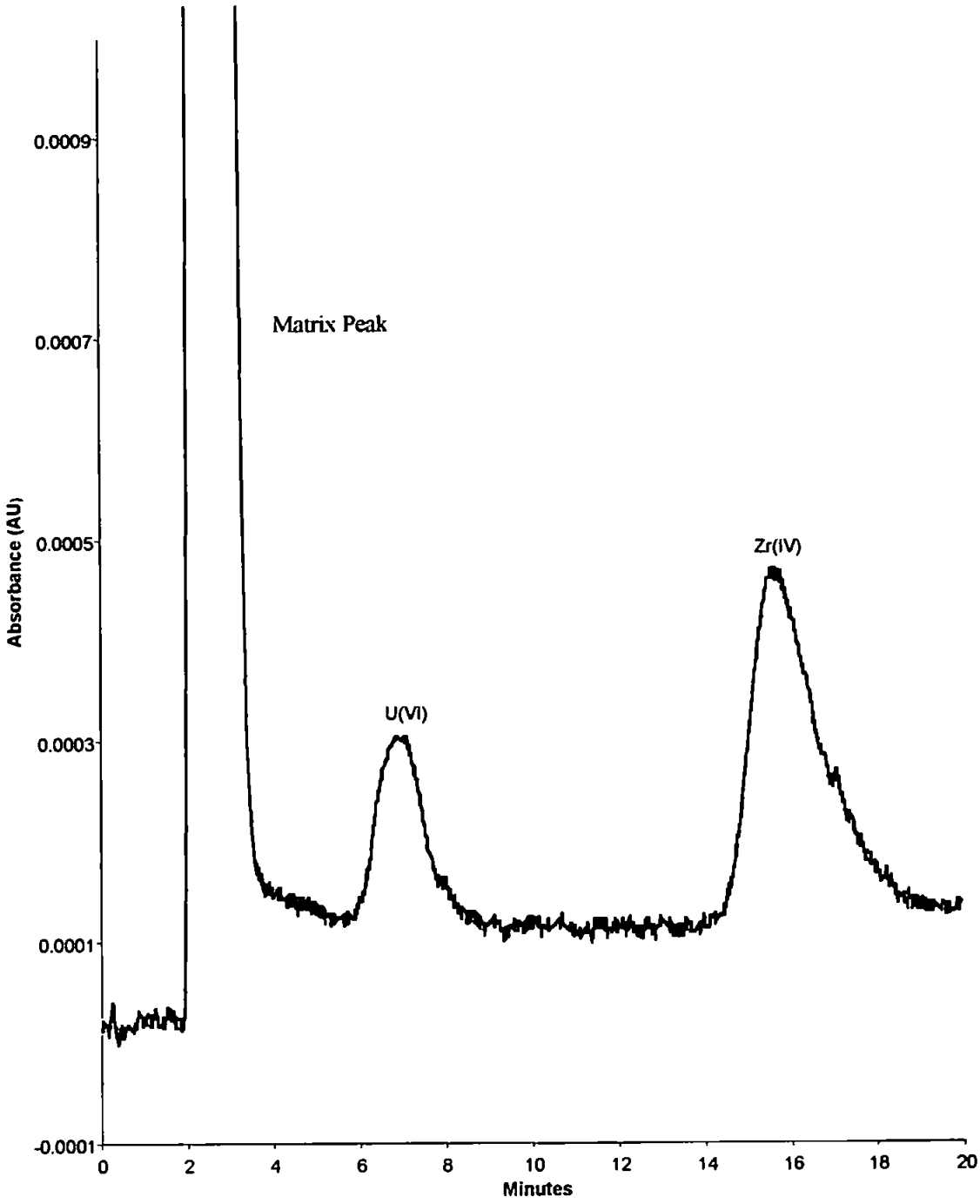

Figure 5.17. Isocratic separation of U(VI) and Zr(IV) in GBW07401 at pH0 on the 15cm PLRP-S column dynamically modified with 0.1mM dipicolinic acid. Injection volume used was 500µl with detection at 654nm with Arsenazo III PCR.

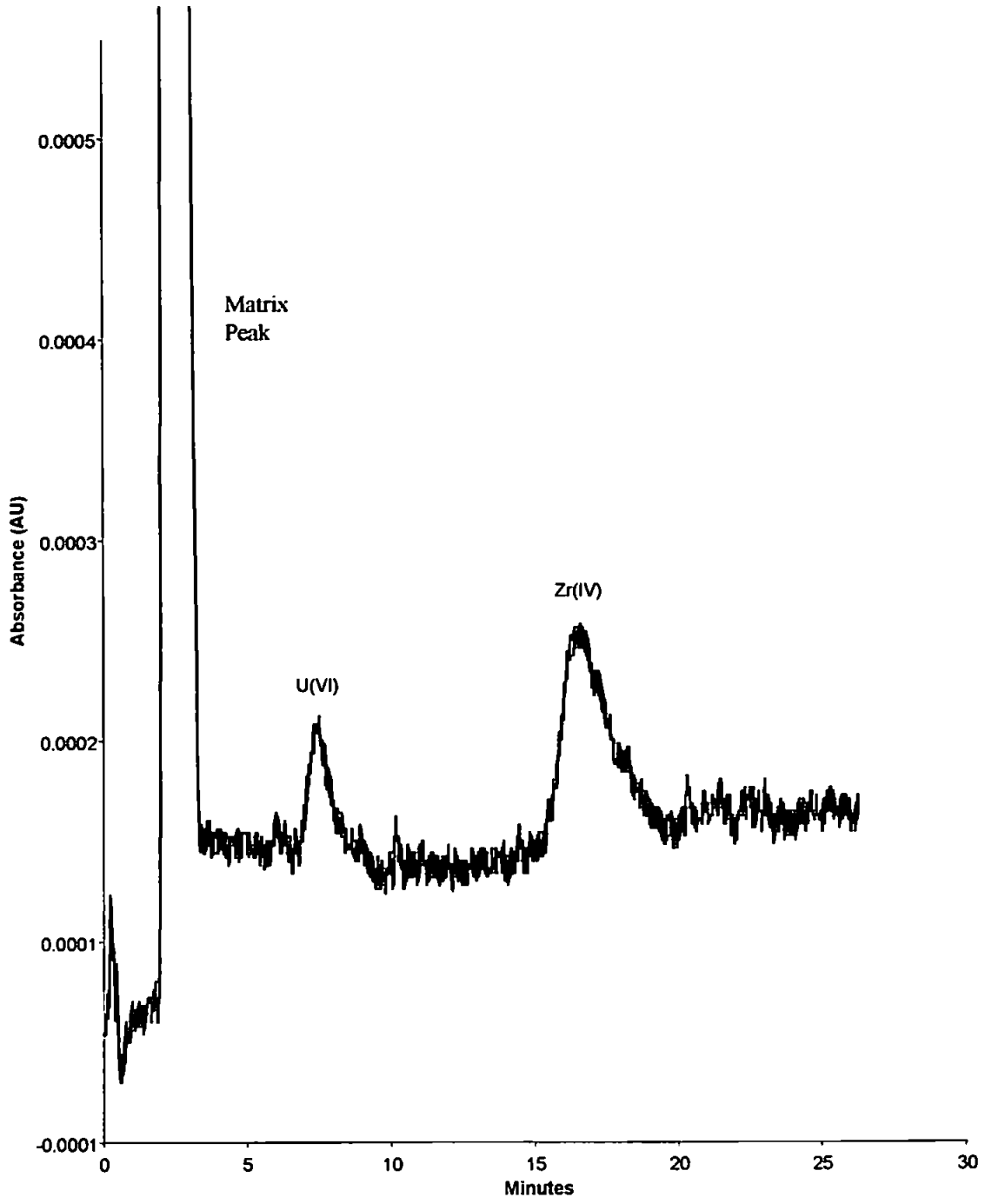

Figure 5.18. Isocratic separation of U(VI) and Zr(IV) in GBW07403 at pH0 on the 15cm PLRP-S column dynamically modified with 0.1mM dipicolinic acid. Injection volume used was 500µl with detection at 654nm with Arsenazo III PCR.

favorably with the certified value. Figure 5.18 shows an example of U(VI) in this sample matrix.

5.7 Summary.

Using a high efficiency PS-DVB resin dynamically modified with dipicolinic acid, a highly selective and sensitive HPCIC system has been developed for the determination of trace levels of U(VI) in complex matrices. U(VI) can de determined at these levels without any adverse affect by the matrix metals using simple isocratic elutions at low pHs. A summary of results and method characteristics is given in Table 5.1.

This system is also suitable for Bi(III) determinations in the complex sample matrices though concentrations of greater than low μgg^{-1} levels are required for analysis using this system as described due to the lack of sensitivity offered by the Arsenazo III PCR. Figures 5.15, 5.17 and 5.18 also show an extra peak which corresponds to Zr(IV). While the system is both selective and sensitive enough for quantitative analysis, problems with the digestion procedure resulted in poor recoveries for this metal.

Table 5.1. Summery of results for the Certified Reference Materials and samples analysed.

Sample	Certified Value	Determined Value	Method Calibration R^2 / %RSD
Drinking Water	10.0 +/- 0.05μgl^{-1}	9.38 +/- 0.13μgl^{-1}	0.9999 / 3.49%
TMDA-54.2	62.3 +/- 13.1μgl^{-1}	6.28 +/- 0.8μgl^{-1}	0.9954 / 1.29%
NASS-4	2.64 +/- 0.12μgl^{-1}	2.59 +/- 0.1μgl^{-1}	0.9986 / 7.56%
Devils Point (Waters Edge)	---	2.37μgl^{-1}	---
Devils Point (Pool)	---	2.50μgl^{-1}	---
GBW 07311	9.1 +/- 1.3μgg^{-1} U(VI)	8.8 +/- 0.02μgg^{-1} U(VI)	0.9995 / 1.73%
	50 +/- 5μgg^{-1} Bi(III)	47.6 +/- 4.4μgg^{-1}Bi(III)	0.9999 / 4.89%
GBW07401	3.3 +/- 0.3μgg^{-1}	3.0 +/- 0.1μgg^{-1}	" / "
GBW07403	1.26 +/- 0.18μgg^{-1}	1.09 +/- 0.01μgg^{-1}	"/ "

Chapter 6 – Conclusions and Further Work.

6.1 Conclusions.

The work presented in this thesis has detailed the investigations carried out for the development of new and improved High Performance Chelation Ion Chromatography (HPCIC) chelating substrates and the subsequent application of these substrates in the determination of trace metals in a variety of complex sample matrices.

Initial studies entailed the development of substrates permanently coated with chelating dyestuffs via a physical impregnation mechanism. Previous work has concentrated principally on the fabrication of this type of substrate as these systems can readily highlight the advantages of HPCIC over more conventional ion chromatography techniques. These advantages include the potential to obtain the desired selectivity for the separation of the metals of interest as well as the ability to determine a single metal in the presence of a large excess of matrix interferences. This is possible due to the separation mechanism being based upon the conditional stability constants of the metal chelates and is therefore governed by the pH of the mobile phase and not simple ion exchange interactions and which also results in a relative insensitivity to ionic strength.

Two chelating dyestuffs were investigated namely Xylenol Orange (XO) and Aurine Tricarboxylic Acid (ATA) and these dyes show the differences in selectivity that can be obtained depending upon the donor ligands present, N, O, O for XO and O, O for ATA. As reported in previous work, XO offers reasonable selectivity towards a variety of transition and heavy metals with the possible exception of Ni(II) for the reasons discussed

in Chapter 2.4.3.3. ATA showed a much stronger preference for Cd(II) as well as Pb(II) and Cu(II) than did XO making this impregnated substrate much more suitable for the determination of these metal cations.

One problem with these dye impregnated substrates is the slow kinetics involved in the retention mechanisms. This results in peaks quickly broadening out as retention increases thereby resulting in separations of greater than four metals being unfeasible under isocratic conditions. To overcome this problem, gradient elution programs were developed. This adds a new dimension to the separations of metal ions on these columns allowing for six, seven or more metal species to be determined within a reasonable time frame by a single elution. Gradient elutions also allows for the determination of Ni(II) in the presence of other transition and heavy metals on a XO impregnated column. The disadvantage to gradient elutions is the increased complexity they bring to the required elution program as well as higher impurity peaks and baseline changes.

The application of these two chelating systems to the analysis of a highly mineralised water is discussed in Chapter 2.6 and highlights the suitability of these chelating substrates for this type of analysis as well as showing the increased suitability of the ATA column over the XO column for the analysis of Cd(II), Pb(II) and Cu(II) even though these metals aren't readily detectable though larger volume injections could overcome this problem.

This relative insensitivity is due to the lack of sensitivity of the PAR/Borate post column reagent especially for Pb(II). However the detection limits obtained for this method, $\leq 10\mu gl^{-1}$ is a vast improvement on previous work. The development and use of the borate based buffer for the PAR post column reagent has shown exceptional increases in

sensitivity for Cd(II) and coupled with the application of the noise reduction system has allowed for much lower levels of detection to be obtained for similar sized injection volumes of past studies.

Other system parameters including column length, particle size and method of impregnation were also investigated with the aim of improving separations. The use of longer columns (25cm) resulted in increased efficiency of separation i.e. greater resolution between the peaks though with greater run times as a result and with smaller particle sizes "sharpening" peaks up. The development of an impregnation method based upon ultrasonic agitation while not necessarily resulting in increased dye loadings did result in a more stable and reproducible chelating substrate.

The use of the noise reduction system not only enhanced the sensitivity of the post column reaction system it also highlighted a problem that is inherent with this method of detection, that being changes in baseline absorbance when using gradient elution programs. Due to the very nature of chromophore containing post column reagents, a change in the pH of the reagent will result in a change in its absorbance and thereby result in a change in a chromatogram's baseline absorbance. This baseline change will invariably occur when a metal is being eluted using gradient elution. As stated in Chapter 3 this change can be compensated for by manipulating the data using suitable computer software.

Dye impregnation was not the only method used to fabricate chelating substrates. A chemisorption mechanism was also studied. This method entailed the dynamic modification of neutral polystyrene based resins with low molecular weight organic molecules. This technique provides a quick and easy method for the preparation of a

chelating substrate and involves the use of an eluent containing the ligand of choice which results in a dynamically sorbed layer building up on the neutral substrate. Eventually equilibrium will be formed between the ligand on the surface of the substrate and that which remains in the mobile phase. The amount of ligand used in the mobile phase has to be of relatively low concentration in order to minimise the competition between the sorbed and mobile ligand as well as to reduce any possible interferences with the post column detection system.

Of the ligands investigated, dipicolinic acid offered the greatest selectivity and efficiency of the selected transition, heavy and high valency metals looked at with five high valency metals including Hf(IV) and Zr(IV) separated within twenty minutes. Studies carried out using both the 2- and 4-chloromandelic acids proved disappointing in that an unstable system was obtained. Whether this is a characteristic of O, O chelators (dipicolinic acid is a N, O, O chelator) when loaded in this manner is uncertain. The final ligand investigated, 4-chlorophenylalanine (a N, O chelator) while not as efficient as dipicolinic acid did produce a stable system. Good separations of selected transition and heavy metals were obtained though the pH required, >4.5, may be too high for some sample matrices. For the high valency metals this column produced a reversal in retention order for U(VI) and Th(IV) when compared to the dipicolinic acid system which could prove useful for Th(IV) determinations in the presence of U(VI).

These dynamic modification studies were carried out using a 5μm PLRP-S resin. As the dipicolinic acid studies appeared to offer the "best" results it was used to dynamically modify the 9μm hypercrosslinked resin "MN 200". This resin differed from the PLRP-S resin in that it has a much higher degree of crosslinking and thereby offers a much greater

surface area. Dynamic modification of this resin produced vastly increased loadings with which it was possible to obtain highly efficient isocratic separations of up to seven transition metals, a feat that is impossible to attain with the dye impregnated substrates within an acceptable time frame.

These dynamic systems do have several problems associated with them. These include gradient elutions are not usable as changes in the dynamic loading occur during the gradient. Also high levels of matrix metals can disturb the sorbed layer though this was never found to be so at the pHs used in this study.

The high efficiency and good separations obtained resulted in the use of the 5μm PLRP-S/dipicolinic acid column for the analysis and determination of U(VI) in various waters and U(VI) and Bi(III) in soil and sediment samples. With the exception of the drinking water CRM all samples reported results that were within the certified value range with the methods used showing good linearity and reproducibility for the metals investigated. The development of these dynamically modified chelating substrates now adds a new dimension to the analysis of trace metals in complex samples by ion chromatographic techniques.

Suggestions for further work on both the dye impregnated and dynamically modified substrates as well as the post column detectors are given in the following section.

6.2 Suggestions for Further Work.

While a lot of work has been carried out using dye impregnated columns, this technique is by no means fully developed. Studies have shown that numerous factors can affect the dye loading obtained including the characteristics of the resin used, dye structure and loading procedure. Optimisation based upon the hydrophilic/hydrophobic nature of the resin, its particle and pore size is needed to determine the procedural requirements of the resin for impregnation. The optimisation of the ultrasonic loading protocols outlined in Chapter 2.4.2.2 also require further study. This may include factors such as sonication frequency, volume of dye solution per weight of resin, concentration and pH of the dye solution as well as the length of time sonicated for. Optimisation of some or all of these factors may produce increased loadings or increased % activities and therefore more efficient separations.

A more efficient eluent clean-up procedure is also required, possibly using a mercury pool, to ensure that only extremely low contamination exists thereby allowing for the full potential of this technique to be further realised.

The results presented in this thesis for the ATA impregnated column are not as impressive as they possibly could be due to the poor loading of the column and so should be investigated further due to its unique selectivity towards Cd(II) and to a lesser extent Pb(II). Other chelating dyestuffs need to be investigated, particularly those that offer N, N or N, S chelation as very little if any work has been done on these types of molecules.

Improvements for the post column detection system can also be made. This may include the investigation of new buffer systems in an attempt to hold the detection pH stable and thereby removing changes in the baseline absorbance. Alternatively, more specific PCR's that will complex with only one or two metal ions, may be investigated which could allow for quicker elution times or suitable isocratic elutions and thereby increase the sensitivity of the system for these metals.

The dynamic modification of neutral substrates can also be studied further. As previously mentioned there are innumerable small organic chelating molecules that could be used for this method. The presence of π-electron accepting groups can be investigated more for example, the synthesis of the stronger NO_2 group onto dipicolinic acid instead of a chlorine group could produce an improved dynamic loading. It is possible though that the presence of stronger π-electron accepting groups could affect the chelating donor atoms by withdrawing electrons from the pyridine group. If this were the case then chemically bonding the dipicolinic acid to the resin backbone, thereby negating the need for it in the mobile phase, could be the answer.

The work reported on the MN 200 resin showed interesting results and warrants further study. This can entail looking at smaller particle sizes e.g. 5μm instead of 9μm to increase the loading further and possibly resulting in a permanently sorbed layer that would require very little (if any) ligand in the mobile phase. If this were so the introduction of gradient elution programs could be made thereby increasing the versatility of the systems.

The methodologies developed for all the samples analysed are also still open to further optimisation by for example, increasing the injection volume, manipulation of sample pH and detection parameters.

REFERENCES

[1] C. F. Mason, Biology of Freshwater Pollution, 2nd Ed., Longman Scientific and Technical, 1993.

[2] H. G. Beere and P. Jones, *Anal. Chim. Acta.*, **293** (1994) 237.

[3] J. P. Riley and R. Chester, Introduction to Marine Chemistry, Academic Press, 1971.

[4] D. Hughes, Environmental Law, 3rd Ed., Butterworths, London, 1996.

[5] R. Helmer and I. Hespanhol, Water Pollution and Control: A Guide to the Use of Water Quality Management Principles, Wiley-VCH, Weinheim, 1997.

[6] D. Gillies, A Guide to EC Environmental Law, Wiley-VCH, Weinheim, 1999.

[7] D. A. Skoog and J. J. Leary, Principles of Instrumental Analysis, 4th Ed., Harcourt Brace and Company, 1992.

[8] H. Small, T. S. Stevens and W. C. Bauman, *Anal. Chem.*, **47** (1975) 1801.

[9] P. Jones and P. N. Nesterenko, *J. Chromatogr. A.*, **789** (1997) 413.

[10] P. R. Haddad and P. E. Jackson, IonChromatography – Principles and Applications, Journal of Chromatography Library, Vol 46, Elsevier, New York, 1990.

[11] A. R. Timerbaev and G. K. Bonn, *J. Chromatogra.*, **640** (1993) 195.

[12] J. Weiss, Ion Chromatography, 2nd Ed., Wiley-VCH, Weinheim, 1995.

[13] J. S. Fritz and D. T. Gjerde, Ion Chromatography, 3rd Ed., Wiley-VCH, Weinheim, 2000.

[14] K. Robards, P. R. Haddad and P. E. Jackson, Principles and Practice of Modern Chromatographic Methods, Academic Press, London, 2001.

[15] R. Chang, Chemistry, 4th Ed., McGraw-Hill Inc., New York, 1991.

[16] C. F. Bell, Principles and Applications of Metal Chelation, Oxford University

Press, 1977

[17] I.M. Kohltoff and P. J. Elving (Eds), Treatise on Analytical Chemistry, Part 1 – Theory and Practice, 2nd Ed., Vol 2, John Wiley and Sons, New York, 1979.

[18] N. N. Greenwood and A. Earnshaw, Chemistry of the Elements, Permagon Press Ltd., 1984.

[19] F. A. Cotton, G. W. Wilkinson and P. L. Gaus, Basic Inorganic Chemistry, 3rd Ed., John Wiley and Sons, New York, 1995.

[20] H. Small, *J. Chromatogra.*, **546** (1991) 3.

[21] K. Robards, P. Starr and E. Patsalides, *Analyst*, **116** (1991) 1247.

[22] C. Sarzanini and E. Mentasti, *J. Chromatogr. A*,, **789** (1997) 301.

[23] C. Sarzanini, *J. Chromatgr. A.*, **850** (1999) 213.

[24] W. T. Frankenberger, H. C. Mehra and G. T. Gjerde, *J. Chromatgra.*, **504** (1990) 211.

[25] P. L. Buldini, S. Cavalli and A. Trifiro, *J. Chromatgr. A.*, **789** (1997) 529.

[26] P. R. Haddad, P. Doble and M. Macka, *J. Chromatgr. A.*, **856** (1999) 145.

[27] C.A. Pohl, J. R. Stillian and P. E. Jackson, *J. Chromatgr A.*, **789** (1997) 29.

[28] DIONEX Product Catalogue, 1997/1998.

[29] A. Rahmalan, M. Zahari Abdullah, M. Marsin Sanagi and M, Rashid, *J. Chromatgr. A.*, **739** (1996) 233.

[30] X. Ding, S. Mou, K. Liu, A. Siriraks and J. M. Riviello, *Anal. Chim. Acta.*, **407** (2000) 319.

[31] K. A. Ruth and R. W. Shaw, *J. Chromatogra.*, **546** (1991) 243.

[32] P. L. Buldini, D. Ferri and J. L. Sharma, *J. Chromatgr. A.*, **789** (1997) 549.

[33] P. L. Buldini, A. Mevoli and J. L. Sharwa, *Analyst*, **123** (1998) 1109.

[34] H. Lu, S. Mou and J. M. Riviello, *J. Chromatgr. A.*, **857** (1999) 343.

[35] M. T. Vasconcelos and C. A. R. Gomes, *J. Chromatgr. A.*, **696** (1995) 227.

[36] P. Janvion, S. Motellier and H. Pitsch, *J. Chromatgr. A.*, **715** (1995) 105.

[37] N. Cardellicchio, S. Cavalli, P. Ragone and J. M. Riviello, *J. Chromatgr. A.*, **847** (1999) 251.

[38] N. Cardellicchio, P. Ragone, S. Cavalli and J. M. Riviello, *J. Chromatgr. A.*, **770** (1997) 185.

[39] N. Cardellicchio, A. Dellatti, S. Giandomenico, A. Dileo and S. Cavalli, *Annali di Chimica*, **88** (1998) 819.

[40] M. Ding, K. Tanaka, W. Hu, K. Hasebe and P. R. Haddad, *Analyst*, **126** (2001) 567.

[41] M. C. Bruzzoniti, E. Mentasti, C. Saranini, M. Braglia, G. Cocito and J. Kraus, *Anal. Chim. Acta.*, **322** (1996) 49.

[42] M. C. Bruzzoniti, E. Mentasti and C. Saranini, *Anal. Chim. Acta.*, **353** (1997) 239.

[43] E.Lane, A. J. Holden and R. A. Coward, *Analyst*, **124** (1999) 245.

[44] A.W. Al-Shawi and R. Dahl, *Anal. Chim. Acta.*, **391** (1999) 35.

[45] M. C. Bruzzoniti, E. Mentasti and C. Saranini, *Anal. Chim. Acta.*, **382** (1999) 291.

[46] I.P. Alimarin, V. I. Fadeeva, G. V. Kudryavtsev, I. M. Loskutova and T. I. Tikhomirovna, *Talanta*, **34** (1987) 103.

[47] K. Ohta, K. Tanaka, B. Paull and P. R. Haddad, *J. Chromatgr. A.*, **770** (1997) 219.

[48] L. M. Nair, R. Saari-Nordhaus and J. M. Anderson, *J. Chromatgra.*, **640** (1993) 41.

[49] M. E. Fernandez-Boy, F. Cabrera, E. Madejon, M. J. Diaz, F. Moreno and J. P.

Calero, *J. Chromatgr. A.*, **823** (1998) 279.

[50] P. N. Nesterenko and G. Z. Amirova, *J. Anal. Chem.*, **49(5)** (1994) 447.

[51] S. Schnell, S. Ratering and K. Jansen, *Environ. Sci. Tech.*, **32** (1998) 1530.

[52] Z. L. Chen, M. A. Adams, *Chromatographia*, **49 (9/10)** (1999) 496.

[53] G. V. Myasoedova and S. B. Savvin, *CRC Crit. Rev. Anal. Chem.*, **17(1)** (1986) 1.

[54] S. K. Sahni and J. Reedijk, *Coord. Chem. Rev.*, **59** (1984) 1.

[55] M. Torre and M. L. Marina, *CRC Crit. Rev. Anal. Chem.*, **24(5 & 6)** (1994) 327.

[56] A.Siriraks, H. M. Kingston and J. M. Riviello, *Anal. Chem.*, **62** (1990) 1185.

[57] J. F. Biernat, P. Konieczka, B. J. Tarbet, J. S. Bradshaw and R. M. Izatt, *Separation and Purification Methods*, **23** (1994) 77.

[58] C. Kantipuly, S. Katragadda, A. Chow and H. D. Gesser, *Talanta*, **37(5)** (1990) 491.

[59] B. S. Garg, R. K. Sharma, N. Bhojak, S. Mittal, *Microchemical Journal*, **61** (1999) 94.

[60] C. Liu, *J. Chin. Chem. Soc.*, **39** (1992) 543.

[61] R. Caprioli and S. Torcini, *J. Chromatgra.*, **640** (1993) 365.

[62] W. Shotyk and I. Immenhauser-Potthast, *J. Chromatgr. A.*, **706** (1995) 167.

[63] H. Lu, S. Mou, Y. Yan, S. Tong, J. M. Riviello, *J. Chromatgr. A.*, **800** (1998) 247.

[64] H. Lu, S. Mou, Y. Hou, F. Liu, K. Li, s. Tong, Z. Li and J. M. Riviello, *J. Liq. Chrom & Rel. Technol.*, **20(19)** (1997) 3173.

[65] H. Lu, S. Mou, Y. Yan, F. Liu, K. Li, S. Tong and J. M. Riviello, *Talanta*, **45** (1997) 119.

[66] M. Laikhtman, J. M. Riviello and J. S. Rohrer, *J. Chromatgr. A.*, **816** (1998)

282.

[67] S. Motellier and H. Pitsch, *J. Chromatgr. A.*, **739** (1996) 119.

[68] N. Cardellicchio, S. Cavalli and J. M. Riviello, *J. Chromatgra.*, **640** (1993) 207.

[69] C.Liu, N. Lee and T. Wang, *Anal. Chim. Acta.*, **337** (1997) 173.

[70] C.Liu, N. Lee and J. Chen, *Anal. Chim. Acta.*, **369** (1998) 225.

[71] M. G. Kolpachnikova, N. A. Penner and P. N. Nesterenko, *J. Chromatgr. A.*, **826** (1998) 15.

[72] O. Abollino, M. Aceto, C. Sarzanini and E. Mentasti, *Anal. Chim. Acta.*, **411** (2000) 223.

[73] C. N. Ferrarello, M. M. Bayon, J. I. G. Alonso and A. Sanz-Medel, *Anal. Chim. Acta.*, **429** (2001) 227.

[74] K. W. Warnken, D. Tang, G. A. Gill and P. H. Santschi, *Anal. Chim. Acta.*, **423** (265.

[75] K. Inagaki, N. Mikuriya, S. Morita. H. Haraguchi, Y. Nakahara, M. Hattori, T. Kinosita and H. Saito, *Analyst*, **125** (2000) 197.

[76] K. Inagaki and H. Haraguchi, *Analyst*, **125** (2000) 191.

[77] M. J. Bloxham, S. J. Hill and P. J. Worsfold, *J. Anal. At. Spec.*, **9** (1994) 935.

[78] M. Kumar, D. P. S. Rathore and A. J. Singh, *Talanta*, **51** (2000) 1187.

[79] M. Kumar, D. P. S. Rathore and A. J. Singh, *Analyst*, **125** (2000) 1221.

[80] H. Bag, A. R. Turker and M. Lale, *Talanta*, **51** (2000) 1035.

[81] H. Bagheri, M. Saraji and M. Naderi, *Analyst*, **125** (2000) 1649.

[82] A.G. S. Prado and C. Airoldi, *Anal. Chim. Acta.*, **432** (2001) 201.

[83] C. H. Lee, M. Y. Suh, K. S. Joe, T. Y. Eom and W. Lee, *Anal. Chim. Acta.*, **351** (1997) 57.

[84] R. Shah and S. Devi, *Talanta*, **45** (1998) 1089.

[85] H. Maeda and H. Egawa, *Anal. Chim. Acta.*, **162** (1984) 339.

[86] M. Ahuja, A. K. Rai and P. N. Mather, *Talanta*, **43** (1996) 1955.

[87] D. Das, A. K. Das and C. Sinha, *Talanta*, **48** (1999) 1013.

[88] K. Inoue, K. Yoshizuka and K. Ohta, *Anal. Chim. Acta.*, **388** (1999) 209.

[89] J. Chwastowska, A. Rogowska, E. Sterlinska and J. Dudek, *Talanta*, **49** (1999) 837.

[90] I. E. DeVito, A. N. Masi and R. A. Olsina, *Talanta*, **49** (1999) 929.

[91] K. Dev, R. Pathak and G.N. Rao, *Talanta*, **48** (1999) 579.

[92] J. D. Glennon and S. Srijaranai, *Analyst*, **115** (1990) 627.

[93] N. Ryan, J. D. Glennon and D. Muller, *Anal. Chim. Acta.*, **283** (1993) 344.

[94] S. Hutchinson, G. A. Kearney, E. Horne, B. Lynch, J. D. Glennon, M. A. McKervey and S. J. Harris, *Anal. Chim. Acta.*, **291** (1994) 269.

[95] L. G. Sillen and A. E. Martell, Stability Constants of Metal Ion Complexes, Spec. Publ., N17 and N24, Chem. Soc., London, 1964 and 1971.

[96] G. Bonn, S. Reiffenstuhl and P. Jandik, *J. Chromatgra.*, **499** (1990) 669.

[97] P. N. Nesterenko and P. Jones, *J. Liq. Chrom & Rel. Technol.*, **19(7)** (1996) 1033.

[98] M. C. Yebra-Biurrun, A. Bernejo-Barrera and M. P. Bernejo-Barrera, *Anal. Chim Acta.*, **264** (1992) 53.

[99] P. N. Nesterenko, O. S. Zhukova, O. A. Shpigun and P. Jones, *J. Chromatgr. A.*, **813** (1998) 47.

[100] P. N. Nesterenko, M. J. Shaw, S. J. Hill and P. Jones, *Microchemical Journal*, **62** (1999) 58.

[101] M. J. Shaw, S. J. Hill, P. Jones and P. N. Nesterenko, *J. Chromatogr. A.*, **876** (2000) 127.

[102] C. Merly, B. Lynch, P. Ross and J. D. Glennon, *J. Chromatgr. A.*, **804** (1998) 187.

[103] A. I. Elefterov, S. N. Nosal, P. N. Nesterenko, O. A. Shpigun, *Analyst*, **119** (1994) 1329.

[104] A. I. Elefterov, P. N. Nesterenko and O. A. Shpigun, *J. Anal. Chem.*, **51(9)** (1996) 964.

[105] I. N. Voloschik, M. L. Litvina, and B. A. Rudenko, *J. Chromatogr. A.*, **706** (1995) 315.

[106] P. N. Nesterenko and P. Jones, *Anal. Comm.*, **34(7/8)** (1997) 7.

[107] P. N. Nesterenko and P. Jones, *J. Chromatogr. A.*, **804** (1998) 223.

[108] P. N. Nesterenko and P. Jones, *J. Chromatogr. A.*, **770** (1997) 129.

[109] W. Bashir and B. Paull, *J. Chromatogr. A.*, **907** (2001) 191.

[110] W. Bashir and B. Paull, *J. Chromatogr. A.*, **910** (2001) 301.

[111] D.Jenson, J. Weiss, M. A. Rey and C. A. Pohl, *J. Chromatgra.*, **640** (1993) 65.

[112] P. Jones and B. Paull, *Anal. Proc.*, **29** (1992) 402.

[113] J. B. Truscott, L. Bromley, P. Jones, E. H. Evans, J. Turner and B. Fairman, *J. Anal. At. Specrom.*, **14** (1999) 627.

[114] P.R. Haddad, *Chromatographia*, **42** (1987) 217.

[115] R. D. Rocklin, *J. Chromatgra.*, 546 (1991) 175.

[116] W. W. Buchberger and P. R. Haddad, *J. Chromatgr A.*, **789** (1997) 67.

[117] O. J. Challenger, Ph.D. Thesis, University of Plymouth, 1993.

[118] R. M. C. Sutton, Ph.D. Thesis, University of Plymouth, 1996.

[119] B. Paull, Ph.D. Thesis, University of Plymouth, 1994.

[120] M. J. Shaw, Ph.D. Thesis, University of Plymouth, 2000.

[121] K. Brajter and E. Olbrych-Sleszynska, *Talanta*, **30(5)** (1983) 355.

[122] H. W. Handley, P. Jones, L. Ebdon and N. W. Barnett, *Anal. Proc.*, **28** (1991)

37.

[123] L. Ebdon, H. W. Handley, P. Jones and N. W. Barnett, *Mikrochim. Acta.*, (1991) II 39.

[124] A.K. Singh and S. K. Dhingra, *Analyst*, **117** (1992) 889.

[125] R. Saxena and A. K. Singh, *Anal. Chim. Acta.*, **340** (1997) 285.

[126] K. Brajter, E. Olbrych-Sleszynska and M. Staskiewicz, *Talanta*, **35** (1988) 65.

[127] P. K. Tewari and A. K. Singh, *Talanta*, **53** (2001) 823.

[128] Z. Molodovan and L. Vladescu, *Talanta*, **43** (1996) 1573.

[129] A. A. Almeida, X. Jun and J. L. F. C. Lima, *Analyst*, **123** (1998) 1283.

[130] K. Brajter and E. Olbrych-Sleszynska, *Analyst*, **113** (1988) 1571.

[131] E. Morosanova, A. Velikorodny and Y. Zolotov, *Fres. J. Anal. Chem.*, **361** (1998) 305.

[132] S. L. C. Ferreira, J. R. Ferreira, A. F. Dantas, V. A. lemos, N. M. L. Araujo and A. C. S. Costa, *Talanta*, **50** (2000) 1253.

[133] S. L. C. Ferreira, C. F. deBrito, A. F. Dantas, N. M. L. Araujo and A. C. S. Costa, *Talanta*, **48** (1999) 1173.

[134] R. M. C. Sutton, S. J. Hill and P. Jones, *J. Chromatogr A.*, **739** (1996) 81.

[135] L. Cornejo-Ponce, P. Peralta-Zamora, H. I. Maretti and S. Bueno, *Talanta*, **46** (1998) 1371.

[136] C. H. Lee, J. S. Kim, M. Y. Suh and W. Lee, *Anal. Chim. Acta.*, **339** (1997) 303.

[137] O. Zaporozhets, N. Petruniock, O. Bessarabova and V. Sukan, *Talanta*, **49** (1999) 899.

[138] R. Saxeena, A. K. Singh and S. S. Sambi, *Anal. Chim. Acta.*, **295** (1994) 199.

[139] P. Jones and G. Schwedt, *J. Chromatogra.*, **482** (1989) 325.

[140] O. J. Challenger, S. J. Hill and P. Jones, *J. Chromatogra.*, **639** (1993) 197.

[141] P. Jones, O. J. Challenger, S. J. Hill and N. W. Barnett, *Analyst*, **117** (1992)

1447.

[142] O. J. Challenger, S. J. Hill, P. Jones and N. W. Barnett, *Anal. Proc.*, **29** (1992) 91.

[143] P. Jones, M. Foulkes and B. Paull, *J. Chromatogr A.*, **673** (1994) 173.

[144] B. Paull and P. Jones, *Chromatographia*, **42(9/10)** (1996) 528.

[145] B. Paull, M. Foulkes and P. Jones, *Analyst*, **119** (1994) 937.

[146] B. Paull, M. Foulkes and P. Jones, *Anal. Proc. Inc. Anal. Comm.*, **31** (1994) 209.

[147] B. Paull and P. R. Haddad, *Anal. Comm.*, **35** (1998) 13.

[148] P. Su and S. Huang, *Anal. Chim. Acta.*, **376** (1998) 305.

[149] Y. A. Zolotov, I. M. Maksimova, E. I. Morosanova and A. A. Velikorodny, *Anal. Chim. Acta.*, **308** (1995) 378.

[150] J. E. DeNunzio, R. W. Yost and E. K. Hutchison, *Talanta*, **32(8b)** (1985) 803.

[151] T. A. Walker, J. Chromatogra., **602** (1992) 97.

[152] J. Toei and N. Baba, *J. Chromatogra.*, **361** (1986) 368.

[153] J. Toei, Fres., *J. Anal. Chem.*, **331** (1988) 735.

[154] J. Toei, *Analyst*, **113** (1988) 247.

[155] J. Toei, *Chromatographia*, **23(5)** (1987) 355.

[156] B. Paull, P. A. Fagan and P. R. Haddad, *Anal. Comm.*, **33** (1996) 193.

[157] B. Paull, M. Macka and P. R. Haddad, *J. Chromatogr A.*, **789** (1997) 329.

[158] B. Paull, P. N. Nesterenko, M. Nurdin and P. R. Haddad, *Anal. Comm.*, **35** (1998) 17.

[159] B. Paull, M. Clow and P. R. Haddad, *J. Chromatogr A.*, **804** (1998) 95.

[160] B. Paull, P. N. Nesterenko and P. R. Haddad, *Anal. Chim. Acta.*, **375** (1998) 117.

[161] B. Paull and P. R. Haddad, *Trends In Anal. Chem.*, **18(2)** (1999) 107.

[162] Z. Holzbecher, L. Divis, M. Kral, L. Sucha and F. Vlacil, Handbook of Organic

Reagents in Inorganic Analysis, John Wiley & Sons, New York, 1976.

[163] F. Smedes, L. G. Decnop-Weever, N. T. Ugen, J. Nieman and J. Kragten, *Talanta*, **30(8)** (1983) 614.

[164] BDH Chemical Catalogue, 1998.

[165] Sigma-Aldrich Chemical Catalogue, 1998.

[166] Z. Wang and K. L. Cheng, *Ultrasonics*, **SEP** (1982) 215.

[167] J. B. Truscott, *Personal Communication*, 1998.

[168] B. Paull and P. Jones, *Chromatographia*, **42** (1996) 528.

[169] J. Emsley, The Elements, 3rd Ed, Oxford University Press, 1998.

[170] X. Ding, S. Mou, K. Liu, A. Siriraks and J. M. Riviello, *J. Chromatogr A.*, **847** (1999) 251.

[171] E.B. Sandell and H. Onishi, Photometric Determination of Traces of Metals – Vol 3, Part1, 4th Ed, John Wiley & Sons, New York, 1978.

[172] P. Jones, *Analyst*, **125** (2000) 803.

[173] M. J. Shaw, S. J. Hill and P. Jones, *Anal. Chim. Acta.*, **401** (1999) 65.

[174] M. J. Shaw, S. J. Hill, P. Jones and P. N. Nesterenko, *Anal. Comm.*, (1999) 399.

[175] M. J. Shaw, S. J. Hill, P. Jones and P. N. Nesterenko, *Chromatographia*, **51(11/12)** (2000) 695.

[176] S. Elchuck, K. I. Burns, R. M. Cassidy and C. A. Lucy, *J. Chromatogra.*, **558** (1991)197.

[177] F.Hao, B. Paull and P.R. Haddad, *J. Chromatogr. A.*, **739** (1996) 151.

[178] F.Hao, B. Paull and P.R. Haddad, *J. Chromatogr A.*, 749 (1996) 103.

[179] P. N. Nesterenko, G. Z. Amirova and T. A. Bol'shova, *Anal. Chim. Acta.*, **285** (1994) 161.

[180] P. N. Nesterenko and G. Z. Amirova, *J. Anal. Chem.*, **49** (1994) 495.

[181] V. K. Jain, A. Handa, S. S. Sait, P. Shrivastav and Y. K. Agrawal, *Anal. Chim. Acta.*, **429** (2001) 237.

[182] J. L. P. Pavon, C. G. Pinto, E. R. Garcia and B. M. Cordero, *Anal., Chim. Acta.*, **264** (1992) 291.

[183] M. J. C. Taylor and J. F. van Staden, *Analyst*, **119** (1994) 1263.

[184] B. Patel, G. E. Henderson, S. J. Haswell and R. Grzeskowiak, *Analyst*, **115** (1990) 1063.

[185] G. Bagur, M. Sanchez and D. Gazquez, *Analyst*, **119** (1994) 1157.

[186] R. G. Wuilloud, J. A. Salonia, J. A. Gazquez, R. A. Olsina and L. D. Martinez, *Anal. Chim. Acta.*, **420** (2000) 73.

[187] S. N. Willie, Y. Tida and J. W. McLaren, *Atom. Spec.*, **19(3)** (1998) 67.

[188] F.W. E. Strelow, *Anal. Chem.*, **59** (1987) 1907.

[189] M. J. Tomlinson, J. Wang and J. A. Caruso, *J. Anal. At. Spec.*, **9** (1994) 957.

[190] B. Gong, X. Li, F. Wang and X. Chang, *Talanta*, **52** (2000) 217.

[191] S. Oszwaldowski, R. Lipka and M. Jarosz, *Anal. Chim. Acta.*, **361** (1998) 177.

[192] S. Oszwaldowski, R. Lipka, T. Majewski and M. Jarosz, *Analyst*, **123** (1998) 1529.

[193] X. Yang and C. Pin, *Analyst*, **125** (2000) 453.

[194] X. Yang and C. Pin, *Anal. Chem.*, **71** (1999) 1706.

[195] D.Trubert, F. M. Guzman, C. Le Naour, L. Brillard, M. Hussonnois and O. Constantinescu, *Anal. Chim. Acta.*, **374** (1998) 149.

[196] M. Qureshi and K. Husain, *Anal. Chem.*, **43(3)** (1971) 447.

[197] R. Purohit and S. Devi, *Talanta*, **44** (1997) 319.

[198] N. A. Penner, P. N. Nesterenko, M. M. Ilyin, M. P. Tsyurupa and V. A. Davankov, *Chromatographia*, **50(9/10)** (1999) 611.

[199] V. A. Davankov and M. P. Tsyurupa, *Angew. Makromol. Chem.*, **91** (1980) 127.

[200] V. A. Davankov and M. P. Tsyurupa, *Pure Appl. Chem.*, **61** (1989) 1881.

[201] M. P. Tsyurupa, T. A. Mrachkovskaya, L. A. Maslova, G. I. Timofeeva and V. A. Davankov, *React. Polym.*, **19** (1993) 55.

[202] V. A. Davankov and M. P. Tsyurupa, *React. Polm.*, **13** (1990) 27.

[203] R. M. C. Sutton, S. J. Hill and P. Jones, *J. Chromatogr. A.*, **789** (1997) 389.

[204] R. M. C. Sutton, S. J. Hill, P. Jones, A. Sanz-Medel and J. I. Garcia-Alonso, *J. Chromatogr. A.*, **816** (1998) 286.

[205] E.Merian (Ed.), Metals and their Compounds in the Environment, VCH, Weinheim, 1991.

[206] D.J. Barkley, L. A. Bennete, J. R. Charbonneau and L. A. Pokrajac, *J. Chromatogra.*, **606** (1992) 195.

[207] P. E. Jackson, J. Carnevale, H. Fuping and P. R. Haddad, *J. Chromatogr. A*,, **671** (1994) 181.

[208] M. P. Harrold, A. Siriraks and J. M. Riviello, *J. Chromatogra.*, **602** (1992) 119.

[209] B. Paull and P. R. Haddad, *Anal. Comm.*, **35** (1998) 13.

[210] A.W. Al-Shawi and R. Dahl, *J. Chromatogra.*, **706** (1995) 175.

[211] M. Merdivan, M. R. Buchmeiser and G. Bonn, *Anal. Chim. Acta.*, **402** (1999) 91.

[212] J. J. Byerley, J. M. Scharer and G. F. Atkinson, *Analyst*, **112** (1987) 41.

[213] P. Goodall and C. Lythgoe, *Analyst*, **124** (1999) 263.

[214] T. Yokoyama, A. Makishima and E. Nakamura, *Anal. Chem.*, **71** (1999) 135.

[215] H. E. Carter, P. Warwick, J. Cobb and G. Longworth, *Analyst*, **124** (1999) 271.

[216] C. H. Lee, M. Y. Suh, J. S. Kim, D. Y. Kim, W. H. Kim and T. Y. Eom, *Anal. Chim. Acta.*, **382** (1999) 199.

[217] S. Rollin and U. B. Eklund, *J. Chromatogr. A.*, **884(1-2)** (2000) 131.

[218] D.K. Mann and G. T. F. Wong, *Marine Chemistry*, **42** (1993), 25.

[219] T. Nakashima, K. Yoshimura and T. Taketatsu, *Talanta*, **39(5)** (1992) 523.

[220] B. Gong, X. Li, F. Wang and X. Chang, *Talanta*, **52** (2000) 215.

[221] B. Gong, X. Li, F. Wang, H. Xu and X. Chang, *Anal. Chim. Acta.*, **42** (2001) 287.

[222] S. Arpadjan, L. Vuchkova and E. Kostadinova, *Analyst*, **122** (1993) 243.

[223] M. S. El-Shahawi and R. S. Al-Mehrezi, *Talanta*, **44** (1997) 483.

[224] R. Kuroda, K Oguma, Y. Mori, H. Okabe and T. Takizawa, *Chromatographia*, **32 (11/12)** (1991) 583.

[225] D.Pozebon, V. L. Dressler and A. J. Curtius, *J. Anal. At. Spectrom.*, **13** (1998) 363.

[226] A.C. Sahayam, *Atom. Spec.*, **19(3)** (1998) 107.

[227] S. Moyano, R. G. Wuilloud, R.A Olsina, J. D. Gasquez and L. D. Martinez, *Talanta*, **54** (2001) 211.

[228] F.W. E. Strelow, *Talanta*, **38(8)** (1991) 923.

[229] N. Uehara, K. Morimoto and Y. Shijo, *Analyst*, **117** (1992) 977.